Functional neuroinflammatory- and serotonergic imaging in Alzheimer's disease

Versijpt, Jan Jozef Albert

RIJKSUNIVERSITEIT
GRONINGEN

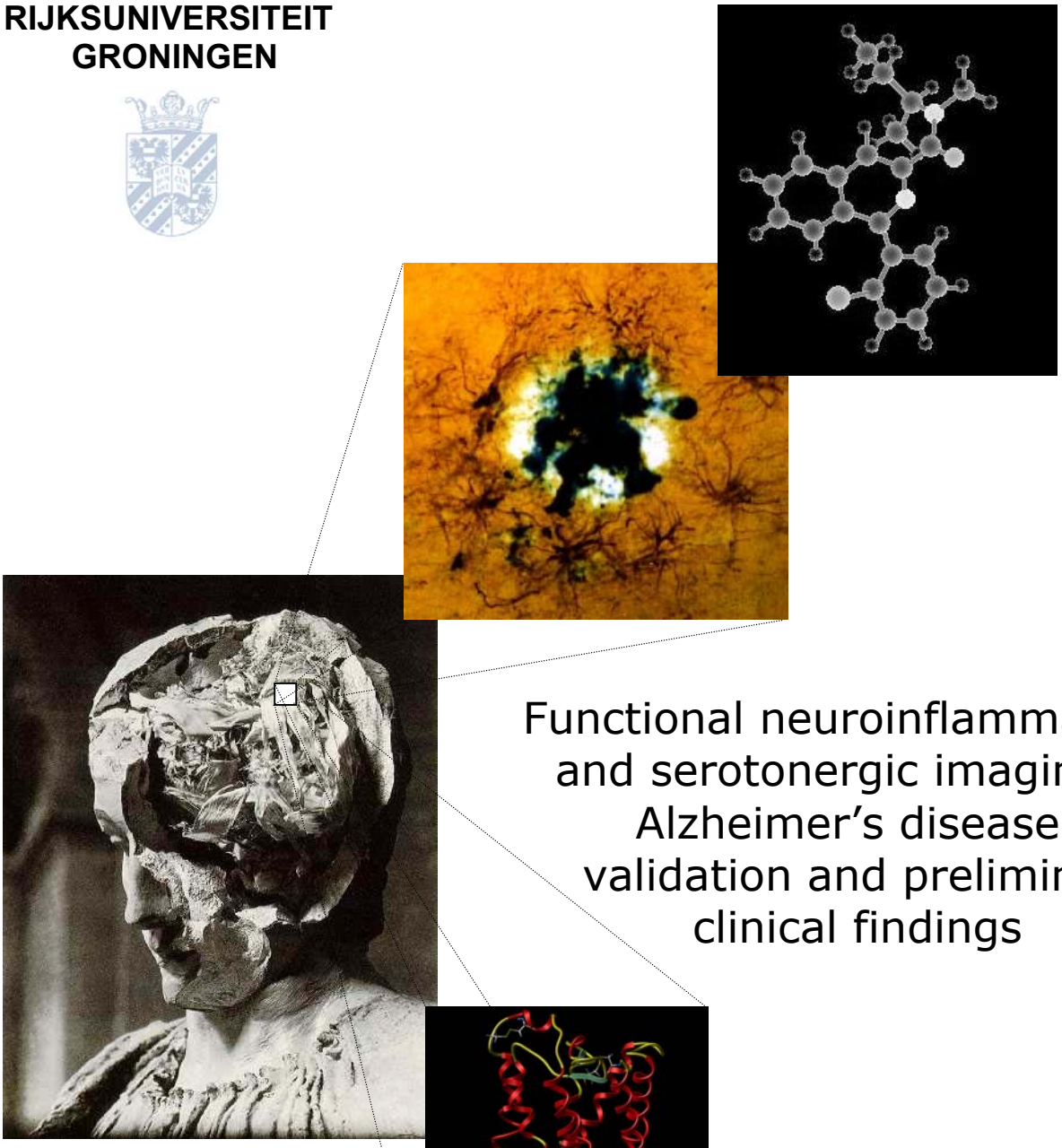

Functional neuroinflammatory- and serotonergic imaging in Alzheimer's disease: validation and preliminary clinical findings

UNIVERSITEIT
GENT

Jan Versijpt

Josef Sudek (°1896 - †1976) was a famous Czechoslovakian photographer known for his lyrical images that show a fine eye for life's intimate details. He once explained that '*everything around us, dead or alive, in the eyes of a crazy photographer mysteriously takes on many variations, so that a seemingly dead object comes to life through light or by its surroundings… To capture some of this – I suppose that's lyricism*'. The cover photograph shows the work *Untitled* (1940) where *in the surrounding* of this PhD thesis one can depict *stoned* plaques and tangles.

The upper row represents the neuroinflammation part of this thesis where the first photograph shows an Alzheimer amyloid plaque (white) surrounded by reactive astrocytes (brown) and a cluster of microglial cells (black) sitting on top. Next to it, a three-dimensional model of the radioligand used in the present thesis PK11195 (either for PET or SPECT) is shown.

The lower row represents the serotonergic part of this thesis where the first picture shows a three-dimensional structure of the 5-HT_{2A} receptor. Next to it, a model of the SPECT radioligand R91150 is shown.

This work was financially supported by the *Internationale stichting Alzheimer onderzoek*.

Aan Sabine

RIJKSUNIVERSITEIT GRONINGEN

Functional neuroinflammatory- and serotonergic imaging in Alzheimer's disease: validation and preliminary clinical findings

PROEFSCHRIFT

ter verkrijging van het doctoraat in de
Medische Wetenschappen
aan de Rijksuniversiteit Groningen
op gezag van de
Rector Magnificus, dr. F. Zwarts,
in het openbaar te verdedigen op
woensdag 16 april 2003
om 14.15 uur

door

Jan Jozef Albert Versijpt
geboren op 10 november 1972
te Sint-Amandsberg

PROMOTORES:

PROF. DR. J. KORF
PROF. DR. R.A. DIERCKX
PROF. DR. G. SLEGERS

BEOORDELINGSCOMMISSIE:

PROF. DR. J. DE REUCK
PROF. DR. W. VAALBURG
PROF. DR. K. LEENDERS

ISBN-nummer: 90 367 1806 6

CONTENTS

We must trust to nothing but facts. These are presented to us by Nature, and cannot deceive. We ought, in every instance, to submit our reasoning to the test of experiment, and never to search for truth but by the natural road of experiment and observation.

Antoine Lavoisier (1743-1794)

INTRODUCTION AND OUTLINE OF THE THESIS

The present thesis aims at clarifying the pathophysiology of Alzheimer's disease by means of functional radionuclide imaging, this in order to finally aid its therapeutic management. It is divided in two parts.

The *first part* deals with neuroinflammatory imaging in general with the ultimate goal of this part being the visualisation and assessment of neuroinflammatory lesions in Alzheimer's disease. Indeed, in the past decades, our understanding of the central nervous system has evolved from one of an immune-privileged site, to one where inflammation is pathognomonic for some of the most prevalent and tragic neurodegenerative diseases. Current research indicates that diseases as diverse as head trauma, multiple sclerosis, stroke and Alzheimer's disease exhibit inflammatory processes sharing this inflammatory pathway as a common mechanism contributing to cellular dysfunction and or neuron loss.

In **chapter two**, Alzheimer's disease as the most common form of dementia is thoroughly reviewed and an introduction is given on firstly Alzheimer's disease as an inflammatory disease and secondly neuroinflammatory imaging in general. In **chapter three**, an attempt is undertaken to visualise neuroinflammatory lesions in Alzheimer's disease with ^{57}Co and single photon emission computed tomography (SPECT), which has previously been proven useful in diseases like stroke and Multiple Sclerosis. To overcome the disadvantages encountered with the previous radioligand, a new radioligand (PK11195) was studied, which is described in **chapter four**. Since multiple sclerosis (MS) is the prototype neuroinflammatory disorder where inflammatory mediators contribute to white matter axonal damage leading to the accumulation of disability, radiolabelled PK11195 as a *neuroinflammatory marker* is validated in a cohort of MS patients. Therefore, its relationship with clinical measures on one hand and structural imaging on the other hand is assessed and described in **chapter five**. In **chapter six**, preliminary findings about radiolabelled PK11195 and its relationship with neuropsychological measures and perfusion imaging in a group of Alzheimer's disease patients are described.

The *second part* deals with the role and distribution of serotonin (5-HT) type 2A receptors in Alzheimer's disease (**chapter seven)**.

In an *introductory part*, the role of serotonin in general and serotonin type 2A (5-HT_{2A}) receptors specifically in cognitive and non-cognitive behaviour and AD is briefly reviewed. In a *second part*, the distribution and comparison of the 5-HT_{2A} system using ^{123}I-5-I-R91150, a selective radio-iodinated 5-HT_{2A} receptor antagonist and SPECT in healthy controls and Alzheimer's disease is described together with its relationship with age, gender, concurrent depression and other neuropsychological measures.

CHAPTER TWO

INTRODUCTION TO NEUROINFLAMMATION, ALZHEIMER'S DISEASE AS AN INFLAMMATORY DISEASE, AND NEUROINFLAMMATORY IMAGING

ALZHEIMER'S DISEASE

Depending on where you set your sights, Alzheimer's disease is a scientific puzzle, a medical whodunit, a psychosocial tragedy, a financial disaster or an ethical, legal and political dilemma. It is all those things and more – a complex problem that is a prototype for the health-care quandaries facing people in developed nations throughout the world. And the solution will need to be equally complex. The disease quietly loots the brain, nerve cell by nerve cell, like a burglar returning to the same house each night. As the brain loses mass, the rest of the body gradually shuts down…

Alzheimer's disease (AD) is the most common cause of dementia in the elderly and is a progressive neurodegenerative disorder that gradually robs the patient of his cognitive function and eventually causes death. The present part reviews the history, epidemiology, clinical features, pathophysiology, and treatment of AD.

HISTORY

Alzheimer's disease had played havoc with people since ancient times. Greek and Roman writers as well as Elizabethan chroniclers accurately described the symptoms of the illness. One of the best examples is in Shakespeare's King Lear. Lear is losing his memory and becoming disorientied; if you read between the lines, he has Alzheimer's disease. But Alzheimer's was not established as a distinct disease until the early part of this century. Alois Alzheimer (figure below, right) who later gave his name to this disease – in 1910 at the suggestion of Emil Kraepelin – first examined Auguste D, now considered as the first person described as having 'AD', in 1901 and followed her up until her death in 1906. After her death, he went on to study the neuropathologic features of her illness, in which he had a great interest due to his friendship with Franz Nissl, whose expertise helped with the development of the histological staining techniques essential in histopathology. Auguste D (figure below, left) was at the time of her first examination a 51-year old woman who initially presented with a strong feeling of jealousy towards her husband with carrying objects to and fro in her flat and hiding them. Later on, she showed progressive cognitive impairment, focal symptoms, hallucinations, delusions and psychosocial incompetence. Sometimes she felt that someone wanted to kill her and would scream loudly. After 4 ½ years of sickness, she died from septicaemia resulting from a decubitis ulcer in the sacral and left trochanteric regions. She presented the neurobiological changes found at necropsy – plaques, neurofibrillary tangles and atherosclerotic changes – now considered characteristic of AD [1]. In 1976 the neurologists Davies, Maloney, and Bowen showed that an enzyme necessary to synthesize acetylcholine was deficient in the brain of patients with AD. Earlier research in neurotransmitter chemistry had shown that cholinergic, or acetylcholine-containing, neurons play an important role in memory. The discovery of a link between a biochemical brain defect – the deficiency of acetylcholine – and AD marked the beginning of modern Alzheimer's research.

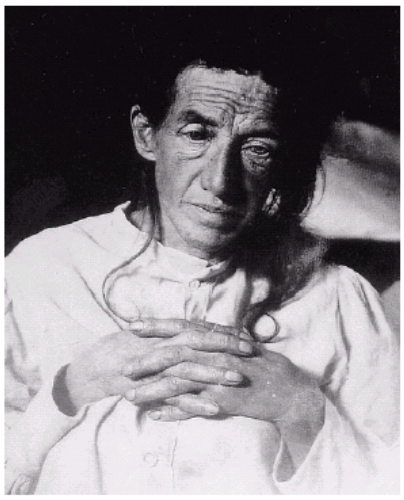

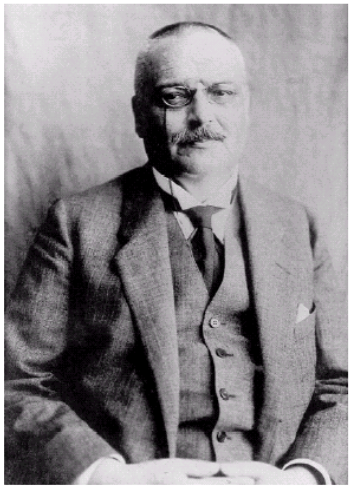

INCIDENCE, PREVALENCE, AND ECONOMIC IMPACT

AD accounts for 60 to 70% of the cases of progressive cognitive impairment in elderly patients. Prevalence of the disease in Europe ranges from 0.02% in people aged 30-39 years to 10.8% in those aged 80-90 years (more than 11 million people worldwide with lower incidence in people of African or Asian origin with even reports suggesting that AD does not occur in Nigerians) [2]. The prevalence of AD in the US doubles every 5 years after the age of 60 increasing from a prevalence of 1% among those 60- to 64-years-old to up to 40% of those aged 85 years and older [3]. The population of patients with AD will nearly quadruple in the next 50 years if the current trend continues [3]. The disease is more common among women than men by a ratio of 1.2 to 1.5 [4].

Most direct costs of care for patients with AD are absorbed by the expense of nursing home care, approximately 47 000,- ε per patient per year [5].

Several risk factors for AD have been identified in epidemiologic studies in addition to age and female sex. The most potent risk factor is the presence of the apolipoprotein ε4 (APOE ε4) allele. Of its 3 forms ε2, ε3, and ε4 only the ε4 allele increases the likelihood of developing AD. The lifetime risk of AD for an individual without the ε4 allele is approximately 9% whereas the lifetime risk of AD for an individual carrying at least one ε4 allele is 29%. While representing a substantial risk of AD, the ε4 genotype is not sufficiently specific or sensitive for the diagnosis of AD to allow its use as a diagnostic test [6]. Other risk factors implicated in a variety of studies include head injury, low serum levels of folate and vitamin B12, elevated plasma and total homocysteine levels, family history of AD or dementia, fewer years of formal education, lower levels of fish in the diet, lower income, no daily wine consumption, lower occupational status, however other undisclosed genetic or environmental factors have yet to be determined [7, 8].

CLINICAL DIAGNOSIS

Although some sources report that AD can be diagnosed with over 90% accuracy during life if standard clinical criteria are followed, some available evidence suggests that mild dementia is rarely

diagnosed and even moderately severe dementia is underrecognized in clinical practice [9]. The specificity of the Mini-Mental State Examination is good (96%) but the sensitivity is poor (63%), indicating that by itself the test (using a standard cutoff score of 24) will leave a substantial proportion of cases of early dementia undetected. The typical clinical syndrome of AD includes three aspects. Firstly, deficits in cognitive functions which cause an amnestic type of memory defect with difficulty in learning and recalling new information, a progressive language disorder beginning with anomia and progressing to fluent aphasia, disturbances of visuospatial skills manifested by environmental disorientation and difficulties in copying figures, the inability to do motor tasks despite intact motor function (apraxia) and the inability to recognise, despite intact sensory functions (agnosia). There are usually deficits in executive function (planning, insight, judgment) and the patient is typically unaware of memory or cognitive compromise. All cognitive deficits progressively worsen. Secondly, neuropsychiatric and behavioural disturbances become apparent in AD, such as personality changes, delusions, hallucinations and misidentifications. Apathy is present early in the clinical course with diminished interest and reduced concern. Agitation becomes increasingly common as the illness advances and is a frequent precipitant of nursing home placement. Depressive symptoms are present in about 50% of patients and approximately 25% exhibit delusions. Thirdly, difficulties with activities of daily living manifest early in the disease, and affect functions such as handling money, use of the telephone, and driving (instrumental), and later, difficulties with dressing, feeding, and toileting (basic). Motor system abnormalities are absent in AD until the final few years of the disease; focal abnormalities, gait changes, or seizures occurring early in the clinical course of dementia make the diagnosis of AD unlikely. Patients with AD usually survive 7 to 10 years after onset of symptoms with a range of 2 to 20 years and typically die from bronchitis or pneumonia [10, 11]. Assessment and diagnosis of AD require identifying the core clinical features and excluding other common causes of dementia in the elderly. Screening for thyroid dysfunction and vitamin B12 deficiency is recommended; syphilis is no longer sufficiently common to warrant routine screening in typical clinical circumstances. Neuroimaging should be obtained to identify vascular contributions to the dementia syndrome and to identify other intracranial pathology. Functional imaging with positron emission tomography or single photon emission computed tomography are helpful particularly when clinical features are ambiguous [12].

PATHOLOGY

The current criteria for the pathologic diagnosis of AD require the presence of both senile neuritic plaques and neurofibrillary tangles in excess of the abundance anticipated for age-matched healthy controls [13]. Neuritic plaques consist of a central core of amyloid protein surrounded by astrocytes, microglia, and dystrophic neurites often containing paired helical filaments. Neurofibrillary tangles are the second major histopathological feature of AD. They contain paired helical filaments of abnormally phosphorylated tau protein that occupy the cell body and extend into the dendrites.

However, current evidence suggests that the neuropathology of AD comprises more than amyloid plaques and neurofibrillary tangles. At least a third of AD cases may exhibit significant

cerebrovascular pathology. Cerebral amyloid angiopathy, microvascular degeneration affecting the cerebral endothelium and smooth muscle cells, basal lamina alterations, hyalinosis and fibrosis are often evident in AD. These changes may be accompanied by perivascular denervation that is causal in the cognitive decline of AD. Peripheral vascular disease such as long-standing hypertension, atrial fibrillation, coronary or carotid artery disease and diabetes could further modify the cerebral circulation such that a sustained hypoperfusion or oligaemia is impacted upon the ageing brain.

In addition to these three major classic histopathologic features, AD also is characterized by reductions in synaptic density, loss of neurons, and granulovacuolar degeneration in hippocampal neurons. Neuronal loss or atrophy in the nucleus basalis, locus ceruleus, and raphe nuclei of the brainstem leads to deficits in cholinergic, noradrenergic, and serotonergic transmitters, respectively with the cholinergic deficit as the most consistent neurochemical abnormality.

MOLECULAR GENETICS AND PATHOGENESIS

A small number of cases – between 2 and 7 percent – result from an inherited genetic mutation and can strike people as young as thirty. Although mutations account for so few cases of AD they have been of great value in the study of the pathogenesis of the disorder. Mutations in the amyloid precursor protein (APP gene, chromosome 21), presenilin 1 (chromosome 14), and the presenilin 2 gene (chromosome 1) produce an autosomal dominant pattern of inheritance with nearly complete penetrance [14]. Together with the apolipoprotein E gene, they account for about half the genetic risk.

The amyloid protein that appears to be central to the pathogenesis of AD is derived from APP (amyloid precursor protein) and its abnormal cleavage finally leads to the deposition of neuritic plaques (figure 2). The accumulation of β-amyloid initiates a series of events contributing to cell death, including activation of cell death programs, oxidation of lipids and disruption of cell membranes, an inflammatory response, and possible tangle formation, a close correlate of neuron loss. All of the identified mutations that cause AD result in increased production of β-amyloid protein [15].

Head injury, educational level, and other risk and protective factors identified through epidemiologic studies may exert effects on the likelihood of developing AD through their impact on cerebral reserve - the ability of the brain to withstand the accumulating amyloid burden without evidencing dysfunction and cognitive impairment [10].

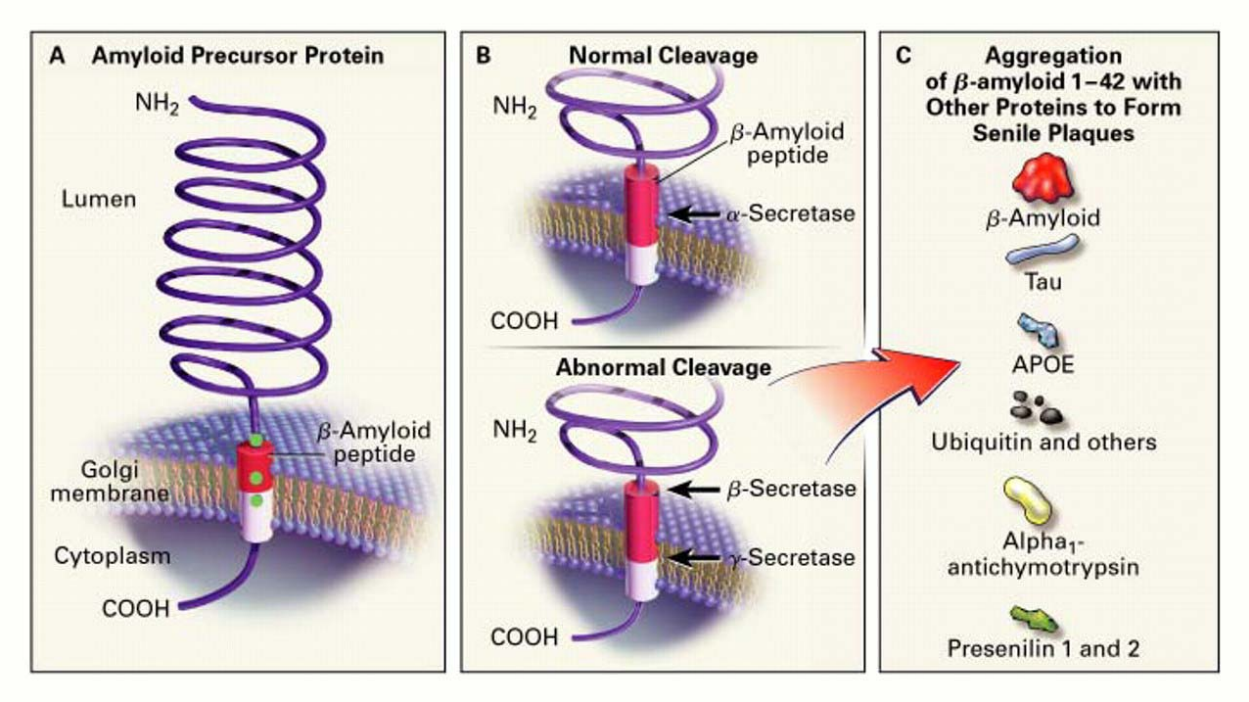

TREATMENT

AD does not have a definite cure, but many psychosocial interventions and caregiver support can help to alleviate strain on carers. Available treatments for AD include cholinesterase inhibitors, disease-modifying treatments, and psychotropic agents. Treatment of AD must always reflect the values and wishes of the patient and their family. Therapeutic strategies may also change in the course of the disease, for example, slowing of disease progression with vitamin E may be desirable early in the clinical course but not in patients with advanced disease.

Cholinesterase inhibitors are the only medications approved by the US Food and Drug Administration as treatment for AD. Sufficient evidence has accumulated for these to be recommended as standard therapy for AD. Four inhibitors are currently available: tacrine, donepezil, rivastigmine, and galantamine. These agents have been shown to produce improvements in global function and cognition. Secondary benefits may include reduction in behavioral disturbances, temporary stabilization of activities of daily living, delay of nursing home placement, and reduced demands on caregiver time. Patients not responding to one agent in the class may respond to another. Discontinuation of treatment should be monitored; deterioration during withdrawal indicates therapeutic benefit and the medication should be reinstated [16].

Vitamin E and selegiline have been shown to reduce the rate of decline of functions in patients with AD. Evidence to support the use of other antioxidants, anti-inflammatory agents, or herbal medications such as ginkgo biloba is insufficient to recommend use as standard therapies. Estrogen in standard doses has been shown not to improve cognition in postmenopausal women with AD [16].

Reducing amyloid production, aggregation, or enhancing its removal are promising avenues of treatment that will address the basic pathophysiology of AD. Immunization, secretase inhibition, and other strategies to accomplish this are being studied.

Epidemiologic data suggest that nonsteroidal anti-inflammatory agents, hormonal treatments, histamine H2 blockers, antihypertensive agents, and statins may decrease the likelihood of developing AD [10, 17]. Clinical trials of these compounds to test their roles in the treatment or prevention of AD are planned or under way.

Psychotropic medications play a critical role in the management of behavioral disturbances of patients with AD. Relatively few psychotropic compounds have been tested specifically in AD populations. Recent double-blind, placebo-controlled trials have established the efficacy of the atypical antipsychotics risperidone and olanzapine for the treatment of psychosis and agitation in patients with AD [18]. Anticonvulsants such as carbamazepine also have been shown to have anti-agitation effects. Depression responds to treatment with selective serotonin reuptake inhibitors or tricyclic antidepressants; there are fewer adverse effects with the former.

Building an alliance with family caregivers is critical to success in the management of patients with AD. Family caregivers provide most of the care received by patients with AD over the course of their illness and are responsible for ensuring adherence to treatment regimens. Caregivers are prone to depression and physical illness as a result of the chronic stress associated with caregiving. Families benefit from short-term education programs and support groups [16].

CHALLENGES

Dramatic progress has been made in understanding the pathogenesis of and developing therapy for AD. Advances so far have had no impact on the prevalence of the disorder and have had limited effects on the clinical course. An effective response to the public health challenge presented by AD requires united efforts in drug discovery, clinical trials of promising agents, implementation in health care delivery systems of programs for screening and treatment of patients with AD, and governmental and public policy initiatives that support patients with AD and their caregivers in all stages of the disease. Much has been achieved but much more remains to be done to prevent the losses of cognitive function, emotional integrity, enjoyment of life, and personal dignity associated with AD. As such, the biggest question now is not whether our research will bear fruit, but how soon – for all those among us and all those to come who might otherwise be doomed to live in the plundered landscape of an eternal present.

REFERENCES

1. Alzheimer A. Über eine eigenartige Erkrankung der Hirnrinde. *Zeit Psychiatrie Psy Gerichtlich Med* 1907; **64**: 146-148.
2. Burns A, Byrne EJ, Maurer K. Alzheimer's disease. *Lancet* 2002; **360**: 163-165.
3. von Strauss E, Viitanen M, De Ronchi D, Winblad B, Fratiglioni L. Aging and the occurrence of dementia: findings from a population-based cohort with a large sample of nonagenarians. *Arch Neurol* 1999; **56**: 587-592.
4. Gao S, Hendrie HC, Hall KS, Hui S. The relationships between age, sex, and the incidence of dementia and Alzheimer disease: a meta-analysis. *Arch Gen Psychiatry* 1998; **55**: 809-815.
5. Rice DP, Fillit HM, Max W, Knopman DS, Lloyd JR, Duttagupta S. Prevalence, costs, and treatment of Alzheimer's disease and related dementia: a managed care perspective. *Am J Manag Care* 2001; **7**: 809-818.
6. Seshadri S, Drachman DA, Lippa CF. Apolipoprotein E □4 allele and the lifetime risk of Alzheimer's disease. What physicians know, and what they should know. *Arch Neurol* 1995; **52**: 1074-1079.
7. Launer LJ, Andersen K, Dewey ME, Letenneur L, Ott A, Amaducci LA, Brayne C, Copeland JR, Dartigues JF, Kragh-Sorensen P, Lobo A, Martinez-Lage JM, Stijnen T, Hofman A. Rates and risk factors for dementia and Alzheimer's disease: results from EURODEM pooled analyses. EURODEM Incidence Research Group and Work Groups. European Studies of Dementia. *Neurology* 1999; **52**: 78-84.
8. Hendrie HC, Ogunniyi A, Hall KS, Baiyewu O, Unverzagt FW, Gureje O, Gao S, Evans RM, Ogunseyinde AO, Adeyinka AO, Musick B, Hui SL. Incidence of dementia and Alzheimer disease in 2 communities: Yoruba residing in Ibadan, Nigeria, and African Americans residing in Indianapolis, Indiana. *JAMA* 2001; **285**: 739-747.
9. Callahan CM, Hendrie HC, Tierney WM. Documentation and evaluation of cognitive impairment in elderly primary care patients. *Ann Intern Med* 1995; **122**: 422-429.
10. Cummings JL, Cole G. Alzheimer disease. *JAMA* 2002; **287**: 2335-2338.
11. Wolfson C, Wolfson DB, Asgharian M, M'Lan CE, Ostbye T, Rockwood K, Hogan DB. A reevaluation of the duration of survival after the onset of dementia. *N Engl J Med* 2001; **344**: 1111-1116.
12. Knopman DS, Dekosky ST, Cummings JL, Chui H, Corey-Bloom J, Relkin N, Small GW, Miller B, Stevens JC. Practice parameter: diagnosis of dementia (an evidence-based review). Report of the Quality Standards Subcommittee of the American Academy of Neurology. *Neurology* 2001; **56**: 1143-1153.
13. The National Institute on Aging and Reagan Institute Working Group on Diagnostic Criteria for the Neuropathological Assessment of Alzheimer's Disease. Consensus recommendations for the postmortem diagnosis of Alzheimer's disease. *Neurobiol Aging* 1997; **18**: S1-S2.
14. George-Hyslop PH. Molecular genetics of Alzheimer's disease. *Biol Psychiatry* 2000; **47**: 183-199.
15. Selkoe DJ. Presenilin, Notch, and the genesis and treatment of Alzheimer's disease. *Proc Natl Acad Sci U S A* 2001; **98**: 11039-11041.
16. Doody RS, Stevens JC, Beck C, Dubinsky RM, Kaye JA, Gwyther L, Mohs RC, Thal LJ, Whitehouse PJ, Dekosky ST, Cummings JL. Practice parameter: management of dementia (an evidence-based review). Report of the Quality Standards Subcommittee of the American Academy of Neurology. *Neurology* 2001; **56**: 1154-1166.
17. Stewart WF, Kawas C, Corrada M, Metter EJ. Risk of Alzheimer's disease and duration of NSAID use. *Neurology* 1997; **48**: 626-632.
18. Street JS, Clark WS, Kadam DL, Mitan SJ, Juliar BE, Feldman PD, Breier A. Long-term efficacy of olanzapine in the control of psychotic and behavioral symptoms in nursing home patients with Alzheimer's dementia. *Int J Geriatr Psychiatry* 2001; **16S1**: S62-S70.

SCINTIGRAPHIC VISUALISATION OF INFLAMMATION IN NEURODEGENERATIVE DISORDERS

Jan Versijpt*¶ MD, Koen Van Laere¶ MD DrSc PhD, Rudi Andre Dierckx¶ MD PhD, Filip Dumont‡ Apr PhD, Peter Paul De Deyn& MD PhD, Guido Slegers‡ Apr MSc PhD, Jakob Korf* PhD

* Department of Biological Psychiatry, Groningen University Hospital, the Netherlands

¶ Division of Nuclear Medicine, Ghent University Hospital, Belgium

‡ Department of Radiopharmacy, Ghent University, Belgium

& Department of Neurology, General Hospital Middelheim, University of Antwerp and Born-Bunge Foundation, Antwerp, Belgium

Nucl Med Commun 2003;24:209-221

SUMMARY

In the past decades, our understanding of the central nervous system has evolved from one of an immune-privileged site, to one where inflammation is pathognomonic for some of the most prevalent and tragic neurodegenerative diseases. Current research indicates that diseases as diverse as multiple sclerosis, stroke and Alzheimer's disease exhibit inflammatory processes that contribute to cellular dysfunction or loss.

Inflammation, whether in the brain or periphery, is almost always a secondary response to a primary pathogen. In head trauma, for example, the blow to the head is the primary event. What typically concerns the neurologist and neurosurgeon more, however, is the secondary inflammatory response that will ensue and likely cause more neuron loss than the initial injury.

The current paper reviews the basic neuroinflammatory mechanisms, the potential neurotoxic mediators during activation of microglia, the brain resident macrophages, and their role in neurodegeneration. To explore these mechanisms, Alzheimer's disease, with the expression of more than 40 inflammatory mediators the most extensively studied disorder in terms of immune-related pathogenesis, is taken as a *prototype*, also because of its importance as the most prevalent dementia type . Visualisation tools for these neuroinflammatory processes, both structural and mainly functional, are critically reviewed and discussed.

NEUROINFLAMMATION AND NEUROIMMUNOMODULATION

Introduction

"In vivo, veritas!" [1]

Current research has shown that the previous concept of the brain as an *immunologically privileged organ* is unvalid. This notion was inferred from the lack of a lymphatic drainage system (now considered to be a lymph-like system [2]), its unusual tolerance to transplanted tissue, and the thought that lymphocytes were excluded from the central nervous system (CNS) by blood-brain and blood-cerebrospinal fluid barriers. As such, the immune and nervous system were considered different compartments acting autonomously in their contribution to physiological homeostasis [3].

One put a lymphocyte into a culture dish, added an antigen, and out came an antibody. So who needed a nervous system? However, already in 1891, Savchenko demonstrated that a CNS lesion could reverse a pigeon's nonsusceptibility to anthrax. Also, inflammatory episodes may be accompanied by behaviour or mood alterations, hypomotility and increased sleep, believed to assist the affected subject in fighting infections and prompting to confine to a safe shelter [1, 4]. Finally, a recent positron emission tomography (PET) study correlated immune measures and regional cerebral blood flow (rCBF). It was found that the natural killer cell activity correlated with rCBF in the secondary sensory cortex, whereas the proliferative lymphocyte response correlated with the rCBF in the secondary visual, motor, and sensory cortices, basal ganglia, and the left hippocampus, providing further support for the brain and immune system interaction [5].

Contemporary research learned that the blood-brain barrier (BBB) is, under certain conditions, less restrictive to the migration of monocytes, lymphocytes, or natural killer cells, irrespective of antigen specificity [6]. Moreover, in vitro ánd *in vivo* studies have clearly established that astrocytes and microglia (brain resident macrophages) can initiate an inflammatory cascade within the CNS [7]. Also, all components of the complement system are found in the brain and are produced by astrocytes, microglia, ànd, surprisingly, neurons.

However, several factors indicate that the CNS inflammation threshold is higher compared to the periphery, leading to a delay between peripheral and CNS inflammation during a general inflammatory status. For example, the rapid recruitment of neutrophils in the CNS is virtually absent, and monocytes are only recruited after a delay of several days. The reason for this higher threshold is at least threefold. Firstly, as only activated T-lymphocytes traverse the BBB, it is the small pool of peripherally activated T-cells that enter the CNS for immune surveillance [8]. Yet, without peripheral T-cell activation, antigens escape detection, thus, brain transplants survive, in spite of an antigen mismatch [9]. Secondly, there is an active suppression of antigen expression leading to T-lymphocytes not recognising their target neither activating inflammatory mechanisms [10]. Thirdly, the adhesion molecule expression, essential in cell-cell contacts during inflammatory cell migration, is low on cerebral endothelial cells [11]. Considered the above, it appears that the CNS, an organ exquisitely sensitive to inflammation, has evolved mechanisms to protect it from the potentially

damaging, even dramatic classical consequences of some acute inflammatory response aspects like redness, heat, swelling and pain, typically seen in the periphery.

Microglia

"Good, bad, or just ugly?" [12]

The concept of the presence of phagocytic brain cells was, although discovered by Nissl, studied in detail in the early part of the last century by Pio del Río-Hortega, a former student of the famous Spanish neuroanatomist Santiago Ramon y Cajal [13]. He identified a population of ramified cells, now considered to be resting microglia [14]. Although Jakob described their morphological changes into activated, macrophage-like cells in neurodegenerative disorders like neurosyphilis, rabies, Creutzfeldt-Jakob, senile dementia and Huntington disease already in 1927 [15], the origin and even the existence of this cell population was contested until recently. Few investigators followed up on these early pioneers during the next 50 years, largely because the staining method proved unreliable. This barrier came down only in the 1980's, after Perry at Oxford University began screening antibodies for their ability to bind microglia. It has only been during the last decade that major progress in microglial studies has been made, and their involvement in neurodegeneration has become apparent.

Microglia represent, next to astrocytes and oligodendroglia, 10-20% of the brain glial cell population (*glia* from Greek, meaning *glue*), located in close vicinity of grey matter neurons and between white matter fibre tracts. In contrast with the ramified shape along with a suppressed genomic activity in the *resting* state, on cellular activation, they assume an amoebic shape associated with a dynamic genome upregulation, characteristic of their phagocytic stage (Figure 1). They are the brain macrophages within the entire neuroaxis sharing the same lineage as monocytes, taking up residence in the CNS antenatally i.e. prior to the BBB completion. Cells of this lineage function as classical *professional* antigen presenting cells in the immune system in all mammals [16].

Figure 1. Morphology of ramified resting microglia with extended pseudopodia with transformation to the activated state with retraction of their branches (phagocytic cells or foamy macrophages, named *gitter cells* after Nissl in 1904 because of the fact they are typically *gitting* rid of dead myelin and other cell debris)

Microglia represent a highly reactive cell population and express antigens in response to microenvironmental stimuli, particularly neuronal damage. During the early neuronal injury stages, when affected brain tissue still appears histologically normal, microglia may carry out subtle microchanges such as the synapse removal from injured neurons. After non-lethal axotomy, for example, microglia interpose between pre- and postsynaptic moieties, cause synapse disconnection and strip the neuron of input (*synaptic stripping*). As such, they represent the primary immunocompetent cells dealing with invasions of any kind and removing cellular debris (i.e. scavenger cell, which may be important, combined with their ability to secrete growth factors, for tissue modelling in the developing CNS). All this, together with their ability to cooperate with immune cells, seems to make microglia function as true sentinels [17].

Conclusion

Immune cells, such as microglia, T-cells, or even neurons are able to produce potentially neurotoxic factors, some of them capable of destroying at picomolar concentrations. These factors, normally required for pathogen elimination, include cytokines, complement components, and reactive intermediates (superoxide anion, hydroxyl radicals, hydrogen peroxide, ...). These factors, however, not only destroy foreign pathogens but may damage local elements as well (*bystander lysis*), leading to neuronal loss [18]. Indeed, direct CNS injection of cytokines results in neurodegeneration, consistent with the potential role of cytokines in neurodegenerative diseases when microglia remain in an activated state and contrast with their potential neurotrophic actions under *transient exposure* or *housekeeping* conditions, where damaging actions are presumably *buffered* by cytoprotective mechanisms [19]. Also, microenvironmental compromises like age, genetic factors, and frank tissue insult will dramatically affect the neuron susceptibility as well as the *buffering capacity* degree for removing neurotoxic mediators. Moreover, there is little or no mitogenesis to repair potential damage. Concerning this postmitotic state, animal experiments already illustrated the neuronal vulnerability during inflammation, in particular of synaptic plasticity, memory, and neurotransmission [20]. Finally, in contrast to peripheral tissues, focal CNS injury not only has local effects, but also causes neuronal and axonal loss at a distance due to retrograde degeneration and Wallerian degeneration.

INFLAMMATION AND MICROGLIA IN CHRONIC NEURODEGENERATION, WITH THE EMPHASIS ON ALZHEIMER'S DISEASE

LINKING BRAIN IMMUNITY TO NEURODEGENERATION

"Good, bad, or irrelevant" [21]

As described above, CNS immune responses usually take milder courses, where it has not been clear yet whether this relative deficit is solely explicable by the lack of immunological structures, or due to counterregulatory mechanisms. Recent evidence indicates that CNS immune responses are indeed downregulated, with a key role for electrically active neurons. For instance, a blockade of neuronal activity in hippocampal cultures significantly increased the antigen expression on microglia [22].

Normally, CNS immune surveillance is effected by patrolling T-cells, freshly activated peripherally with an ensuing release of pro-inflammatory cytokines inducing glial cells to produce immunologically relevant molecules. Intriguingly, pro-inflammatory signals very similar to those provided by T-cells are also produced by degenerating brain cells. This pro-inflammatory milieu of neurodegeneration can be due to active induction signals communicated by degenerating neurons or cellular by-products of neurodegeneration (DNA, neurofilaments, and myelin fragments) [23], or, alternatively, it could reflect an escape from the anti-inflammatory control mentioned above [24].

Neurodegenerative diseases with immune system involvement are listed in Table I.

CLINICAL CONDITION	**FINDINGS** (REFERENCES)
Diffuse Lewy Body disease	Microglia [25]
Progressive supranuclear palsy	Complement activation [26] Glial activation [27]
Corticobasal degeneration	Glial activation [27]
Parkinson's disease	Microglia [28] Complement activation [26] TNF-α [29]
Pick's dementia	(Micro)glial activation [27] Complement activation [30]
Huntington's disease	Microglia [31]
Creutzfeldt-Jakob disease	Microglia [32]
Multi system atrophy	Microglia [33]

Table 1. Neurodegenerative diseases (next to AD) associated with increased numbers of activated (micro)glia, increased CNS cytokines or complement activation

INFLAMMATION AS A CAUSE OF DAMAGE TO THE ALZHEIMER'S DISEASE BRAIN

Introduction

Alzheimer's disease (AD) is the most common form of dementia and the number of affected persons is expected to triple over the next 50 years. It is characterised by intraneuronal neurofibrillary tangles

(NFT), neuronal and synaptic loss, neurotransmitter deficits and amyloidosis. The latter results from the aggregation of β-amyloid peptides (i.e. Aβ, derived from the abnormal cleavage of amyloid precursor protein or β-APP), giving rise to amyloid or neuritic plaques [34].

Interestingly, when Alois Alzheimer in 1907 described its features, he also noticed a close association between brain phagocytes and amyloid plaques [35]. Nowadays, the pathophysiological relevance of inflammation to AD has been established by multiple lines of converging tangential and direct evidence. For example, transgenic animals (over)expressing inflammatory proteins exhibit neuropathological changes similar to AD,[36] whereas human beings without dementia but sufficient Aβ/NFT to qualify for AD show only modest elevations of inflammatory markers [37].

The following sections briefly review the inflammatory mechanisms in AD.

Genetic risk factors and epidemiological data

AD shows an Apolipoprotein E (ApoE) genotype susceptibility with ApoE4 as a risk factor. Interestingly, ApoE4 seems essential for APP-induced microglial activation and the expression of several inflammatory indicators [38]. Also, several genetic cytokine risk factors have already been identified with a decreased cytokine activity associated with a reduced risk and delayed onset [39].

There are now about 20 reports which studied the AD incidence in populations with a long anti-inflammatory drug consumption history. Nearly all of these studies showed a lower AD incidence with a decrease of 50% or a delay in onset of 5 to 7 years, where, in one prospective study, the relative risk fell with increasing duration of drug use [40]. Clinical trials with indomethacin or propentofylline, another agent with anti-inflammatory properties, showed both a significant cognitive improvement [41, 42], while, however, one study with diclofenac and one recent study with hydroxychloroquine did not demonstrate a positive effect on AD progression [43, 44].

Immunopathological, in vitro, and in vivo data

A summary of these mechanisms is shown in Figure 2.

BACKGROUND

Just as foreign materials and damaged tissue are classical stimulants of peripheral, sometimes overtly cytotoxic, inflammation, so are also Aβ and the ensuing neurodegeneration the most likely sources for inflammation in AD. From this point, a nearly bewildering number of inflammatory mediators comes in to play, each characterized by an abundance of amplifying and dampening loops, as well as multiple interactions with other subsystems. Like a web, all these inflammatory pathways make it likely for one set of mediators to induce most of the others. For this reason, the selection of any particular starting point for explaining the AD inflammatory mechanism must be taken as a matter of convenience [45].

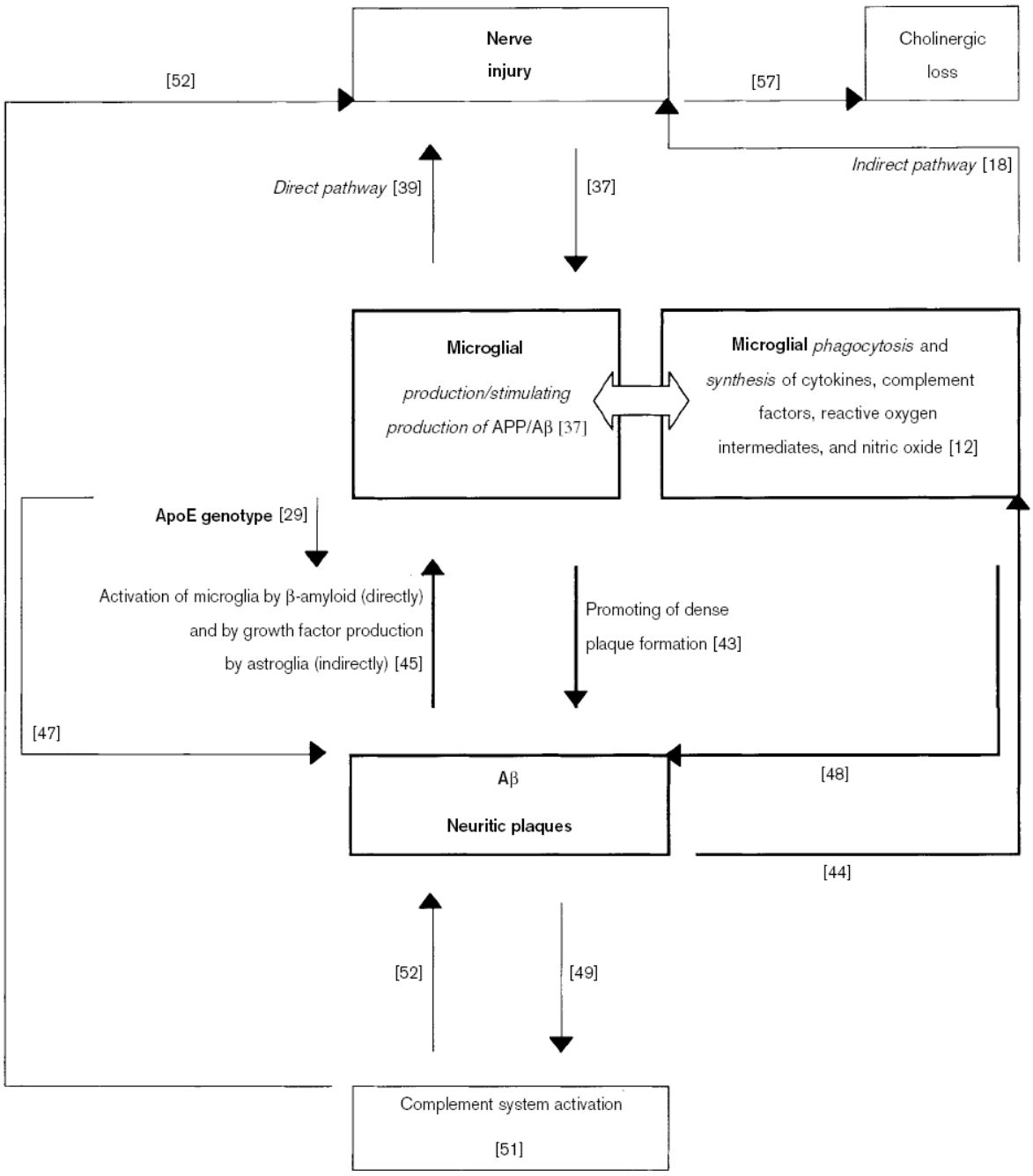

Figure 2. Inflammatory hypothesis in Alzheimer's disease emphasising the main loops with the interaction between microglia and the amyloid plaques and neurofibrillary tangles

SOURCES, TOXICITY, AND REMOVAL OF Aβ

The cellular source of Aβ is still a matter of debate. Microglia are able to synthesise Aβ in response to nerve injury or even Aβ itself [46]. As for toxicity, although it has been hypothesised that the presence of amyloid is the direct cause of AD pathology, the *in vivo* confirmation of Aβ toxicity has not yet been conclusively demonstrated, while there is even evidence that Aβ may be neuroprotective [47]. Moreover, in one study, a fulminant hippocampal neuron loss by neuritic plaques was only seen in the presence of microglia [48].

As for Aβ phagocytosis, the degradation rate seems limited and results in the release of potentially neurodestructive compounds [49]. However, that microglia càn remove amyloid was strongly suggested by the demonstration of Aβ co-localised with microglia in *Aβ-immunised* transgenic mice, where amyloid was apparently cleared, where this removal also protected against a further cognitive decline [50]. Interestingly, C1q, a complement protein which binds Aβ, apparently inhibits the microglial Aβ uptake [51].

PLAQUE FORMATION AND MICROGLIAL INTERACTION THROUGH CYTOKINES AND COMPLEMENT SYSTEM

The fact that activated microglia are the sole and consistent accompaniment of neuritic plaques and not readily found in association with non-neuritic plaques suggests their pivotal role in the promotion of neuritic plaque formation, a role similar to that ascribed to peripheral macrophages in systemic amyloidosis [52].

Aβ may also act in a feedforward mechanism to maintain microglial activation, directly and indirectly by stimulating cytokine production, hereby increasing the amount of APP and rendering neurons subject to deleterious effects of activated microglia [53, 54].

Some cytokines cause neuronal injury ànd microglial activation with a further overexpression of the same cytokines, producing feedback amplification and self-propagation (*cytokine cycle*) [55]. Also, some cytokines who are on their own not neurotoxic are able to enhance the Aβ-induced cell death [56]. Finally, because APP/Aβ expression is regulated by the same transcriptional factors that are involved in the expression of most acute phase proteins, Aβ not only induces microglial cytokine release, but, once released, these same cytokines increase the Aβ aggregation process. The resulting vicious cycle could explain the chronicity of the disease [55, 57].

Recent studies suggested that Aβ and NFT bind C1q and activate the complement system in an antibody-independent fashion [58]. Also, both C5a and Aβ synergistically augment the release of proinflammatory cytokines. Moreover, the very modest upregulation of C1-inhibitor mRNA and the decrease of CD59 expression, both regulatory molecules protecting the cell from bystander while permitting foreign cell lysis, compared to the high upregulation for the other complement components, could lead to ongoing activation at the C1 level [59]. One study even indicated that complement production in the AD brain may be as great as in the liver, the primary source of complement [60]. This complement activation, of which direct evidence of its toxicity in the AD brain was recently observed, is also able to promote both Aβ aggregation ánd enhance the neurotoxicity of Aβ in neuronal cultures [61].

REGIONAL CELL LOSS AND COGNITIVE IMPAIRMENT

Cytokines affect acetylcholine, glutamate, and nitric oxide, all playing a key role in cognition [62]. Indeed, basal forebrain mixed neuronal/microglial cultures revealed cholinergic neuron losses, demonstrating their selective susceptibility to the toxic actions of activated microglia. More recently,

microglial secreted IL-1 was reported to induce the expression of the acetylcholinesterase protein ánd to increase its enzymatic activity [63]. Also, a disrupted memory-based performance in the water maze was shown after a sub-lethal bacterial injection while mice administered concurrently with IL-1 antibodies had normal learning rates [64]. Finally, IL-2 within the physiological range was capable of suppressing the hippocampal acetylcholine release, an effect related to the cognitive side effects during IL-2 immunotherapy in e.g. cancer patients [65]. Presumably, these data partly explain the cholinergic dysfunction in AD by demonstrating their susceptibility to toxic actions of activated microglia and suggest a basis for the regional loss of only selected neuronal populations in AD [66].

Remarks on the inflammatory hypothesis of AD

It should be stressed that the theory of inflammation as a primary disease-aggravating hallmark, opposed to a secondary or even a disease-ameliorating factor, remains a hypothesis and one should be aware that our current knowledge of microglia is still incomplete, speculative, and mainly based upon *in vitro* observations rather than *in vivo* studies [67]. Indeed, B- or T-cells and immunoglobulins are not readily detectable in the AD brain and are only in very small amounts found in relation to amyloid plaques (without IgM/IgA) [68]. Likewise, although leukocytes hàve been demonstrated, their role in AD has not been established [69]. As such, the evidence for an antigen-driven *acquired* immune response in AD, with T-cells eliminating amyloid and B-cells producing Aβ-specific antibodies, is not that overt as e.g. in multiple sclerosis (MS), although some authors see this *acquired immune response* inability as the support for the chronic overreaction of the *innate immune system* (phagocytic cells) [70].

NEUROINFLAMMATORY IMAGING

INTRODUCTION

Visualising neuroinflammation would be of interest, firstly for clarifying the pathophysiology, secondly for selecting patient subgroups that are more eligible for anti-inflammatory treatment and finally, for monitoring patients during trials with these anti-inflammatory agents. In the following section the currently available neuroinflammatory imaging modalities, both structural and mainly functional, will be reviewed and discussed.

STRUCTURAL IMAGING

As its name implies, the capability of structural imaging lies in visualising its (non-specific) structural changes and describing the detailed spatial relationship of inflammatory consequences like mass effects, oedema, vascular congestion, thrombosis, petechial haemorrhages, secondary demyelinisation, gliosis, and finally neuronal destruction, necrosis, or atrophy. As such, computed tomography (CT) and to a greater extent (Gadolinium-enhanced) magnetic resonance imaging (MRI), with its excellent soft tissue contrast resolution (mainly for evaluation of white matter and posterior fossa) are able to detect CNS inflammatory changes caused by mostly localised processes like cerebral abscess, encephalitis, granulomatous disease (tuberculosis, sarcoidosis, ...), meningitis, empyema, AIDS, chronic inflammatory demyelinating polyneuropathy, and MS [71]. For example, Brück *et al.* found that demyelinating lesions in MS, presenting as isointense lesions with a massive gadolinium-DTPA enhancement on T1-weighted scans, correlated neuropathologically with activated macrophages in the zone of myelin destruction at the plaque border [72].

However, in general, inflammation must be already at an advanced stage before it can be depicted by one of these imaging modalities, giving rise to its poor sensitivity at the early stages of inflammation (when anatomical changes are not detectable yet). Also, for chronic processes, structural changes may be detectable that do not reflect the actual state of disease activity. Indeed, Ketonen *et al.* noted already that in early AIDS dementia encephalitis, post-mortem characterised by scattered microglial nodules and HIV-infected multinucleated giant cells located primarily in the white matter and correlating with the severity of dementia, both CT and MRI are insensitive enough to detect these microglial nodules and for this reason, the neuroimaging appearance early in the disease is usually normal [73]. Similarly, Kim et al noted that, although CT and MRI are able to detect general or basal ganglia atrophy and white matter lesions that appear to increase in severity with the progression of the HIV infection, these techniques are relatively insensitive to the presence of clinical dementia, neurological signs, or positive findings on neuropsychological tests. In addition, they show poor correlation with histopathological findings [74].

METABOLIC IMAGING

As for the newer structural or *metabolic* imaging tools in brain inflammation, Cecil *et al.* reviewed proton MR spectroscopy as a sensitive and specific imaging tool in Creutzfeldt-Jakob, herpes simplex encephalitis, and AIDS, indicating its applicability for longitudinal studies to predict and monitor the

response to therapy, leading to an individual optimised treatment [75]. Likewise, Bitsch *et al.* found that the measured increases of choline and myo-inositol corresponded to the histopathologically verified glial proliferation and the infiltration of subcortical grey matter structures with foamy macrophages [76]. Recently, Rovaris *et al.* reported about the value of magnetisation transfer imaging (MTI) in measuring brain involvement in systemic immune mediated diseases. It was found that MTI provides information about brain damage with increased pathological specificity and detects subtle microscopic abnormalities in the normal brain tissue, which go undetected with conventional scanning. However, in some immune mediated diseases microscopic brain tissue damage seemed to be absent despite macroscopic MRI lesions or clinical evidence of CNS involvement [77].

FUNCTIONAL RADIONUCLIDE IMAGING

Background

Nuclear medicine provides several techniques for the detection of inflammation. Studies demonstrating inflammatory lesions started as early as in 1959, when Athens *et al.* labelled leukocytes by intravenous injection of diisopropylfluoro-phospate labelled with ^{32}P with which they demonstrated skin blisters in volunteers [78]. Classically, scintigraphic imaging of inflammation has been done with ^{67}Gallium-citrate, radiolabelled leukocytes, nanocolloids, non-specific human immunoglobulins (HIG), and ^{18}F-deoxyglucose (FDG). Their uptake mechanism ranges from direct binding to relevant inflammatory cells or proteins (radiolabelled leukocytes, ^{67}Gallium-citrate, HIG) over hyperaemia, binding to lactoferrin excreted *in loco* by leukocytes or to siderophores produced by micro-organisms (^{67}Gallium-citrate), non-specific locally increased blood supply, extravasation through vessels with increased vascular permeability giving rise to an expanded local interstitial fluid space (^{67}Gallium-citrate, nanocolloid, HIG), to high glucose uptake in inflammatory cells (FDG) [79]. As such, studies with radiolabelled leukocytes in cerebral ischemia have been undertaken where several authors reported on the higher accumulation in massive infarcts with severe neurological impairments and little improvement [80]. As far as chronic mononuclear cell infiltrates are concerned, however, most radiopharmaceuticals show inadequate diagnostic accuracy [81]. This is due to the minor haemodynamic and permeability changes (little or no vasodilatation), the slow cellular turnover and the predominant mononuclear cell infiltrate of chronic processes.

In the last decade, attempts have also been made to visualise inflammation by means of Cobalt radioisotopes. Indeed, both *in vivo* and *in vitro* experiments have shown that Ca^{2+} accumulates in the (ir)reversibly damaged nerve cell body and degenerating axons [82, 83]. Cobalt radioisotopes, as Ca^{2+}-analogues, probably reflect Ca^{2+}-influx in ischaemically or neurotoxically damaged cerebral tissue. Moreover, the time sequence of the radioligand uptake seems to correlate with cell death and glial proliferation in the ipsilateral thalamus following supratentorial ischaemic stroke in an experimental rat stroke model [84]. In this way, both ^{57}Co (for single photon emission tomography or SPET) and ^{55}Co (for PET) were able to visualise some of the focal neurodegenerative changes, reactive gliosis, endangered brain tissue and/or ongoing neuronal tissue decay including inflammatory lesions in various brain diseases e.g. multiple sclerosis, trauma, tumours, and stroke [80, 85, 86]. A

recent study however, concluded that ^{57}Co SPET was not able to show any regional raised uptake in AD patients, irrespective of the depth or extent of the associate perfusion defects, the presence of atrophy on MRI, or the neuropsychological test results [87]. Moreover, the long physical half-life with its resulting low count rate and statistics and the incomplete knowledge about the specific cellular uptake mechanisms all limit the application of Cobalt radioisotopes.

Radiolabelled receptor-specific proteins and peptides

Over the last decade, there has been a shift in scintigraphic inflammatory imaging from large proteins with non-specific uptake mechanisms via receptor-specific large proteins to receptor-specific small proteins and peptides (i.e. mediators of the inflammatory response), allowing the non-invasive detection of specific cells and tissues [88]. Monoclonal antibodies (against leukocyte antigens or endothelial adhesion molecules) were the first example of this new class of radiopharmaceuticals and in the past few years several new radiolabelled receptor ligands have been developed. As such, radiolabelled monoclonal antibodies against granulocyte and lymphocyte antigens, adhesion molecules, cytokines, chemokines, chemotactic peptides, and macrophages were developed [81]. For example, Paul *et al.* recently reported the detection and quantitation of neuroinflammation through BBB permeability changes during experimental allergic encephalomyelitis using a radiolabelled tuftsin analogue [89]. Tuftsin is a tetrapeptide derived from the Fc portion of IgG that promotes chemotaxis and phagocytosis of neutrophils, monocytes, and macrophages by binding to receptors on these cells. In addition, the radiopharmaceutical was able to successfully monitor glucocorticoid suppression of inflammation, recording a typical dose-response to increasing steroid concentrations.

All of these mediators came available for application in several fields by synthesis or recombinant DNA techniques. In nuclear medicine, they have emerged as a promising class of agents with attractive characteristics for scintigraphic detection of inflammation. Theoretically, the high binding affinity for their receptors – expressed in inflammatory tissue – facilitates retention of these agents in inflammation while the small size permits rapid clearance from blood and other non-target tissues. Whether this small radiolabelled receptor-binding agent specifically localises in an inflammatory focus depends firstly on the receptor expression in the particular inflammatory response. Secondly, the receptors should be accessible for the ligand and thirdly, the interaction of the ligand and its receptor should be characterized by high affinity and specificity (shown by autoradiography, receptor blockade, or studies with control agents). For neuroimaging studies in pathologies without BBB breakdown, the ligand should also easily penetrate the BBB.

Toxicity is still the major drawback of using receptor-specific small proteins and peptides for scintigraphic imaging. The tested agents are mediators of the inflammatory response and most of them elicit a specific response after binding to the receptor, i.e. express biological agonistic activity, which is undesirable for scintigraphic imaging. The use of receptor antagonists is therefore a logical choice, however, antagonists behave differently from agonists. Alternatives are the development of

partial antagonists with significantly reduced biological activity, obtained by synthesis or modification of the agonists, or the development of high specific activity labelling of agonists [90].

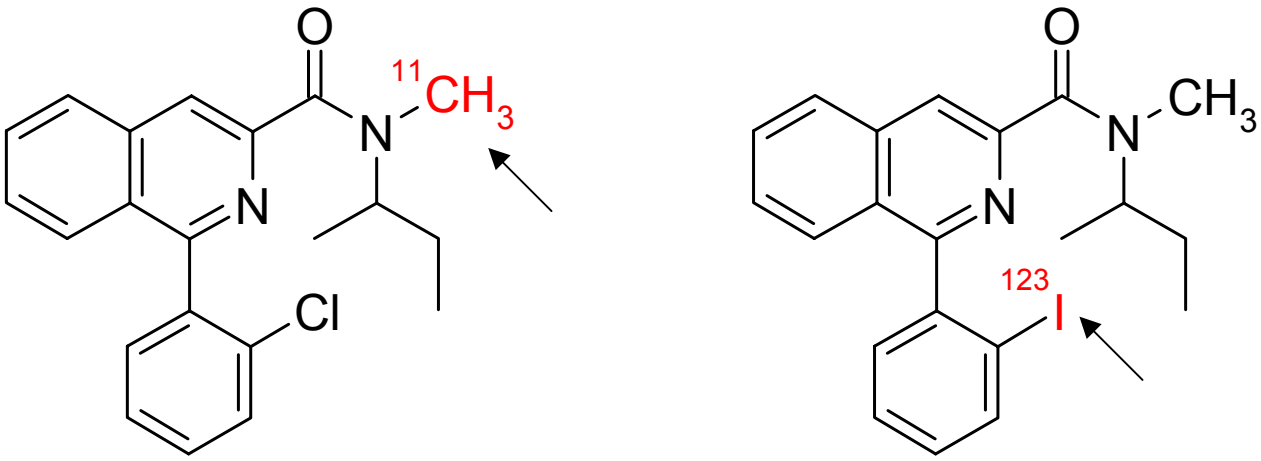

Figure 3. Chemical structure of PK11195 (the arrows indicate the site for radiolabelling with I^{123} (SPET, right) or C^{11} (PET, left))

Imaging of Microglia

The scintigraphic visualisation of microglia can be performed with radiolabelled PK11195, a ligand that binds the peripheral benzodiazepine receptor (PBR), present on microglia and upregulated under inflammatory circumstances. The PBR is structurally and pharmacologically distinct from the central benzodiazepine receptor (associated with GABA-regulated chloride-channels), and earned his name based on its localisation outside the CNS and its high affinity for several 1,4-benzodiazepines. The PBR is found in highest concentrations in kidneys, colon membranes, heart, steroid hormone producing cells of adrenal cortex, ovaries and testes, and several cell types of the immune system, such as mast cells and macrophages. It is also present in low concentrations throughout the brain, primarily associated with the choroid plexus, ependymal linings, and glial cells [91].

Although the specific function of the PBR remains unknown, it is generally accepted to be involved in lipid metabolism and/or transport, heme biosynthesis, cell proliferation, or ion channel functions [91]. Its immunomodulatory role includes the ability to induce monocyte chemotaxis, modulate cytokine expression and superoxide generation, and stimulate antibody-producing cell formation [92]. Interestingly, the PBR has the ability to reflect neuronal injury and neurotoxicity, by a rise in the number of binding sites in the case of activated microglia [93, 94].

PK11195 (1-(2-chlorophenyl)-N-(1-methyl-propyl)-3-isoquinoline carboxamide) is a specific and selective high affinity ligand for the PBR and, in this way, can be used as a marker for neuroinflammatory lesions (Figure 3). It has neither anxiolytic nor spasmolytic activity, nor interactions with other receptors and has been classified as an antagonist or partial agonist [95]. As such, Banati

et al. showed an increased PK11195 binding to activated microglia after facial nerve axotomy - a lesion causing a retrograde neuronal reaction without nerve cell death with a rapid proliferation and activation of microglia while keeping the BBB intact - where the peak of PK11195 binding was observed 4 days after the peripheral nerve lesion, which is consistent with the well-known time course of microglial activation. Moreover, photoemulsion microautoradiography confirmed the restriction of PK11195 binding to activated (i.e. PBR-expressing) microglia, where the full transformation of microglia into parenchymal phagocytes is not necessary to reach maximal levels of PK11195 binding. It was concluded that PK11195 is a well-suited marker of microglial activation in areas of subtle brain pathology, without BBB disturbance, or the presence of macrophages [96].

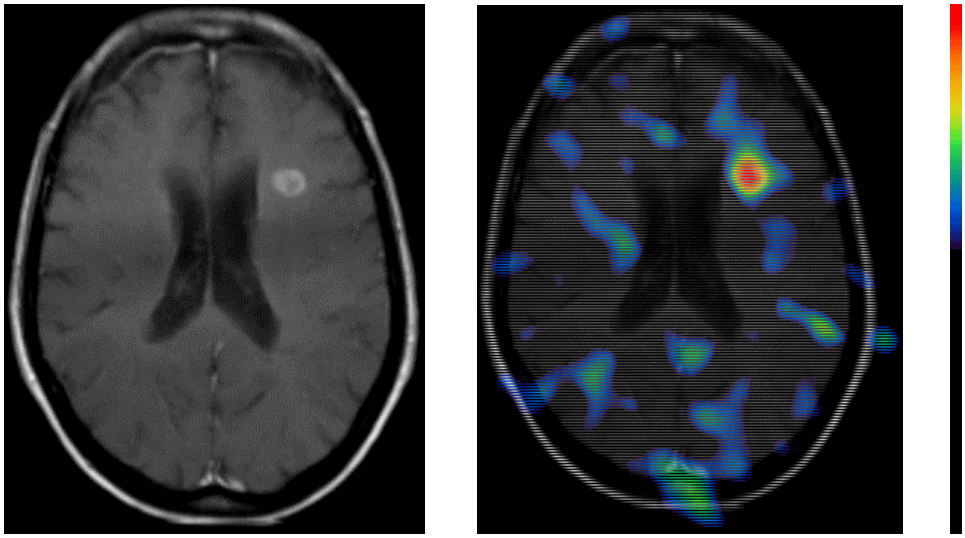

Figure 4. Transaxial slice of an MRI of an MS patient showing gadolinium-enhancement on a T1-weighted scan (left) and overlaid MRI-^{11}C PK11195 PET image showing the focus of radioligand uptake at the same site (right)

In vivo visualisation of the human PBR, and in this way of neuronal damage, cellular inflammatory infiltration, or microgliosis, has previously been done with ^{11}C radiolabelled PK11195 for PET in various diseases like glial neoplasms, ischemic stroke, MS, Rasmussen's encephalitis, AD and Parkinson's disease, producing a signal of activated microglia unrelated to the influx of blood-borne macrophages (Figure 4) [97-100]. Also, significant ^{11}C-PK11195 binding was detected in MS patients in areas where MRI did not show any abnormalities, e.g. PK11195-related signals localised to deafferented grey matter regions such as the lateral geniculate body (to which the optic nerve projects) and visual cortex in patients with previous optic neuritis. In patients with transient speech dyspraxia, regionally increased PK11195 binding was found in the left frontal operculum close to Broca's area, which contains the superior longitudinal fascicle [101]. Finally, ^{11}C-PK11195 has also been applied in early and mild dementia patients revealing an increased regional binding in the entorhinal, temporoparietal, and cingulate cortex. Moreover, serial volumetric MRI scans revealed that areas with high ^{11}C-PK11195 binding subsequently showed the highest rate of atrophy up to 12-24 months later indicating that the presence of a local immune response in cortical areas did indeed reflect an active disease process associated with tissue loss. Also, measurement of cerebral glucose

metabolism revealed that areas with high ^{11}C-PK11195 binding were also characterised by decreased regional glucose use. Finally, in one patient with isolated memory impairment without dementia, the pattern of atrophy as seen by volumetric MRI imaging was predicted by the initial distribution of increased ^{11}C-PK11195 binding [102].

Recently, the biodistribution and dosimetry of PK11195 radiolabelled with Iodine for SPET has been studied. It was concluded that ^{123}I labelled iodo-PK 11195 is a suitable agent for the visualisation of the PBR and indirectly for the imaging of neuroinflammatory lesions [103]. In a recent pilot study, [^{123}I]iodo-PK 11195 was also applied in AD which showed a distinct difference in ligand uptake between AD patients and controls, indicating the pathophysiological involvement of microglia, in frontal, temporal and parietal cortical regions, pathognomonically compromised in AD [103]. Moreover, inverse correlations were found between regional [^{123}I]iodo-PK11195 uptake values and cognitive test results. In this way, the radioligand PK11195, developed both for SPET and PET, can be considered as a highly sensitive cellular marker for the functional monitoring of microglia *in vivo*, useful for the visualisation of chronic neurodegeneration without BBB breakdown nor other imaging findings.

CONCLUSION

In this review, the current status of inflammation with respect to neurodegeneration has been highlighted. From the basic neuroinflammatory mechanisms and its biochemical characteristics, the role of its potential mediators playing a key role in neurodegenerative disorders has been explored, with Alzheimer's disease as a prototype. Currently, the overwhelming amount of *in vitro* data has to be translated to *in vivo* human data. Whereas structural imaging shows merely late anatomical consequences of an inflammatory response, functional imaging is a strong potential candidate to bridge this gap between *in vitro* and *in vivo* knowledge. A number of radioligands have been recently explored which allow the early *in vivo* visualisation of inflammatory responses, and, as such, open a promising window on both *understanding* as well as possible *clinical management* of inflammatory neurodegenerative disorders.

REFERENCES

1. Spector NH. Neuroimmunomodulation: a brief review. *Regul Toxicol Pharmacol* 1996; **24**: S32-S38.
2. Cserr HF, Knopf PM. Cervical lymphatics, the blood-brain barrier and the immunoreactivity of the brain: a new view. *Immunol Today* 1992; **13**: 507-512.
3. Barker CF, Billingham RE. Immunologically privileged sites. *Adv Immunol* 1977; **25**: 1-54.
4. Straub RH, Mannel DN. How the immune system puts the brain to sleep [news; comment]. *Nat Med* 1999; **5**: 877-879.
5. Wik G, Lekander M, Fredrikson M. Human brain-immune relationships: a PET study. *Brain Behav Immun* 1998; **12**: 242-246.
6. Mucke L, Eddleston M. Astrocytes in infectious and immune-mediated diseases of the central nervous system. *FASEB J* 1993; **7**: 1226-1232.
7. Owens T, Renno T, Taupin V, Krakowski M. Inflammatory cytokines in the brain: Does the CNS shape immune responses? *Immunol Today* 1994; **15**: 566-570.
8. Hickey WF, Hsu BL, Kimura H. T-lymphocyte entry into the central nervous system. *J Neurosci Res* 1991; **28**: 254-260.
9. Head JR, Griffin WS. Functional capacity of solid tissue transplants in the brain: evidence for immunological privilege. *Proc R Soc Lond B Biol Sci* 1985; **224**: 375-387.
10. Hart MN, Fabry Z. CNS antigen presentation. *Trends Neurosci* 1995; **18**: 475-481.
11. Lassmann H, Rossler K, Zimprich F, Vass K. Expression of adhesion molecules and histocompatibility antigens at the blood-brain barrier. *Brain Pathol* 1991; **1**: 115-123.
12. Rogers J, Shen Y. Markers of inflammation and their role in Alzheimer's pathophysiology. Neurobiol Aging 1998; **19**: S224.
13. Nissl F. Über einige Beziehungen zwischen Nervenzellerkrankungen und gliösen Erscheinungen bei verschiedenen Psychosen. *Arch Psychiatr* 1899; **32**: 656-676.
14. del Río-Hortega P. El "tercer elemento" de centros nervisos: poder fagocitario y movilidad de la microglia. *Biol Soc Exp Bio Ano* 1919; **9**: 154-166.
15. Jakob A. Normale und pathologische Anatomie und Histologie des Grosshirns. In: Aschaffenburg G, ed. Handbuch der Psychiatrie algemeiner Teil. Wien: Deuticke, 1927: 1.
16. Barron KD. The microglial cell. A historical review. *J Neurol Sci* 1995; **134**: 57-68.
17. Kreutzberg GW. Microglia: a sensor for pathological events in the CNS. *Trends Neurosci* 1996; **19**: 312-318.
18. Banati RB, Gehrmann J, Schubert P, Kreutzberg GW. Cytotoxicity of microglia. *Glia* 1993; **7** : 111-118.
19. Rothwell NJ, Strijbos PJLM. Cytokines in neurodegeneration and repair. *Int J Dev Neurosci* 1995; **13**: 179-185.
20. Patterson PH. Cytokines in Alzheimer's disease and multiple sclerosis. *Curr Opin Neurobiol* 1995; **5**: 642-646.
21. Honig LS. Inflammation in neurodegenerative disease: good, bad, or irrelevant? *Arch Neurol* 2000; **57**: 786-788.
22. Neumann H, Wekerle H. Neuronal control of the immune response in the central nervous system: linking brain immunity to neurodegeneration. *J Neuropathol Exp Neurol* 1998; **57**: 1-9.
23. Tchelingerian JL, Quinonero J, Booss J, Jacque C. Localization of TNF and IL-1 immunoreactivities in striatal neurons after surgical injury to the hippocampus. *Neuron* 1993; **10**: 213-224.
24. Becher B, Prat A, Antel JP. Brain-immune connection: immuno-regulatory properties of CNS-resident cells. *Glia* 2000; **29**: 293-304.
25. MacKenzie IR. Activated microglia in dementia with Lewy bodies. *Neurology* 2000; **55**: 132-134.

26. Yamada T, Akiyama H, McGeer PL. Complement-activated oligodendroglia: a new pathogenetic entity identified by immunostaining with antibodies to human complement proteins C3d and C4d. *Neurosci Lett* 1990; **112**: 161-166.
27. Komori T. Tau-positive glial inclusions in progressive supranuclear palsy, corticobasal degeneration and Pick's disease. *Brain Pathol* 1999; **9**: 663-679.
28. Hunot S, Boissiere F, Faucheux B, Brugg B, Mouatt-Prigent A, Agid Y, et al. Nitric oxide synthase and neuronal vulnerability in Parkinson's disease. *Neuroscience* 1996; **72**: 355-363.
29. Mogi M, Harada M, Riederer P, Narabayashi H, Fujita K, Nagatsu T. Tumor necrosis factor-alpha (TNF-a) increases both in the brain and in the cerebrospinal fluid from parkinsonian patients. *Neurosci Lett* 1994; **165**: 208-210.
30. Singhrao SK, Neal JW, Gasque P, Morgan BP, Newman GR. Role of complement in the aetiology of Pick's disease? *J Neuropathol Exp Neurol* 1996; **55**: 578-593.
31. McGeer PL, Itagaki S, McGeer EG. Expression of the histocompatibility glycoprotein HLA-DR in neurological disease. *Acta Neuropathol* 1988; **76**: 550-557.
32. Brown DR, Schmidt B, Kretzschmar HA. Role of microglia and host prion protein in neurotoxicity of a prion protein fragment. *Nature* 1996; **380**: 345-347.
33. Arai N, Nishimura M, Oda M, Morimatsu Y, Ohe R, Nagatomo H. Immunohistochemical expression of microtubule-associated protein 5 (MAP5) in glial cells in multiple system atrophy. *J Neurol Sci* 1992; **109**: 102-106.
34. Fowler CJ, Cowburn RF, Joseph JA. Alzheimer's, ageing and amyloid: an absurd allegory? *Gerontology* 1997; **43**: 132-142.
35. Alzheimer A. Über eine eigenartige Erkrankung der Hirnrinde. *Zeit Psychiatrie Psy Gerichtlich Med* 1907; **64**: 146-148.
36. Wyss-Coray T, Masliah E, Mallory M, McConlogue L, Johnson-Wood K, Lin C, et al. Amyloidogenic role of cytokine TGF-b1 in transgenic mice and in Alzheimer's disease. *Nature* 1997; **389**: 603-606.
37. Lue LF, Brachova L, Civin WH, Rogers J. Inflammation, Ab deposition, and neurofibrillary tangle formation as correlates of Alzheimer's disease neurodegeneration. *J Neuropathol Exp Neurol* 1996; **55**: 1083-1088.
38. Egensperger R, Kosel S, von Eitzen U, Graeber MB. Microglial activation in Alzheimer disease: Association with APOE genotype. *Brain Pathol* 1998; **8**: 439-447.
39. McGeer PL, McGeer EG. Polymorphisms in inflammatory genes and the risk of Alzheimer disease. *Arch Neurol* 2001; **58**: 1790-1792.
40. in 't Veld BA, Ruitenberg A, Hofman A, Launer LJ, van Duijn CM, Stijnen T, et al. Nonsteroidal antiinflammatory drugs and the risk of Alzheimer's disease. *N Engl J Med* 2001; **345**: 1515-1521.
41. Rogers J, Kirby LC, Hempelman SR, Berry DL, McGeer PL, Kaszniak AW, et al. Clinical trial of indomethacin in Alzheimer's disease. *Neurology* 1993; **43**: 1609-1611.
42. Rother M, Erkinjuntti T, Roessner M, Kittner B, Marcusson J, Karlsson I. Propentofylline in the treatment of Alzheimer's disease and vascular dementia: a review of phase III trials. *Dement Geriatr Cogn Disord* 1998; **9S1**: 36-43.
43. Scharf S, Mander A, Ugoni A, Vajda F, Christophidis N. A double-blind, placebo-controlled trial of diclofenac/misoprostol in Alzheimer's disease. *Neurology* 1999; **53**: 197-201.
44. van Gool WA, Weinstein HC, Scheltens PK, Walstra GJ. Effect of hydroxychloroquine on progression of dementia in early Alzheimer's disease: an 18-month randomised, double-blind, placebo- controlled study. *Lancet* 2001; **358**: 455-460.
45. Akiyama H, Barger S, Barnum S, Bradt B, Bauer J, Cole GM, et al. Inflammation and Alzheimer's disease. *Neurobiol Aging* 2000; **21**: 383-421.

46. Bitting L, Naidu A, Cordell B, Murphy GMJr. b-amyloid peptide secretion by a microglial cell line is induced by b-amyloid-(25-35) and lipopolysaccharide. *J Biol Chem* 1996; **271**: 16084-16089.
47. Mattson MP, Cheng B, Culwell AR, Esch FS, Lieberburg I, Rydel RE. Evidence for excitoprotective and intraneuronal calcium-regulating roles for secreted forms of the b-amyloid precursor protein. *Neuron* 1993; **10**: 243-254.
48. Giulian D, Haverkamp LJ, Yu JH, Karshin W, Tom D, Li J, et al. Specific domains of b-amyloid from Alzheimer plaque elicit neuron killing in human microglia. *J Neurosci* 1996; **16**: 6021-6037.
49. Paresce DM, Chung H, Maxfield FR. Slow degradation of aggregates of the Alzheimer's disease amyloid b-protein by microglial cells. *J Biol Chem* 1997; **272**: 29390-29397.
50. Ingram DK. Vaccine development for Alzheimer's disease: a shot of good news. *Trends Neurosci* 2001; **24**: 305-307.
51. Webster SD, Yang AJ, Margol L, Garzon-Rodriguez W, Glabe CG, Tenner AJ. Complement component C1q modulates the phagocytosis of Ab by microglia. *Exp Neurol* 2000; **161**: 127-138.
52. Mackenzie IRA, Hao CH, Munoz DG. Role of microglia in senile plaque formation. *Neurobiol Aging* 1995; **16**: 797-804.
53. Weldon DT, Rogers SD, Ghilardi JR, Finke MP, Cleary JP, O'Hare E, et al. Fibrillar b-amyloid induces microglial phagocytosis, expression of inducible nitric oxide synthase, and loss of a select population of neurons in the rat CNS in vivo. *J Neurosci* 1998; **18**: 2161-2173.
54. Meda L, Cassatella MA, Szendrei GI, Otvos L, Baron P, Villalba M, et al. Activation of microglial cells by b-amyloid protein and interferon-g. *Nature* 1995; **374**: 647-650.
55. Griffin WS, Sheng JG, Royston MC, Gentleman SM, McKenzie JE, Graham DI, et al. Glial-neuronal interactions in Alzheimer's disease: the potential role of a 'cytokine cycle' in disease progression. *Brain Pathol* 1998; **8**: 65-72.
56. Blasko I, Schmitt TL, Steiner E, Trieb K, Grubeck-Loebenstein B. Tumor necrosis factor alpha augments amyloid beta protein (25-35) induced apoptosis in human cells. *Neurosci Lett* 1997; **238**: 17-20.
57. Blasko I, Marx F, Steiner E, Hartmann T, Grubeck-Loebenstein B. TNFa plus IFNg induce the production of Alzheimer b-amyloid peptides and decrease the secretion of APPs. *FASEB J* 1999; **13**: 63-68.
58. Webster S, Bradt B, Rogers J, Cooper N. Aggregation state-dependent activation of the classical complement pathway by the amyloid beta peptide. *J Neurochem* 1997; **69**: 388-398.
59. Shen Y, Yang LB, Rogers J. Complement defense protein CD59 is deficient in the Alzheimer's brain. Neuroscience 1999; **25**: 1102.
60. Yasojima K, Schwab C, McGeer EG, McGeer PL. Up-regulated production and activation of the complement system in Alzheimer's disease brain. *Am J Pathol* 1999; **154**: 927-936.
61. Webster S, Lue LF, Brachova L, Tenner AJ, McGeer PL, Terai K, et al. Molecular and cellular characterization of the membrane attack complex, C5b-9, in Alzheimer's disease. *Neurobiol Aging* 1997; **18**: 415-421.
62. Gahtan E, Overmier JB. Inflammatory pathogenesis in Alzheimer's disease: biological mechanisms and cognitive sequeli. *Neurosci Biobehav Rev* 1999; **23**: 615-633.
63. Li Y, Liu L, Kang J, Sheng JG, Barger SW, Mrak RE, et al. Neuronal-glial interactions mediated by interleukin-1 enhance neuronal acetylcholinesterase activity and mRNA expression. *J Neurosci* 2000; **20**: 149-155.
64. Gibertini M, Newton C, Friedman H, Klein TW. Spatial learning impairment in mice infected with Legionella pneumophila or administered exogenous interleukin-1-b. *Brain Behav Immun* 1995; **9**: 113-128.
65. Hanisch UK, Seto D, Quirion R. Modulation of hippocampal acetylcholine release: a potent central action of interleukin-2. *J Neurosci* 1993; **13**: 3368-3374.

66. McMillian M, Kong LY, Sawain SM, Wilson B, Das K, Hudson P, et al. Selective killing of cholinergic neurons by microglial activation in basal forebrain mixed neuronal/glial cultures. *Biochem Biophys Res Commun* 1995; **215**: 572-577.
67. Rozemuller JM, Van Muiswinkel FL. Microglia and neurodegeneration [see comment]. *Eur J Clin Invest* 2000; **30**: 469-470.
68. Eikelenboom P, Stam FC. Immunoglobulins and complement factors in senile plaques. *Acta Neuropathol* 1982; **57**: 242.
69. Myllykangas-Luosujarvi R, Isomaki H. Alzheimer's disease and rheumatoid arthritis. *Br J Rheumatology* 1994; **33**: 501-502.
70. Marx F, Blasko I, Pavelka M, Grubeck-Loebenstein B. The possible role of the immune system in Alzheimer's disease. *Exp Gerontol* 1998; **33**: 871-881.
71. Sze G, Zimmerman RD. The magnetic resonance imaging of infections and inflammatory diseases. *Radiol Clin North Am* 1988; **26**: 839-859.
72. Brück W, Bitsch A, Kolenda H, Bruck Y, Stiefel M, Lassmann H. Inflammatory central nervous system demyelination: correlation of magnetic resonance imaging findings with lesion pathology. *Ann Neurol* 1997; **42**: 783-793.
73. Ketonen L, Tuite MJ. Brain imaging in human immunodeficiency virus infection. *Semin Neurol* 1992; **12**: 57-69.
74. Kim DM, Tien R, Byrum C, Krishnan KR. Imaging in acquired immune deficiency syndrome dementia complex (AIDS dementia complex): a review. *Prog Neuropsychopharmacol Biol Psychiatry* 1996; **20**: 349-370.
75. Cecil KM, Lenkinski RE. Proton MR spectroscopy in inflammatory and infectious brain disorders. *Neuroimaging Clin N Am* 1998; **8**: 863-880.
76. Bitsch A, Bruhn H, Vougioukas V, Stringaris A, Lassmann H, Frahm J, et al. Inflammatory CNS demyelination: histopathologic correlation with in vivo quantitative proton MR spectroscopy. *AJNR Am J Neuroradiol* 1999; **20**: 1619-1627.
77. Rovaris M, Viti B, Ciboddo G, Gerevini S, Capra R, Iannucci G, et al. Brain involvement in systemic immune mediated diseases: magnetic resonance and magnetisation transfer imaging study. *J Neurol Neurosurg Psychiatry* 2000; **68**: 170-177.
78. Athens JW, Mauer AM, Ashenbrucker H, Cartwright GE, Wintrobe MM. Leukokinetic studies. I. A method for labeling leukocytes with diisopropylfluorophosphate (DFP^{32}). *Blood* 1959; **14**: 303-333.
79. Corstens FH, van der Meer JW. Nuclear medicine's role in infection and inflammation. *Lancet* 1999; **354**: 765-770.
80. Stevens H, Van de Wiele C, Santens P, Jansen HM, De Reuck J, Dierckx R, et al. Cobalt-57 and Technetium-99m-HMPAO-labeled leukocytes for visualization of ischemic infarcts. *J Nucl Med* 1998; **39**: 495-498.
81. Chianelli M, Mather SJ, Martin-Comin J, Signore A. Radiopharmaceuticals for the study of inflammatory processes: a review. *Nucl Med Commun* 1997; **18**: 437-455.
82. Linde R, Laursen H, Hansen AJ. Is calcium accumulation post-injury an indicator of cell damage? *Acta Neurochir* 1995; **66**: 15-20.
83. Gramsbergen JBP, Veenma-van der Duin L, Loopuit L, Paans AMJ, Vaalburg W, Korf J. Imaging of the degeneration of neurons and their processes in rat or cat brain by $^{45}CaCl_2$ autoradiography or $^{55}CoCl_2$ positron emission tomography. *J Neurochem* 1988; **50**: 1798-1807.
84. Iizuka H, Sakatani K, Young W. Neural damage in the rat thalamus after cortical infarcts. *Stroke* 1990; **21**: 1485-1488.

85. Jansen HM, Dierckx RA, Hew JM, Paans AM, Minderhoud JM, Korf J. Positron emission tomography in primary brain tumours using Cobalt-55. *Nucl Med Commun* 1997; **18**: 734-740.
86. De Reuck J, Stevens H, Jansen H, Keppens J, Strijckmans K, Goethals P, et al. Cobalt-55 positron emission tomography of ipsilateral thalamic and crossed cerebellar hypometabolism after supratentorial ischaemic stroke. *Cerebrovasc Dis* 1999; **9**: 40-44.
87. Versijpt J, Decoo D, Van Laere KJ, Achten E, Audenaert K, D'Asseler Y, et al. ^{57}Co SPECT, ^{99m}Tc-ECD SPECT, MRI and neuropsychological testing in senile dementia of the Alzheimer type. *Nucl Med Commun* 2001; **22**: 713-719.
88. van der Laken CJ, Boerman OC, Oyen WJG, van de Ven MTP, van der Meer JWM, Corstens FHM. Scintigraphic detection of infection and inflammation: new developments with special emphasis on receptor interaction. *Eur J Nucl Med* 1998; **25**: 535-546.
89. Paul C, Peers SH, Woodhouse LE, Thornback JR, Goodbody AE, Bolton C. The detection and quantitation of inflammation in the central nervous system during experimental allergic encephalomyelitis using the radiopharmaceutical ^{99m}Tc-RP128. *J Neurosci Methods* 2000; **98**: 83-90.
90. van der Laken CJ, Boerman OC, Oyen WJ, van de Ven MT, Claessens RA, van der Meer JW, et al. Different behaviour of radioiodinated human recombinant interleukin-1 and its receptor antagonist in an animal model of infection. *Eur J Nucl Med* 1996; **23**: 1531-1535.
91. Zisterer DM, Williams DC. Peripheral-type benzodiazepine receptors. *Gen Pharmacol* 1997; **29**: 305-314.
92. Zavala F, Taupin V, Descamps-Latscha B. In vivo treatment with benzodiazepines inhibits murine phagocytic oxidative metabolism and production of interleukin 1, tumor necrosis factor and interleukin-6. *J Pharmacol Exp Ther* 1990; **255**: 442-450.
93. Guilarte TR, Kuhlmann AC, O'Callaghan JP, Miceli RC. Enhanced expression of peripheral benzodiazepine receptors in trimethyltin-exposed rat brain: a biomarker of neurotoxicity. *Neurotoxicology* 1995; **16**: 441-450.
94. Banati RB, Newcombe J, Gunn RN, Cagnin A, Turkheimer F, Heppner F, et al. The peripheral benzodiazepine binding site in the brain in multiple sclerosis: quantitative in vivo imaging of microglia as a measure of disease activity. *Brain* 2000; **123**: 2321-2337.
95. Parola AL, Yamamura HI, Laird HE. Peripheral-type benzodiazepine receptors. *Life Sci* 1993; **52**: 1329-1342.
96. Banati RB, Myers R, Kreutzberg GW. PK ('peripheral benzodiazepine') – binding sites in the CNS indicate early and discrete brain lesions: microautoradiographic detection of [^{3}H]PK11195 binding to activated microglia. *J Neurocytol* 1997; **26**: 77-82.
97. Groom GN, Junck L, Foster NL, Frey KA, Kuhl DE. PET of peripheral benzodiazepine binding sites in the microgliosis of Alzheimer's disease. *J Nucl Med* 1995; **36**: 2207-2210.
98. Junck L, Olson JM, Ciliax BJ, Koeppe RA, Watkins GL, Jewett DM, et al. PET imaging of human gliomas with ligands for the peripheral benzodiazepine binding site. *Ann Neurol* 1989; **26**: 752-758.
99. Ramsay SC, Weiller C, Myers R, Cremer JE, Luthra SK, Lammertsma AA, et al. Monitoring by PET of macrophage accumulation in brain after ischaemic stroke [letter]. *Lancet* 1992; **339**: 1054-1055.
100. Banati RB, Cagnin A, Myers R, Gunn RN, Piccini P, Olanow CW, et al. In vivo detection of activated microglia by [^{11}C]PK11195–PET indicates involvement of the globus pallidum in idiopathic Parkinson's disease. Movement Disord 1999; **5**: S56.
101. Banati RB, Goerres GW, Myers RN, Gunn RN, Turkheimer FE, Kreutzberg GW, et al. [^{11}C](R)-PK11195 positron emission tomography imaging of activated microglia in vivo in Rasmussen's encephalitis. *Neurology* 1999; **53**: 2199-2203.

102. Cagnin A, Brooks DJ, Kennedy AM, Gunn RN, Myers R, Turkheimer FE, et al. In-vivo measurement of activated microglia in dementia. *Lancet* 2001; **358**: 461-467.

103. Versijpt J, Dumont F, Thierens H, Jansen H, De Vos F, Slegers G, et al. Biodistribution and dosimetry of [^{123}I]iodo-PK 11195: a potential agent for SPET imaging of the peripheral benzodiazepine receptor. *Eur J Nucl Med* 2000; **27**: 1326-1333.

CHAPTER THREE

COBALT AS AN INFLAMMATORY TRACER IN ALZHEIMER'S DISEASE

^{57}Co SPECT, ^{99m}Tc-ECD SPECT, MRI, AND NEUROPSYCHOLOGICAL TESTING IN SENILE DEMENTIA OF THE ALZHEIMER TYPE

J Versijpt[1,2], D Decoo[3], KJR Van Laere[2], E Achten[4], K Audenaert[5], Y D'Asseler[6], G Slegers[7], RA Dierckx[2], J Korf[1]

[1]Department of Biological Psychiatry, Groningen University Hospital, the Netherlands
[2]Division of Nuclear Medicine, Ghent University Hospital, Belgium
[4]Department of Radiology, Ghent [3]Department of Neurology, Elisabeth Hospital, Sijsele, Belgium
University Hospital, Belgium
[5]Department of Psychiatry, Ghent University Hospital, Belgium
[6]Medical Signal and Image Processing Department (MEDISIP), Faculty of Applied Sciences, Ghent University, Belgium
[7]Department of Radiopharmacy, Ghent University, Belgium

Nucl Med Commun 2001;22(6):713-9

SUMMARY

Introduction: Inflammatory mechanisms contribute to the pathophysiology in senile dementia of the Alzheimer type (sDAT). Previous studies showed that ^{57}Co SPECT is able to visualise inflammatory lesions, probably by means of the final common pathway of the Ca^{2+}-homeostasis disturbance in both neuronal degeneration and inflammation. The aim of this study was (1) to detect ^{57}Co SPECT changes in sDAT patients, (2) correlate these findings with conventional neuroimaging techniques and neuropsychological testing (NPT), and (3) compare ^{57}Co SPECT findings in sDAT patients with other types of dementia.

Patients and methods: Six patients suffering from probable sDAT were included and compared with 4 patients suffering from other types of dementia. All patients had a MRI-scan, NPT, ^{57}Co and a ^{99m}Tc-ECD SPECT scan. Perfusion SPECT images were semiquantitatively evaluated by comparison with an age-matched normal database while ^{57}Co SPECT scans were assessed qualitatively.

Results and conclusions: MRI and ^{99m}Tc-ECD SPECT scans yielded conclusive results as to the exclusion of other pathologies and confirmation of diagnosis. Using visual analysis, ^{57}Co SPECT scans were not able to show any regional raised uptake, irrespective of the disorder, depth or extent of the perfusion defects, presence of atrophy on MRI, or the results of NPT.

INTRODUCTION

In most industrialised countries, senile dementia of the Alzheimer type (sDAT), a primary degenerative disease of the brain, either alone or in combination with other illnesses, accounts for about 70% of dementia cases. The typical course in sDAT is one of progressive decline with an average survival of 8 to 10 years. The most characteristic feature is progressive memory impairment, predominantly loss of short-term memory. However, other cognitive dysfunctions or behavioral symptoms, as well as changes in the neurological status (especially late sDAT) are important [1].

Pathophysiologically, sDAT is characterised by dense and neuritic amyloid plaques, cerebral intraneuronal neurofibrillary tangles (NFT), neuronal and synaptic loss and deficits in neurotransmitter functions [2]. However, over the last years, it has become clear that inflammatory mechanisms may contribute to the neurodegenerative process in sDAT. Indeed, epidemiological data from about 20 studies have shown the protective and progression-retarding effect of non-steroidal anti-inflammatory drugs (NSAIDs) which would reduce the prevalence by 50% of sDAT in people who regularly take these drugs for various reasons [3]. As such, Breitner et al. concluded from twin studies that the use of NSAIDs could delay the onset of sDAT by 5 to 7 years [4]. As for treatment, there is only one double-blind placebo-controlled clinical trial showing this same progression-retarding effect [5].

Visualising this inflammation with positron emission tomography (PET) or single photon emission computed tomography (SPECT) would be of interest, firstly for clarifying the underlying pathophysiology, secondly for selecting subgroups of patients that are more eligible for anti-inflammatory treatment and finally, for monitoring patients during trials with anti-inflammatory agents.

Both *in vivo* and *in vitro* experiments have shown that Ca^{2+} accumulates in the (ir)reversibly damaged nerve cell body and degenerating axons, this through a passive influx due to a shortage of ATP following ischemia, resulting in the disappearance of the membrane potential, ánd through neuronal and glial uptake by divalent cation-permeable kainate-activated non-NMDA glutamate receptor-operated channels in the membrane [6-11]. ^{57}Co (SPECT) and ^{55}Co (PET), both as Ca^{2+}-analogues, reflect Ca^{2+}-influx in ischaemically or neurotoxically damaged cerebral tissue. In this way, both ^{57}Co SPECT and ^{55}Co PET have been shown capable of visualising focal neurodegenerative changes, reactive gliosis, endangered brain tissue and/or ongoing neuronal tissue decay including inflammatory lesions in various brain diseases e.g. multiple sclerosis, trauma, tumours, and stroke [12-18]. Moreover, the time sequence of the ^{55}Co-load seems to correlate well with cell death and glial proliferation in the ipsilateral thalamus following supratentorial ischaemic stroke in an experimental rat stroke model [19]. The visualisation of these inflammatory processes in sDAT can be expected to occur by means of the final common pathway of the Ca^{2+}-homeastasis-disturbance in both neuronal degeneration and inflammation [20-24].

A previous study by Oosterink et al. with PET and ^{55}Co suggested that this technique could generate additional specific information, which cannot be obtained with conventional neuroimaging techniques

like perfusion and ^{18}FDG PET [25]. The objectives of this study were (1) to visualise inflammation *in vivo* in sDAT patients by detecting ^{57}Co SPECT changes and investigate whether ^{57}Co SPECT can generate additional information which cannot be obtained with conventional neuroimaging techniques or neuropsychological testing (NPT); (2) to search for a possible correlation of findings with data obtained from MRI, perfusion SPECT, and NPT; and (3) to compare findings in sDAT patients with patients suffering from vascular dementia (VaD) and frontal lobe-type dementia (FLD).

PATIENTS AND METHODS

PATIENTS

The study was approved by the medical ethics committee and all patients gave informed (proxy-)consent. Six patients suffering from probable sDAT (mean age 79 ± 7 yrs; range 68 to 87 yrs) according to the NINCDS-ADRDA criteria were included [26]. As controls, 3 VaD patients (mean age 67 ± 5 yrs) according to the NINDS-AIREN criteria and one FLD patient (75 yrs) according to the criteria suggested by Gustafson et al. were included [27, 28].

METHODS

Magnetic Resonance Imaging

All patients had a MRI scan (1,5 Tesla, Siemens, Erlangen, Germany). After the administration of Gadolinium, 5 mm axial slices were scanned with protondensity-, T_2- and T_1-weighting. Subsequently, the head was scanned with a 3D-MPRAGE sequence yielding 128 sagittal T_1-weighted images with a thickness of 1.25 mm. From the MPRAGE series, axial, sagittal, and coronal planes were reconstructed. The images were hard copied and then viewed to assess global/regional atrophy, white matter lesions (periventricular, frontoparietal, occipital, and temporal), and the presence of infarcts.

Neuropsychological testing

Patients underwent the following battery: mini mental state examination (MMSE; N=10), Rey auditory verbal learning test for verbal learning and memory (AVLT; N=9), Trail making test for attention, sequencing, mental flexibility, and visual search and motor function (TMT, N=7), Controlled Oral Word Association Task for semantic and syntactic verbal fluency (COWAT, N=8), and the Money Road map test for spatial orientation (MRMT, N=8). Not all tests could be performed in every patient due to non-compliance.

^{57}Co SPECT scan

^{57}Co was purchased from Amersham (Amersham Cygne, Eindhoven, the Netherlands). Approximately 37 MBq (1 mCi) of ^{57}Co was injected. The patient was scanned on a triple-headed gamma camera (Toshiba GCA-9300A, Dutoit Medical, Wijnegem, Belgium) equipped with low energy, high-resolution parallel hole collimators (FWHM 9.5 mm), 15 ± 10 hours (range 3 to 24) after injection, in the same session as the ^{99m}Tc-ECD SPECT scan, enabling image registration. Images were acquired in a 128×128 matrix with a step angle of 6, frame time of 90 seconds, and a 1.25 zoom. Images were reconstructed with filtered backprojection (FBP, Butterworth filter 0.9 cycles/cm, order 8). Uniform attenuation correction was performed (μ=0.09), no scatter correction was applied. A visual qualitative assessment of the ^{57}Co SPECT images was made.

^{99m}Tc-ECD SPECT scan

Nine patients underwent a ^{99m}Tc-ECD SPECT scan, after the injection of 925 MBq ^{99m}Tc-ECD (ethyl cysteinate dimer; Dupont Pharmaceuticals Ltd., Belgium). Images were acquired in a 128×128 matrix with a frame time of 60 seconds, a step angle of 6, and a 1.25 zoom. Images were reconstructed with FBP (Butterworth filter 0.9 cycles/cm, order 8). Uniform attenuation correction was performed (μ=0.09), without scatter correction. Perfusion SPECT images were automatically fitted and realigned into Talaraich co-ordinates where 26 cortical, 6 subcortical, 2 cerebellar, and one pons 3D-volumes of interest were assessed semiquantitatively (normalisation total number of counts) (Brass software, Nuclear Diagnostics, Sweden). Comparison was done to a database consisting of 20 healthy controls (mean age 70.4 ± 6.2 yrs) [29]. Mean counts per voxel were averaged in the sDAT group to assess a group perfusion deficit. A hypoperfusion in a specific region was considered as

significant when the uptake was less than the averaged uptake for the healthy volunteers minus two times the SD for that specific region.

RESULTS

Age, pathology, MMSE-score, the presence of cerebral infarcts on MRI and the perfusion defects are presented in Table 1. Age was inversely correlated with the relative perfusion in the left temporal lobe, temporal atrophy, the MMSE-score and the number of hyoperfused regions ($p = 0.04$, Pearson correlation; $p = 0.01$, $p = 0.02$, and $p = 0.02$, Spearman correlation coefficient) respectively.

Age	Pathology	MMSE	Infarcts on MRI	Significant perfusion defects
75	sDAT	12	(-)	L and R temporal superior, medial inferior, and parietal inferior region
68	sDAT	19	(-)	L prefrontal and superior frontal region; posterior cingulate gyrus
84	sDAT	16	(+)	L temporal superior and parietal inferior region; cerebellum
83	sDAT	0	(-)	L temporal superior region
87	sDAT	10	(-)	L lateral frontal, temporal medial inferior, and parietal inferior region R lateral frontal and temporal anterior region
77	sDAT	22	(-)	R prefrontal region and posterior cingulate gyrus; thalamus
68	VaD	17	(+)	Not performed
71	VaD	18	(+)	R lateral/superior frontal, temporal medial inferior, and parietal superior region
61	VaD	24	(+)	R temporal anterior region, cerebellum
75	FLD	17	(-)	L lateral frontal and R prefrontal region

sDAT = senile dementia of the Alzheimer type; VaD = vascular dementia; FLD = frontal lobe-type dementia

Table 1: Age, pathology, MMSE-score, presence of infarcts on MRI and the significant perfusion defects detected on the ^{99m}Tc-ECD SPECT scans

Structural imaging

MRI scans yielded conclusive results as to the exclusion of other pathologies and the confirmation of diagnosis. One patient had a lenticulostriate infarct but was however classified as a sDAT patient. No significant correlation was found between the rCBF deficits and the regional atrophy rating scores derived from the MRI scans. Vascular dementia patients had more white matter lesions than sDAT patients (10.5 vs. 2.2 ml) did, whereas the periventricular hyperintensities did not differ between groups. The total amount of periventricular white matter hyperintensities correlated significantly with the memory performance on the AVLT and the MMSE score ($p = 0.02$ and 0.03 respectively; Spearman correlation coefficient).

^{57}Co SPECT scans

By visual analysis, ^{57}Co SPECT scans were unable to show any regional raised uptake (and in this way inflammatory lesions), irrespective of the disorder, depth or extent of the associate lesions on the perfusion images or MRI, and irrespective of the results of the NPT.

Perfusion SPECT - Neuropsychological testing

Perfusion SPECT scans in sDAT patients showed significant deficits in the anterior, superior and inferior mesiotemporal region, the inferior parietal region, the orbitofrontal, prefrontal, superior frontal and lateral frontal region, the posterior cingulate gyrus, the caput caudate nucleus, thalamus, and the cerebellum. A group perfusion defect for the sDAT patients was found in the left inferior parietal and the right temporal anterior region. The FLD patient showed perfusion deficits in the left lateral frontal and the right prefrontal region. The VaD patients showed mixed defects in the frontal, temporal and parietal lobes but also in the cerebellar region. The MMSE-score correlated significantly with the relative left temporal perfusion ($p = 0.002$, Pearson correlation coefficient). Results of the spatial orientation task correlated significantly with the relative perfusion in the right lateral frontal, right medial temporal and the right parietal region ($p = 0.03$, 0.005, and 0.03; Pearson correlation coefficient).

DISCUSSION

Neuroinflammatory imaging

Scintigraphic visualisation of inflammation has previously been done with Ga^{67}, radiolabelled leukocytes, nanocolloid and human immunoglobulins [30]. The application of these techniques in sDAT for the visualisation of the inflammatory process would pose several difficulties. Indeed, despite repeated efforts by several laboratories, neutrophil invasion has until now not yet been documented in sDAT and a consistent lymphocytic or immunoglobulin involvement appears to lack [31]. The absence of these phenomena makes the application of the former mentioned techniques inadequate. As such, the aim of the present study was to visualise inflammatory lesions in sDAT patients with ^{57}Co SPECT and compare this with findings in patients suffering from other types of dementia. Inflammation as a pathogenic mechanism has been described to a lesser extent for VaD but not for FLD [32]. The evidence of inflammation in the group of frontotemporal dementia patients is to our knowledge limited to one study where some cases of Pick's disease were found to exhibit a neuronal expression of class II major histocompatibility complex with a dramatic microglial response suggesting an inflammatory process [33].

Limitations of the study

The limitations of ^{57}Co SPECT are manifold. Due to the long physical half-life of 270 days, only a limited dose can be injected which is responsible for the low count rate and the resulting low statistics. Moreover, whether ^{57}Co visualises specific aspects of neuronal damage or blood-brain barrier integrity is still uncertain. To what extent ^{57}Co really visualises calcium-mediated processes (*in vitro* and more importantly *in vivo*), and therefore resembles identical molecular uptake mechanisms, has yet to be determined, although the cerebral uptake of intravenously administered radioactive ^{45}Ca and ^{60}Co in neuronal damage is highly similar [7]. Finally, the exact cellular site of accumulation of radioactivity is, as yet, not known. As for inflammatory imaging, however, it is interesting to note that calcium may also accumulate in activated leukocytes and that both for ^{55}Co and ^{57}Co, only 12% of the total fraction is in its free form where the remainder is bound to leukocytes or plasma proteins [34-36].

Perfusion SPECT and sDAT

The role of perfusion SPECT in dementia, both for clinical (early diagnosis and follow-up) and research objectives has been well described in literature, even in the very early stages of the disease [37]. As such, the Therapeutics and Technology Assessment Subcommittee of the American Academy of Neurology evaluated the use of perfusion SPECT for sDAT as *established to support the clinical diagnosis* with a sensitivity of up to 95% [38]. Perfusion defects in sDAT patients have been mainly described in the posterior temporal and parietal lobe region, in concordance with the group perfusion defect in the temporal and parietal region found in this series. The frontal association cortex is said to be mostly unaffected until late in the course of the disease, however, this is contested by several SPECT and PET studies [38-40]. In this way, none of the dementia diseases can be identified with certainty by any characteristic topography of regional cerebral blood flow deficits, with an incidence of an exclusive or predominant bilateral reduction of perfusion tracer uptake in the

temporoparietal cortex ranging in literature from 26 to 100% [37, 41-43]. As such, group comparisons provide less information due to the heterogeneity of the disease (different stages and progression patterns), as already pointed out by Waldemar et al. [37].

Perfusion SPECT and other types of dementia, correlation with neuropsychological tests

The frontal perfusion defects found in the FLD patient is in agreement with the finding of Risberg et al. where bilateral frontal or frontotemporal defects were found in 25 out of 26 autopsy-verified cases of frontal lobe degeneration of the non-Alzheimer type [44]. Moreover, Pickut et al. identified bifrontal hypoperfusion as the most powerful predictor of clinical classification of sDAT versus FLD on perfusion SPECT [45]. The defects in the cerebellar region in the VaD patient are probably caused by functional diaschisis related to deafferentiation, where metabolic findings in any specific brain region represent complex relationships between a local and remote pathology. [46, 47]. The significant correlation between the orientation task and parietal perfusion confirms previous reports of this parietal hypoperfusion being associated with deficits in visuospatial function whereas a correlation between the MMSE-score and the relative temporal lobe perfusion was also described by O'Brien et al. [48] and Waldemar et al. [49].

MRI and sDAT

Not or only a partial correlation (right parietal region) was found between the rCBF deficits and the regional atrophy rating scores or the number of white matter lesions found on MRI. This is in agreement with studies performed by Eagger et al. and Waldemar et al. which indicates firstly that the hypoperfusion really reflects a reduced metabolism per gram brain tissue and secondly is not caused by a deafferentiation from underlying white matter hyperintensities [40, 50, 51]. The relationship between periventricular hyperintensities and cognitive functions as indicated in this study was already pointed out by Harrel at al [52]. Also, VaD patients having significantly more white matter lesions but not periventricular hyperintensities compared to sDAT patients, was previously indicated by Bowen et al. [53]. Although MRI is useful in the workout of patients with dementia since it shows the presence of space-occupying lesions, ventricular dilatation, cerebral atrophy, widening of sulci or infarcts, this technique is not of particular value in the direct diagnosis of sDAT, although promising results have been made with volumetric measurements of the (para)hippocampal and amygdala region [54].

Conclusions

In conclusion, ^{57}Co SPECT scans are not able to show any regional raised uptake and in this way ongoing tissue decay or inflammation, irrespective of the type of dementia, the depth or extent of perfusion defects, the presence of atrophy on MRI, or the results of NPT.

REFERENCES

1. Geldmacher DS, Whitehouse PJ. Evaluation of dementia. *N Engl J Med* 1996; **335**: 330-336.
2. Fowler CJ, Cowburn RF, Joseph JA. Alzheimer's, ageing and amyloid: an absurd allegory? *Gerontology* 1997; **43**: 132-142.
3. McGeer PL, Schulzer M, McGeer EG. Arthritis and anti-inflammatory agents as possible protective factors for Alzheimer's disease: a review of 17 epidemiologic studies. *Neurology* 1996; **47**: 425-432.
4. Breitner JCS, Welsh KA, Helms MJ, Gaskell PC, Gau BA, Roses AD, et al. Delayed onset of Alzheimer's disease with nonsteroidal anti-inflammatory and histamine H2 blocking drugs. *Neurobiol Aging* 1995; **16**: 523-530.
5. Rogers J, Kirby LC, Hempelman SR, Berry DL, McGeer PL, Kaszniak AW, et al. Clinical trial of indomethacin in Alzheimer's disease. *Neurology* 1993; **43**: 1609-1611.
6. Linde R, Laursen H, Hansen AJ. Is calcium accumulation post-injury an indicator of cell damage? *Acta Neurochir* 1995; **66**: 15-20.
7. Gramsbergen JBP, Veenma-van der Duin L, Loopuit L, Paans AMJ, Vaalburg W, Korf J. Imaging of the degeneration of neurons and their processes in rat or cat brain by $^{45}CaCl_2$ autoradiography or $^{55}CoCl_2$ positron emission tomography. *J Neurochem* 1988; **50**: 1798-1807.
8. Dubinsky JM. Examination of the role of calcium in neuronal death. *Ann N Y Acad Sci* 1993; **679**: 34-40.
9. Gibbons SJ, Brorson JR, Bleakman D, Chard PS, Miller RJ. Calcium influx and neurodegeneration. *Ann N Y Acad Sci* 1993; **679**: 22-33.
10. Hartley DM, Kurth MC, Bjerkness L, Weiss JH, Choi DW. Glutamate receptor-induced $^{45}Ca^{2+}$ accumulation in cortical cell correlates with subsequent neuronal degeneration. *J Neurosci* 1993; **13**: 1993-2000.
11. Müller T, Möller T, Berger T, Schnitzer J, Kettenmann H. Calcium entry through kainate receptors and resulting potassium-channel blockade in Bergmann glial cells. *Science* 1992; **256**: 1563-1566.
12. Pruss RM, Akeson RL, Racke MM, Wilburn JL. Agonist-activated cobalt uptake identifies divalent cation-permeable kainate receptors on neurons and glial cells. *Neuron* 1991; **7**: 509-518.
13. Williams LR, Pregenzer JF, Oostveen JA. Induction of cobalt accumulation by excitatory amino acids within neurons of the hippocampal slice. *Brain Res* 1992; **581**: 181-189.
14. De Reuck J, Stevens H, Jansen H, Keppens J, Strijckmans K, Goethals P, et al. Cobalt-55 positron emission tomography of ipsilateral thalamic and crossed cerebellar hypometabolism after supratentorial ischaemic stroke. *Cerebrovasc Dis* 1999; **9**: 40-44.
15. Jansen HM, Willemsen AT, Sinnige LG, Paans AM, Hew JM, Franssen EJ, et al. Cobalt-55 positron emission tomography in relapsing-progressive multiple sclerosis. *J Neurol Sci* 1995; **132**: 139-145.
16. Jansen HM, van der Naalt J, van Zomeren AH, Paans AM, Veenma-van der Duin L, Hew JM, et al. Cobalt-55 positron emission tomography in traumatic brain injury: a pilot study [published erratum appears in J Neurol Neurosurg Psychiatry 1996 Jul;61(1):121]. *J Neurol Neurosurg Psychiatry* 1996; **60**: 221-224.
17. Jansen HM, Dierckx RA, Hew JM, Paans AM, Minderhoud JM, Korf J. Positron emission tomography in primary brain tumours using Cobalt-55. *Nucl Med Commun* 1997; **18**: 734-740.
18. Stevens H, Van de Wiele C, Santens P, Jansen HM, De Reuck J, Dierckx R, et al. Cobalt-57 and Technetium-99m-HMPAO-labeled leukocytes for visualization of ischemic infarcts. *J Nucl Med* 1998; **39**: 495-498.
19. Iizuka H, Sakatani K, Young W. Neural damage in the rat thalamus after cortical infarcts. *Stroke* 1990; **21**: 1485-1488.
20. Thibault O, Porter NM, Chen K-C, Blalock EM, Patrick GK, Clodfelter GV, et al. Calcium dysregulation in neuronal aging and Alzheimer's disease: history and new directions. *Cell Calcium* 1998; **24**: 417-433.

21. Pascale A, Etcheberrigaray R. Calcium alterations in Alzheimer's disease: pathophysiology, models and therapeutic opportunities. *Pharmacol Res* 1999; **39**: 81-88.
22. Holscher C. Possible causes of Alzheimer's disease: amyloid fragments, free radicals, and calcium homeostasis. *Neurobiol Dis* 1998; **5**: 129-141.
23. Eckert A, Forstl H, Zerfass R, Hartmann H, Muller W. Lymphocytes and neutrophils as peripheral models to study the effect of beta-amyloid on cellular calcium signalling in Alzheimer's disease. *Life Sci* 1996; **59**: 499-510.
24. Mattson M, Rydel R, Lieberburg I, Smith-Swintosky V. Altered calcium signaling and neuronal injury: stroke and Alzheimer's disease as examples. *Ann N Y Acad Sci* 1993; **679**: 1-21.
25. Oosterink BJ, Jansen HML, Paans AMJ, Willemsen ATM, Hew JM, van Zomeren AH, et al. Cobalt-55 positron emission tomography in senile dementia: a pilot study. J Cereb Blood Flow Metab 1995; **15**: S794.
26. McKhann G, Drachman D, Folstein M, Katzman R, Price D, Stadlan EM. Clinical diagnosis of Alzheimer's disease: report of the NINCDS-ADRDA work group under the auspices of the Department of Health and Human Services Task Force on Alzheimer's Disease. *Neurology* 1984; **34**: 939-944.
27. Roman GC, Tatemichi TK, Erkinjuntti T, Cummings JL, Masdeu JC, Garcia JH, et al. Vascular dementia: diagnostic criteria for research studies. Report of the NINDS-AIREN International Workshop [see comments]. *Neurology* 1993; **43**: 250-260.
28. Gustafson L. Clinical picture of frontal lobe degeneration of the non-Alzheimer type. *Dementia* 1993; **4**: 143-148.
29. Van Laere KJ, Versijpt J, Audenaert K, Goethals I, Koole M, De Winter O, et al. An age and gender stratified, high-resolution normal database for ^{99m}Tc-ECD rCBF in adults. J Nucl Med 2000; **41**: *212*.
30. van der Laken CJ, Boerman OC, Oyen WJG, van de Ven MTP, van der Meer JWM, Corstens FHM. Scintigraphic detection of infection and inflammation: new developments with special emphasis on receptor interaction. *Eur J Nucl Med* 1998; **25**: 535-546.
31. Rogers J. Inflammation as a pathogenic mechanism in Alzheimer's disease. *Arzneimittelforschung* 1995; **45**: 439-442.
32. Rother M, Erkinjuntti T, Roessner M, Kittner B, Marcusson J, Karlsson I. Propentofylline in the treatment of Alzheimer's disease and vascular dementia: a review of phase III trials. *Dement Geriatr Cogn Disord* 1998; **9S1**: 36-43.
33. Hollister RD, Xia M, McNamara MJ, Hyman BT. Neuronal expression of class II major histocompatibility complex (HLA-DR) in 2 cases of Pick disease. *Arch Neurol* 1997; **54**: 243-248.
34. Haverstick DM, Gray LS. Increased intracellular Ca^{2+} induced Ca^{2+} influx in human T lymphocytes. *Mol Biol Cell* 1993; **4**: 173-184.
35. Clementi E, Martino G, Grimaldi LM, Brambilla E, Meldolesi J. Intracellular Ca^{2+} stores of T lymphocytes: Changes induced by *in vitro* and *in vivo* activation. *Eur J Immunol* 1994; **24**: 1365-1371.
36. Jansen HM, Knollema S, van-der-Duin LV, Willemsen AT, Wiersma A, Franssen EJ, et al. Pharmacokinetics and dosimetry of cobalt-55 and cobalt-57. *J Nucl Med* 1996; **37**: 2082-2086.
37. Waldemar G. Functional brain imaging with SPECT in normal aging and dementia. Methodological, pathophysiological, and diagnostic aspects. *Cerebrovasc Brain Metab Rev* 1995; **7**: 89-130.
38. Report of the Therapeutics and Technology Assessment Subcommittee of the American Academy of Neurology. Assessment of brain SPECT. *Neurology* 1996; **46**: 278-285.
39. Rapoport SI. Positron emission tomography in Alzheimer's disease in relation to disease pathogenesis: a critical review. *Cerebrovasc Brain Metab Rev* 1991; **3**: 297-335.

40. Waldemar G, Bruhn P, Kristensen M, Johnsen A, Paulson OB, Lassen NA. Heterogeneity of neocortical cerebral blood flow deficits in dementia of the Alzheimer type: a [99mTc]-d,l-HMPAO SPECT study. *J Neurol Neurosurg Psychiatry* 1994; **57**: 285-295.
41. Ryding E. SPECT measurements of brain function in dementia; a review. *Acta Neurol Scand Suppl* 1996; **168**: 54-58.
42. Holman BL, Johnson KA, Gerada B, Carvalho PA, Satlin A. The scintigraphic appearance of Alzheimer's disease: a prospective study using technetium-99m-HMPAO SPECT [published erratum appears in J Nucl Med 1992 Apr;33(4):484] [see comments]. *J Nucl Med* 1992; **33**: 181-185.
43. Masterman DL, Mendez MF, Fairbanks LA, Cummings JL. Sensitivity, specificity, and positive predictive value of technetium 99-HMPAO SPECT in discriminating Alzheimer's disease from other dementias. *J Geriatr Psychiatry Neurol* 1997; **10**: 15-21.
44. Risberg J, Passant U, Warkentin S, Gustafson L. Regional cerebral blood flow in frontal lobe degeneration of non-Alzheimer type. *Dementia* 1993; **4**: 186-187.
45. Pickut BA, Saerens J, Marien P, Borggreve F, Goeman J, Vandevivere J, et al. Discriminative use of SPECT in frontal lobe-type dementia versus (senile) dementia of the Alzheimer's type. *J Nucl Med* 1997; **38**: 929-934.
46. Waldemar G, Larsson HB, Lassen NA, Paulson OB. Tomographic measurements of regional cerebral blood flow by SPECT in vascular dementia. In: Hartmann A, Kuschinsky W, Hoyer S, eds. Cerebral ischemia and dementia. Berlin: Springer-Verlag, 1991: 310-315.
47. Flores LG, Futami S, Hoshi H, Nagamachi S, Ohnishi T, Jinnouchi S, et al. Crossed cerebellar diaschisis: analysis of iodine-123-IMP SPECT imaging. *J Nucl Med* 1995; **36**: 399-402.
48. O'Brien JT, Eagger S, Syed GM, Sahakian BJ, Levy R. A study of regional cerebral blood flow and cognitive performance in Alzheimer's disease. *J Neurol Neurosurg Psychiatry* 1992; **55**: 1182-1187.
49. Waldemar G, Bruhn P, Schmidt E, Kristensen M, Lassen NA, Paulson OB. Cognitive profiles and regional cerebral blood flow patterns in dementia of the Alzheimer type. *Eur J Neurol* 1994; **1**: 81-89.
50. Eagger S, Syed GM, Burns A, Barrett JJ, Levy R. Morphologic (CT) and functional (rCBF-SPECT) correlates in Alzheimer's disease. *Nucl Med Commun* 1992; **13**: 644-647.
51. Waldemar G, Christiansen P, Larsson HB, Hogh P, Laursen H, Lassen NA, et al. White matter magnetic resonance hyperintensities in dementia of the Alzheimer type: morphological and regional cerebral blood flow correlates. *J Neurol Neurosurg Psychiatry* 1994; **57**: 1458-1465.
52. Harrel LE, Duvall E, Folks DG. The relationship of high-intensity signals on magnetic resonance images to cognitive and psychiatric state in Alzheimer's disease. *Arch Neurol* 1991; **48**: 1136-1140.
53. Bowen BC, Barker WW, Loewenstein DA, Sheldon J, Duara R. MR signal abnormalities in memory disorder and dementia. *AJNR Am J Neuroradiol* 1990; **11**: 283-290.
54. Scheltens P. Early diagnosis of dementia: neuroimaging. *J Neurol* 1999; **246**: 16-20.

CHAPTER FOUR

DEVELOPMENT AND VALIDATION OF RADIOLABELLED PK11195 FOR SINGLE PHOTON EMISSION COMPUTED TOMOGRAPHY

BIODISTRIBUTION AND DOSIMETRY OF [^{123}I]iodo-PK 11195: A POTENTIAL AGENT FOR SPET IMAGING OF THE PERIPHERAL BENZODIAZEPINE RECEPTOR

Jan Versijpt*¶ MD, Filip Dumont‡ Apr, Hubert Thierens§ MSc PhD, Hugo Jansen¶ MSc MD PhD, Filip De Vos‡ Apr, Guido Slegers‡ MSc PhD, Patrick Santens** MD, Rudi Andre Dierckx¶ MD PhD, Jakob Korf* PhD

* Department of Biological Psychiatry, Groningen University Hospital, the Netherlands

‡ Department of Radiopharmacy, Ghent University, Belgium

§ Department of Biomedical Physics & Radiation Protection, Ghent University, Belgium

¶ Division of Nuclear Medicine, Ghent University Hospital, Belgium

** Department of Neurology, Ghent University Hospital, Belgium

Eur J Nucl Med 2000;27(9):1326-33

ABSTRACT

The peripheral benzodiazepine receptor (PBR) is found in highest concentrations in kidneys and heart. In addition, it was reported to reflect neuro-inflammatory damage by a colocalisation with activated microglia. PK 11195 is a high affinity ligand for the PBR. The aim of the present study was to investigate in humans the biodistribution and dosimetry of [^{123}I]iodo-PK 11195, a potential SPET tracer for the PBR. Five healthy volunteers were injected with 112 MBq of ^{123}I labelled iodo-PK 11195. Sequential whole body scans were performed up to 72 hours post-injection. Multiple blood samples were taken, and urine was collected to measure the fraction voided by the renal system. Decay corrected *ROIs* of the whole-body images were analysed, and geometric mean count rates were used to determine organ activity. Organ absorbed doses and effective dose were calculated using the MIRD method. [^{123}I]iodo-PK 11195 was rapidly cleared from the blood, mainly by the hepatobiliary system. Approximately 22% was voided in urine after 48 hours. Average organ residence times were 0.74, 0.44, and 0.29 hrs for the liver, upper large intestine, and lower large intestine respectively. The testes received the highest dose, 109.4 μGy/MBq. All other organs investigated received doses of less than 50 μGy/MBq. The effective dose was 40.3 μSv/MBq. In conclusion, ^{123}I labelled iodo-PK 11195 can be used for the visualisation of the PBR and indirectly for the imaging of neuroinflammatory lesions. Taking into account the radiation burden of 7.46 mSv following an administration of 185 MBq, a ^{123}I labelled iodo-PK 11195 investigation has to be considered as an ICRP risk category IIb investigation.

INTRODUCTION

The central-type benzodiazepine receptor (CBR) with the known clinically relevant anxiolytic, anticonvulsant and muscle-relaxant effect of benzodiazepines is coupled to GABA receptors and their associated chloride channels. Unexpectedly, rat peripheral tissues used as negative controls for radioligand binding experiments also demonstrated high affinity [^{3}H]diazepam binding [1]. These peripheral binding sites were structurally and pharmacologically distinct from the CBR. Based on their localisation outside of the central nervous system and the high affinity for several 1,4-benzodiazepines, these sites were designated "peripheral-type" benzodiazepine receptors (PBR) [2]. Although present in virtually all mammalian peripheral tissues, marked differences in PBR density and distribution of various species have been shown using autoradiographic techniques [3,4]. It is found in highest concentrations in kidneys, colon membranes, heart, steroid hormone producing cells of adrenal cortex, ovaries and testes, and several cell types of the immune system, such as mast cells and macrophages [2,5-7]. It is also present in low concentrations throughout the brain, primarily associated with the choroid plexus, ependymal linings, and glial cells [8-10]. Subcellular, the PBR is found in greatest abundance in the mitochondrial outer membrane and plasma membrane, however, other localisations are possible. Although the specific function of the PBR remains unknown, it is generally accepted to be involved in lipid metabolism and/or transport, heme biosynthesis, cell proliferation, or ion channel functions [2,11,12].

The immunomodulatory role for this receptor includes the ability to induce monocyte chemotaxis [13], modulate cytokine expression and superoxide generation [14], and stimulate formation of antibody-producing cells [6,15]. Moreover, it has the ability to reflect the effect of neuronal injury and neurotoxicity, by a colocalisation with activated microglia (brain resident macrophages) [16-18].

Iodo-PK 11195 [1-(2-iodophenyl)-N-methyl-N-(1-methyl-propyl)-3-isoquinolone carboxamide] is a specific and selective high affinity ligand (K_D 8.0 ± 1.7 nM) for the PBR in all species, comparable with PK 11195 itself (K_D 14.0 ± 3.4 nM) and, in this way, can be used as a diagnostic marker for the PBR. It has neither anxiolytic nor spasmolytic activity, nor interactions with other receptors and has thermodynamically been classified as an antagonist or partial agonist [2]. In vitro work revealed that iodinated PK 11195 binds specifically to the PBR, a binding that was dramatically increased at the sites of brain lesions [19].

In vivo visualisation of the human PBR, and in this way of glial neoplasms, neuronal damage, cellular inflammatory infiltration and microgliosis, has previously been done with ^{11}C radiolabelled PK 11195 [20-28]. Research with this ligand, however, is restricted to institutions with a positron emission tomography (PET) system and an in-house cyclotron that have access to these short-lived positron emitters. Therefore, the availability of a radiolabelled single photon emission computed tomography (SPET) ligand for the study of the PBR would allow a wider application. Similarly, Chalon et al. concluded already that iodinated PK 11195 could be suitable to detect brain injuries in humans by SPET [19].

In a previous study, the *in vivo* behaviour in mice (biodistribution, displacement and metabolisation) and humans (metabolisation) was assessed [29]. In the present study, the in vivo biodistribution and radiation dosimetry of [^{123}I]iodo-PK 11195 following a single intravenous-bolus administration was investigated in 5 healthy volunteers. The [^{123}I]iodo-PK 11195 blood and plasma pharmacological profile was determined. Data obtained from the biodistribution combined with basic pharmacokinetics of [^{123}I]iodo-PK 11195 were used to work out the dosimetry of [^{123}I]iodo-PK 11195 according to the MIRD formulation [30].

PATIENTS AND METHODS

Radionuclide synthesis and quality control

^{123}I was purchased from Amersham Cygne (the Netherlands) and PK 11195 was obtained from RBI (USA). ^{123}I labelled 1-(2-iodophenyl)-N-(1-methyl-propyl)-3-isoquinoline carboxamide ([^{123}I]iodo-PK 11195) was synthesised according to the method described previously [29,31], using a direct displacement of aromatic chlorine under solid-state conditions. The specific activity of the labelled compound was 6.7-17.6 GBq/μmol (180-475 mCi/μmol). The total labelling yield was 50-60% and the radiochemical purity of the final product, as assessed with high performance liquid chromatography (HPLC), was >99%.

Subject accrual and assessment

The study protocol was approved by the Institutional Review Board of the University Hospital. Five healthy volunteers (with regard to medical history and physical examination) consisting of 4 males and 1 female, with a mean weight of 72.4 kg (range 55 to 94 kg), and a mean age of 30.2 years (range 19 to 56 yrs) gave written informed consent. None of them had a clinical history that could have affected the biodistribution or elimination of the radioligand. Thyroid was blocked with Lugol's solution for all volunteers (5% iodine and 10% potassium iodide; one-day protocol of 20 drops one hr before the radioligand injection).

Administered activity measurements

The amount of radioactivity in each syringe containing [^{123}I]iodo-PK 11195 was measured in a dose calibrator before and after injection. The mean dose administered was 112 MBq with a range of 51.8 to 181.7 MBq (1.7-4.9 mCi).

[^{123}I]iodo-PK 11195 gamma camera emission images

Scanning was done with a two-headed large-field-of-view gamma camera system (Helix, GE Medical Systems, Milwaukee, USA) equipped with a medium energy, general purpose, parallel-hole collimator (256×1024 byte-mode matrix). A 20% photopeak window was symmetrically centred on 159 keV. The volunteers were lying supine with a 0.9% saline infusion (Baxter, Belgium) in the left arm (where blood sampling was performed), while the [^{123}I]iodo-PK 11195 was injected in bolus via a peripheral right arm vein. Sequential anterior and posterior whole body scans were performed immediately post-injection and at 0.5, 1, 1.5, 2, 6, 24, 48 and 72 hours post-injection, with a scan speed varying from 12 cm/min for the early to 6 cm/min for the late images. The mean number of total counts of the first scan was 536 kcts in the AP- and 473 kcts in the PA-direction. Conversion from counts to activity was performed based on the initial whole body scan.

Pharmacokinetics and metabolite analysis

Blood samples (citrate tubes) were taken immediately post-injection and 15, 30, 45 sec, 1, 1.5, 2, 3, 5, 7.5, 10, 15, 20, 36, 50, 90 min, 4, 8, 24, 48 h post-injection. Radioactivity was determined with a 3 × 3" NaI (Tl) detector. The amount of radioactivity in the blood was calculated using total blood volume based on the individual haematocrit and expressed as % of injected activity of [^{123}I]iodo-PK 11195. Urine was collected up to 48 hr to measure the fraction of the activity voided by the renal system. Activity not excreted in urine was assumed to be eliminated in faeces. Radioactivity in urine was measured using a well-type ionisation chamber (Radcal Corporation, Monrovia, USA). Analysis of metabolites in plasma and urine was performed with a HPLC system, as described previously [29].

Count rate measurements and organ residence times

Irregularly shaped regions of interests (ROIs) were drawn with a digital track ball along the outer border of those organs that accumulated sufficient activity to be seen clearly on the images. All ROIs were drawn by a single operator, minimising variability in region definition. The ROI set, determined in the anterior image with the best visualisation of the specific organ, was applied to all images, after translation to correct for any difference in subject position at the different acquisition times. Finally, ROIs were mirrored about their long axis for the posterior whole body images. Shapes and sizes were kept constant for all individual emission images. Decay corrected ROIs of the whole-body images were analysed and geometric mean count rates were used to determine source organ time-activity curves. A soft tissue region in the upper thigh was used for background subtraction. A multi-exponential fit was applied to the time-activity curves for the organs and tissues of each subject using in-house software. Residence times of the gall bladder, heart wall, liver and testes were calculated for each of the 5 volunteers. The residence time of the urinary bladder was calculated using the dynamic bladder model of Cloutier et al. with a voiding interval of 4.8 h [32]. For each volunteer the measured fraction of the activity leaving through the kidney – bladder pathway was taken into account. Residence times of the gastrointestinal tract were determined assuming the *ICRP 30* model. The gallbladder was assumed to empty its content every 6 h into the small intestine. Using the obtained individual residence times, target organ absorbed doses and effective dose were calculated using the MIRD method (3.0 software package) [30] with organ weighting factors from *ICRP 60* [33].

RESULTS

Pharmacokinetics and metabolite analysis

Figure 1 shows the percentage of the injected activity of [^{123}I]iodo-PK 11195 in whole blood, plasma, and plasma corrected for metabolites up to 60 minutes post-injection for one subject.

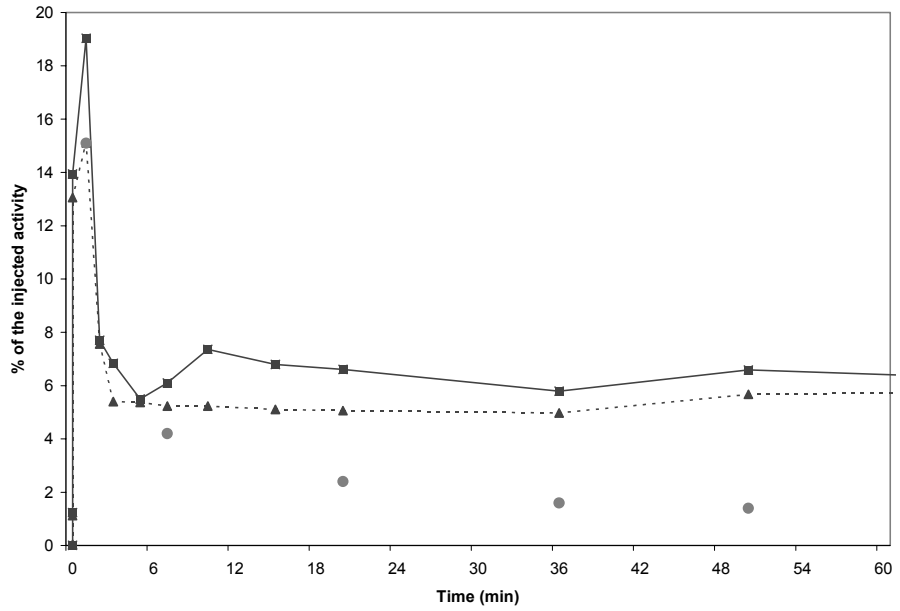

FIGURE 1. Percentage of the injected activity of [^{123}I]iodo-PK 11195 in whole blood, plasma, and plasma corrected for metabolites up to 60 minutes post-injection for one subject

■ whole blood; ▲ plasma; ● plasma corrected for metabolites

The [^{123}I]iodo-PK 11195 was rapidly cleared from the blood pool, primarily by the hepatobiliary system. An average of 77.5 ± 10.2% (range 60.0 to 85.3%) of the administered tracer remained in the soft tissues, which necessitated the background subtraction, especially for small organs.

Analysis of the metabolites in plasma showed a decomposition of the original tracer into two polar metabolites. Figure 2 shows the time course for the average percentage of parent radioactivity of [I^{123}]iodo-PK 11195 and the two major metabolites in venous plasma immediately post-injection, 7.5, 20, 37 and 50 minutes post-injection.

The mean measured urinary excretion was 22.0 ± 3.2% (range 18.9 to 25.2%) of the administered activity at 48 hr post-injection. No unchanged [^{123}I]iodo-PK 11195 was detected in urine.

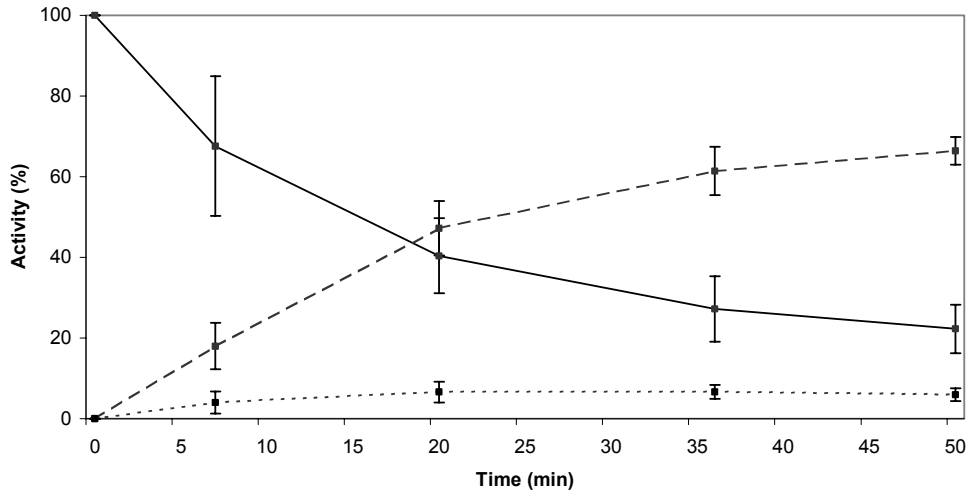

FIGURE 2. Time course for the average percentage (± SD) of parent radioactivity of [123I]iodo-PK 11195 and two major metabolites in venous plasma immediately post-injection, 7.5, 20, 36 and 50 minutes post-injection from five individuals studied.

_____ [123I]iodo-PK 11195

_ _ _ _ _ major metabolite (probably free ^{123}I)

..... other metabolite

Biodistribution and dosimetry

All subjects completed successfully the imaging protocol. No adverse or subjective effects of the tracer on any of the subjects were observed. Serial anterior whole body images of one subject are presented in Figure 3. Visual analysis of the acquired body scans showed avid and rapid liver uptake of the radiopharmaceutical. Activity noted within the gall bladder and bowel provides clear evidence of excretion through the enterohepatic route. No other major organ systems showed significant uptake of [^{123}I]iodo-PK 11195, except for some activity in the heart (average uptake 1.9%, highest uptake 3.1% immediately post-injection) and a small amount of activity in the testes for 2 of the 4 males (average uptake 0.5%, highest uptake 0.6% 7 hr post-injection) and thyroid for 3 subjects (average uptake 0.4%, highest uptake 0.7% 24 hr post-injection). Figure 4 displays the time-activity curves for heart, liver, gallbladder and testis for one subject. Concerning the equilibrium concentrations of tracer (%/ID/g) in various tissues, the following levels for the specific uptake were obtained in the steady-state situation two hours after administration: liver 4.5×10^{-3} %/ID/g (SD=0.5×10^{-3}), heart 9.7×10^{-3} %/ID/g (1.3×10^{-3}) and testes 2.7×10^{-2} %/ID/g (0.5×10^{-2}).

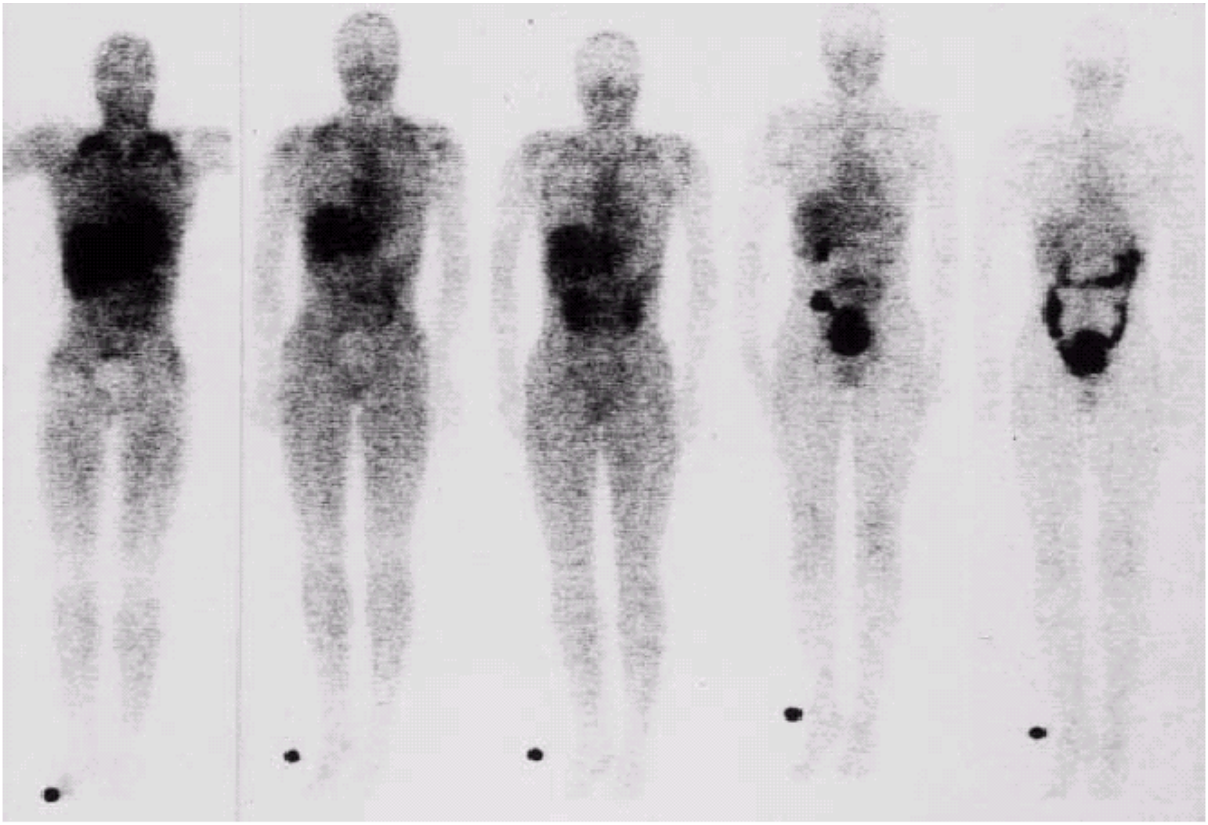

FIGURE 3. Serial anterior whole body images immediately post-injection, 1, 2, 6 and 24-hr post-injection. An intense gallbladder activity is seen on the 6-hr images along with activity in the liver and large bowel system. On the 2-hr images both kidneys can be clearly visualised

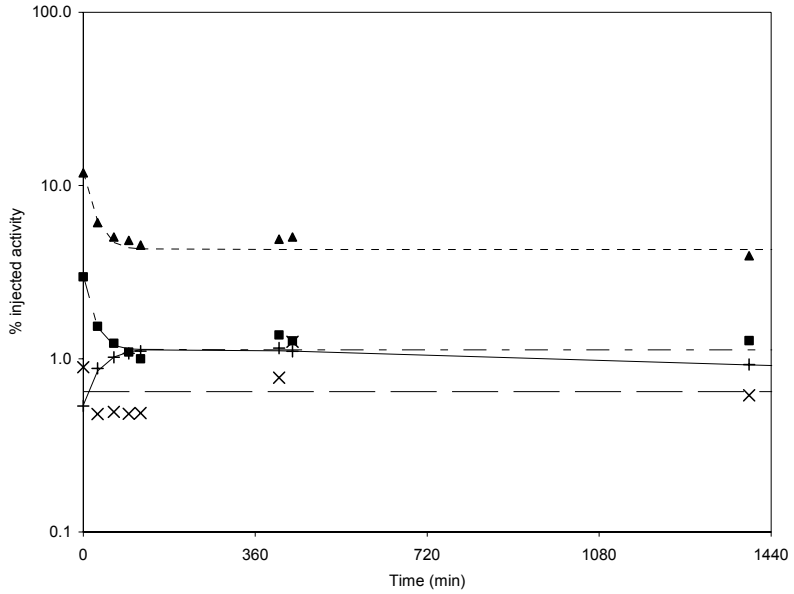

FIGURE 4. Time-activity curves for liver, heart, gallbladder and testis for one subject (expressed as % of the injected activity)▲ Liver (-------- fit line); ■ Heart (— - — fit line); × Gall bladder (— — fit line); + Testes (——— fit line)

Table 1 shows the residence times for each of the 5 volunteers. Except for the remainder compartment, the values were highest for the liver in all subjects. Average organ residence times were 0.74 ± 0.18 hr (range 0.47 to 0.87 hr), 0.44 ± 0.29 hr (range 0.15 to 0.76 hr), and 0.29 ± 0.19 hr (range 0.10 to 0.49 hr) for the liver, upper large intestine, and lower large intestine respectively. Average organ residence time of the testes (4 male volunteers) was 0.17 ± 0.03 (range 0.12 to 0.19 hr). For the one female volunteer the ovary residence time was estimated, based on literature data, assuming a similar specific activity (activity/g) as in the testes [5,34-36]. This procedure was necessary because of the impossibility to draw ROIs in the ovary region due to the superimposed gastrointestinal tract. For testes and ovaries mass, standard values were adopted [37].

TABLE 1. Residence times (hr) in each organ for all subjects

Organ	Subject				
	1	2	3	4	5
GB	0.17	0.15		0.12	0.25
SI	0.12	0.09	0.35	0.34	0.47
ULI	0.20	0.15	0.56	0.54	0.76
LLI	0.13	0.10	0.36	0.35	0.49
Heart wall	0.24	0.39	0.36	0.22	0.17
Liver (* +GB)	0.47	0.85	*0.80	0.71	0.87
UB	0.23	0.22	0.20	0.23	0.27
Testes/Ovaries*	0.12	0.19	0.19	0.18	*0.05
Remainder	15.50	15.30	16.20	15.20	14.10

GB = gallbladder; LLI = lower large intestine; SI = small intestine; ULI = upper large intestine; UB = urinary bladder

Table 2 lists the absorbed dose estimates and effective dose for [^{123}I]iodo-PK 11195 in this sample. The testes received the largest radiation burden: 109.4 ± 19.3 μGy/MBq. Gallbladder wall, upper large intestine and lower large intestine received doses of respectively 48.7 ± 19.4, 39.9 ± 16.2 and 38.3 ± 14.8 μGy/MBq. The ovary dose was estimated to be 138.0 ± 24.3 μGy/MBq. All other organs investigated received doses of 31.5 μGy/MBq or less. The mean effective dose for the normal adult was estimated to be 40.3 ± 6.6 μSv/MBq.

TABLE 2. Radiation absorbed dose estimates for [^{123}I]iodo-PK 11195

Target organ	Mean (μGy/MBq)	Standard deviation
Adrenals	16.2	0.6
Bone surfaces	23.7	1.0
Brain	11.7	0.6
Breasts	10.1	0.5
Gallbladder wall	48.7	19.4
Heart Wall	31.5	7.8
Kidneys	15.2	0.6
Liver	21.9	3.4
LLI wall	38.3	14.8
Lungs	14.2	0.7
Muscle	13.1	0.6
Ovaries	138.0	24.3
Pancreas	17.5	0.5
Red marrow	13.0	0.6
Skin	9.1	0.4
Small intestine	24.9	6.8
Spleen	14.7	0.6
Stomach	15.8	0.7
Testes	109.4	19.3
Thymus	14.0	0.9
Thyroid	13.4	0.7
Total body	14.3	0.7
ULI wall	39.9	16.2
Urinary bladder wall	29.9	1.6
Uterus	19.4	1.5
Effective dose (μSv/MBq)	40.3	6.6

LLI = lower large intestine; ULI = upper large intestine

DISCUSSION

The present study is the first study to describe the biodistribution and dosimetry of radiolabelled PK 11195 for SPET in humans. Although several reports described the use of [^{11}C]PK 11195 in various diseases, there has been to date no report of a biodistribution, dosimetry or quantitative compartmental modelling of [^{11}C]PK 11195 data because of inconsistent plasma data hampering the application of quantification methods that rely on establishing a plasma input function, the lack of procedures for the determination and quantification of circulating radiolabelled metabolites in healthy volunteers and the lack of a "reference" brain region devoid of specific signal. Recently however, a cluster analytical approach, that functionally extracts a distinct kinetic component representing normal ligand kinetics, was proposed as a viable means of generating an input function to the simplified reference tissue model in the analysis of [^{11}C]PK 11195 clinical data [38]. Thus, in normal brain tissue, only the use of a saturation procedure (coinjection with saturating amounts of cold PK 11195) has been able to demonstrate the specific binding of [^{11}C]PK 11195, but its precise quantification was complicated due to the displacement, and subsequent release into the systemic circulation, of radiotracer bound specifically to peripheral organ tissues, resulting in transiently enhanced uptake in the brain [39]. In this way, Petit-Taboué et al. and Sette et al. performed challenge studies in baboons with saturating doses of cold ligands which confirmed the specific in vivo binding, both in the unlesioned, physiological state as after focal induced ischaemia [40,41].

[^{123}I]iodo-PK 11195 appears to be a radiopharmaceutically safe radioligand and did not produce any subjective or objective pharmacological effects in human volunteers in this series. This is consistent with literature since PK 11195 was not reported to have a perceptible effect on humans, certainly in the nanomolar dose range administered as a radioligand [2,42].

The biodistribution of radiolabelled iodo-PK 11195 has previously been described in mice [29,43], rats, and dogs [44]. In rats, the tracer exhibited preferential accumulation in organs known to be high in PBR density, such as heart and especially adrenal gland. This accumulation could be decreased with as much as 87% by pre-treatment of rats with 5 mg/kg cold PK 11195 [31]. Similarly, Hashimoto et al. found that the radioactivity after administration of ^{3}H-PK 11195 in mice was significantly decreased by the coadministration of carrier PK 11195 [43]. In none of the subjects in the present study, however, an uptake of activity was seen in the adrenal gland. In dogs, the highest activity was found in bile [44], which is consistent with the observed activity in gallbladder in the present study. Moreover, the secondary peak in plasma concentration noted in one volunteer at approximately 24 hrs can be explained by an enterohepatic recycling phenomenon, as previously described by Ferry et al. [42].

From the first hr up to 24 hr post-injection, testis activity could be clearly seen in 2 of the 4 males, which is consistent with the known presence of PBRs in the Leydig secreting cells of the testis. This testis activity is reflected in the rather high gonadal dose with this dose contributing primarily for 57% to the effective dose. However, the estimated dose received by the ovaries is probably an overestimation due to the fact that, although not properly compared in humans and given the influence

of various endocrine and paracrine hormones, the number of peripheral benzodiazepine receptors in human ovaries is probably not as high as in testes, corresponding to the fact that the ovaries could not be traced on the whole-body sections [34,45,46]. In this way, the assumption of a similar specific activity in ovaries as in testes has probably made us overestimate the dose. Moreover, one has to take into consideration that [^{123}I]iodo-PK 11195 will be predominantly used in patients with neurodegenerative diseases outside the reproductive age range.

Also, thyroid showed significant accumulation of the tracer in 3 of the 5 subjects on the late images, despite thyroid blockage with Lugol's solution. In spite of the presence of PBRs in thyroid tissue [44], the uptake of radioactivity at this time point most likely reflects the uptake of free iodide resulting from the *in vivo* dehalogenation.

Previous metabolite analysis in mice showed a dramatic metabolisation of [^{123}I]iodo-PK 11195 in blood (± 55%) within 2.5 minutes, with the major metabolite most likely being free ^{123}I. In brain and heart however, the only radioactive compound found was the original product [29], probably due to the fact that the major metabolites do not enter the heart and brain. Similarly, Hashimoto et al. found no radioactive metabolites in heart, lung and brain 20 minutes after intravenous administration of ^{3}H-PK 11195 [43]. In spite of this rapid metabolisation, the absence of radioactive metabolites in the organs mentioned above makes this an appropriate radioligand to study peripheral benzodiazepine receptors in man. Also, the specific activity of [^{123}I]iodo-PK 11195 is comparable with the specific activity of [^{11}C]PK 11195 (18.5-74 GBq/μmol) required for quantitative PET studies as stated by Pike et al. [47].

A rapid penetration of an intact blood-brain barrier is possible, as the level of radioactivity in brain of mice exceeded the one in blood 40 sec. after injection, and thereafter, rapidly cleared from cerebral tissue, with radioactivity levels decreasing below blood levels 10 min. after injection [29]. This rapid rise in cortical and grey matter activity has also been demonstrated by Petit-Taboué et al. with [^{11}C]PK 11195 in baboons [40]. Likewise, Banati et al. showed an increased PK 11195 binding to activated microglia after facial nerve axotomy - a lesion causing a retrograde neuronal reaction without nerve cell death while keeping the blood-brain barrier intact - where the peak of PK 11195 binding was observed 4 days after the peripheral nerve lesion, which is consistent with the well-known time course of microglial activation. Moreover, photoemulsion microautoradiography confirmed the restriction of PK 11195 binding to activated microglia, where the full transformation of microglia into parenchymal phagocytes is not necessary to reach maximal levels of PK 11195 binding. The authors concluded that PK 11195 is a well-suited marker to detect microglial activation in areas of subtle brain pathology, where neither a disturbance of blood-brain barrier function nor the presence of macrophages and inflammatory cells indicate an on-going disease process [48]. In the present study, the highest brain uptake was approximately 2.0 ± 0.5% (range 1.0 to 3.1%), which is expected due to the low concentration of PBRs throughout the brain in healthy volunteers.

Probably, the agent is not appropriate for SPET imaging of the gastrointestinal tract due to the main excretion by the gastrointestinal system and the high abdominal activity. Even so, [^{123}I]iodo-PK 11195 seems theoretically promising for imaging of the heart, due to the electrophysiological and pharmacological evidence that PBRs are coupled to calcium channels in the heart [49]. However, cardiac imaging may prove difficult, due to the large liver and gallbladder uptake.

These findings suggest that [^{123}I]iodo-PK 11195 can be used safely in clinical investigations of the PBR for the imaging of neuroinflammatory lesions. The radiation absorbed doses are low enough to allow 185 MBq of activity to be administered to a healthy volunteer during each study, giving an average effective dose of 7.46 mSv. This administered dose is comparable with other [^{123}I]labelled receptor ligands as β-CIT, FP-CIT and IBZM [50,51]. For quantitative PET studies with [^{11}C]PK 11195, 185-888 MBq is required to be injected intravenously [26,27,47].

Concerning the proper imaging time post-injection, no dynamic SPET scans were performed in the present study, but a period of 30 to 90 minutes post-injection seems adequate. Indeed, Sette et al. noticed stable [^{11}C]PK 11195 uptake ratios across various gray matter structures analysed as early as 20 minutes after injection with no significant relation between [^{11}C]PK 11195 uptake and corresponding cerebral blood flow ratios between 20 and 60 minutes post-injection [41]. Likewise, Pappata et al found in a patient with a glioblastoma a tumor/normal gray matter ratio of 2.12 at 10 min which remained quite constant until the end of the study (60 min post-injection) [21].

CONCLUSIONS

^{123}I labelled iodo-PK 11195 is a suitable agent for the visualisation of the PBR and indirectly for the imaging of neuroinflammatory lesions. Taking into account the acceptable radiation burden of 7.46 mSv following an administration of 185 MBq, a ^{123}I labelled iodo-PK 11195 investigation has to be considered as an ICRP risk category IIb investigation with minor to intermediate risk, requiring a moderate benefit [52].

REFERENCES

1. Braestrup C, Squires RF. Specific benzodiazepine receptors in rat brain characterized by high-affinity (^{3}H)diazepam binding. *Proc Natl Acad Sci U S A* 1999; 74:3805-3809.
2. Parola AL, Yamamura HI, Laird HE. Peripheral-type benzodiazepine receptors. *Life Sci* 1993; 52:1329-1342.
3. Awad M, Gavish M. Peripheral-type benzodiazepine receptors in human cerebral cortex, kidney, and colon. *Life Sci* 1991; 49:1155-1161.
4. Cymerman V, Pazo SA, Palacios JM. Evidence for species differences in "peripheral" benzodiazepine receptors: an autoradiographic study. *Neurosci Lett* 1986; 66:153-158.
5. Weizman R, Gavish M. Molecular cellular and behavioral aspects of peripheral-type benzodiazepine receptors. *Clin Neuropharmacol* 1993; 16:401-417.
6. Zavala F, Haumont J, Lenfant M. Interaction of benzodiazepines with mouse macrophages. *Eur J Pharmacol* 1984; 106:561-566.
7. Taniguchi T, Spector S. Properties of [^{3}H]-diazepam binding to rat peritoneal mast cells. *Life Sci* 1980; 27:171-178.
8. Schoemaker H, Bliss M, Yamamura HI. Specific high affinity saturable binding of [3H]Ro5-4864 to benzodiazepine binding sites in rat cerebral cortex. *Eur J Pharmac* 1981; 71:173-175.
9. Richards JG, Mohler H. Benzodiazepine receptors. *Neuropharmacology* 1984; 23:233-242.
10. Benavides J, Quarteronet D, Plouin PF, Imbault F, Phan T, Uzan A, Renault C, Dubroeucq MC, Gueremy C, Le-Fur G. Characterization of peripheral type benzodiazepine binding sites in human and rat platelets by using [3H]PK 11195. Studies in hypertensive patients. *Biochem Pharmacol* 1984; 33:2467-2472.
11. Zisterer DM, Williams DC. Peripheral-type benzodiazepine receptors. *Gen Pharmac* 1997; 29:305-314.
12. Olson JM, Ciliax BJ, Mancini WR, Young AB. Presence of peripheral-type benzodiazepine binding sites on human erythrocyte membranes. *Eur J Pharmacol* 1988; 152:47-53.
13. Ruff MR, Pert CB, Weber RJ, Wahl LM, Wahl SM, Paul SM. Benzodiazepine receptor-mediated chemotaxis of human monocytes. *Science* 1985; 229:1281-1283.
14. Zavala F, Taupin V, Descamps-Latscha B. In vivo treatment with benzodiazepines inhibits murine phagocytic oxidative metabolism and production of interleukin 1, tumor necrosis factor and interleukin-6. *J Pharmacol Exp Ther* 1990; 255:442-450.
15. Zavala F, Lenfant M. Benzodiazepines and PK 11195 exert immunomodulating activities by binding on a specific receptor on macrophages. *Ann N Y Acad Sci* 1987; 496:240-249.
16. Guilarte TR, Kuhlmann AC, O'Callaghan JP, Miceli RC. Enhanced expression of peripheral benzodiazepine receptors in trimethyltin-exposed rat brain: a biomarker of neurotoxicity. *Neurotoxicology* 1995; 16:441-450.
17. Stephenson DT, Schober DA, Smalstig EB, Mincy RE, Gehlert DR, Clemens JA. Peripheral benzodiazepine receptors are colocalized with activated microglia following transient global forebrain ischemia in the rat. *J Neurosci* 1995; 15:5263-5274.
18. Myers R, Manjil LG, Cullen BM, Price GW, Frackowiak RS, Cremer JE. Macrophage and astrocyte populations in relation to [3H]PK 11195 binding in rat cerebral cortex following a local ischaemic lesion. *J Cereb Blood Flow Metab* 1991; 11:314-322.
19. Chalon S, Pellevoisin C, Bodard S, Vilar MP, Besnard JC, Guilloteau D. Iodinated PK 11195 as an ex vivo marker of neuronal injury in the lesioned rat brain. *Synapse* 1996; 24:334-339.
20. Banati RB, Goerres G, Perkin D, et al. Imaging microglial activation in vivo. J Cereb Blood Flow Metab 1997; 17: S435(Abstract)

21. Pappata S, Cornu P, Samson Y, Prenant C, Benavides J, Scatton B, Crouzel C, Hauw JJ, Syrota A. PET study of carbon-11-PK 11195 binding to peripheral type benzodiazepine sites in glioblastoma: a case report. *J Nucl Med* 1991; 32:1608-1610.
22. Junck L, Olson JM, Ciliax BJ, Koeppe RA, Watkins GL, Jewett DM, McKeever PE, Wieland DM, Kilbourn MR, Starosta RS, et a. PET imaging of human gliomas with ligands for the peripheral benzodiazepine binding site. *Ann Neurol* 1989; 26:752-758.
23. Junck L, Jewett DM, Kilbourn MR, Young AB, Kuhl DE. PET imaging of cerebral infarcts using a ligand for the peripheral benzodiazepine binding site. Neurology 1990; 40: 265(Abstract)
24. Banati RB, Myers R, Goerres G, Kreutzberg GW, Brooks DJ. [11C] PK11195 PET-imaging of microglial Activation in Multiple Sclerosis. Neurology 1997; 48: A313(Abstract)
25. Ramsay SC, Weiller C, Myers R, Cremer JE, Luthra SK, Lammertsma AA, Frackowiak RS. Monitoring by PET of macrophage accumulation in brain after ischaemic stroke [letter]. *Lancet* 1992; 339:1054-1055.
26. Vowinckel E, Reutens D, Becher B, Verge G, Evans A, Owens T, Antel JP. PK11195 binding to the peripheral benzodiazepine receptor as a marker of microglia activation in multiple sclerosis and experimental autoimmune encephalomyelitis. *J Neurosci Res* 1997; 50:345-353.
27. Groom GN, Junck L, Foster NL, Frey KA, Kuhl DE. PET of peripheral benzodiazepine binding sites in the microgliosis of Alzheimer's disease. *J Nucl Med* 1995; 36:2207-2210.
28. Banati RB, Goerres GW, Myers RN, Gunn RN, Turkheimer FE, Kreutzberg GW, Brooks DJ, Jones T, Duncan JS. [^{11} C](R)-PK11195 positron emission tomography imaging of activated microglia in vivo in Rasmussen's encephalitis. *Neurology* 1999; 53:2199-2203.
29. Dumont F, De Vos F, Versijpt J, Jansen HML, Korf J, Dierckx RA, Slegers G. In *vivo* evaluation in mice and metabolism in blood of human volunteers of [^{123}I] Iodo-PK11195: a possible SPECT tracer for visualization of inflammation. *Eur J Nucl Med* 1999; 26:194-200.
30. Loevinger R, Budinger TF, Watson EE. MIRD primer for absorbed dose calculations. New York: Society of Nuclear Medicine; 1991:1-21.
31. Gildersleeve DL, Lin TY, Wieland DM, Ciliax BJ, Olson JM, Young AB. Synthesis of a high specific activity ^{125}I-labeled analog of PK 11195, potential agent for SPECT imaging of the peripheral benzodiazepine binding site. *Int J Rad Appl Instrum B* 1989; 16:423-429.
32. Cloutier R, Smith S, Watson E, Snyder W, Warner G. Dose to the fetus from radionuclides in the bladder. *Health Phys* 1973; 25:147-161.
33. International Commission on Radiological Protection. *1990 recommendations of the international commission on radiological protection, ICRP Publication 60.* Oxford: Pergamon Press; 1990:6-8.
34. Bar-Ami S., Fares F, Gavish M. Altered peripheral benzodiazepine receptor density in human granulosa-lutein cells in relation to follicular maturity. *Mol Cell Endocrinol* 1991; 82:285-291.
35. Toranzo D, Tong Y, Tonon MC, Vaudry H, Pelletier G. Localization of diazepam-binding inhibitor and peripheral type benzodiazepine binding sites in the rat ovary. *Anat Embryol Berl* 1994; 190:383-388.
36. Amsterdam A, Suh BS. An inducible functional peripheral benzodiazepine receptor in mitochondria of steroidogenic granulosa cells. *Endocrinology* 1991; 129:503-510.
37. Snyder WS, Cook MJ, Karhausen LR, Nasset ES, Howells GP, Tipton IH. *Report of the task group on reference man*. Oxford: Pergamon Press, 1974.
38. Myers R, Gunn RN, Cunningham VJ, Banati RB, Jones T. Cluster analysis and the reference tissue model in the analysis of clinical [^{11}C]PK11195 PET. J Cereb Blood Flow Metab 1999; 19: S789-S789(Abstract)
39. Petit-Taboue MC, Baron JC, Gourand F, Ravenel N, Barré L, Travere JM, MacKenzie ET. Specific binding of [^{11}C]-PK 11195 to w_3 sites in the baboon brain as demonstrated by positron emission tomography. *Circ Metab Cerv* 1991; 8:285-297.

40. Petit-Taboue MC, Baron JC, Barre L, Travere JM, Speckel D, Camsonne R, MacKenzie ET. Brain kinetics and specific binding of [^{11}C]PK 11195 to w_3 sites in baboons: positron emission tomography study. *Eur J Pharmacol* 1991; 200:347-351.
41. Sette G, Baron JC, Young AR, Miyazawa H, Tillet I, Barre L, Travere JM, Derlon JM, MacKenzie ET. In vivo mapping of brain benzodiazepine receptor changes by positron emission tomography after focal ischemia in the anesthetized baboon. *Stroke* 1993; 24:2046-2057.
42. Ferry A, Jaillon P, Lecocq B, Lecocq V, Jozefczak C. Pharmacokinetics and effects on exercise heart rate of PK 11195 (52028 RP), an antagonist of peripheral benzodiazepine receptors, in healthy volunteers. *Fundam Clin Pharmacol* 1989; 3:383-392.
43. Hashimoto K, Inoue O, Suzuki K, Yamasaki T, Kojima M. Synthesis and evaluation of 11C-PK 11195 for in vivo study of peripheral-type benzodiazepine receptors using positron emission tomography. *Ann Nucl Med* 1989; 3:63-71.
44. Gildersleeve DL, Van-Dort ME, Johnson JW, Sherman PS, Wieland DM. Synthesis and evaluation of [^{123}I]-iodo-PK11195 for mapping peripheral-type benzodiazepine receptors (omega 3) in heart. *Nucl Med Biol* 1996; 23:23-28.
45. Bovolin P, Schlichting J, Miyata M, Ferrarese C, Guidotti A, Alho H. Distribution and characterization of diazepam binding inhibitor (DBI) in peripheral tissues of rat. *Regul Pept* 1990; 29:267-281.
46. Calvo DJ, Ritta MN, Calandra RS, Medina JH. Peripheral-type benzodiazepine receptors are highly concentrated in mitochondrial membranes of rat testicular cells. *Neuroendocrinology* 1990; 52:350-353.
47. Pike VW, Halldin C, Crouzel C, Barre L, Nutt DJ, Osman S, Shah F, Turton DR, Waters SL. Radioligands for PET studies of central benzodiazepine receptors and PK (peripheral benzodiazepine) binding sites--current status [published erratum appears in Nucl Med Biol 1993 Aug;20(6):I]. *Nucl Med Biol* 1993; 20:503-525.
48. Banati RB, Myers R, Kreutzberg GW. PK ('peripheral benzodiazepine')--binding sites in the CNS indicate early and discrete brain lesions: microautoradiographic detection of [3H]PK11195 binding to activated microglia. *J Neurocytol* 1997; 26:77-82.
49. Mestre M, Carriot T, Belin C, Uzan A, Renault C, Dubroeucq MC, Gueremy C, Doble A, Le-Fur G. Electrophysiological and pharmacological evidence that peripheral type benzodiazepine receptors are coupled to calcium channels in the heart. *Life Sci* 1985; 36:391-400.
50. Brucke T, Podreka I, Angelberger P, Wenger S, Topitz A, Kufferle B, Muller C, Deecke L. Dopamine D2 receptor imaging with SPECT: studies in different neuropsychiatric disorders. *J Cereb Blood Flow Metab* 1991; 11:220-228.
51. Seibyl JP, Marek K, Sheff K, Zoghbi S, Baldwin RM, Charney DS, van-Dyck CH, Innis RB. Iodine-123-beta-CIT and iodine-123-FPCIT SPECT measurement of dopamine transporters in healthy subjects and Parkinson's patients. *J Nucl Med* 1998; 39:1500-1508.
52. Radiological protection in biomedical research. Annals of the ICRP. (22, No. 3). 1992. Oxford, Pergamon Press. ICRP publication 62.

CHAPTER FIVE

VALIDATION OF RADIOLABELLED PK11195 AS AN INFLAMMATORY TRACER IN MULTIPLE SCLEROSIS

MULTIPLE SCLEROSIS

Multiple Sclerosis (MS) is the prototype inflammatory autoimmune disorder of the central nervous system and, with a lifetime risk of one in 400, potentially the most common cause of neurological disability in young adults. As with all complex traits, the disorder results from an interplay between as yet unidentified environmental factors and susceptibility genes. Together, these factors trigger a cascade of events, involving engagement of the immune system, acute inflammatory injury of axons and glia, recovery of function and structural repair, post-inflammatory gliosis, and neurodegeneration. The sequential involvement of these processes underlies the clinical course characterised by episodes with recovery, episodes leaving persistent deficits, and secondary progression. The aim of treatment is to reduce the frequency, and limit the lasting effects, of relapses, relieve symptoms, prevent disability arising from disease progression, and promote tissue repair. Despite limited success in each of these categories, everyone touched by multiple sclerosis looks for a better dividend from applying an improved understanding of the pathogenesis to clinical management.

The present part reviews the history, epidemiology, pathophysiology, clinical features and disease course, and treatment of MS.

HISTORY AND EPIDEMIOLOGY

Previously unrecognised, multiple sclerosis makes a fleeting appearance in the early 19th century before taking centre stage as clinical neurology began to flourish in the 1860s. By the beginning of the 20th century, a disease only a few years earlier meriting individual case reports had become one of the most common reasons for admission to a neurological ward. The incidence of MS is greatest at the extremes of latitude in both the northern and southern hemispheres (hence rarely observed in Asians or Africans) and affects almost twice as many women as it does men (at least in the most common relapsing remitting type of MS); this unexplained bias mimics that seen in other putative autoimmune diseases. The disease has an incidence of about seven per 100 000 every year, prevalence of around 50 to 150 per 100 000 for Caucasians, and a lifetime risk ranging from one in 1000 to one in 250. Now, multiple sclerosis is recognised throughout the world, with around 2.5 million affected individuals. These crude statistics conceal the harsh reality of a frightening and potentially disabling disease for young adults.

PATHOPHYSIOLOGY

The oligodendrocyte, a principal target of immune attack in multiple sclerosis, synthesises and maintains the myelin sheath of up to 40 neighbouring nerve axons in the central nervous system. Compact myelin consists of a condensed membrane, spiralled around axons to form the insulating segmented sheath needed for saltatory axonal conduction: voltage-gated sodium channels cluster at the unmyelinated nodes of Ranvier, between myelin segments, from where the action potential is

propagated and spreads passively down the myelinated nerve segment to trigger another action potential at the next node.

The consequences of demyelination for saltatory conduction explain many clinical and laboratory features of multiple sclerosis. Partially demyelinated axons conduct impulses at reduced velocity - explaining the characteristic delays in conduction of evoked potentials. Demyelinated axons can discharge spontaneously and show increased mechanical sensitivity - accounting for the flashes of light on eye movement (phosphenes) and electrical sensation running down the spine or limbs on neck flexion (Lhermitte's sign). Partially demyelinated axons, whose safety factor for conduction is compromised, cannot sustain the fall in membrane capacitance induced by a rise in temperature, and conduction fails - leading to the characteristic appearance of symptoms and signs after exercise or a hot bath (Uhthoff's phenomenon). Ephaptic transmission (cross-talk) can arise between neighbouring demyelinated axons, resulting in paroxysmal symptoms - trigeminal neuralgia, ataxia, and dysarthria, or painful tetanic posturing of the limbs, lasting one or two minutes and often triggered by touch or movement. Individuals with multiple sclerosis characteristically tire during physical and cognitive tasks, and take longer to recover: although poorly understood, and probably multifactorial, fatigue in multiple sclerosis can be very disabling, even in isolation.

The symptoms and signs of multiple sclerosis merely reflect the functional anatomy of impaired saltatory conduction at affected sites. The cerebrum is almost always involved when assessed with magnetic resonance imaging (MRI), but most white matter abnormalities cannot be linked to specific events or clinical symptoms, anyway, new lesions appear to occur at least seven to ten times more frequently than clinical attacks, where especially the correlation between T2 lesions and disability is poor (clinicoradiological paradox) [1]. Involvement of the anterior visual pathway is the rule. Lesions of the brainstem and cerebellar pathways produce precise clinicopathological correlations; typically, coordinated movement of the eyes, limbs, bulbar musculature, and axial muscles is disrupted. The spinal cord is frequently affected, leading to alterations in motor, sensory, and autonomic functions.

One hypothesis to explain the breakdown of immune regulation in autoimmune diseases is molecular mimicry, which suggests that a peptide (the environmental factor), presented in the groove of specific class II molecules (one component of inherited risk), is immunologically indistinguishable from self-antigen and, hence, an appropriate response to infection generates inappropriate inflammation against some component of the oligodendrocyte-myelin unit. Also, damage to normal tissue may expose novel antigens to the immune system that would otherwise not be contacted and further direct attack against nearby self-antigens, i.e. epitope spreading. In common with all organ-specific autoimmune diseases, this systemic defect results not in a sustained autoimmune attack on the entire target organ but, rather, in inflammatory lesions that are temporally and spatially segregated.

MOLECULAR GENETICS AND ENVIRONMENTAL FACTORS

Multiple sclerosis is caused by an interplay between genes and environment. There is a familial recurrence rate of about 15%. The age-adjusted risk is higher for siblings (3-5%), parents (2%), and children (2%) than for second-degree and third-degree relatives. Recurrence in monozygotic twins is around 25-35%. Recurrence is higher in the children of conjugal pairs with multiple sclerosis (20%) than in the offspring of single affecteds (2%). Conversely, the risk is not increased either for individuals adopted into a family with an affected individual or in the non-biological relatives of adoptees who themselves develop multiple sclerosis.

Multiple sclerosis seems to be genuinely polygenic in which the genes responsible for the complex traits are not mutations coding for aberrant gene products but normal polymorphisms [2]. They act independently or through epistasis, and each polymorphism can exert a small contributory effect on some as yet undefined structure or physiological function. Extensive searches have yielded few secure candidate regions. Results of population studies suggest an association between the human leucocyte antigen (HLA) class II MHC alleles which code for molecules that participate in antigen recognition by T lymphocytes and the gene for TNF-α encoded within the same linkage group. The list of candidate genes that have been screened includes many adhesion molecules, immune receptors or accessory molecules, cytokines and their receptors or antagonists, chemokines, growth promoting molecules, and structural genes of the myelin-oligodendrocyte unit. Disappointingly, the low yield from this trawl is not definitively advanced by eight whole genome linkage screens done in several countries [3]. In common with most other complex traits, no major susceptibility gene has yet been identified, although several promising chromosomal linkages are provisionally linked and associated with multiple sclerosis - at 1p, 6p, 10p, 17q, and 19q [4].

The distribution of multiple sclerosis cannot be explained on the basis of population genetics alone. Outside Europe, prevalence rates among white people are half those documented for many parts of northern Europe. In Australia and New Zealand, there are gradients in frequency that do not follow genetic clines. The risk is higher for English-speaking white people who migrate into South Africa as adults than as children. The low frequency of multiple sclerosis in Africans increases substantially for first-generation descendants raised in the UK. Results of surveys of multiple sclerosis have prompted speculation on the occurrence of epidemics in Iceland, the Orkney and Shetland Islands, and the Faroes (where MS was unknown until 1940 when British soldiers landed on its shores), although others prefer the interpretation that these merely indicate improved case recognition. There is age-linked susceptibility to viral exposure in those who are constitutionally at risk of developing the disease. Attempts to reliably implicate specific environmental agents are frustrating. Recent, yet unsubstantiated candidates, include Chlamydia pneumoniae [5], Ebstein-Barr Virus, and human herpesvirus type 6 [6].

CLINICAL DIAGNOSIS

Revised diagnostic criteria classify individuals in the categories of multiple sclerosis, not multiple sclerosis, or possible multiple sclerosis, and incorporate evidence from MRI. As with the previous diagnostic criteria, individuals must have a minimum of two attacks, affecting more than one anatomical site, but, assuming an initial presentation suggestive of multiple sclerosis, the second lesion need not necessarily be clinically expressed [7].

Investigations are done for four main reasons in patients with multiple sclerosis: they allow to see the anatomical dissemination of lesions in time and space (imaging); they permit the assessment of intrathecal inflammation (spinal fluid analysis); they show that conduction has altered in a pattern consistent with demyelination (evoked potentials); and they allow the exclusion of conditions that mimic the disease.

More than 95% of patients with multiple sclerosis have T2-weighted white matter abnormalities, but these are not diagnostic. They occur about 10 times more frequently than new clinical events. Imaging is not necessary for diagnostic purposes in patients with a history of relapsing disease, affecting multiple sites within the central nervous system. The major practical use is in the investigation of individuals with clinically isolated lesions or progressive disease at a single site. There is less cerebral involvement in patients with primary progressive multiple sclerosis than in those who have comparable disability from secondary progression. Variations in imaging protocols are beginning to distinguish separate components of the underlying pathological process - inflammation (gadolinium DTPA enhancement of T1-weighted lesions, reflecting a breach in the normal blood-brain barrier and indicating that the lesion is of recent origin), demyelination (magnetisation transfer ratio), astrocytosis (T2-weighted lesions, the signal arising from increased water content), and axonal damage (reduction in diffusion tensor imaging anisotrophy and N-acetyl-aspartate spectra with chemical shift imaging, or the presence of focal atrophy and T1-weighted black holes) [8].

Cerebrospinal fluid protein electrophoresis shows oligoclonal IgG bands in more than 90% of cases. Their role in the pathogenesis of multiple sclerosis is unresolved. Screening spinal fluid against cDNA expression, phage display, or random peptide libraries has not distinguished common antigen specificities; some antibodies are directed against components of the oligodendrocyte or its myelin membranes, and others recognise extrinsic antigens including viruses, but collectively these specificities only account for a minority of the bands. Diagnostically, spinal fluid oligoclonal bands confirm that the underlying pathology is inflammatory, which can be useful in excluding alternative explanations, especially in the context of progressive spinal cord syndromes and in elderly patients in whom imaging abnormalities are not discriminatory.

Demyelination characteristically delays the latencies of visual, auditory, and somatosensory evoked potentials, as well as central motor conduction times, leaving the amplitude of responses unchanged. Before the advent of MRI, these abnormalities provided evidence for clinically silent lesions; now, their

role is confined to the provision of circumstantial evidence for demyelination in diagnostically difficult situations, such as syndromes that progress from onset.

NATURAL HISTORY AND EVOLUTION OF THE PLAQUES

80-90% of patients present with relapsing - remitting disease and, typically, the illness passes through phases of relapse with full recovery, relapse with persistent deficit, and secondary progression. In about a quarter of patients, multiple sclerosis never affects activities of daily living; conversely, up to 15% become severely disabled within a short time. Episodes happen at random intervals, but initially average about one per year, decreasing steadily thereafter. In 10-20% of patients, the disease is progressive from onset, hence termed primary progressive - affecting the spinal cord and, less frequently, the optic nerve, cerebrum, or cerebellum. Disease onset is usually in the third or fourth decade, but 2% of patients with multiple sclerosis present before the age of 10 years, and 5% before age 16 years. In children, the distinction from acute disseminated encephalomyelitis can often only be established by observing the subsequent natural history. Overall, life expectancy is at least 25 years from disease onset with most patients dying from unrelated causes.

The prognosis is relatively good when sensory or visual symptoms dominate the course of multiple sclerosis in adults, and there is complete recovery from individual episodes. This pattern is most common in young women. Conversely, motor involvement, especially when coordination or balance are disturbed, has a less positive prognosis. The outlook is also poor in older men who develop the disease. Frequent and prolonged relapses with incomplete recovery at onset and a short interval between the initial episode and first relapse are adverse prognostic features [9], but the main determinant of disability is onset of the progressive phase [10].

Fixed disability in multiple sclerosis is acquired through two distinct mechanisms: incomplete recovery from relapse and disease progression. Patients with relapsing-remitting multiple sclerosis accumulate disability from disease onset more slowly than those with primary progressive multiple sclerosis. However, beyond a degree of disability sufficient to limit walking to less than 500 m without aid or rest (Kurtzke expanded disability status scale [EDSS] of 4.0), subsequent accumulation no longer correlates with mode of presentation, suggesting that the pathological substrate for progression determines disability at this stage of the disease [11].

Prospective studies show that around 10% of upper respiratory (adenovirus) and gastrointestinal infections, arising in patients with multiple sclerosis, are followed by relapse, and about 30% of new episodes relate to infection. There is no evidence that trauma causes multiple sclerosis, triggers latent disease in someone who has the underlying disease process, or alters the course in individuals who have already experienced symptoms. People with multiple sclerosis cope less well with symptoms while exposed to stress, but psychological factors do not directly affect disease activity.

Maturation of the individual lesion involves several stages: a) immune engagement, b) acute inflammatory injury of axons and glia, c) recovery of function and structural repair and d) post-inflammatory gliosis and neurodegeneration. Healthy individuals harbour autoreactive myelin T cells, normally kept in check by regulatory T cells. Failure of regulation leads to proliferation, activation, and entry into the circulation of autoreactive T cells; they express adhesion molecules and induce reciprocal changes in endothelia, allowing access across the blood-brain barrier into the central nervous system. There, activated T cells re-encounter antigen and activate microglia (the CNS macrophage); they, in turn, express HLA class II molecules, re-present antigen to T cells, and set up a proinflammatory loop, which provides an infiltrate rich in activated T cells and microglia with some neutrophils. On the figure below perivascular inflammation is shown (panel 1) which causes acute axonal transection (panel 2), and microglia-mediated removal of myelin (panel 3) with persistent demyelination despite some remyelination (panel 4); chronic lesions show further axonal loss (panel 5) and gliosis (panel 6). This scheme does not depict primary progressive multiple sclerosis in which there is pronounced axonal degeneration with or without a preceding inflammatory phase [12].

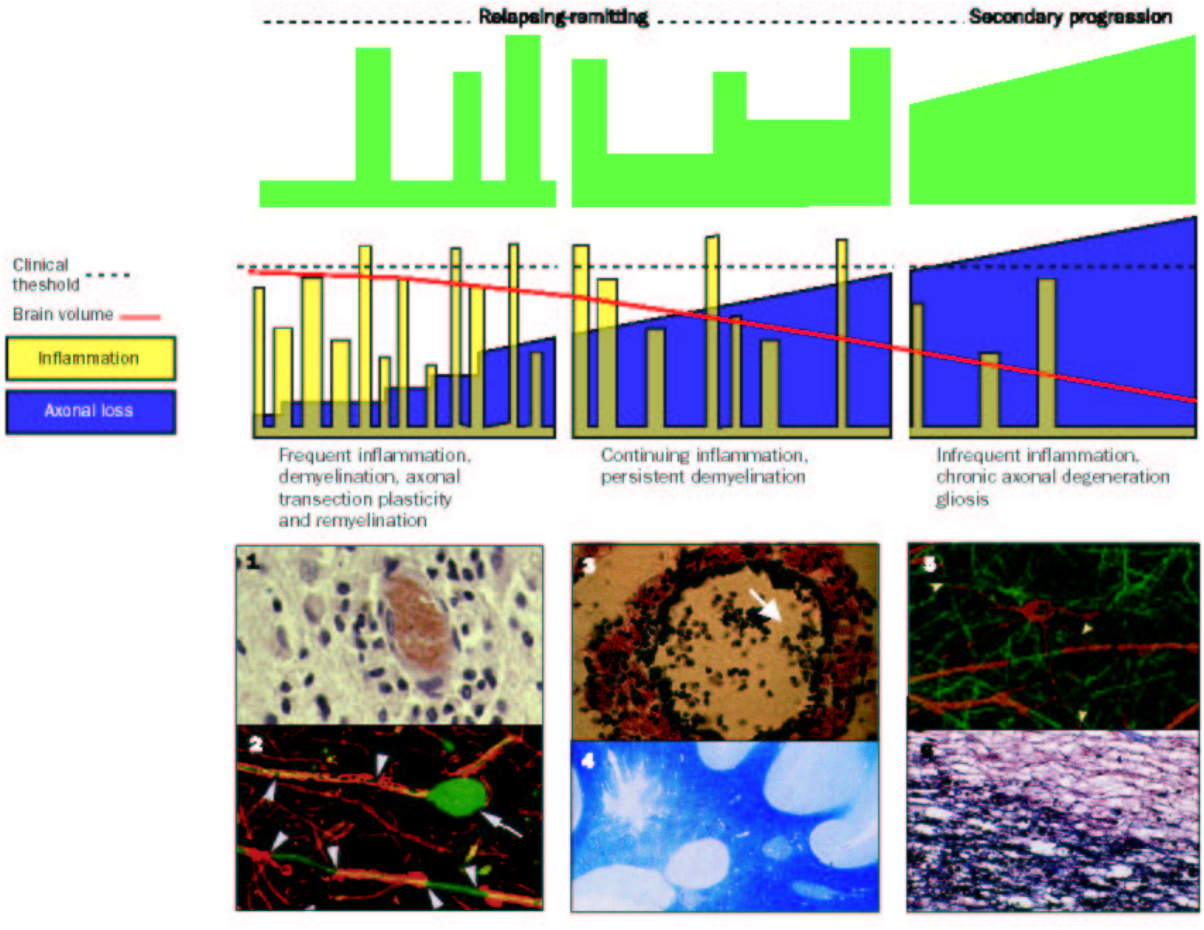

Toxic inflammatory mediators are released, sustaining breakdown of the blood-brain barrier and leading to injury of axons and glia. Nitric oxide might act directly on normal or hypomyelinated axons, transiently blocking conduction [13] and reversibly increasing deficits arising from already compromised pathways. Symptoms also improve as surviving functional pathways are reorganised at

the cellular [14] and systems level [15]. Together, these mechanisms account for remission early in the disease. But tissue vulnerability is easily exposed. When compounded by high axonal firing frequency, nitric oxide causes structural (and hence irreversible) changes to axons [16]. Axonal transection in acute inflammatory plaques is shown histologically [17] and radiologically through reduction in the neuronal spectroscopic marker, N-acetyl aspartate (NAA) [18]. These transected axons undergo Wallerian degeneration during the subsequent 18 months [19], but this action does not seem to extend the lesion or shape the clinical deficit.

Cytokines and growth-promoting factors released by reactive astrocytes and microglia as part of the acute inflammatory process promote endogenous remyelination. But, over time, astrocyte reactivity seals the lesion and gliosis causes a physical barrier to further remyelination, reducing the capacity to accommodate cumulative deficits, and marking transition to the stage of persistent deficit.

Most axonal loss is seen in secondary progressive multiple sclerosis [20]. It is proposed that chronic axonopathy is not due directly to inflammation nor does it occur only colocalised with discrete pathological lesions, but results from loss of trophic support normally provided to axons by myelin or glia, acting directly or through the maintenance of electrical activity, or both [21,22]. As such, chronic axonal degeneration might slowly increase the clinical deficit, decaying a compromised but functioning pathway and leading to disease progression.

TREATMENT

The aims of treatment are to: a) reduce relapse rates, b) prevent fixed disability directly attributable to relapse, c) provide symptomatic management of fixed neurological deficit, d) prevent disability acquired through progression, e) treat established progression.

Reducing relapse rates in multiple sclerosis

Since permanent disability can be caused by incomplete recovery from episodes, relapse frequency is bound to correlate with accumulation of disability during the relapsing-remitting phase of multiple sclerosis. The dividend from reducing the relapse rate is best shown by use of the β-interferons: interferon β-1a, and interferon β-1b. These type-1 interferons were first used in multiple sclerosis for their antiviral action, in view of the known propensity of viral infections to trigger relapses. Their predominant mechanism of action is unknown, but they have been found to suppress T cell proliferation, reduce T cell migration from the systemic circulation into the CNS, alter the T cell cytokine secretion repertoire from relatively proinflammatory Th1 to relatively anti-inflammatory Th2 response, and downregulate class II MHC antigen expression [23]. The annual relapse rate for individuals treated with interferon-β is significantly reduced by 30-37%, however, only with interferon β-1a this change in relapse rate is also accompanied by a reduction in the accumulation of disability [24].

Three other agents reduce relapse frequency, and the accumulation of disability, in relapsing-remitting multiple sclerosis; each has similar efficacy to the β-interferons and acceptable adverse effects profiles. Glatiramer acetate was noted serendipitously to suppress experimental allergic encephalomyelitis, the animal model of demyelinating disease, perhaps by inhibiting the binding of myelin basic protein (MBP) to the T cell receptor or by altering the phenotype of myelin-autoreactive T cells [25], and is able to reduce the annual relapse rate by 25% [26]. Secondly, azathioprine inhibits lymphocyte proliferation by inhibiting purine synthesis, and probably has similar efficacy to the β-interferons, although trial data were less clear-cut [27]. Thirdly, mitoxantrone inhibits DNA repair and synthesis in dividing and non-dividing cells through inhibition of DNA topoisomerase II; it is potentially much more toxic than the β-interferons, and is mainly used for the treatment of aggressive relapsing disease, including patients with high relapse frequency in the progressive phase [28].

Prevention of disability attributable to relapse

Mild attacks causing little or no functional impairment may require no treatment other than rest and often resolve spontaneously. Relapses causing functional impairment (e.g., visual loss, weakness, significant gait impairment) are typically treated with corticosteroids where they reduce the duration of relapses and hence their short-term morbidity, but not the ensuing permanent deficits. Corticosteroids, bound to their cytoplasmic receptors, enter the cell nucleus and inhibit transcription of proinflammatory cytokines, such as interleukin-1, interleukin-2, tumour necrosis factor-α (TNF-α) and proinflammatory enzymes, including collagenase, elastase, and plasminogen activator [29].

Symptomatic management of fixed neurological deficits

Fixed neurological deficits in multiple sclerosis are best managed by a multidisciplinary team, attending to physical therapies, psychological, and social interventions supplemented by medical treatments. The benefits of intense inpatient rehabilitation outlast the duration of therapy by up to 9 months [30]. The symptoms that are most amenable to treatment are spasticity and sphincter dysfunction. Spasticity causes discomfort and hinders care and is usefully treated by baclofen, which acts on spinal cord GABA-B receptors to suppress reflex arcs that have been released from higher inhibitory control; or tizanidine, which acts through spinal cord α_2 receptors to modulate presynaptic release of excitatory aminoacids. Bladder symptoms are most easily categorised by measuring the postmicturition bladder volume. If greater than 100 mL, there is primarily failure to empty and the treatment is ideally intermittent self-catheterisation; if the bladder empties fully but stores poorly, the detrusor might be inhibited by anti-cholinergics such as oxybutynin [31]. In fact, most patients have a combination and experience the urge frequently to empty a partially filled bladder against a closed sphincter. Erectile impotence is successfully treated with sildenafil citrate, a phosphodiesterase inhibitor that acts predominantly on nitric oxide within the penile vasculature. Paroxysmal attacks respond well to membrane-stabilising drugs - typically carbamazepine. No pharmacological treatment has shown a useful effect on the tremor of multiple sclerosis. There are advocates for thalamotomy and thalamic stimulation in highly selected patients. Fatigue cannot be satisfactorily treated; lowering body temperature might help and small trials report some benefit from amantadine and modafanil [32].

Prospects for improved treatment of disease activity

In view of the fact that the ability to suppress relapses and limit their consequences is partial, no informed analyst could reasonably conclude that (despite their achievements) the β-interferons are a definitive therapy in multiple sclerosis. The pharmaceutical industry has responded by sponsoring studies with combinations of established drugs (such as β-interferon and cyclophosphamide) without compelling evidence for synergistic benefit to date, together with a significant investment in novel immunotherapeutic strategies.

There are two approaches to reduce the activation and proliferation of autoreactive T cells. One is to search for new agents that suppress immune activity non-specifically and have acceptable safety profiles. Past attempts (with cyclophosphamide, ciclosporin, lymphoid irradiation, cladribine) have shown evidence for efficacy but with major side-effects; examples of this legacy are paclitaxel, teriflunomide, and autologous bone marrow transplantation, in which the limited efficacy seen to date must be weighed against the procedural mortality of around 5% [33]. The second strategy is to assume that the specific interaction between MBP, T cells, and antigen-presenting cells is the pivotal event driving multiple sclerosis. Several drugs have been designed to manipulate this interaction - for instance, vaccination with T cell receptor subtypes [34], MBP specific T cell clones [35], or disrupted MBP peptides. Although the results were disappointing, it would be premature to judge whether the strategy is wrong or the reagents insufficiently active. The hope was that, by minor changes in the presumed immunodominant peptide, autoaggressive MBP-reactive T cells might be tolerised. Alternatively, there are treatment strategies to reduce the effect of activated T cells; by blocking their entry into the brain (with an antibody against the α-4 integrin) or by neutralising putative toxic products [36].

Prevention of disability acquired through progression

Despite several attempts, immunomodulatory drugs are of little use once axonal degeneration has reached a critical threshold and clinical progression is established [37]. It follows that there might be an opportunity, early in the disease course, to suppress those components of the inflammatory process that initiate the cascade leading to delayed progression. Thus, the aim of immunotherapies is not only to reduce relapse frequency, but also to prevent transition to the secondary progressive phase of the illness. These essential issues in the therapy of multiple sclerosis - does early effective antiinflammatory therapy reduce the proportion of patients who ever enter the secondary progressive phase, or usefully affect the slope of that progression? - are now being addressed in trial design [38].

Can surviving axons be remyelinated?

The informed patient often expresses disappointment that management aims merely to limit further damage without seeking to restore the neurological past. Endogenous remyelination is limited to the acute inflammatory phase, and this timing raises the issue of whether, paradoxically, anti-inflammatory treatment might contribute to the failure of repair. For those axons that degenerate early as a direct result of the inflammatory process, efforts at remyelination might have little to offer; conversely, if the

naked axon is resistant to the inflammatory milieu but has poor survival properties, remyelination might be neuroprotective and its timing important.

The therapeutic challenge is whether to enhance endogenous remyelination or develop exogenous cell-based therapies. Experimentally, endogenous remyelination restores conduction and function in young and adult nervous systems [39]. The lesions of multiple sclerosis do contain oligodendrocyte progenitors, but these seem unable to usefully engage naked axons [40]. Manipulation of mechanisms involved in receptor-ligand growth factor interactions during the inflammatory phase of tissue injury might energise these indolent progenitors and improve remyelination. Thus, one option is to wait until a therapy is available that can be given systemically and delivered simultaneously to all affected parts of the central nervous system. The alternative is first to prove that structure and function can usefully be restored in a single informative lesion before tackling the secondary task of making this intervention diffusely available in the central nervous system. The initial proof of principle will almost certainly involve cell implantation; at present, the most promising candidates are autologous peripheral nerve Schwann cells [41] or olfactory bulb ensheathing cells [42]. How best to plan the difficult transition from experimental to clinical science in the context of a multifocal and multiphasic disease has been much discussed. The ideal lesion would be accessible, responsible for clinically significant and stable deficits, resulting from persistent demyelination, and at a site where the risks of failure would be acceptable (perhaps through the presence of an intact paired structure or pathway) and where tissue was shown to be undergoing progressive axonal degeneration in the absence of active inflammation. The optic nerve is perhaps the best candidate, because the symptoms are clinically eloquent, physiological assessment and imaging are well developed, and serial atrophy is seen after unilateral optic neuritis despite recovery of vision [43]; this combination suggests postinflammatory axonal degeneration consistent with loss of trophic support from myelin [22].

CHALLENGES

For the pathologist, multiple sclerosis is a disorder of the central nervous system, manifesting as acute focal inflammatory demyelination and axonal loss with limited remyelination, culminating in the chronic multifocal sclerotic plaques from which the disease gets its name. For the patient, multiple sclerosis threatens an apparently infinite variety of symptoms but with certain recurring themes and an unpredictable course. For the neurologist, multiple sclerosis is a disorder of young adults diagnosed on the basis of clinical and paraclinical evidence for at least two demyelinating lesions, affecting different sites within the brain or spinal cord, separated in time. For the clinical scientist, multiple sclerosis is the prototype inflammatory autoimmune disease of the central nervous system in which knowledge gained across a range of basic and clinical neuroscience disciplines has already allowed rational strategies for treatment. For all these groups, multiple sclerosis remains a difficult disease for which solutions seem attainable yet remain elusive.

A major part of future studies will be to resolve the question of disease heterogeneity [44,45]. Because primary progressive multiple sclerosis affects an older (predominantly male) population, has a less favourable prognosis, and is associated with fewer radiological and histological inflammatory lesions - such that these patients are disenfranchised with respect to clinical trials of immunomodulatory drugs - this type of multiple sclerosis is considered by many to be a separate disorder [46]. Genetic analyses suggest specifically different MHC associations in northern Europeans and the Mediterranean (especially Sardinians), and (perhaps) between primary progressive and relapsing-remitting multiple sclerosis. This notion of heterogeneity is further developed in pathological studies with biopsy and necropsy material, in which four distinct but overlapping histological types are described. The histopathological appearances are generally similar between lesions from each patient, but the nature of necropsy or biopsy material makes it more difficult to show subtype consistency over time [45].

Within 40 years of its first depiction, the clinical and pathological details of multiple sclerosis had been adequately characterised. Over the past 120 years, ideas have consolidated on the cause and mechanisms of inflammatory demyelination and axonopathy. In the past 10 years, therapies have emerged that modestly affect the course of the illness. Current research is increasingly seen as coherent and focused on the hot topics that need to be solved to limit, repair, and prevent the damage caused by multiple sclerosis.

REFERENCES

1. Keegan BM, Noseworthy JH. Multiple sclerosis. *Annu Rev Med* 2002; 53:285-302.
2. Compston A. The genetic epidemiology of multiple sclerosis. *Philos Trans R Soc Lond B Biol Sci* 1999; 354:1623-1634.
3. The transatlantic muliple sclerosis genetics cooperative. A meta-analysis of genome screens in multiple sclerosis. *Multiple Sclerosis* 2001; 7:3-11.
4. Sawcer S, Maranian M, Setakis E, Curwen V, Akesson E, Hensiek A, Coraddu F, Roxburgh R, Sawcer D, Gray J, Deans J, Goodfellow PN, Walker N, Clayton D, Compston A. A whole genome screen for linkage disequilibrium in multiple sclerosis confirms disease associations with regions previously linked to susceptibility. *Brain* 2002; 125:1337-1347.
5. Derfuss T, Gurkov R, Then BF, Goebels N, Hartmann M, Barz C, Wilske B, Autenrieth I, Wick M, Hohlfeld R, Meinl E. Intrathecal antibody production against Chlamydia pneumoniae in multiple sclerosis is part of a polyspecific immune response. *Brain* 2001; 124:1325-1335.
6. Challoner PB, Smith KT, Parker JD, MacLeod DL, Coulter SN, Rose TM, Schultz ER, Bennett JL, Garber RL, Chang M, . Plaque-associated expression of human herpesvirus 6 in multiple sclerosis. *Proc Natl Acad Sci U S A* 1995; 92:7440-7444.
7. McDonald WI, Compston A, Edan G, Goodkin D, Hartung HP, Lublin FD, McFarland HF, Paty DW, Polman CH, Reingold SC, Sandberg-Wollheim M, Sibley W, Thompson A, van den NS, Weinshenker BY, Wolinsky JS. Recommended diagnostic criteria for multiple sclerosis: guidelines from the International Panel on the diagnosis of multiple sclerosis. *Ann Neurol* 2001; 50:121-127.
8. Miller DH, Thompson AJ. Nuclear magnetic resonance monitoring of treatment and prediction of outcome in multiple sclerosis. *Philos Trans R Soc Lond B Biol Sci* 1999; 354:1687-1695.
9. Weinshenker BG, Bass B, Rice GP, Noseworthy J, Carriere W, Baskerville J, Ebers GC. The natural history of multiple sclerosis: a geographically based study. 2. Predictive value of the early clinical course. *Brain* 1989; 112 (Pt 6):1419-1428.
10. Weinshenker BG, Bass B, Rice GP, Noseworthy J, Carriere W, Baskerville J, Ebers GC. The natural history of multiple sclerosis: a geographically based study. I. Clinical course and disability. *Brain* 1989; 112 (Pt 1):133-146.
11. Confavreux C, Vukusic S, Moreau T, Adeleine P. Relapses and progression of disability in multiple sclerosis. *N Engl J Med* 2000; 343:1430-1438.
12. Compston A, Coles A. Multiple sclerosis. *Lancet* 2002; 359:1221-1231.
13. Redford EJ, Kapoor R, Smith KJ. Nitric oxide donors reversibly block axonal conduction: demyelinated axons are especially susceptible. *Brain* 1997; 120 (Pt 12):2149-2157.
14. England JD, Gamboni F, Levinson SR, Finger TE. Changed distribution of sodium channels along demyelinated axons. *Proc Natl Acad Sci U S A* 1990; 87:6777-6780.
15. Werring DJ, Bullmore ET, Toosy AT, Miller DH, Barker GJ, MacManus DG, Brammer MJ, Giampietro VP, Brusa A, Brex PA, Moseley IF, Plant GT, McDonald WI, Thompson AJ. Recovery from optic neuritis is associated with a change in the distribution of cerebral response to visual stimulation: a functional magnetic resonance imaging study. *J Neurol Neurosurg Psychiatry* 2000; 68:441-449.
16. Smith KJ, Kapoor R, Hall SM, Davies M. Electrically active axons degenerate when exposed to nitric oxide. *Ann Neurol* 2001; 49:470-476.
17. Trapp BD, Peterson J, Ransohoff RM, Rudick R, Mork S, Bo L. Axonal transection in the lesions of multiple sclerosis. *N Engl J Med* 1998; 338:278-285.

18. Brex PA, Gomez-Anson B, Parker GJ, Molyneux PD, Miszkiel KA, Barker GJ, MacManus DG, Davie CA, Plant GT, Miller DH. Proton MR spectroscopy in clinically isolated syndromes suggestive of multiple sclerosis. *J Neurol Sci* 1999; 166:16-22.
19. Bjartmar C, Kinkel RP, Kidd G, Rudick RA, Trapp BD. Axonal loss in normal-appearing white matter in a patient with acute MS. *Neurology* 2001; 57:1248-1252.
20. Kornek B, Storch MK, Weissert R, Wallstroem E, Stefferl A, Olsson T, Linington C, Schmidbauer M, Lassmann H. Multiple sclerosis and chronic autoimmune encephalomyelitis: a comparative quantitative study of axonal injury in active, inactive, and remyelinated lesions. *Am J Pathol* 2000; 157:267-276.
21. Barres BA, Raff MC. Proliferation of oligodendrocyte precursor cells depends on electrical activity in axons. *Nature* 1993; 361:258-260.
22. Wilkins A, Chandran S, Compston A. A role for oligodendrocyte-derived IGF-1 in trophic support of cortical neurons. *Glia* 2001; 36:48-57.
23. Hall GL, Compston A, Scolding NJ. Beta-interferon and multiple sclerosis. *Trends Neurosci* 1997; 20:63-67.
24. The PRISMS (Prevention of Relapses and Disability by Interferon-□-1a Subcutaneously in MultipleSclerosis) Study Group, and the University of British Columbia MS/MRI Analysis Group. PRISMS-4: Long-term efficacy of interferon-beta-1a in relapsing MS. *Neurology* 2001; 56:1628-1636.
25. Neuhaus O, Farina C, Wekerle H, Hohlfeld R. Mechanisms of action of glatiramer acetate in multiple sclerosis. *Neurology* 2001; 56:702-708.
26. Johnson KP, Brooks BR, Cohen JA, Ford CC, Goldstein J, Lisak RP, Myers LW, Panitch HS, Rose JW, Schiffer RB. Copolymer 1 reduces relapse rate and improves disability in relapsing- remitting multiple sclerosis: results of a phase III multicenter, double-blind placebo-controlled trial. The Copolymer 1 Multiple Sclerosis Study Group. *Neurology* 1995; 45:1268-1276.
27. Palace J, Rothwell P. New treatments and azathioprine in multiple sclerosis. *Lancet* 1997; 350:261
28. Millefiorini E, Gasperini C, Pozzilli C, D'Andrea F, Bastianello S, Trojano M, Morino S, Morra VB, Bozzao A, Calo' A, Bernini ML, Gambi D, Prencipe M. Randomized placebo-controlled trial of mitoxantrone in relapsing-remitting multiple sclerosis: 24-month clinical and MRI outcome. *J Neurol* 1997; 244:153-159.
29. Barnes D, Hughes RA, Morris RW, Wade-Jones O, Brown P, Britton T, Francis DA, Perkin GD, Rudge P, Swash M, Katifi H, Farmer S, Frankel J. Randomised trial of oral and intravenous methylprednisolone in acute relapses of multiple sclerosis. *Lancet* 1997; 349:902-906.
30. Freeman JA, Langdon DW, Hobart JC, Thompson AJ. Inpatient rehabilitation in multiple sclerosis: do the benefits carry over into the community? *Neurology* 1999; 52:50-56.
31. Fowler CJ. The cause and management of bladder, sexual and bowel symptoms in multiple sclerosis. *Baillieres Clin Neurol* 1997; 6:447-466.
32. Rammohan KW, Rosenberg JH, Lynn DJ, Blumenfeld AM, Pollak CP, Nagaraja HN. Efficacy and safety of modafinil (Provigil) for the treatment of fatigue in multiple sclerosis: a two centre phase 2 study. *J Neurol Neurosurg Psychiatry* 2002; 72:179-183.
33. Comi G, Kappos L, Clanet M, Ebers G, Fassas A, Fazekas F, Filippi M, Hartung HP, Hertenstein B, Karussis D, Martino G, Tyndall A, van der Meche FG. Guidelines for autologous blood and marrow stem cell transplantation in multiple sclerosis: a consensus report written on behalf of the European Group for Blood and Marrow Transplantation and the European Charcot Foundation. BMT-MS Study Group. *J Neurol* 2000; 247:376-382.
34. Appel H, Seth NP, Gauthier L, Wucherpfennig KW. Anergy induction by dimeric TCR ligands. *J Immunol* 2001; 166:5279-5285.
35. Zhang J. T-cell vaccination in multiple sclerosis: immunoregulatory mechanism and prospects for therapy. *Crit Rev Immunol* 2001; 21:41-55.

36. Tubridy N, Behan PO, Capildeo R, Chaudhuri A, Forbes R, Hawkins CP, Hughes RA, Palace J, Sharrack B, Swingler R, Young C, Moseley IF, MacManus DG, Donoghue S, Miller DH. The effect of anti-alpha4 integrin antibody on brain lesion activity in MS. The UK Antegren Study Group. *Neurology* 1999; 53:466-472.
37. Li DK, Zhao GJ, Paty DW. Randomized controlled trial of interferon-beta-1a in secondary progressive MS: MRI results. *Neurology* 2001; 56:1505-1513.
38. Comi G, Filippi M, Barkhof F, Durelli L, Edan G, Fernandez O, Hartung H, Seeldrayers P, Sorensen PS, Rovaris M, Martinelli V, Hommes OR. Effect of early interferon treatment on conversion to definite multiple sclerosis: a randomised study. *Lancet* 2001; 357:1576-1582.
39. Jeffery ND, Blakemore WF. Locomotor deficits induced by experimental spinal cord demyelination are abolished by spontaneous remyelination. *Brain* 1997; 120 (Pt 1):27-37.
40. Chang A, Tourtellotte WW, Rudick R, Trapp BD. Premyelinating oligodendrocytes in chronic lesions of multiple sclerosis. *N Engl J Med* 2002; 346:165-173.
41. Kohama I, Lankford KL, Preiningerova J, White FA, Vollmer TL, Kocsis JD. Transplantation of cryopreserved adult human Schwann cells enhances axonal conduction in demyelinated spinal cord. *J Neurosci* 2001; 21:944-950.
42. Barnett SC, Alexander CL, Iwashita Y, Gilson JM, Crowther J, Clark L, Dunn LT, Papanastassiou V, Kennedy PG, Franklin RJ. Identification of a human olfactory ensheathing cell that can effect transplant-mediated remyelination of demyelinated CNS axons. *Brain* 2000; 123 (Pt 8):1581-1588.
43. Hickman SJ, Behan CMH. Continuing optic nerve atrophy following optic neuritis: a serial MRI study. *Multiple Sclerosis* 2002; in press:
44. Lassmann H, Bruck W, Lucchinetti C. Heterogeneity of multiple sclerosis pathogenesis: implications for diagnosis and therapy. *Trends Mol Med* 2001; 7:115-121.
45. Lucchinetti C, Bruck W, Parisi J, Scheithauer B, Rodriguez M, Lassmann H. Heterogeneity of multiple sclerosis lesions: implications for the pathogenesis of demyelination. *Ann Neurol* 2000; 47:707-717.
46. Revesz T, Kidd D, Thompson AJ, Barnard RO, McDonald WI. A comparison of the pathology of primary and secondary progressive multiple sclerosis. *Brain* 1994; 117 (Pt 4):759-765.

PET VISUALISATION OF MICROGLIA IN MULTIPLE SCLEROSIS PATIENTS USING [^{11}C]PK11195

Jan C Debruyne MD[2,7], Jan Versijpt MD[1,7], Koenraad J Van Laere MD PhD DrSc[3], Filip De Vos Pharm PhD[4], Johan Keppens Eng[3], Karel Strijckmans MrSc PhD[5], Eric Achten MD PhD[6], Guido Slegers Apr MrSc PhD[4], Rudi A Dierckx MD PhD[3], Jakob Korf MrSc PhD[1], Jacques L De Reuck MD PhD[2]

[1] Department of Biological Psychiatry, University Hospital, Groningen, the Netherlands

[2] Department of Neurology, Ghent University Hospital, Ghent, Belgium

[3] Division of Nuclear Medicine, Ghent University Hospital

[4] Laboratory of Radiopharmacy, Ghent University

[5] Laboratory of Analytical Chemistry, Institute for Nuclear Sciences, Ghent University

[6] Department of Radiology, MR-Unit, Ghent University Hospital

[7] Both authors contributed equally to this manuscript

Eur J Neurol 2003; in press

ABSTRACT

Activated microglia are involved in the immune response of multiple sclerosis (MS). The peripheral benzodiazepine receptor (PBR) is expressed on microglia and upregulated after neuronal injury. [^{11}C]PK11195 is a positron emission tomography (PET) radioligand for the PBR. The objective of the present study was to investigate [^{11}C]PK11195 imaging in MS patients and its additional value over MRI concerning the immuno-pathophysiological process. Seven healthy and 22 MS subjects were included. Semiquantitative [^{11}C]PK11195 uptake values were assessed with normalisation on cortical gray matter. Uptake in Gadolinium-lesions was significantly increased compared to normal white matter. Uptake in T2-lesions was generally decreased, suggesting a PBR downregulation. However, uptake values increased whenever a clinical or MR-relapse was present, suggestive for a dynamic process with a transient PBR upregulation. During disease progression, an increase of normal-appearing white matter (NAWM) uptake was found, propagating NAWM as the possible real burden of disease. In conclusion, [^{11}C]PK11195 and PET are able to demonstrate inflammatory processes with microglial involvement in MS.

INTRODUCTION

Microglia, the brain's intrinsic macrophages, play a major role in the inflammatory process of autoimmune demyelinating diseases and particularly multiple sclerosis (MS). They initiate the immunological process in the early stages of the disease. More specifically, microglial activation in experimental allergic encephalomyelitis (EAE) and MS contributes to CNS damage through several mechanisms such as the production of proinflammatory cytokines (e.g. TNF-α), matrix metalloproteinases and free radicals, even as still ramified but activated cells (Benveniste, 1997). Indeed, by releasing myelinotoxic factors with direct injury to the oligodendrocyte-myelin unit, activated microglia stimulate this demyelinating process (Sriram and Rodriguez, 1997). Additionally, during relapses when the blood-brain barrier (BBB) opens, they are thought to act as antigen presenting cells having the capacity of activating perivascular myelin-reactive T lymphocytes by costimulatory molecules on their surface (Dangond *et al.*, 1997; Vowinckel *et al.*, 1997).

One of the characteristic features of microglia is their rapid activation in response to brain injury with a concomitant higher expression of the peripheral benzodiazepine receptor (PBR) (Banati *et al.*, 2000). Visualisation of this PBR is possible by means of radiolabeled PK11195, a selective and specific high affinity ligand, allowing as such the assessment of microglial activity and providing more specific in vivo information concerning the underlying histopathological features. Indeed, high resolution microautoradiography combined with immunohistochemical cell identification in MS and EAE tissue demonstrated that in focal inflammation, when the BBB is disrupted, the PBR is expressed on invading blood-borne cells such as macrophages (Banati *et al.*, 2000). However in brain lesions without direct damage to the BBB, the predominant cell type expressing PBR binding sites is the activated microglial cell (Banati *et al.*, 1997).

PK11195 has been labeled with ^{11}C for the study of the lesioned brain with positron emission tomography (PET) in various neuroinflammatory conditions like stroke, Rasmussen's encephalitis and cerebral vasculitis (Goerres *et al.*, 2001; Ramsay *et al.*, 1992). A previous feasibility study showed the value of a straightforward semiquantitative approach by means of defining an accurate confidence interval for the [^{11}C]PK11195 uptake values in controls for the eventual detection of microglial activation in acute and chronic neuroinflammatory diseases (Debruyne *et al.*, 2002).

Up till now, magnetic resonance imaging (MRI) has been widely used in MS to evaluate disease activity and to monitor clinical trials or the natural course of the disease process itself. Although MRI is of paramount value for diagnostic procedures, there remains a weak correlation between MRI parameters and disability as measured with the expanded disability status scale (EDSS). The reason for this clinicoradiological paradox may be the lack of histological specificity of conventional MRI lesions and the underestimation of disease burden in the normal-appearing white matter (NAWM) and spinal cord (Barkhof and van Walderveen, 1999; Nijeholt *et al.*, 1998). The aims of the present study are, firstly, to

assess the [^{11}C]PK11195 uptake in MS patient subgroups with chronic and active white matter lesions on MRI and, secondly, to investigate the additional value of [^{11}C]PK11195 imaging over MRI concerning the immuno-pathophysiological process during the disease course in this cohort of patients with different clinical manifestations and invalidity.

PATIENTS AND METHODS

Subjects

The study was approved by the Ethical Committee of the Ghent University Hospital and written informed consent was obtained from each subject. Seven healthy volunteers (3 males, mean age 33 ± 8, range 23-41 yrs) and 22 out of 27 initially randomly included clinical definite and laboratory proven MS patients referring to the Poser criteria (Poser *et al.*, 1983) (mean age 43 ± 11, range 26-64 yrs) were finally included. Demographic and clinical parameters of the MS patients are described in table 1. Four MS patients were treated with IFN-ß at the time of inclusion. Thirteen patients had the relapsing-remitting type (RR) of the disease while 7 patients were secondary progressive (SP), having a continuous worsening of invalidity over a follow-up period of at least 6 months. Two patients had a primary progressive course (PP) without relapses from the very beginning of the disease. Six patients had a clinical relapse during the time of scanning, defined as the occurrence or worsening of neurological dysfunction lasting more than 24 hours. In 3 of them, corticosteroids needed to be administered after all imaging was performed. Ten patients showed Gd-enhancing lesions on the MR scan, 5 of them with a concomitant clinical relapse. One patient with the RR type of disease was scanned twice within a time interval of 4 months, the first imaging session at the time of a clinical relapse with Gd-lesions and the second session at the time of remission. The average disease duration was 9.3 ± 8.3, range 0.3-32.7 yrs. The average EDSS was 4.0 ± 2.0, range 1.0-7.0. To assess differences between moderate and severe impairment, patients were, for some analyses, subdivided into a low and high invalidity category (cut-off EDSS 4.0).

Age	Sex	Type	Disease duration (yrs)	EDSS	Clinical relapse	Gd-lesions	Sampled T2-lesions	Total T2-lesions
44	M	RR	2.3	3.0	no	7	4	32
37	F	RR	3.6	1.5	no	1	4	30
51	F	RR	22.7	2.5	yes	1	3	8
64	F	PP	13.7	7.0	no	-	2	9
45	F	PP	12.7	6.0	no	-	-	6
32	F	RR	3.1	3.0	no	1	3	25
45	F	RR	14.8	3.0	no	1	4	30
27	M	RR	3.8	1.0	yes	1	1	6
49	M	SP	8.8	7.0	no	-	3	33
50	F	SP	8.7	5.5	no	-	2	27
38	F	RR	0.3	1.5	yes	11	4	10
51	F	SP	23.7	4.5	no	-	2	28
36	M	RR	0.7	5.5	no	-	6	19
31	M	RR	13.2	3.5	no	-	5	41
35	F	SP	7.7	4.5	no	1	3	19
60	M	SP	32.7	6.5	no	-	6	21
64	F	SP	7.6	4.5	no	-	6	28
26	M	RR	2.2	1.5	yes	-	2	2
45	F	SP	9.7	6.5	yes	2	6	16
42	M	RR	3.1	1.0	yes	1	2	12
37	M	RR	6.9	5.5	no	-	-	5
31	F	RR	3.5	3.0	no	-	1	15

Table 1 Clinical characteristics of the MS patients.

Radiochemistry

PK11195 [1-(2-chlorophenyl)-N-methyl-N-(1-methylpropyl)-3-isoquinolinecarboxamide] was obtained from RBI (Natick, MA, USA). [^{11}C]PK11195 was synthesized according to a procedure described by Camsonne et al. (Camsonne *et al.*, 1984). Briefly, 3 µmol N-desmethyl PK11195 was dissolved in 150 µL dimethylsulphoxide, containing 3 µmol tetrabutylammonium hydroxide. After trapping of [^{11}C]CH_3I, the vial was closed and heated at 80°C for 3 min. Purification was done by HPLC using a RP-C18 column (Econosil, 250 mm x 10 mm, 10 µm particle size) and an ethanol/water (70/30) mixture as mobile phase. Radiochemical yield towards [^{11}C]CH_3I was 57 ± 2 %. Finally, 3.7 GBq [^{11}C]PK11195 was obtained with a specific activity of 25 GBq/µmol. Chemical and radiochemical purity were higher than 99%. All subjects were injected intravenously with 370 ± 10 % MBq [^{11}C]PK11195 with a slow bolus in a time course of 30 seconds.

Data acquisition and processing

All subjects underwent MR and PET scanning on the same day.

MR imaging was performed on a 1.5 T commercial MR scanner (Siemens, Magnetom 1.5 T, SP4000; Erlangen, Germany). Prior to the administration of gadolinium (Gd), standard spin-echo imaging was carried out in 5 mm thick axial planes (pixel size=0.9 $\times$ 0.9 mm^2) with proton density- (TR/TE/NEX=2170/20/1), T2- (TR/TE/NEX=2170/80/1) and T1-weighted (TR/TE/NEX=600/12/1) contrast. Five minutes after Gd injection, the axial slices were rescanned with T1-weighting (TR/TE/NEX=800/20/1).

PET studies were performed on a Siemens ECAT 951/31 PET scanner (Siemens, Knoxville, TN, USA) with a transaxial and axial resolution (FWHM) of 5.8 and 5 mm respectively, operating in 2D mode. All subjects were placed in supine position with dimmed lights and low ambient noise. Recontruction was done using filtered backprojection with a Hanning filter with a (cut-off 0.5 cycles/cm). Sequential transmission scanning was performed using a germanium - 68 / gallium - 68 ring source. Correction for scatter was done using the standard software provided by the manufacturer (CTI). Subsequently, regional cerebral blood flow (rCBF) images were acquired by [^{15}O]CO_2 inhalation at 900 MBq/min. For this, the steady state technique using [^{15}O]CO_2 was applied (Frackowiak *et al.*, 1980). Eight min later, a one-hour dynamic PET study was conducted following the injection of 370 MBq [^{11}C]PK11195. Nineteen frames each consisting of thirty-one planes of 3.375 mm thickness were recorded over 60 min with an increasing duration of 2 * 5 s, 5 * 10 s, 4 * 1 min, 2 * 3 min, 1 * 4 min, 1 * 5 min and 4 * 10 min. No partial volume correction was applied. Since a previous feasibility study showed that the time-activity curves for both volunteers and patients had a similar decline with a steady-state period from 40 min postinjection, data obtained from 40-60 min postinjection were summed (static scans). Automatic radioactive decay correction was applied to all images. Individual automatic coregistration of MR and perfusion PET data was achieved using SPM99 (Statistical Parametric Mapping, Functional Imaging Laboratory, Wellcome Department of Cognitive Neurology, Institute of Neurology, London, UK) (Friston *et al.*, 1991). Spatial normalisation was done on the normal templates for T1-weighted MR in MNI space (Montreal Neurological Institute), using non-linear warping with 7×8×7 basic functions (5 iterations), and to a voxel size of 3×3×3 mm^3. T2-, Gd- and coregistered PET data underwent the same transformation as the original T1-image. The same spatial transformation as for the perfusion PET studies was applied to all [^{11}C]PK11195 data. Five patients were excluded because of head movement and subsequent incorrect coregistration between the perfusion and receptor PET scan.

Volumes of interest and semiquantification

Since no generally accepted model of absolute quantification of [^{11}C]PK11195 specific binding in normal brain has been widely validated, and moreover, as no dynamic data for all volunteers were available and no arterial sampling was carried out, a straightforward semiquantitative approach was performed on the static scans. Volumes of interest (VOIs, on average 400 voxels ranging from 5 to more than 3000) were manually defined on the reoriented high-resolution MR scans in white and gray matter for volunteers and NAWM, gray matter, T2- and T1-Gd-lesions for MS patients and automatically transferred onto the reoriented [^{11}C]PK11195 scans by means of PMOD, a kinetic modeling and image fusion environment tool in JAVA (Zurich, Switzerland) (Mikolajczyk *et al.*, 1998). When drawing VOIs, care was taken to avoid the carotid and major cerebral arteries as well as the ventricles and venous sinuses. For all controls, 52 VOIs were sampled in white matter and 264 in gray matter. For all MS patients, 153 VOIs were sampled in NAWM and 84 in gray matter. Gray matter was divided in cortical and central gray matter (thalamus and striatum) because higher binding of [^{3}H]PK11195 was described in diencephalic structures notably in several thalamic nuclei (Doble *et al.*, 1987). The normalised specific uptake for a particular VOI was defined as the mean number of counts per volume unit in this VOI divided by the mean number of counts per volume unit in cortical gray matter. Since there was a significant age difference between patients and controls, the effect of age in controls for white matter, cortical and subcortical gray matter, and thalamic [^{11}C]PK11195 uptake values was studied.

Statistical analysis

Data were analysed by means of SPSS v10.0 for Windows (Chicago, IL, USA). For normality testing, a Kolmogorov-Smirnov test statistic was applied. For differences between groups, an independent samples t or a Mann-Whitney U test was applied when appropriate. A p-value lower than 0.05 was considered as significant while a value lower than 0.10 was considered as a meaningful trend. No Bonferroni correction was performed. Data are given as means ± one standard deviation.

RESULTS

[^{11}C]PK11195 uptake values for MS patients versus controls and effect of age

A [^{11}C]PK11195 uptake value of 100.3 ± 9.9 in white matter and 100.5 ± 9.4 in gray matter for controls was found. In patients, NAWM and gray matter uptake was respectively 101.7 ± 11.1 and 101.0 ± 9.4, both higher, however, not statistically significant different from white and gray matter in controls (p=0.3 and 0.7 respectively). No effect of age was found in controls for white, cortical and subcortical gray matter, or thalamic [^{11}C]PK11195 uptake values. In T2-lesions, the uptake tended to be lower compared to white matter in controls (97.3 ± 13.8, p=0.06). Regarding Gd-lesions, [^{11}C]PK11195 uptake was significantly higher (p=0.001) compared to normal white matter (110.9 ± 14.7). Figure 1A shows the raised [^{11}C]PK11195 uptake corresponding with a Gd-lesion on MRI.

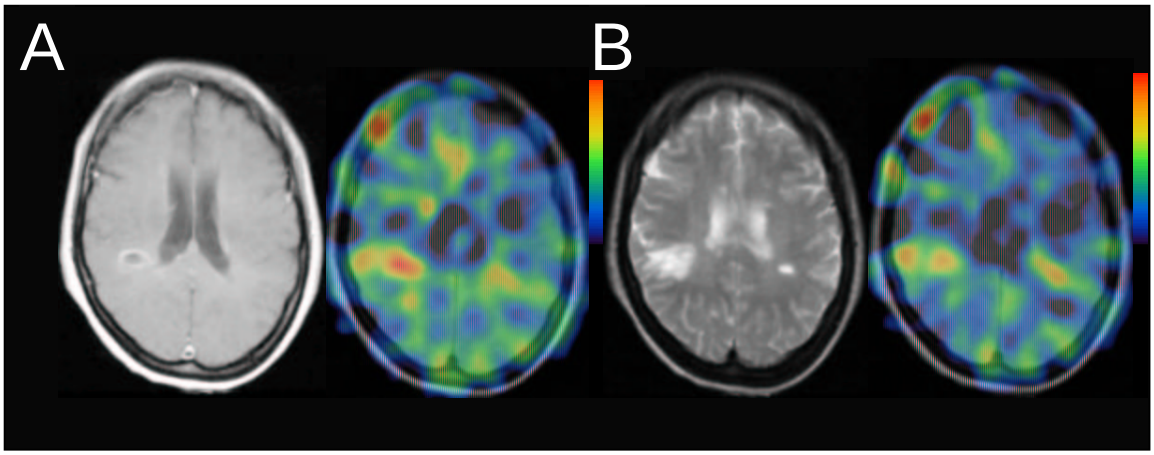

FIGURE 1: Illustration of the remote projected neuroinflammatory response in the wake of a primary lesion elsewhere. Gd-lesion located in the right periventricular parietal region in a patient with active relapsing-remitting MS with the corresponding focally increased uptake on the [^{11}C]PK11195 image (A). On a slightly higher level, the patient has a T2-weighted MR-lesion in the left periventricular parietal region corresponding with the concomitantly raised uptake on the [^{11}C]PK11195 image (B). On the same image, the increased uptake of the upper border of the Gd-lesion in the right parietal region is still visible. Note the uptake in the frontal meningeal area on both [^{11}C]PK11195 images, indicating the aspecific signal of [^{11}C]PK11195. Both [^{11}C]PK11195 images are superimposed on the corresponding proton density-weighted MR scan.

Figure 2 shows the mean [^{11}C]PK11195 normalised uptake values for different types of MRI-lesions in MS patients.

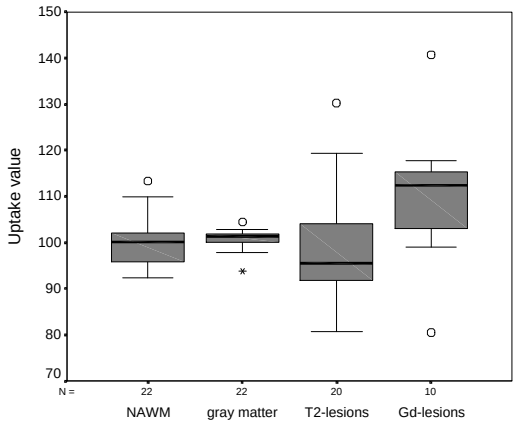

FIGURE 2: Boxplot of [^{11}C]PK11195 normalized uptake values in different types of MRI-lesions.

[^{11}C]PK11195 uptake values for MRI-lesions subdivided according to the presence of a relapse (clinical or MR-relapse)

A higher [^{11}C]PK11195 uptake for T2-lesions was found in patients presenting at the time of scanning with an attack, defined as a clinical relapse or the presence of Gd-lesions on MRI (100.7 ± 14.2 versus 93.7 ± 12.5; p=0.01, figure 3). Also, when subdivided according to the presence of Gd-lesions on MRI or a clinical relapse separately, [^{11}C]PK11195 uptake values were higher in both situations (respectively p= 0.05 and 0.02). Table 2 shows the T2-lesional [^{11}C]PK11195 uptake values for the distinct conditions. The single patient with the RR type of disease, which was scanned twice, had a mean T2-lesional uptake value of 130.3, which dropped to 100.9 four months later at the time of remission. Figure 1 shows the raised [^{11}C]PK11195 uptake corresponding with a T2-lesion in a patient with the RR type of disease during a clinical and MR-relapse.

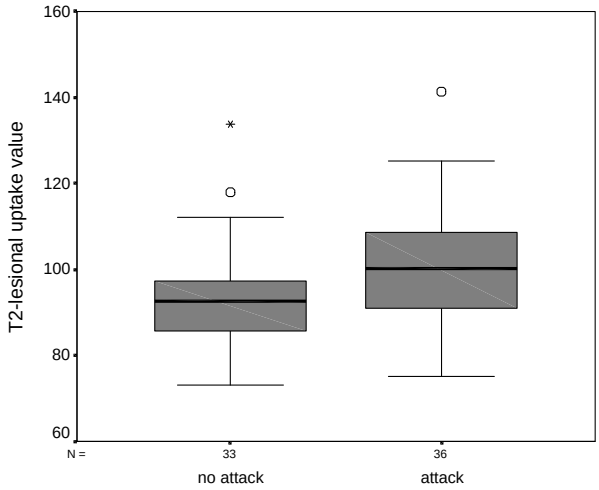

FIGURE 3: Boxplot of [^{11}C]PK11195 uptake values for all T2-lesions subdivided according to the presence of an attack (clinical or MR-relapse).

o = outlier value (cases with values between 1.5 and 3 box lengths from the upper or lower edge of the box. The box length is the interquartile range); * = extreme value (cases with values more than 3 box lengths from the upper or lower edge of the box)

	Clinical relapse	**MR-relapse**	**Attack**
present	105.0 ± 16.6	101.7 ± 13.9	100.7 ± 14.2
not present	94.6 ± 11.7	93.1 ± 12.5	93.7 ± 12.5
p-value	0.02	0.05	0.01

Table 2 [^{11}C]PK11195 uptake values for T2-lesions, subdivided according to the presence of a relapse (clinical or MR-relapse).

When the [^{11}C]PK11195 uptake for Gd-lesions was subdivided according to the coinciding presence of a clinical relapse, uptake was higher when a relapse was present (104.4 ± 17.0 versus 115.4 ± 11.3; p = 0.05).

No significantly different NAWM [^{11}C]PK11195 uptake was found when a relapse was present.

Correlation of lesional [^{11}C]PK11195 uptake values with disease duration and invalidity

Concerning the relationship between NAWM [^{11}C]PK11195 uptake values and disease duration, a steady rising slope during the progression of the disease was found (r=0.4; p=0.05; figure 4). Without the outlier value (see figure 4), the positive correlation remained, however, statistically non-significant (p>0.1). Concerning the correlation between gray matter [^{11}C]PK11195 uptake and disease duration, subdivided according to high and low invalidity category patients, significance was reached for the high invalidity patients only (r=0.6; p=0.05). The correlations between [^{11}C]PK11195 uptake values for both T2-weighted lesions and Gd-lesions on one side and EDSS or disease duration on the other side did not reach statistical significance.

Thalamic and NAWM [^{11}C]PK11195 uptake in PP MS patients

For the two patients with the PP type of MS, a substantially higher uptake was found both in the thalamus (mean values respectively 109.9 for PP, 104.0 for RR and 104.3 for SP; p-value of 0.3 PP versus RR) and the NAWM (mean values for all lesions respectively 104.1 for PP, 99.8 for RR and 100.7 for SP; p-value of 0.1 PP versus RR).

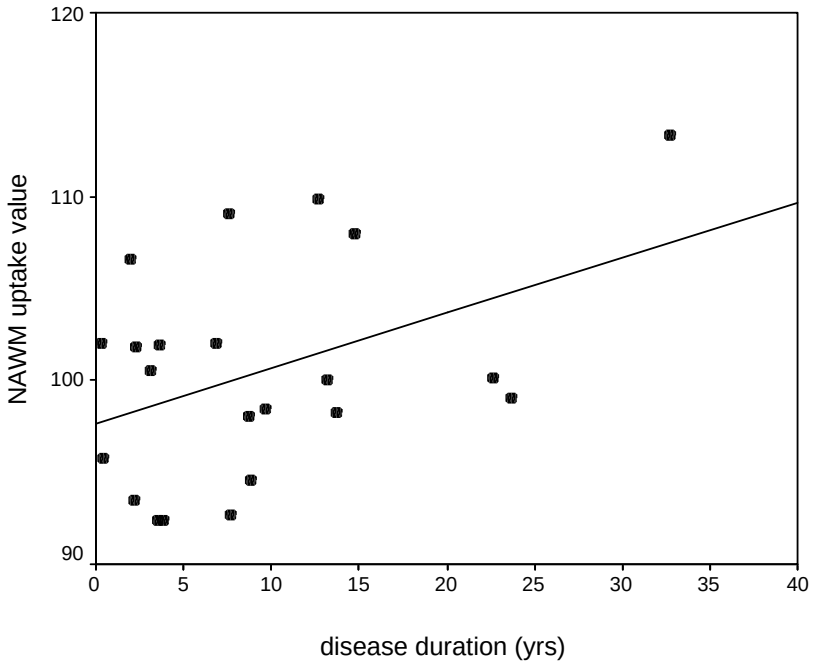

FIGURE 4: Correlation of NAWM [^{11}C]PK11195 uptake and disease duration.

DISCUSSION

Radiolabeled PK11195 has been validated as a marker of microglial proliferation, with its ensuing increased PBR density, in ample neuropathological and animal experimental work involving lesions with or without BBB damage. Moreover, the full transformation of microglia into parenchymal phagocytes, absent in areas with chronic or subtle brain pathology, is not necessary to reach maximal levels of PK11195 binding (Banati *et al.*, 1997; Benavides *et al.*, 1988). An equal observation was made in a previous study in MS patients, where a high [^{11}C]PK11195 uptake occurred in active white matter inflammation defined by MR, reflecting the presence of activated microglia (Vowinckel *et al.*, 1997). The latter findings were confirmed in the present study where significantly increased [^{11}C]PK11195 uptake values were found in patients with active focal inflammatory lesions defined by Gd-enhanced T1-MRI (figure 1 and 2). The increased uptake in Gd-lesions is in accordance with the known histology of these conventional MR lesions. Indeed, in focal Gd-enhanced T1-weighted MRI lesions, the BBB breakdown is related to an extensive inflammatory response including macrophages and T-cells (Nesbit *et al.*, 1991).

Microglia occupy 5 to 12% of the total number of cells in the normal brain. Gray matter contains more microglia than white matter, especially in sensory, limbic and subcortical gray matter structures (Lawson *et al.*, 1990). The latter was also demonstrated in a previous feasibility study where a higher mean gray matter [^{11}C]PK11195 uptake was detected in seven controls (Debruyne *et al.*, 2002). Although a larger group of MS patients of the PP type is needed to make a clearer statement, the higher thalamic [^{11}C]PK11195 uptake found in the present study could be explained by a projected neuroinflammatory response secondary to descending corticothalamic tract lesions but, alternatively, also due ascending to spinal cord long tract lesions such as in myelopathic syndromes, typically seen in this subgroup of MS patients (Andersson *et al.*, 1999; Banati *et al.*, 2000; Sorensen *et al.*, 1996). This hypothesis of a remote neuroinflammatory response in the wake of primary lesions elsewhere along a neural pathway was already formulated by Banati et al. where an increased thalamic [^{11}C]PK11195 uptake was found in a patient with a spinal cord MRI lesion, and also in a case of EAE where PBR expression was induced in the midbrain caused by an injured spinothalamic tract (Banati *et al.*, 2000).

T2-lesions on MRI are known for their high sensitivity but low specificity with regard to histopathology. The [^{11}C]PK11195 uptake for T2-weighted lesions in the present study was low (figure 2). As such, these findings may be related to a PBR downregulation of chronic, immunologically less triggered microglia due to the disappearance of myelin fibers, which are over time replaced by axonal scars (Johnson *et al.*, 1986; Schlumpf *et al.*, 1993; Trapp *et al.*, 1998). Then, whenever a temporarily reactivation of the autoimmune process occurs, PBR expression will be higher compared to lesions in an existing steady state, as demonstrated in the present study where an overall global T2-lesional upgrading of [^{11}C]PK11195 uptake was noticed when imaging was performed during a clinical or MR-relapse (figure 3). This upgrading of [^{11}C]PK11195 uptake is illustrated in figure 1 and was also seen in the single RR patient who was scanned twice and showed a much larger mean T2-lesional [^{11}C]PK11195 uptake value at the time of

relapse compared to the time of remission. These findings confirm earlier in vitro and in vivo observations showing activated microglia remote from the primary inflammatory site (Banati *et al.*, 2000). As such, the molecular analogue of the natural disease course in which clinical and MR relapses are followed by periods of a relative stagnation is a waxing and waning phenomenon for the PBR expression in the T2-weighted lesions.

In the present study, a slightly higher value of NAWM [^{11}C]PK11195 uptake compared to white matter of controls was found, without any significantly different radioligand uptake when a relapse was present. This is also in agreement with histopathological studies, where an increased number of MHC class II microglia attributing to a loss of myelin extending far beyond visible detectable inflammatory foci was found (Hayes *et al.*, 1987), as well as with autoradiographic studies both in EAE and human post-mortem tissue demonstrating regions of an increased number of non-phagocytic, still ramified, but activated microglia along NAWM tracts (Banati *et al.*, 2000). Also, a tendency to a rising of the NAWM [^{11}C]PK11195 uptake during disease progression was found (figure 4). These findings are in line with the hypothesis that the demyelinating process is initiated by microglia from the very beginning of the disease, unrelated to BBB disruption and autoreactive T-cell function (Kesselring, 1990), the latter being involved in clinical and MR-relapses (Miller *et al.*, 1995). As such, NAWM microglia constitutes a real burden of the disease, causing invisible demyelinisation independent from relapses. With this regard, Confavreux et al. recently concluded already that relapses do not significantly influence the progression of irreversible disability (Confavreux *et al.*, 2000).

In conclusion, with [^{11}C]PK11195 PET as a marker of the immuno-pathophysiological process, we in vivo raise evidence to the hypothesis that microglia may play an important role in the immunopathogenesis of multiple sclerosis. For T1-Gadolinium-weighted MR lesions, the [^{11}C]PK11195 uptake was significantly increased. Concerning T2-weighted MR lesions, the microglial activity was decreased suggesting a PBR downregulation related to the gradual vanishing of myelin fibers towards the chronic degenerative phase. An increased uptake in these lesions was found in patients with a clinical relapse or the presence of remote Gd-lesions, indicating a dynamic process with a transient upregulation following the natural course of the disease. In NAWM, the increase of [^{11}C]PK11195 uptake with disease duration is in line with the theory proposing NAWM microglia as a real burden of the disease, causing invisible demyelinisation independent from relapses.

REFERENCES

Andersson PB, Waubant E, Gee L, Goodkin DE (1999). Multiple sclerosis that is progressive from the time of onset: clinical characteristics and progression of disability. *Arch Neurol.* **56**:1138-1142.

Banati RB, Myers R, Kreutzberg GW (1997). PK ('peripheral benzodiazepine') - binding sites in the CNS indicate early and discrete brain lesions: microautoradiographic detection of [^{3}H]PK11195 binding to activated microglia. *J Neurocytol* **26**:77-82.

Banati RB, Newcombe J, Gunn RN, Cagnin A, Turkheimer F, Heppner F, Price G, Wegner F, Giovannoni G, Miller DH, Perkin GD, Smith T, Hewson AK, Bydder G, Kreutzberg GW, Jones T, Cuzner ML, Myers R (2000). The peripheral benzodiazepine binding site in the brain in multiple sclerosis: quantitative in vivo imaging of microglia as a measure of disease activity. *Brain* **123**:2321-2337.

Barkhof F, van Walderveen M (1999). Characterization of tissue damage in multiple sclerosis by nuclear magnetic resonance. *Philos.Trans.R.Soc.Lond B Biol.Sci.* **354**:1675-1686.

Benavides J, Cornu P, Dennis T, Dubois A, Hauw JJ, MacKenzie ET, Sazdovitch V, Scatton B (1988). Imaging of human brain lesions with an □□ site radioligand. *Ann Neurol* **24**:708-712.

Benveniste EN (1997). Role of macrophages/microglia in multiple sclerosis and experimental allergic encephalomyelitis. *J Mol.Med* **75**:165-173.

Camsonne R, Crouzel C, Comar D, Maziere M, Prenant C, Sastre J, Moulin MA, Syrota A (1984). Synthesis of n-(C-11) methyl, n-(methyl-1 propyl), (chloro-2 phenyl)-1 isoquinoleine carboxamide-3 (PK-11195) – a new ligand for peripheral benzodiazepine receptors. *J Labelled Compd Rad* **21**:985-991.

Confavreux C, Vukusic S, Moreau T, Adeleine P (2000). Relapses and progression of disability in multiple sclerosis. *N Engl J Med* **343**:1430-1438.

Dangond F, Windhagen A, Groves CJ, Hafler DA (1997). Constitutive expression of costimulatory molecules by human microglia and its relevance to CNS autoimmunity. *J Neuroimmunol.* **76**:132-138.

Debruyne JC, Van Laere KJ, Versijpt J, De Vos F, Eng JK, Strijckmans K, Santens P, Achten E, Slegers G, Korf J, Dierckx RA, De Reuck JL (2002). Semiquantification of the peripheral-type benzodiazepine ligand [^{11}C]PK11195 in normal human brain and application in multiple sclerosis patients. *Acta Neurol Belg* **102**:127-35.

Doble A, Malgouris C, Daniel M, Daniel N, Imbault F, Basbaum A, Uzan A, Gueremy C, Le Fur G (1987). Labelling of peripheral-type benzodiazepine binding sites in human brain with [^{3}H]PK 11195: anatomical and subcellular distribution. *Brain Res Bull* **18**:49-61.

Frackowiak RS, Lenzi GL, Jones T, Heather JD (1980). Quantitative measurement of regional cerebral blood flow and oxygen metabolism in man using ^{15}O and positron emission tomography: theory, procedure, and normal values. *J Comput.Assist.Tomogr.* **4**:727-736.

Friston KJ, Frith CD, Liddle PF, Frackowiak RS (1991). Comparing functional (PET) images: the assessment of significant change. *J Cereb Blood Flow Metab* **11**:690-699.

Goerres GW, Revesz T, Duncan J, Banati RB (2001). Imaging cerebral vasculitis in refractory epilepsy using [^{11}C](R)-PK11195 positron emission tomography. *Am J Roentgenol* **176**:1016-1018.

Hayes GM, Woodroofe MN, Cuzner ML (1987). Microglia are the major cell type expressing MHC class II in human white matter. *J Neurol.Sci.* **80**:25-37.

Johnson MD, Wang JK, Morgan JI, Spector S (1986). Downregulation of [^{3}H]Ro5-4864 binding sites after exposure to peripheral-type benzodiazepines in vitro. *J Pharmacol Exp Ther* **238**:855-859.

Kesselring J (1990). The pathogenesis of multiple sclerosis. *Schweiz Med Wochenschr* **120**:1083-1090.

Lawson LJ, Perry VH, Dri P, Gordon S (1990). Heterogeneity in the distribution and morphology of microglia in the normal adult mouse brain. *Neuroscience* **39**:151-170.

Mikolajczyk K, Szabatin M, Rudnicki P, Grodzki M, Burger C (1998). A JAVA environment for medical image data analysis: initial application for brain PET quantitation. *Med Inform.(Lond)* **23**:207-214.

Miller SD, McRae BL, Vanderlugt CL, Nikcevich KM, Pope JG, Pope L, Karpus WJ (1995). Evolution of the T-cell repertoire during the course of experimental immune-mediated demyelinating diseases. *Immunol.Rev.* **144**:225-244.

Nesbit GM, Forbes GS, Scheithauer BW, Okazaki H, Rodriguez M (1991). Multiple sclerosis: histopathologic and MR and/or CT correlation in 37 cases at biopsy and three cases at autopsy. *Radiology* **180**:467-474.

Nijeholt GJ, van Walderveen MA, Castelijns JA, van Waesberghe JH, Polman C, Scheltens P, Rosier PF, Jongen PJ, Barkhof F (1998). Brain and spinal cord abnormalities in multiple sclerosis. Correlation between MRI parameters, clinical subtypes and symptoms. *Brain* **121**:687-697.

Poser CM, Paty DW, Scheinberg L, McDonald WI, Davis FA, Ebers GC, Johnson KP, Sibley WA, Silberberg DH, Tourtellotte WW (1983). New diagnostic criteria for multiple sclerosis: guidelines for research protocols. *Ann Neurol* **13**:227-231.

Ramsay SC, Weiller C, Myers R, Cremer JE, Luthra SK, Lammertsma AA, Frackowiak RS (1992). Monitoring by PET of macrophage accumulation in brain after ischaemic stroke. *Lancet* **339** :1054-1055.

Schlumpf M, Parmar R, Lichtensteiger W (1993). Prenatal diazepam induced persisting downregulation of peripheral (omega 3) benzodiazepine receptors on rat splenic macrophages. *Life Sci.* **52**:927-934.

Sorensen JC, Dalmau I, Zimmer J, Finsen B (1996). Microglial reactions to retrograde degeneration of tracer-identified thalamic neurons after frontal sensorimotor cortex lesions in adult rats. *Exp Brain Res* **112**:203-212.

Sriram S, Rodriguez M (1997). Indictment of the microglia as the villain in multiple sclerosis. *Neurology* **48**:464-470.

Trapp BD, Peterson J, Ransohoff RM, Rudick R, Mork S, Bo L (1998). Axonal transection in the lesions of multiple sclerosis. *N.Engl.J Med* **338**:278-285.

Vowinckel E, Reutens D, Becher B, Verge G, Evans A, Owens T, Antel JP (1997). PK11195 binding to the peripheral benzodiazepine receptor as a marker of microglia activation in multiple sclerosis and experimental autoimmune encephalomyelitis. *J Neurosci Res* **50** :345-353.

IMAGING OF MICROGLIAL ACTIVATION WITH PET AND ATROPHY WITH MRI IN MULTIPLE SCLEROSIS: INTERRELATIONSHIP AND CLINICAL CORRELATES

Jan Versijpt MD[1,6], Jan C Debruyne MD[2], Koenraad J Van Laere MD PhD DrSc[1], Filip De Vos Pharm PhD[3], Johan Keppens Eng[1], Karel Strijckmans DrSc[4], Eric Achten MD PhD[5], Guido Slegers Pharm DrSc[3], Rudi A Dierckx MD PhD[1], Jakob Korf DrSc[6], Jacques L De Reuck MD PhD[2]

[1] Division of Nuclear Medicine, Ghent University Hospital

[2] Department of Neurology, Ghent University Hospital, Ghent, Belgium

[3] Laboratory of Radiopharmacy, Ghent University

[4] Laboratory of Analytical Chemistry, Institute for Nuclear Sciences, Ghent University

[5] Department of Radiology, MR-Unit, Ghent University Hospital

[6] Department of Biological Psychiatry, University Hospital, Groningen, the Netherlands

J Neurol Sci, submitted

ABSTRACT

Objective: The objectives of the present study were to assess brain atrophy in MS patients during different disease stages and to investigate by PET and [^{11}C]PK11195, a marker of microglial activation, the relationship between inflammation, atrophy, and clinical relevant measures.

Methods: Eight healthy subjects and 22 MS patients were included. Semiquantitative [^{11}C]PK11195 uptake values, with normalization on cortical gray matter, were measured for magnetic resonance imaging T_2- and T_1-lesions and normal appearing white matter (NAWM). As atrophy index we used the ratio of the amount of white and gray matter divided by the ventricular size, using an optimized a priori based segmentation algorithm (SPM99).

Results: Atrophy was significantly greater in MS patients compared to age-matched controls. A significant correlation was found between brain atrophy and both disease duration and disability, as measured with the expanded disability status scale (EDSS). For NAWM, [^{11}C]PK11195 uptake increased with the amount of atrophy, while T_2-lesional [^{11}C]PK11195 uptake values decreased according to increasing brain atrophy.

Conclusions: Brain atrophy, correlating with disease duration and disability, is directly related to NAWM and T_2-lesional inflammation as measured by microglial activation.

INTRODUCTION

In MS, neuroinflammation is the pivotal event that causes demyelination and oligodendrocyte cell death [1]. Whereas over the past decade most attention was focused on the theory of a T-cell mediated autoimmune process [2], in vitro studies however showed that microglia also can be activated by various stimuli resulting in the expression of proinflammatory cytokines, matrix metalloproteinases, and free radicals [3]. In addition, activated microglia serve as the major antigen-presenting cell in the CNS, likely contributing to aberrant immune reactivity at this site. Accordingly, it has been hypothesized that demyelination may, at least partly, be the result of microglial activation leading to the release of myelinotoxic factors that directly injure the oligodendrocyte-myelin unit [4]. As a consequence, it is believed that microglia play a prominent role in autoimmune mediated demyelinating disorders of the central nervous system.

One of the characteristic features of microglia is their rapid activation in response to brain *injury* with a concomitant higher expression of the peripheral benzodiazepine receptor (PBR) [5]. Visualization of the PBR can be performed by means of radiolabeled PK11195. This specific high-affinity ligand, allows as such the assessment of microglial activation giving more specific *in vivo* information concerning the underlying histopathological features due to neuroinflammation in general and to MS in particular [6]. PK11195 has been labeled with ^{11}C for PET and applied in various neuroinflammatory conditions like Rasmussen's encephalitis [7], cerebral vasculitis [8], and Herpes simplex encephalitis [9].

Previously, we demonstrated characteristic [^{11}C]PK11195 uptake patterns for chronic and active white matter lesions and normal appearing white matter (NAWM) in subgroups of MS patients, exemplifying an additional value of [^{11}C]PK11195 imaging over MRI concerning the assessment and monitoring of the *immuno-pathophysiological* process in MS. Moreover, a significant steady rising amount of NAWM [^{11}C]PK11195 uptake during disease progression was found, propagating NAWM as a major burden of the disease [10]. Concordingly with the hypothesis that microglia can directly induce myelin damage through the release of proinflammatory mediators [11], this study suggested that during the disease process invisible demyelination is an increasingly ongoing NAWM process.

On the other hand, atrophy of the brain and spinal cord at postmortem examination is considered to be a hallmark of irreversible CNS damage. Indeed, MS involves substantial loss of both axonal density and volume, in addition to the well-recognized loss of myelin within lesions [12,13]. Whereas in healthy controls, the progressive loss of brain parenchyma occurs with magnitudes ranging from 0.1 to 0.3 % per year, for MS patients the reduction in brain volume is estimated at 0.4 to 5 % per year where most published patient cohorts narrow this annual loss range to 0.6 to 1 % per year [13-15], starting already in the early stage of the disease, and being associated with short-term clinical disease activity [16,17]. Although the pathologic basis of MS-related atrophy is still unclear, there seems to be a connection with the NAWM inflammatory process. As such, a rather global process, such as (MRI-)invisible demyelination with consequently a steady axonal loss might underlie this brain atrophy [18]. This was

also demonstrated by Trapp *et al.* in a postmortem study showing axonal transection as a consistent feature in NAWM [19]. Newer MR techniques, such as magnetization transfer imaging and magnetization resonance spectroscopy have confirmed this loss of brain parenchyma in the NAWM as being a major burden of disease contributing to whole brain atrophy [20,21].

The objectives of the present study were threefold: firstly, the assessment of brain atrophy in MS patients compared to age-matched normal controls, secondly, the correlation of brain atrophy with clinical measures, and thirdly, the correlation of [^{11}C]PK11195 uptake with brain atrophy measures.

PATIENTS AND METHODS

Subjects

The study was approved by the Ethical Committee of the Ghent University Hospital and written informed consent was obtained from each subject. Eight controls (3 men, five women; mean age 37.2 ± 13, range 23-65 y) and 27 clinical definite and laboratory proven MS patients referring to the criteria of the International Panel on the Diagnosis of Multiple Sclerosis were randomly included [22]. Five patients had to be removed from the study because of head movement and subsequent coregistration errors between perfusion and receptor PET scanning. Finally, 22 patients were eligible (9 men, 13 women; mean age 42.6 ± 11, range 26-64 y). There was no statistically significant age difference between patients and controls ($p = 0.3$). Demographic and clinical parameters of the MS patients are described in table 1. Four MS patients were treated with IFN-ß at the time of inclusion. Thirteen patients had the relapsing-remitting type (RR) of the disease while 7 patients were secondary progressive (SP), having a continuous worsening of invalidity over a follow-up period of at least 6 months. Two patients had a primary progressive course (PP) without relapses from the very beginning of the disease. Six patients had a clinical relapse at the time of scanning, defined as the occurrence or worsening of neurological dysfunction lasting more than 24 hours. In 3 of them, corticosteroids needed to be administered after all imaging was performed. Ten patients showed Gd-enhancing lesions on the MRI scan, 5 of them with a concomitant clinical relapse. The average disease duration was 9.3 ± 8.3 y (range 0.3-33 y). The average expanded disability status scale (EDSS) was 4.0 ± 2.0 (range 1.0-7.0).

Age	Sex	Type	disease duration (y)	EDSS
44	M	RR	2.3	3.0
37	F	RR	3.6	1.5
51	F	RR	22.7	2.5
64	F	PP	13.7	7.0
45	F	PP	12.7	6.0
32	F	RR	3.1	3.0
45	F	RR	14.8	3.0
27	M	RR	3.8	1.0
49	M	SP	8.8	7.0
50	F	SP	8.7	5.5
38	F	RR	0.3	1.5
51	F	SP	23.7	4.5
36	M	RR	0.7	5.5
31	M	RR	13.2	3.5
35	F	SP	7.7	4.5
60	M	SP	32.7	6.5
64	F	SP	7.6	4.5
26	M	RR	2.2	1.5
45	F	SP	9.7	6.5
42	M	RR	3.1	1.0
37	M	RR	6.9	5.5
31	F	RR	3.5	3.0

RR = relapsing-remitting; SP = secondary progressive; PP = primary progressive; EDSS = expanded disability status scale

Table 1 Clinical characteristics of the MS patients

Radiochemistry

PK11195 [1-(2-chlorophenyl)-N-methyl-N-(1-methylpropyl)-3-isoquinoline carboxamide] was obtained from RBI (Natick, MA, USA). [^{11}C]PK11195 was synthesized according to a procedure described by Camsonne et al [23]. Briefly, 3 µmol N-desmethyl PK11195 was dissolved in 150 µL dimethylsulphoxide, containing 3 µmol tetrabutylammonium hydroxide. After trapping of [^{11}C]CH_3I, the vial was closed and heated at 80°C for 3 min. Purification was done by HPLC using a RP-C18 column (Econosil, 250 mm x 10 mm, 10 µm particle size) and an ethanol/water (70/30) mixture as mobile phase. Radiochemical yield towards [^{11}C]CH_3I was 57% (confidence interval 2 %, 30 experiments). Finally, 3.7 GBq [^{11}C]PK11195 was obtained with a specific activity of 25 GBq/µmol. Chemical and radiochemical purity were higher than 99%. All subjects were injected intravenously with 370 ± 10 % MBq [^{11}C]PK11195 with a slow bolus in a time course of 30 seconds.

Data acquisition and processing

All subjects underwent MR and PET scanning on the same day.

MR imaging was performed on a 1.5 T MR scanner (Siemens, Magnetom SP4000; Erlangen, Germany). Prior to the administration of gadolinium, standard spin-echo imaging was carried out in 5 mm thick axial planes (pixel size of 0.9 $\times$ 0.9 mm^2) with proton density- (TR/TE/NEX=2170/20/1), T_2- (TR/TE/NEX=2170/80/1) and T_1-weighted (TR/TE/NEX=600/12/1) contrast. Five minutes after gadolinium injection, the axial slices were rescanned with T_1-weighting (TR/TE/NEX=800/20/1).

PET studies were performed on a Siemens ECAT 951/31 PET scanner (Siemens, Knoxville, TN, USA) with a transaxial and axial resolution (FWHM) of 5.8 and 5 mm respectively (values provided by Siemens, operating in 2D mode). All subjects were placed in supine position with dimmed lights and low ambient noise. Realignment of the head to the orbitomeatal line was performed by laser guidance. Reconstruction was done using filtered backprojection with a Hanning filter (cut-off of 0.5 cycles/cm). Sequential transmission scanning was performed using a ^{68}Ge/^{68}Ga ring source. Correction for scatter was done using the standard software provided by the manufacturer. Subsequently, regional cerebral blood flow (rCBF) images were acquired by [^{15}O]CO_2 inhalation at 900 MBq/min. For this, the steady state technique using [^{15}O]CO_2 was applied [24]. Eight minutes later, a one-hour dynamic PET study was conducted after the injection of 370 MBq [^{11}C]PK11195. Nineteen frames, each consisting of thirty-one planes of 3.375 mm thickness, were recorded over 60 min with an increasing duration of 2×5 s, 5×10 s, 4×1 min, 2×3 min, 1×4 min, 1×5 min and 4×10 min. Automatic radioactive decay correction was applied to all images. No partial volume correction was applied. Since a previous feasibility study showed that the time-activity curves for both volunteers and patients had a similar decline with a steady-state period from 40 min post-injection, data obtained from 40-60 min post-injection were summed (static scans) [25]. Individual automatic coregistration of MR and perfusion PET data was achieved using SPM99 (Statistical Parametric Mapping, Functional Imaging Laboratory, Wellcome Department of Cognitive Neurology, Institute of Neurology, London, UK) [26]. Spatial normalization was done on the normal templates for T_1-weighted MR in MNI space (Montreal Neurological Institute), using non-linear warping with 7×8×7 basic functions (5 iterations), and to a voxel size of 3×3×3 mm^3. T_2-, Gd- and coregistered PET data underwent the same transformation as the original T_1-image. The same spatial transformation parameters as for the perfusion PET studies were subsequently applied to the [^{11}C]PK11195 data.

Volumes of interest and [^{11}C]PK11195 uptake semiquantification

Since no generally accepted model of absolute quantification of [^{11}C]PK11195 specific binding in normal brain has been widely validated and no dynamic data for all volunteers were obtained neither was arterial sampling carried out, a validated semiquantitative approach was carried out on the static images obtained during the steady-state period of the [^{11}C]PK11195 brain uptake [25]. Volumes of interest (VOIs) were defined on the individual's spatially standardized high-resolution MR scan in white and gray matter for volunteers and in NAWM, gray matter, T_2- and T_1-

Gd-lesions for MS patients and automatically transferred onto the coregistered [^{11}C]PK11195 scan by means of PMOD (University Hospital Zurich, Switzerland), a kinetic modeling and image fusion environment tool in Java [27]. When drawing VOIs, care was taken to avoid the carotid and major cerebral arteries as well as the ventricles or venous sinuses. Three global regions were defined namely white matter, cortical and central gray matter (thalamus and striatum, this was done because high labeling of [^{3}H]PK11195 was described in diencephalic structures notably in several thalamic nuclei [28]). The normalized specific uptake for a particular area of interest was defined as the mean activity per volume unit in this area divided by the mean activity per volume unit in cortical gray matter.

Atrophy measures

Relative parenchymal fractions were assessed with the whole-brain probabalistic segmentation and volumetry module incorporated within SPM99. T_1-weighted images were used. Since relative brain atrophy measures have shown to be superior to absolute measures for cross-sectional studies [29], images were first normalized to the MNI template using the default SPM spatial pre-processing method (normalization with bilinear interpolation, 7×8×7 nonlinear basic functions, 12 iterations and medium nonlinear regularization). Then, images were segmented, without lesion extraction using the '*lots of inhomogeneity correction*' option into gray and white matter and CSF maps for which the respective volume was determined as the proportion of voxels, worked out from a subregion of the volume that encloses the brain [30]. Finally, the brain atrophy index was defined as the relative CSF volume divided by the relative white and gray matter volume. Figure one shows an image of a segmented axial MR slice of a 37-year old MS patient (panel A) and a 39-year old healthy control subject (panel B).

Statistical analysis

Data were analyzed by means of SPSS v10.0 for Windows (Chicago, IL, USA). For normality testing, a Kolmogorov-Smirnov test statistic was applied. For differences between groups, an *independent samples T test* or a *Mann-Whitney U test* was applied whereas for the correlational analysis, a Pearson or Spearman correlation coefficient was calculated, when appropriate. A *p value* lower than or equal to 0.05 was considered as significant. Data are given as means ± one standard deviation.

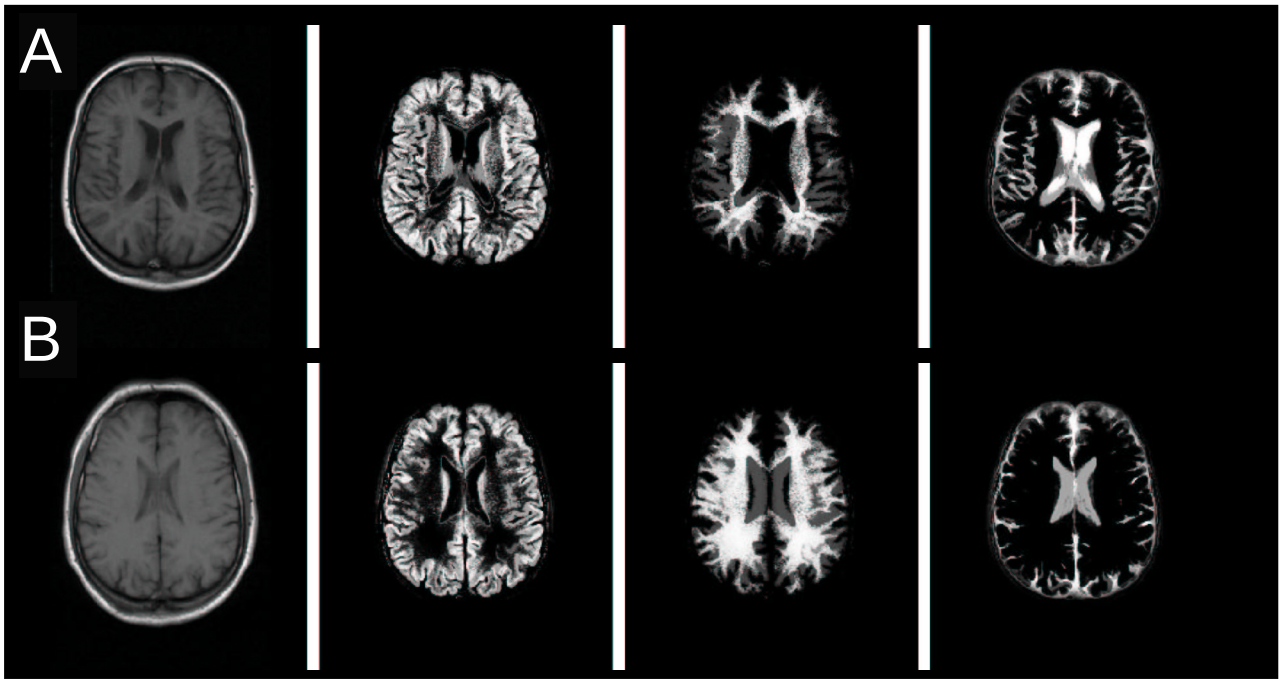

Figure 1. Example of a segmented axial MR slice into gray and white matter and cerebrospinal fluid for a 37-year old MS patient (panel A) and a 39-year old healthy control (panel B), after anatomical standardization

RESULTS

Atrophy measures for MS patients versus age-matched controls

Table 2 shows the atrophy measures for the different brain compartments. Atrophy as measured by the atrophy index was significantly greater in MS patients compared to age-matched controls (p = 0.04). When considering the brain compartments separately, the relative amount of gray matter, (normal appearing) white matter and CSF were all indicative of the loss of brain tissue for MS patients, however, only the difference in ventricular size (CSF) was statistically significant (p = 0.04). Whereas for controls a significant correlation was found between age and the amount of gray matter, CSF and the atrophy index (p = 0.009, p = 0.03 and p = 0.02 respectively), no statistically significant correlation was found between age and any atrophy measure for patients.

	MS patients	**age-matched controls**	***p-value***
gray matter	0.183 ± 0.011	0.186 ± 0.012	0.6
(normal appearing) white matter	0.102 ± 0.009	0.106 ± 0.007	0.3
CSF	0.089 ± 0.012	0.080 ± 0.007	**0.04**
$\frac{CSF}{gray + white}$	0.314 ± 0.047	0.275 ± 0.034	**0.04**

Table 2: Atrophy comparison between MS patients and age - matched controls

Correlation of the atrophy index with disease duration and disability

As shown in figure two, there was a statistically significant correlation between disease duration and brain atrophy (r = 0.5; p = 0.03). The correlation between atrophy and disability as measured by the EDSS yielded also statistical significance (r = 0.4, p = 0.05; figure three).

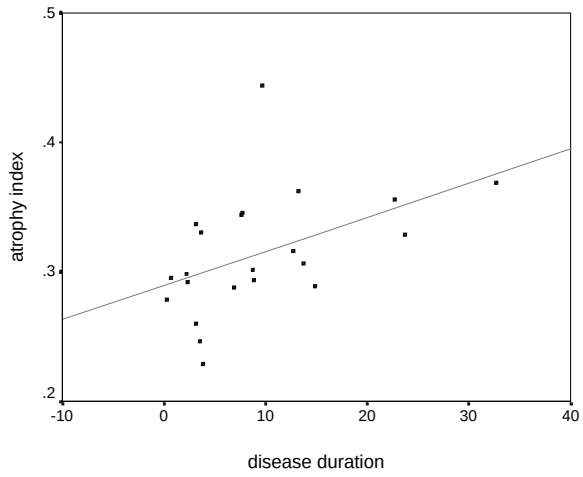

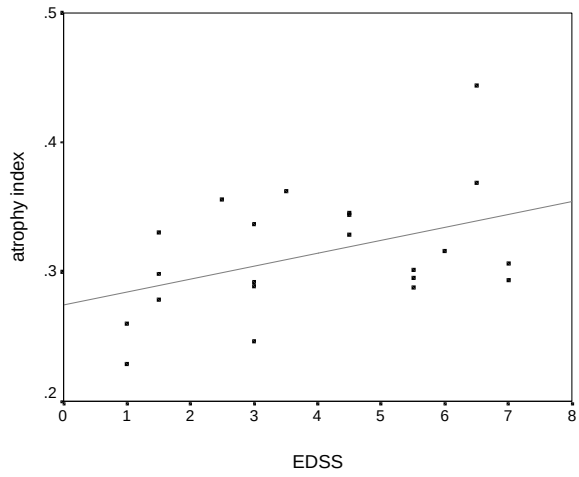

Figure 2 (left). Scatterplot of atrophy as measured by the atrophy index with disease duration (y)
Figure 3 (right). Scatterplot of atrophy as measured by the atrophy index with disability (EDSS)

Correlation of lesional [^{11}C]PK11195 uptake values with atrophy

Figure four demonstrates the relation of NAWM [^{11}C]PK11195 uptake with atrophy, indicating that the amount of NAWM microglial activation as measured with [^{11}C]PK11195 PET scanning is statistically

significant corelated to the amount of atrophy (r = 0.2; p = 0.03). It was also shown that the [^{11}C]PK11195 uptake for T_2-lesions decreases significantly with increasing brain atrophy (r = -0.3, p = 0.03; Figure five). There was no relation between [^{11}C]PK11195 uptake in gadolinium-enhancing lesions and brain atrophy (r = -0.01; p = 0.9).

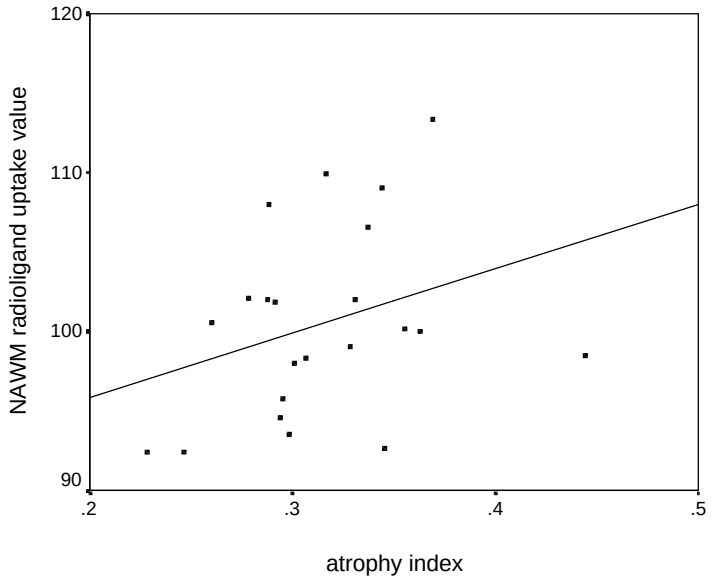

Figure 4. Scatterplot of the NAWM [^{11}C]PK11195 uptake value with atrophy as measured by the atrophy index

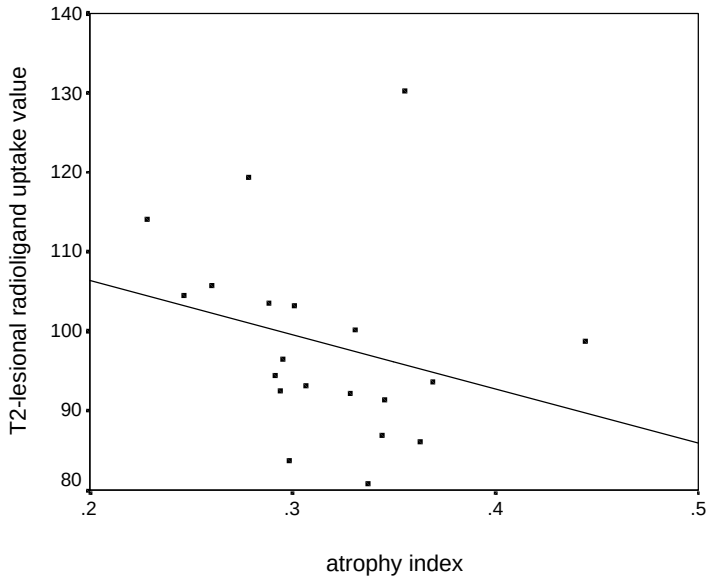

Figure 5. Scatterplot of the T_2-lesional [^{11}C]PK11195 uptake value with atrophy as measured by the atrophy index

DISCUSSION

Recent MRI studies in MS have emphasized that brain atrophy is a robust and pivotal marker of disease progression, reflecting the destructive processes as a result of extensive axonal damage [15,16]. However, the assessment of cerebral atrophy by MRI is difficult due to general factors such as (small) inter-individual variations in head size and intracranial volume, inconsistencies in the acquisition sequence like differences in the measured voxel size or slice thickness, movement artifacts, magnetic field inhomogeneities and variations in MR image intensity scales. In addition, also disease-specific aspects like fluctuations of tissue water content such as in vasogenic edema coupled to active lesions or the administration of 'anti-inflammatory' treatment are potential sources of error [31,32]. Atrophy has been measured with MRI both by manual techniques as well as by semi-automated contour or thresholding segmentation techniques. Actual atrophy measures ranged from linear atrophy measures like the intercaudate distance, whole brain or ventricular width to absolute or relative volumes of ventricles, whole brain, hemisphere or some adherent slices, corpus callosum, or more specific brain structures like the cerebellum or brainstem [16,33-35].

Ideally however, the measurement technique should be fully reproducible, automated, accurate and very sensitive. In the present study the statistical parametric mapping software package (SPM99) was used for the assessment of brain atrophy which is a relatively robust method and requires no manual intervention [36]. SPM software uses prior spatial information from a database of normal brain images to classify voxels, according to their location and signal intensity characteristics, as gray matter, white matter or CSF and can be applied to both 2D or 3D images. This method was recently introduced by Chard *et al.* for the measurement of brain parenchymal, white and gray matter fractions in early relapsing-remitting MS patients making use of three-dimensional fast spoiled gradient recall MR scans with a slice thickness of 1.5 mm [37].

Measures of brain atrophy have been found to correlate to varying degrees with intellectual and memory dysfunction, dementia, and scores for neuropsychological tests [38,39]. Concerning the relationship between atrophy and disability, several conflicting results have been reported, most likely also enhanced by varying atrophy measures throughout different studies. The present study found a significant correlation between atrophy and disability, as measured by the EDSS, which is in agreement with most previously reported findings [40-47]. However, Wilson et al found no correlation between cerebral volume and clinical disability [48] while Ge et al as well found no significant correlation between fractional white nor gray matter volume and disability in a group of 27 RR MS patients [49].

In a previous study, we demonstrated a slightly higher NAWM [^{11}C]PK11195 uptake compared to normal white matter where the NAWM [^{11}C]PK11195 uptake showed a steady rising slope with disease progression indicating the growing amount of activated microglia, undetectable for MRI in this brain area [10]. The present study demonstrates the weak, however significant correlation between this rising NAWM [^{11}C]PK11195 uptake during disease progression and the decrease in brain parenchymal volume.

It has to be noted however that this study was not a longitudinal study but rather a snapshot study of patients with a different disease duration, making it rather difficult to draw formal conclusions about disease progression and as such necessitating extrapolations. Yet, this is the first study to reveal *in vivo* the direct relationship between NAWM inflammation or microglial activation as measured with radiolabeled PK11195 on one hand and atrophy on the other hand and demonstrates that abnormalities in the NAWM are one factor, if not one of the most important, contributing to neurological impairment [50,51]. The mechanism of neuroinflammation leading to atrophy is most probably mediated by a steady ongoing NAWM process of invisible demyelination by activated microglia. Indeed, a study by Yin *et al.* with myelin-associated glycoprotein (MAG) deficient mice demonstrated already this relationship between demyelination and atrophy where the absence of MAG leaded to chronic atrophy of myelinated axons and axonal degeneration [52]. This process of (hypo)myelination seems pivotal in the evolution of brain atrophy and is maintained by the lack of neurotrophic factors like MAG in the myelin sheat which are important for the protection of the cytoplasmic collar and the periaxonal space [53].

The present study did not reveal any correlation between T_1-Gadolinium-enhanced lesional [^{11}C]PK11195 uptake and brain atrophy. This is in concordance with Saindane *et al.* where the relationship between the Gadolinium-enhancing T_1 lesion load and the development of whole brain atrophy over a 2-years period was investigated and no correlation was found [18]. This suggests that the breakdown in the blood-brain barrier may be considered as an epiphenomenon in the process of brain atrophy giving rise to localized inflammation with reversible edema and some degree of focal axonal damage. Moreover, both magnetization transfer and magnetic resonance spectroscopy studies established that a rather global process underlies atrophy in MS [18,54,55], which was confirmed in the present study indicating the NAWM as a substantial contributor to brain atrophy.

The results of this study implicate the role of activated microglia in the overall demyelinating process especially in NAWM and emphasize the important long-term relationship between neuroinflammation and brain atrophy, the latter evolving by mechanisms that are at least partly independent of those mechanisms responsible for MRI lesions.

REFERENCES

[1] Dinter H, Onuffer J, Faulds D, Perez HD. Phosphodiesterase type IV inhibitors in the treatment of multiple sclerosis. J Mol Med 1997;75:95-102.

[2] Awad M, Gavish M. Peripheral-type benzodiazepine receptors in human cerebral cortex, kidney, and colon. Life Sci 1991;49:1155-61.

[3] Gebicke-Haerter PJ, Van Calker D, Norenberg W, Illes P. Molecular mechanisms of microglial activation. A. Implications for regeneration and neurodegenerative diseases. Neurochem Int 1996;29:1-12.

[4] Sriram S, Rodriguez M. Indictment of the microglia as the villain in multiple sclerosis. Neurology 1997;48:464-70.

[5] Agnello D, Carvelli L, Muzio V, Villa P, Bottazzi B, Polentarutti N, Mennini T, Mantovani A, Ghezzi P. Increased peripheral benzodiazepine binding sites and pentraxin 3 expression in the spinal cord during EAE: relation to inflammatory cytokines and modulation by dexamethasone and rolipram. J Neuroimmunol 2000;109:105-11.

[6] Vowinckel E, Reutens D, Becher B, Verge G, Evans A, Owens T, Antel JP. PK11195 binding to the peripheral benzodiazepine receptor as a marker of microglia activation in multiple sclerosis and experimental autoimmune encephalomyelitis. J Neurosci Res 1997;50:345-53.

[7] Banati RB, Goerres GW, Myers R, Gunn RN, Turkheimer FE, Kreutzberg GW, Brooks DJ, Jones T, Duncan JS. [^{11}C](R)-PK11195 positron emission tomography imaging of activated microglia in vivo in Rasmussen's encephalitis. Neurology 1999;53:2199-203.

[8] Goerres GW, Revesz T, Duncan J, Banati RB. Imaging cerebral vasculitis in refractory epilepsy using [^{11}C](R)-PK11195 positron emission tomography. Am J Roentgenol 2001;176:1016-8.

[9] Cagnin A, Myers R, Gunn RN, Lawrence AD, Stevens T, Kreutzberg GW, Jones T, Banati RB. In vivo visualization of activated glia by [^{11}C] (R)-PK11195-PET following herpes encephalitis reveals projected neuronal damage beyond the primary focal lesion. Brain 2001;124:2014-27.

[10] Debruyne JC, Versijpt J, Van Laere K, De Vos F, Keppens J, Strijckmans K, Achten E, Slegers G, Dierckx R, Korf J, De Reuck JL. PET visualisation of microglia in multiple sclerosis patients using [^{11}C]PK11195. Eur J Neurol 2003;in press:

[11] Brenner T, Brocke S, Szafer F, Sobel RA, Parkinson JF, Perez DH, Steinman L. Inhibition of nitric oxide synthase for treatment of experimental autoimmune encephalomyelitis. J Immunol 1997;158:2940-6.

[12] Evangelou N, Esiri MM, Smith S, Palace J, Matthews PM. Quantitative pathological evidence for axonal loss in normal appearing white matter in multiple sclerosis. Ann Neurol 2000;47:391-5.

[13] Liu C, Edwards S, Gong Q, Roberts N, Blumhardt LD. Three dimensional MRI estimates of brain and spinal cord atrophy in multiple sclerosis. J Neurol Neurosurg Psychiatry 1999;66:323-30.

[14] Filippi M, Grossman RI. MRI techniques to monitor MS evolution: the present and the future. Neurology 2002;58:1147-53.

[15] Simon JH, Jacobs LD, Campion MK, Rudick RA, Cookfair DL, Herndon RM, Richert JR, Salazar AM, Fischer JS, Goodkin DE, Simonian N, Lajaunie M, Miller DE, Wende K, Martens-Davidson A, Kinkel RP, Munschauer FE, III, Brownscheidle CM. A longitudinal study of brain atrophy in relapsing multiple sclerosis. The Multiple Sclerosis Collaborative Research Group (MSCRG). Neurology 1999;53:139-48.

[16] Rudick RA, Fisher E, Lee JC, Simon J, Jacobs L. Use of the brain parenchymal fraction to measure whole brain atrophy in relapsing-remitting MS. Multiple Sclerosis Collaborative Research Group. Neurology 1999;53:1698-704.

[17] Brex PA, Jenkins R, Fox NC, Crum WR, O'Riordan JI, Plant GT, Miller DH. Detection of ventricular enlargement in patients at the earliest clinical stage of MS. Neurology 2000;54:1689-91.

[18] Saindane AM, Ge Y, Udupa JK, Babb JS, Mannon LJ, Grossman RI. The effect of gadolinium-enhancing lesions on whole brain atrophy in relapsing-remitting MS. Neurology 2000;55:61-5.

[19] Trapp BD, Peterson J, Ransohoff RM, Rudick R, Mork S, Bo L. Axonal transection in the lesions of multiple sclerosis. N Engl J Med 1998;338:278-85.

[20] Tortorella C, Viti B, Bozzali M, Sormani MP, Rizzo G, Gilardi MF, Comi G, Filippi M. A magnetization transfer histogram study of normal-appearing brain tissue in MS. Neurology 2000;54:186-93.

[21] Rooney WD, Goodkin DE, Schuff N, Meyerhoff DJ, Norman D, Weiner MW. ^{1}H MRSI of normal appearing white matter in multiple sclerosis. Mult Scler 1997;3:231-7.

[22] McDonald WI, Compston A, Edan G, Goodkin D, Hartung HP, Lublin FD, McFarland HF, Paty DW, Polman CH, Reingold SC, Sandberg-Wollheim M, Sibley W, Thompson A, van den NS, Weinshenker BY, Wolinsky JS. Recommended diagnostic criteria for multiple sclerosis: guidelines from the International Panel on the diagnosis of multiple sclerosis. Ann Neurol 2001;50:121-7.

[23] Camsonne R, Crouzel C, Comar D, Maziere M, Prenant C, Sastre J, Moulin MA, Syrota A. Synthesis of n-(C-11) methyl, n-(methyl-1 propyl), (chloro-2 phenyl)-1 isoquinoleine carboxamide-3 (PK-11195) – a new ligand for peripheral benzodiazepine receptors. J Labelled Compd Rad 1984;21:985-91.

[24] Frackowiak RS, Lenzi GL, Jones T, Heather JD. Quantitative measurement of regional cerebral blood flow and oxygen metabolism in man using ^{15}O and positron emission tomography: theory, procedure, and normal values. J Comput Assist Tomogr 1980;4:727-36.

[25] Debruyne JC, Van Laere KJ, Versijpt J, De Vos F, Keppens J, Strijckmans K, Santens P, Achten E, Slegers G, Korf J, Dierckx RA, De Reuck JL. Semiquantification of the peripheral-type benzodiazepine ligand [^{11}C]PK11195 in normal human brain and application in multiple sclerosis patients. Acta Neurol Belg 2002;102:127-35.

[26] Friston KJ, Frith CD, Liddle PF, Frackowiak RS. Comparing functional (PET) images: the assessment of significant change. J Cereb Blood Flow Metab 1991;11:690-9.

[27] Mikolajczyk K, Szabatin M, Rudnicki P, Grodzki M, Burger C. A JAVA environment for medical image data analysis: initial application for brain PET quantitation. Med Inform (Lond) 1998;23:207-14.

[28] Doble A, Malgouris C, Daniel M, Daniel N, Imbault F, Basbaum A, Uzan A, Gueremy C, Le Fur G. Labelling of peripheral-type benzodiazepine binding sites in human brain with [^{3}H]PK 11195: anatomical and subcellular distribution. Brain Res Bull 1987;18:49-61.

[29] Zivadinov R, Fisher E, Grop A, et al. Normalized vs. absolute brain atrophy measures in multiple sclerosis. Mult Scler 2001; 7: P117.

[30] Ashburner J, Friston K. Multimodal image coregistration and partitioning--a unified framework. Neuroimage 1997;6:209-17.

[31] Blatter DD, Bigler ED, Gale SD, Johnson SC, Anderson CV, Burnett BM, Parker N, Kurth S, Horn SD. Quantitative volumetric analysis of brain MR: normative database spanning 5 decades of life. AJNR Am J Neuroradiol 1995;16:241-51.

[32] Whitwell JL, Crum WR, Watt HC, Fox NC. Normalization of cerebral volumes by use of intracranial volume: implications for longitudinal quantitative MR imaging. AJNR Am J Neuroradiol 2001;22:1483-9.

[33] Stevenson VL, Miller DH. Measures of brain and spinal cord atrophy. In: Rudick RA, Goodkin DE, editors. Multiple sclerosis therapeutics. London: Martin Dunitz Ltd, 1999:107-17.

[34] Bermel RA, Bakshi R, Tjoa C, Puli SR, Jacobs L. Bicaudate ratio as a magnetic resonance imaging marker of brain atrophy in multiple sclerosis. Arch Neurol 2002;59:275-80.

[35] Miller DH, Barkhof F, Frank JA, Parker GJ, Thompson AJ. Measurement of atrophy in multiple sclerosis: pathological basis, methodological aspects and clinical relevance. Brain 2002;125:1676-95.

[36] Ashburner J, Friston KJ. Voxel-based morphometry--the methods. Neuroimage 2000;11:805-21.

[37] Chard DT, Griffin CM, Parker GJ, Kapoor R, Thompson AJ, Miller DH. Brain atrophy in clinically early relapsing-remitting multiple sclerosis. Brain 2002;125:327-37.

[38] Zivadinov R, Sepcic J, Nasuelli D, De Masi R, Bragadin LM, Tommasi MA, Zambito-Marsala S, Moretti R, Bratina A, Ukmar M, Pozzi-Mucelli RS, Grop A, Cazzato G, Zorzon M. A longitudinal study of brain atrophy and cognitive disturbances in the early phase of relapsing-remitting multiple sclerosis. J Neurol Neurosurg Psychiatry 2001;70:773-80.

[39] Arnold DL, Matthews PM. MRI in the diagnosis and management of multiple sclerosis. Neurology 2002;58:S23-S31

[40] Bakshi R, Benedict RH, Bermel RA, Jacobs L. Regional brain atrophy is associated with physical disability in multiple sclerosis: semiquantitative magnetic resonance imaging and relationship to clinical findings. J Neuroimaging 2001;11:129-36.

[41] Berg D, Maurer M, Warmuth-Metz M, Rieckmann P, Becker G. The correlation between ventricular diameter measured by transcranial sonography and clinical disability and cognitive dysfunction in patients with multiple sclerosis. Arch Neurol 2000;57:1289-92.

[42] Fisher E, Rudick RA, Cutter G, Baier M, Miller D, Weinstock-Guttman B, Mass MK, Dougherty DS, Simonian NA. Relationship between brain atrophy and disability: an 8-year follow-up study of multiple sclerosis patients. Mult Scler 2000;6:373-7.

[43] Kalkers NF, Bergers E, Castelijns JA, van Walderveen MA, Bot JC, Ader HJ, Polman CH, Barkhof F. Optimizing the association between disability and biological markers in MS. Neurology 2001;57:1253-8.

[44] Luks TL, Goodkin DE, Nelson SJ, Majumdar S, Bacchetti P, Portnoy D, Sloan R. A longitudinal study of ventricular volume in early relapsing-remitting multiple sclerosis. Mult Scler 2000;6:332-7.

[45] Paolillo A, Pozzilli C, Gasperini C, Giugni E, Mainero C, Giuliani S, Tomassini V, Millefiorini E, Bastianello S. Brain atrophy in relapsing-remitting multiple sclerosis: relationship with 'black holes', disease duration and clinical disability. J Neurol Sci 2000;174:85-91.

[46] Pelletier J, Suchet L, Witjas T, Habib M, Guttmann CR, Salamon G, Lyon-Caen O, Cherif AA. A longitudinal study of callosal atrophy and interhemispheric dysfunction in relapsing-remitting multiple sclerosis. Arch Neurol 2001;58:105-11.

[47] Rovaris M, Comi G, Rocca MA, Wolinsky JS, Filippi M. Short-term brain volume change in relapsing-remitting multiple sclerosis: effect of glatiramer acetate and implications. Brain 2001;124:1803-12.

[48] Wilson M, Morgan PS, Lin X, Turner BP, Blumhardt LD. Quantitative diffusion weighted magnetic resonance imaging, cerebral atrophy, and disability in multiple sclerosis. J Neurol Neurosurg Psychiatry 2001;70:318-22.

[49] Ge Y, Grossman RI, Udupa JK, Babb JS, Nyul LG, Kolson DL. Brain atrophy in relapsing-remitting multiple sclerosis: fractional volumetric analysis of gray matter and white matter. Radiology 2001;220:606-10.

[50] Filippi M, Tortorella C, Rovaris M, Bozzali M, Possa F, Sormani MP, Iannucci G, Comi G. Changes in the normal appearing brain tissue and cognitive impairment in multiple sclerosis. J Neurol Neurosurg Psychiatry 2000;68:157-61.

[51] Fu L, Matthews PM, De Stefano N, Worsley KJ, Narayanan S, Francis GS, Antel JP, Wolfson C, Arnold DL. Imaging axonal damage of normal-appearing white matter in multiple sclerosis. Brain 1998;121:103-13.

[52] Yin X, Crawford TO, Griffin JW, Tu P, Lee VM, Li C, Roder J, Trapp BD. Myelin-associated glycoprotein is a myelin signal that modulates the caliber of myelinated axons. J Neurosci 1998;18:1953-62.

[53] Li C, Tropak MB, Gerlai R, Clapoff S, Abramow-Newerly W, Trapp B, Peterson A, Roder J. Myelination in the absence of myelin-associated glycoprotein. Nature 1994;369:747-50.

[54] Narayanan S, Fu L, Pioro E, De Stefano N, Collins DL, Francis GS, Antel JP, Matthews PM, Arnold DL. Imaging of axonal damage in multiple sclerosis: spatial distribution of magnetic resonance imaging lesions. Ann Neurol 1997;41:385-91.

[55] Davie CA, Barker GJ, Thompson AJ, Tofts PS, McDonald WI, Miller DH. ^{1}H magnetic resonance spectroscopy of chronic cerebral white matter lesions and normal appearing white matter in multiple sclerosis. J Neurol Neurosurg Psychiatry 1997;63:736-42.

CHAPTER SIX

RADIOLABELLED PK11195 IN ALZHEIMER'S DISEASE

ASSESSMENT OF NEUROINFLAMMATION AND MICROGLIAL ACTIVATION IN ALZHEIMER'S DISEASE WITH RADIOLABELLED PK11195 AND SINGLE PHOTON EMISSION COMPUTED TOMOGRAPHY: A PILOT STUDY

Jan J Versijpt*[1,2] MD, Filip Dumont[3] PhD, Koen J Van Laere[2] PhD, Danny Decoo[4] MD, Patrick Santens[5] MD, Kurt Audenaert[6] MD, Eric Achten[7] PhD, Guido Slegers[3] PhD, Rudi A Dierckx[2] PhD, Jakob Korf[1] PhD

[1]Department of Biological Psychiatry, University Hospital, Groningen, the Netherlands
[2]Division of Nuclear Medicine, Ghent University Hospital, Belgium
[3]Department of Radiopharmacy, Faculty of Pharmaceutical Sciences, Ghent University, Belgium
[4]Department of Neurology, Elisabeth Hospital, Sijsele, Belgium
[5]Department of Neurology, Ghent University Hospital, Belgium
[6]Department of Psychiatry, Ghent University Hospital, Belgium
[7]Department of Radiology, Ghent University Hospital, Belgium

Eur Neurol 2003;in press

ABSTRACT

Objectives: Inflammation contributes to degeneration in Alzheimer's disease (AD), not simply as a secondary phenomenon, but primarily as a significant source of pathology. [^{123}I]iodo-PK11195 is a single photon emission computed tomography (SPECT) ligand for the peripheral benzodiazepine receptor, the latter being expressed on microglia (brain resident macrophages) and upregulated under inflammatory circumstances. The objectives were to assess AD inflammation by detecting [^{123}I]iodo-PK11195 uptake changes and investigate how uptake values relate with perfusion SPECT and neuropsychological findings. **Methods:** Ten AD and 9 control subjects were included. [^{123}I]iodo-PK11195 SPECT images were realigned into stereotactic space where binding indices, normalized on cerebellar uptake, were calculated. **Results:** The mean [^{123}I]iodo-PK11195 uptake was increased in AD compared to controls in nearly all neocortical regions, however, statistical significance was only reached in the frontal and right mesotemporal regions. Significant correlations were found between regional increased [^{123}I]iodo-PK11195 uptake and cognitive deficits. **Conclusions:** [^{123}I]iodo-PK11195 is a cellular disease activity marker and allows in vivo assessment of microglial inflammation in AD.

INTRODUCTION

Alzheimer's disease (AD), accounting for about 70% of the dementia cases is neuropathologically characterized by dense and neuritic amyloid plaques and cerebral intraneuronal neurofibrillary tangles [1,2]. However, neither plaques nor tangles correlate strongly with the degree of dementia, loss of synapses and neurons, and abnormalities of the cytoskeleton [3,4]. Over the last few years, it has become clear that inflammatory mechanisms and more specifically activated microglia, i.e. the brain resident macrophages, may contribute to the AD neurodegenerative process, not only as a purely secondary phenomenon, but also as a possible primary source of its clinical pathology [5-8]. Epidemiologically, almost 20 retrospective studies have already shown the protective effect of non-steroidal anti-inflammatory drugs (NSAIDs) in populations with a long history of NSAIDs consumption which would reduce the AD prevalence by 50% and delay its onset by 5 to 7 years [9-13]. This progression-retarding and neuroprotective effect of NSAIDs has up till now only been shown in one prospective, double-blind, placebo-controlled clinical trial of indomethacin where a significant decrease in the rate of mental deterioration in 28 AD patients was shown over a 6-months period [14]. On the other hand, other studies with diclofenac, hydroxychloroquine or nimesulide did not demonstrate this positive effect on AD progression, hence possibly indicating that influencing this neuroinflammation should be done in an early stage and maybe for a prolonged period of time [15-17].

Visualizing activated microglia and in this way inflammatory lesions in AD with positron emission tomography (PET) or single photon emission computed tomography (SPECT) would be of interest for clarifying the underlying pathophysiology, for selecting subgroups of patients that are more eligible for anti-inflammatory treatment, and, finally, for monitoring patients during trials with anti-inflammatory agents or ultimately during immunization treatment for monitoring the effective removal of amyloid deposits by activated microglia [18].

The peripheral benzodiazepine receptor (PBR) is structurally and pharmacologically distinct from the central benzodiazepine receptor (associated with GABA-regulated chloride channels), and earned his name based on his localization outside of the CNS and his high affinity for several 1,4-benzodiazepines. It is found in highest concentrations in kidneys, colon membranes, heart, steroid hormone producing cells of adrenal cortex, ovaries and testes, and several cell types of the immune system, such as mast cells and macrophages. It is also present in low concentrations throughout the brain, primarily associated with the choroid plexus, ependymal linings, and microglia [19]. Although the specific function of the PBR remains unknown, it is generally accepted to be involved in lipid metabolism and/or transport, steroid regulation, and cell proliferation [3]. The immunomodulatory role for this receptor includes the ability to modulate monocyte chemotaxis [20], cytokine expression, and to stimulate the formation of antibody-producing cells [7]. Interestingly, the PBR has the ability to reflect neuronal injury and inflammatory lesions without blood-brain barrier (BBB) damage, by an increased expression of the number of binding sites on proliferating and activated microglia, as previously indicated autoradiographically for AD [2,21].

PK11195 (1-(2-chlorophenyl)-N-(1-methyl-propyl)-3-isoquinoline carboxamide) is a specific and selective high affinity ligand for the PBR and can thus be used as a diagnostic marker for microglial activation, neuroinflammatory lesions, and finally neuronal damage. Moreover, the full transformation of microglia into parenchymal phagocytes, absent in areas with chronic or subtle brain pathology, is not necessary to reach maximal levels of PK11195 binding [22]. In vivo visualization of the human PBR, and in this way of cellular inflammatory infiltration, by means of radiolabelled PK11195 has previously been done with ^{11}C radiolabelled PK11195 for PET in various diseases like glial neoplasms, ischemic stroke, multiple sclerosis (MS), Rasmussen's encephalitis, hepatic encephalopathy, cerebral vasculitis, and herpes encephalitis [23-27]. Recently, ^{11}C-PK11195 has also been applied in early and mild dementia patients revealing an increased regional binding in the entorhinal, temporoparietal, and cingulate cortex. Moreover, serial volumetric MRI scans revealed that areas with high ^{11}C-PK11195 binding subsequently showed the highest rate of atrophy up to 12-24 months later indicating that the presence of a local immune response in cortical areas did indeed reflect an active disease process associated with tissue loss. Also, measurement of cerebral glucose metabolism revealed that areas with high ^{11}C-PK11195 binding were also characterized by decreased regional glucose use. Finally, in one patient with isolated memory impairment without dementia, the pattern of atrophy as seen by volumetric MRI imaging was predicted by the initial distribution of increased ^{11}C-PK11195 binding [28].

The application of this ligand, however, is restricted to institutions with a PET system and an in-house cyclotron that have access to these short-lived positron emitters. Therefore, the availability of a radiolabelled SPECT ligand for the study of the PBR would allow wider *clinical* application on a larger scale. Recently, we therefore assessed the biodistribution and dosimetry of ^{123}I radiolabelled PK11195 [29]. It was concluded that [^{123}I]iodo-PK11195 is a suitable and safe agent for the assessment of the PBR with a high enough specific activity required for quantitative studies [30]. The objectives of the present study were to visualize inflammation in vivo in AD patients by detecting [^{123}I]iodo-PK11195 uptake changes compared to controls and to investigate whether [^{123}I]iodo-PK11195 SPECT relates with findings obtained from perfusion SPECT and neuropsychological testing, both sensitive markers of functional brain integrity in AD [31,32,32].

PATIENTS AND METHODS

PATIENTS

The study was approved by the medical ethics committee of the Ghent University Hospital and all patients gave informed (proxy-)consent. Ten patients suffering from probable AD (4 men; mean age 77 ± 10.7 yrs (SD); range 55 to 87 yrs) according to the NINCDS-ADRDA criteria were included [33]. All had a cerebral MRI scan negative for focal lesions. As a control group, 9 normal subjects (6 men; mean age 67 ± 8.6 yrs; range 53 to 76 yrs) were included. This control group formed part of a perfusion SPECT normal database consisting of nearly 100 healthy controls, which all underwent thorough medical screening including high-resolution MRI, a complete history and physical examination, blood and urine tests, and full clinical neurological, neuropsychological, and psychiatric examination. Detailed exclusion criteria for the healthy controls are described elsewhere [34]. For ethical reasons, the AD patients' current treatment was continued during this study. Only the use of anti-inflammatory medication in general and more specifically NSAIDs for the last six months by patients ànd controls was an exclusion criterium for this study. Age, sex, MMSE-score, neuropsychological profile and significant perfusion defects for the AD patients are given in table 1.

Age (yrs)	Sex	MMSE	Major neuropsychological dysfunction	Perfusion defects
62.2	F	18	memory, executive, visuospatial, verbal	/
79.2	F	23	-	right frontal, right parietal
80.1	F	23	-	-
84.5	F	9	(visual) memory, executive, visuospatial	bilateral frontal, right lateral temporal, bilateral caudate head
86.5	F	14	-	left prefrontal, lateral frontal
87.3	F	25	visual	-
55.4	M	20	visuospatial	right lateral temporal, right parietal
73.3	M	23	visuospatial	left frontal
75.7	M	22	executive, visuospatial	left lateral temporal, left parietal, right frontal
85.3	M	10	memory, executive, visuospatial, verbal	right frontal, left striatum, right caudate head

Table 1 Age, sex, MMSE-score, neuropsychological profile and perfusion defects for the AD patients

METHODS

[^{123}I]IODO-PK11195 SPECT scan

Radionuclide synthesis and injection

^{123}I was purchased from Dupont (Dupont Pharmaceuticals Ltd., Brussels, Belgium) and PK11195 (1-(2-chlorophenyl)-N-(1-methyl-propyl)-3-isoquinoline carboxamide) was obtained from RBI (Natick, Massachusetts, USA). ^{123}I labelled PK11195 ([^{123}I]iodo-PK11195) was synthesized according to the method described previously [35], using a direct displacement of aromatic chlorine under solid-state conditions. The specific activity of the

labelled compound was 6.7-17.6 GBq/μmol (180-475 mCi/μmol). The total labelling yield was 50-60% and the radiochemical purity of the final product, as assessed with high performance liquid chromatography (HPLC), was more than 99%. Thyroid was blocked with Lugol's solution for all subjects (5% iodine and 10% potassium iodide; one-day protocol of 20 drops one hr before radioligand injection). The mean dose administered was 185 MBq.

Imaging and reconstruction

All subjects were scanned on a triple-headed gamma camera (Toshiba GCA-9300A, Dutoit Medical, Wijnegem, Belgium) equipped with low energy, super-high-resolution lead fan-beam collimators (measured resolution 8.1 mm) and ^{153}Gd transmission rod sources allowing transmission before emission scanning, enabling image coregistration [36]. Imaging was performed one hour after injection since stable [^{11}C]PK11195 uptake ratios were noticed as early as 20 minutes after injection reflecting pseudo-equilibrium [37]. Emission images were acquired during 20 min in a 128×128 matrix with 90 projections. After triple-energy window scatter correction and uniform attenuation correction (μ=0.09), images were processed by means of filtered backprojection and a Butterworth postfilter (order 8; cut-off 0.07) [38].

Estimation of binding index

After image registration into Talairach co-ordinates using a 9-parameter rigid transformation, a predefined volume of interest (VOI) analysis was performed consisting of 26 cortical, 6 subcortical, and 2 cerebellar 3D-volumes of interest for each patient (Brass, Nuclear Diagnostics, Hägersted, Sweden) [36]. Every registration with the subsequent VOI analysis was carefully checked for errors where in some cases, a manual adjustment was made when the lower cerebellar slices were not completely imaged due to subject positioning on the camera (at least five cerebellar slices had to be visualized for final inclusion). A binding index for every VOI was calculated by normalization to the cerebellum i.e. dividing the counts per volume unit in a given VOI through the counts per volume unit in the cerebellum, the latter being free of pathophysiological involvement. Comparison of binding index between patients and controls was assessed by means of a one-tailed Mann-Whitney *U* test since, out of neuropathological data, an increased binding index was expected for AD patients [21].

Neuropsychological testing

All patients underwent the Mini-Mental State Examination (MMSE) and a screening battery for cognitive impairment (Amsterdam dementia screening test, ADS6) containing the following subtests: picture recognition (n=8), orientation (n=8), drawing alternating sequences (n=7), verbal fluency (n=8), copying geometric figures (n=8), and free recall (n=8) [39]. Not every (sub)test could be performed in all patients due to non-compliance.

^{99m}Tc-ECD perfusion SPECT scan

All patients, except for one, underwent a ^{99m}Tc-ECD perfusion SPECT scan. On average 30 minutes after the injection of 925 MBq ^{99m}Tc-ECD (ethyl cysteinate dimer; Dupont Pharmaceuticals Ltd., Brussels, Belgium). Images were acquired in a 128×128 matrix with 90 projections and a frame time of 40 seconds. After triple-energy window scatter correction and uniform attenuation correction, images were processed by means of filtered backprojection and a Butterworth postfilter (order 8; cut-off 0.12). Perfusion SPECT images were automatically fitted and realigned into Talairach co-ordinates where a similar VOI analysis was performed using the same predefined VOI-map (normalization on cerebellar uptake). All patient perfusion data were averaged to assess a global group perfusion deficit. Comparison was done to 20 healthy controls (mean age 70.5 ± 6.2 yrs) [34]. For the individual patient, a hypoperfusion in a specific region was considered as significant when the uptake was less than the averaged uptake for the group of healthy volunteers minus two times the standard deviation for that specific region.

RESULTS

[^{123}I]IODO-PK11195 SPECT scan

No effect of age was found on radiolabelled PK11195 uptake for cortical regions in controls. Grouped mean [^{123}I]iodo-PK11195 uptake values for patients and controls are shown in table 2.

		AD patients		Controls		p-value
Orbitofrontal	Left	133.8	60.6	99.2	15.4	0.04*[1]
	Right	141.9	68.6	112.8	17.8	0.2
Prefrontal	Left	143.9	55.8	100.8	20.3	0.02*
	Right	139.4	62.6	102.0	21.3	0.02*
Lateral frontal	Left	126.7	32.6	101.1	17.7	0.02*
	Right	125.7	42.9	97.7	16.4	0.03*
Superior frontal	Left	115.5	32.0	97.4	12.4	0.1
	Right	110.1	32.8	92.2	14.3	0.1
Cingulate gyri	Anterior	90.7	17.1	94.0	13.1	0.3
	Posterior	93.3	10.7	101.0	15.1	0.1
Sensorimotor	Left	109.2	41.5	106.1	14.4	1
	Right	94.4	30.4	100.6	12.1	0.2
Temporal anterior	Left	123.5	61.7	109.8	18.7	0.3
	Right	146.4	80.8	110.8	21.1	0.3
Temporal superior	Left	97.7	9.0	99.3	10.9	0.3
	Right	93.8	12.1	94.1	13.2	0.3
Temporal medial inferior	Left	106.2	15.7	99.6	11.9	0.1
	Right	103.6	28.9	92.8	12.2	0.2
Mesotemporal	Left	102.9	37.6	101.5	15.4	0.3
	Right	117.7	31.6	98.5	15.3	0.05*
Parietal inferior	Left	115.9	34.8	102.8	13.8	0.2
	Right	93.6	31.8	97.6	18.4	0.3
Parietal superior	Left	118.8	60.3	102.3	21.4	0.4
	Right	119.3	54.7	104.6	17.4	1
Occipital	Left	102.0	16.4	103.5	15.8	0.4
	Right	102.3	12.1	99.9	10.2	0.3
Basal ganglia		77.4	11.7	88.7	9.3	0.02

[1] p-values indicating significantly raised uptake values

Table 2. [^{123}I]iodo-PK11195 regional uptake values and standard deviation for AD patients compared to controls.

Elevated mean uptake values for AD patients were found in all frontal regions, temporal anterior, temporal medial inferior and mesotemporal region, left parietal inferior and parietal superior region, left sensorimotor cortex, and the right occipital region. Grouped mean [^{123}I]iodo-PK11195 uptake values for AD patients and controls are displayed in figure 1. Significantly increased uptake values were reached in the left orbitofrontal, bilateral prefrontal and lateral frontal region, and the right mesotemporal region (one-tailed Mann-Whitney *U* test). Figure 2 shows the [^{123}I]iodo-PK11195 uptake values for the left prefrontal and the right mesotemporal area.

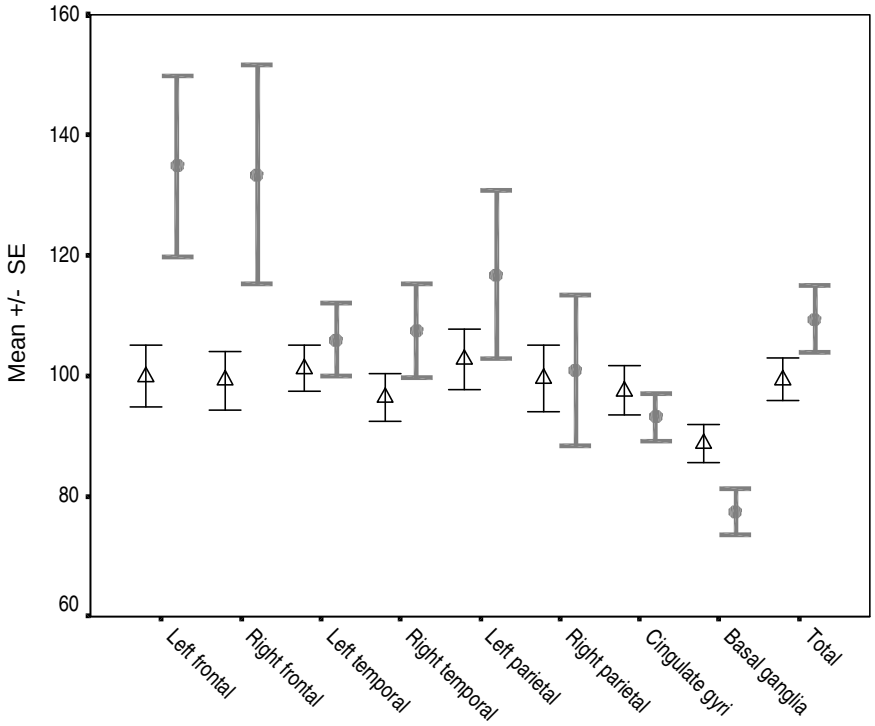

Figure 1. Grouped mean (+/- standard error of the mean) [^{123}I]iodo-PK11195 uptake values
△ controls; ● AD patients

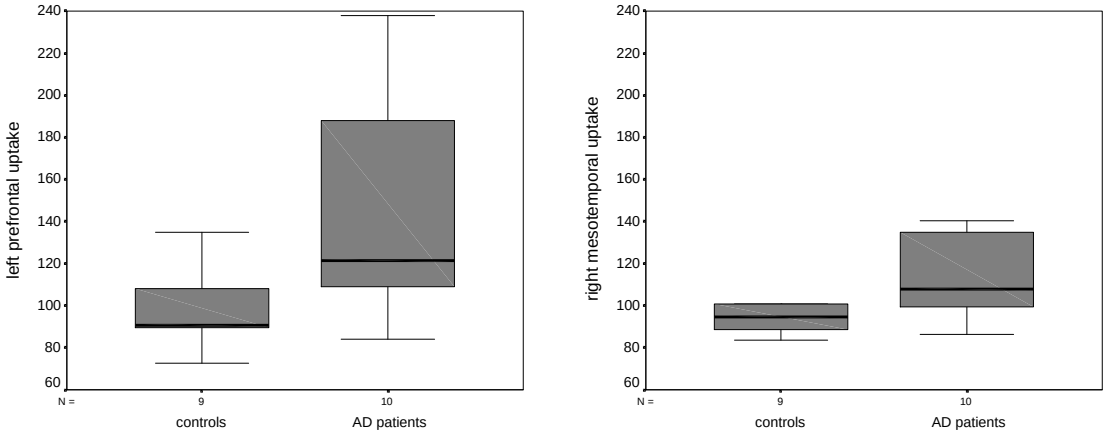

Figure 2. Boxplot of the [^{123}I]iodo-PK11195 uptake values for the left prefrontal (left) and the right mesotemporal area (right)

Neuropsychological testing and correlation with [^{123}I]iodo-PK11195 uptake values

The mean MMSE score of the AD patients was 19 ± 6 (range 9-25). Results from the picture recognition task correlated inversely with the [^{123}I]iodo-PK11195 uptake value in the right superior frontal region (two-tailed Spearman's correlation coefficient, p=0.005). Results of the orientation task correlated inversely with the left lateral frontal, right superior frontal and the left parietal (figure 3, left) [^{123}I]iodo-PK11195 uptake values (two-tailed Spearman's correlation coefficient, p=0.03, 0.04, and 0.006 respectively). Verbal fluency results correlated inversely with the left parietal inferior [^{123}I]iodo-PK11195 uptake value (two-tailed Spearman's correlation coefficient, p=0.007). Results of the free recall task correlated inversely with [^{123}I]iodo-PK11195 uptake values in the left and right frontal (figure 3, right), left temporal, and the left parietal superior region (two-tailed Pearson correlation coefficient, p=0.02, 0.03, 0.03, and 0.01 respectively). No correlations were found between [^{123}I]iodo-PK11195 uptake values and the neuropsychological test results of the controls.

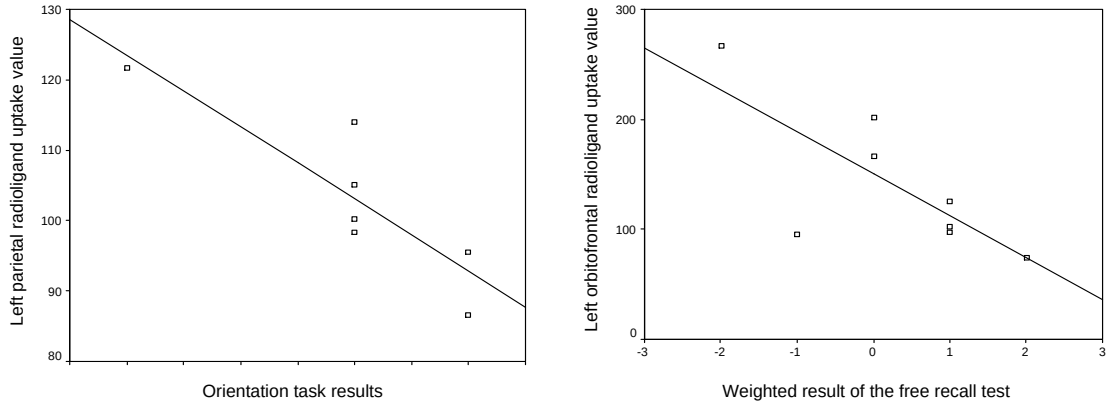

Inverse correlation between results of the orientation task with the left parietal [^{123}I]iodo-PK11195 uptake value (left, Spearman's correlation coefficient -0.896, p=0.006) and the free recall test with the left orbitofrontal [^{123}I]iodo-PK11195 uptake value (right, Pearson correlation coefficient -0.742; p=0.03)

^{99m}Tc-ECD SPECT scan

Group perfusion defects were found in the bilateral frontal, temporal and parietal inferior regions, basal ganglia and the cingulate gyri (Independent samples t-test, $p < 0.01$, < 0.03, < 0.02, < 0.01, and 0.001 respectively).

DISCUSSION

The present study describes the in vivo assessment of activated microglia in AD using radiolabelled PK11195 and SPECT. As such, this is the first SPECT study to show inflammatory lesions in AD and hence may be a potential parameter for investigational studies or therapeutic trials aiming for the inflammatory component. A previous PET study did not show an increased ^{11}C PK11195 uptake in a series of 8 AD patients [40]. However, the use of only one normal elderly subject together with glioma patients as controls could have hampered this analysis. On the other hand, the present findings are in line with more recent findings with PET and ^{11}C-PK11195 in early and mild dementia patients revealing increased regional binding in the entorhinal, temporoparietal, and cingulate cortex [28]. The discrepancy between these two studies however could be due the use of ^{123}I in the present study with its higher lipophilicity facilitating brain uptake influencing both specific binding and tracer kinetics [41].

With regard to regional uptake values, the fact that mean [^{123}I]iodo-PK11195 uptake values are increased in various regions probably indicates a widespread and diffuse inflammatory process. Likewise, increased ^{11}C PK11195 signals were found well beyond focal lesions in multiple sclerosis patients, supporting the notion that additional mechanisms apart from the focal macrophage accumulations found in the areas of BBB leakage must contribute to disease progression [25]. Moreover, the concordance between raised [^{123}I]iodo-PK11195 uptake values and perfusion deficits in frontal regions together with the significant inverse correlation between [^{123}I]iodo-PK11195 uptake values and several neuropsychological test results support the *bystander lysis* theory where activated microglia contribute to neuronal lysis by direct cytotoxic actions of some of their mediators.

Although mean uptake values were increased in various neocortical regions pathognomonically compromised in AD, significance was particularly reached in frontal neocortical regions. Although somewhat unexpected, this is in concordance with a very recent study where an intense immunoreactivity for the immune and inflammatory mediator CD40L, expressed on microglia and involved in microglia-dependent neuron death, was found throughout the frontal cortex of AD patients [8,42]. Also, this frontal increase in [^{123}I]iodo-PK11195 uptake could possibly indicate the progression together with the spreading of active inflammation towards more frontal regions in patients already at an advanced stage of the disease, although the mean MMSE score in the present study was still at a moderate level of 19. This advanced *neuropathological* stage is in concordance with the frontal perfusion deficits observed in the present study, typically seen later in the course of the disease [43]. Concerning this progression towards more frontal regions, also recent biopsy results showed that the progressive neurological impairment in AD is accompanied by a significant increase in senile plaques, neurofibrillary tangles and microglial cell activation in the frontal cortex [44]. However, group analyses should be carefully interpreted since there is a marked heterogeneity in AD patients concerning stage of the disease, progression pattern, predominant topographical lesion and cognitive subtype, with a substantial overlap between AD and other neurodegenerative conditions [43,45,46]. This heterogeneity, to which we actually contributed due to the rather large range of MMSE-score for the included AD patients, is also reflected in the larger standard deviations of [^{123}I]iodo-PK11195 uptake

values in AD patients compared to controls. Concerning this heterogeneity, behavioural as well as cognitive variability has been correlated with PET and SPECT findings [47]. Two subgroups with distinct progression rates were already distinguished segregated by neuropsychological and cerebral metabolic profiles where one rapidly deteriorating group had a significantly greater impairment in executive functions attributed to the frontal lobe and a concomitant greater frontal hypometabolism revealed by PET scanning [48].

Where the age difference between AD patients and controls could explain at least some of the perfusion SPECT findings, it cannot explain the increased [^{123}I]iodo-PK11195 uptake in AD patients since age-related increases in ^{11}C PK11195 uptake only have been described in the thalamus and no age-related effect at all was found in the present study [49]. Moreover, this age discrepancy between AD patients and controls probably made us underestimate the actual [^{123}I]iodo-PK11195 uptake due to the fact that for the current measurement no atrophy correction was performed while atrophy will be more present in the older AD group (next to the atrophy already present pathognomonically), giving rise to a loss of signal. This can be seen for example on one hand in the decreased basal ganglia radioligand uptake but also on the other hand in the lack a significantly increased radioligand uptake in the left mesotemporal region since this area, encompassing the hippocampus, is known for its substantial atrophy in AD [50].

In the present study, a semiquantitative analysis was performed with a regional normalization and the cerebellum as reference region and thus normalization factor. A regional rather than a global normalization (with whole brain as normalization factor) was preferred since a region-specific normalization is known to be more sensitive for diseases with various regions pathophysiologically involved, like AD [51]. Although some reports described the pathological involvement of the cerebellum in AD [52], this region was chosen as the normalization region since its taken together low pathologic susceptibility and the absence or at least minimal presence of upregulated inflammatory mediators in the cerebellum [53]. A previous study concluded already that the cerebellum is the more appropriate choice of reference region in the quantification of perfusion SPECT in primary degenerative dementia [54]. With regard to perfusion SPECT imaging, the cerebellum was shown to be scintigraphically uninvolved [55].

In conclusion, [^{123}I]iodo-PK11195 provides a cellular marker of disease activity (progression), able to indicate inflammatory pathology in AD patients. Interestingly, the combination of perfusion *defects* and *increased* [^{123}I]iodo-PK11195 uptake values could be able to discriminate AD patients from controls or other dementia patients, although for diagnostic purposes additional information concerning for example the test-retest reliability of [^{123}I]iodo-PK11195 SPECT scanning should be assessed. Also, the marked heterogeneity in regional increased uptake values and the concomitant large standard deviations for the different neocortical regions could probably hamper the (diagnostic) use of the present radioligand for individual patient studies. Finally, it is at present not known whether [^{123}I]iodo-PK11195 SPECT would be able to detect pathological changes in a preclinical or a very early

stage of the disease. Worthy of note is the fact that, since the PBR also has an immunomodulatory role and, moreover, PK11195 appears to possess anti-inflammatory properties [56-58], the PBR may be itself a target for therapeutic intervention. This broadens the applicability of this radioligand for the monitoring of anti-inflammatory drug treatment trials in neurodegenerative diseases.

REFERENCES

1. Geldmacher DS, Whitehouse PJ: Evaluation of dementia. N Engl J Med 1996;335:330-336.
2. Kuhlmann AC, Guilarte TR: Cellular and subcellular localization of peripheral benzodiazepine receptors after trimethyltin neurotoxicity. J Neurochem 2000;74:1694-1704.
3. Neve RL, Robakis NK: Alzheimer's disease: a re-examination of the amyloid hypothesis. Trends Neurosci 1998;21:15-19.
4. Mesulam MM: Neuroplasticity failure in Alzheimer's disease: bridging the gap between plaques and tangles. Neuron 1999;24:521-529.
5. Akiyama H, Barger S, Barnum S, Bradt B, Bauer J, Cole GM, Cooper NR, Eikelenboom P, Emmerling M, Fiebich BL, Finch CE, Frautschy S, Griffin WS, Hampel H, Hull M, Landreth G, Lue L, Mrak R, MacKenzie IR, McGeer PL, O'Banion MK, Pachter J, Pasinetti G, Plata-Salaman C, Rogers J, Rydel R, Shen Y, Streit W, Strohmeyer R, Tooyoma I, Van Muiswinkel FL, Veerhuis R, Walker D, Webster S, Wegrzyniak B, Wenk G, Wyss-Coray T: Inflammation and Alzheimer's disease. Neurobiol Aging 2000;21:383-421.
6. Gonzalez-Scarano F, Baltuch G: Microglia as mediators of inflammatory and degenerative diseases. Annu Rev Neurosci 1999;22:219-240.
7. McCusker SM, Curran MD, Dynan KB, McCullagh CD, Urquhart DD, Middleton D, Patterson CC, McIlroy SP, Passmore AP: Association between polymorphism in regulatory region of gene encoding tumour necrosis factor a and risk of Alzheimer's disease and vascular dementia: a case-control study. Lancet 2001;357:436-439.
8. McGeer PL, McGeer EG: Polymorphisms in inflammatory genes and the risk of Alzheimer disease. Arch Neurol 2001;58:1790-1792.
9. McGeer PL, Schulzer M, McGeer EG: Arthritis and anti-inflammatory agents as possible protective factors for Alzheimer's disease: a review of 17 epidemiologic studies. Neurology 1996;47:425-432.
10. Stewart WF, Kawas C, Corrada M, Metter EJ: Risk of Alzheimer's disease and duration of NSAID use. Neurology 1997;48:626-632.
11. in 't Veld BA, Ruitenberg A, Hofman A, Launer LJ, van Duijn CM, Stijnen T, Breteler MM, Stricker BH: Nonsteroidal antiinflammatory drugs and the risk of Alzheimer's disease. N Engl J Med 2001;345:1515-1521.
12. Zandi PP, Breitner JCS: Do NSAIDs prevent Alzheimer's disease? And, if so, why? The epidemiological evidence. Neurobiol Aging 2001;22:811-817.
13. De Strooper B, Konig G: An inflammatory drug prospect. Nature 2001;414:159-160.
14. Rogers J, Kirby LC, Hempelman SR, Berry DL, McGeer PL, Kaszniak AW, Zalinski J, Cofield M, Mansukhani L, Wilson P, Kogan F: Clinical trial of indomethacin in Alzheimer's disease. Neurology 1993;43:1609-1611.
15. Scharf S, Mander A, Ugoni A, Vajda F, Christophidis N: A double-blind, placebo-controlled trial of diclofenac/misoprostol in Alzheimer's disease. Neurology 1999;53:197-201.
16. van Gool WA, Weinstein HC, Scheltens PK, Walstra GJ: Effect of hydroxychloroquine on progression of dementia in early Alzheimer's disease: an 18-month randomised, double-blind, placebo- controlled study. Lancet 2001;358:455-460.
17. Aisen PS, Schmeidler J, Pasinetti GM: Randomized pilot study of nimesulide treatment in Alzheimer's disease. Neurology 2002;58:1050-1054.
18. Morgan D, Diamond DM, Gottschall PE, Ugen KE, Dickey C, Hardy J, Duff K, Jantzen P, DiCarlo G, Wilcock D, Connor K, Hatcher J, Hope C, Gordon M, Arendash GW: Ab peptide vaccination prevents memory loss in an animal model of Alzheimer's disease. Nature 2000;408:982-985.
19. Richards JG, Mohler H: Benzodiazepine receptors. Neuropharmacology 1984;23:233-242.
20. Ruff MR, Pert CB, Weber RJ, Wahl LM, Wahl SM, Paul SM: Benzodiazepine receptor-mediated chemotaxis of human monocytes. Science 1985;229:1281-1283.

21. Diorio D, Welner SA, Butterworth RF, Meaney MJ, Suranyi CB: Peripheral benzodiazepine binding sites in Alzheimer's disease frontal and temporal cortex. Neurobiol Aging 1991;12:255-258.
22. Banati RB, Myers R, Kreutzberg GW: PK ('peripheral benzodiazepine') – binding sites in the CNS indicate early and discrete brain lesions: microautoradiographic detection of [^{3}H]PK11195 binding to activated microglia. J Neurocytol 1997;26:77-82.
23. Ramsay SC, Weiller C, Myers R, Cremer JE, Luthra SK, Lammertsma AA, Frackowiak RS: Monitoring by PET of macrophage accumulation in brain after ischaemic stroke [letter]. Lancet 1992;339:1054-1055.
24. Banati RB, Goerres GW, Myers RN, Gunn RN, Turkheimer FE, Kreutzberg GW, Brooks DJ, Jones T, Duncan JS: [^{11}C](R)-PK11195 positron emission tomography imaging of activated microglia in vivo in Rasmussen's encephalitis. Neurology 1999;53:2199-2203.
25. Banati RB, Newcombe J, Gunn RN, Cagnin A, Turkheimer F, Heppner F, Price G, Wegner F, Giovannoni G, Miller DH, Perkin GD, Smith T, Hewson AK, Bydder G, Kreutzberg GW, Jones T, Cuzner ML, Myers R: The peripheral benzodiazepine binding site in the brain in multiple sclerosis: quantitative in vivo imaging of microglia as a measure of disease activity. Brain 2000;123:2321-2337.
26. Cagnin A, Myers R, Gunn RN, Lawrence AD, Stevens T, Kreutzberg GW, Jones T, Banati RB: In vivo visualization of activated glia by [11C] (R)-PK11195-PET following herpes encephalitis reveals projected neuronal damage beyond the primary focal lesion. Brain 2001;124:2014-2027.
27. Goerres GW, Revesz T, Duncan J, Banati RB: Imaging cerebral vasculitis in refractory epilepsy using [(11)C](R)- PK11195 positron emission tomography. AJR Am J Roentgenol 2001;176:1016-1018.
28. Cagnin A, Brooks DJ, Kennedy AM, Gunn RN, Myers R, Turkheimer FE, Jones T, Banati RB: In-vivo measurement of activated microglia in dementia. Lancet 2001;358:461-467.
29. Dumont F, De Vos F, Versijpt J, Jansen HM, Korf J, Dierckx RA, Slegers G: In vivo evaluation in mice and metabolism in blood of human volunteers of [^{123}I]iodo-PK11195: a possible single-photon emission tomography tracer for visualization of inflammation. Eur J Nucl Med 1999;26:194-200.
30. Versijpt J, Dumont F, Thierens H, Jansen H, De Vos F, Slegers G, Santens P, Dierckx RA, Korf J: Biodistribution and dosimetry of [^{123}I]iodo-PK 11195: a potential agent for SPET imaging of the peripheral benzodiazepine receptor. Eur J Nucl Med 2000;27:1326-1333.
31. Jagust W, Thisted R, Devous MD, Sr., Van Heertum R, Mayberg H, Jobst K, Smith AD, Borys N: SPECT perfusion imaging in the diagnosis of Alzheimer's disease: A clinical-pathologic study. Neurology 2001;56:950-956.
32. Morgan CD, Baade LE: Neuropsychological testing and assessment scales for dementia of the Alzheimer's type1. Psychiatr Clin North Am 1997;20:25-43.
33. McKhann G, Drachman D, Folstein M, Katzman R, Price D, Stadlan EM: Clinical diagnosis of Alzheimer's disease: report of the NINCDS-ADRDA work group under the auspices of the Department of Health and Human Services Task Force on Alzheimer's Disease. Neurology 1984;34:939-944.
34. Van Laere K, Versijpt J, Audenaert K, Koole M, Goethals I, Achten E, Dierckx R: ^{99m}Tc-ECD brain perfusion SPET: variability, asymmetry and effects of age and gender in healthy adults. Eur J Nucl Med 2001;28:873-887.
35. Gildersleeve DL, Lin TY, Wieland DM, Ciliax BJ, Olson JM, Young AB: Synthesis of a high specific activity ^{125}I-labeled analog of PK 11195, potential agent for SPECT imaging of the peripheral benzodiazepine binding site. Int J Rad Appl Instrum B 1989;16:423-429.
36. Van Laere K, Koole M, D'Asseler Y, Versijpt J, Audenaert K, Dumont F, Dierckx R: Automated stereotactic standardization of brain SPECT receptor data using single-photon transmission images. J Nucl Med 2001;42:361-375.

37. Sette G, Baron JC, Young AR, Miyazawa H, Tillet I, Barre L, Travere JM, Derlon JM, MacKenzie ET: In vivo mapping of brain benzodiazepine receptor changes by positron emission tomography after focal ischemia in the anesthetized baboon. Stroke 1993;24:2046-2057.
38. Van Laere K, Koole M, Kauppinen T, Monsieurs M, Bouwens L, Dierckx R: Nonuniform transmission in brain SPECT using ^{201}Tl, ^{153}Gd, and ^{99m}Tc static line sources: anthropomorphic dosimetry studies and influence on brain quantification. J Nucl Med 2000;41:2051-2062.
39. de Jonghe JF, Krijgsveld S, Staverman K, Lindeboom J, Kat MG: Differentiation between dementia and functional psychiatric disorders in a geriatric ward of a general psychiatric hospital using the 'Amsterdam Dementia-Screening Test'. Ned Tijdschr Geneeskd 1994;138:1668-1673.
40. Groom GN, Junck L, Foster NL, Frey KA, Kuhl DE: PET of peripheral benzodiazepine binding sites in the microgliosis of Alzheimer's disease. J Nucl Med 1995;36:2207-2210.
41. De Vos F, Dumont F, Slegers G, Dierckx RA. Pharmacological comparison between ^{11}C-2'-Iodo-PK11195 and ^{123}I-2'-Iodo-PK11195. J Nucl Med 2001; 42: 252P(Abstract)
42. Calingasan NY, Erdely HA, Anthony AC: Identification of CD40 ligand in Alzheimer's disease and in animal models of Alzheimer's disease and brain injury. Neurobiol Aging 2002;23:31-39.
43. Report of the Therapeutics and Technology Assessment Subcommittee of the American Academy of Neurology: Assessment of brain SPECT. Neurology 1996;46:278-285.
44. Di Patre PL, Read SL, Cummings JL, Tomiyasu U, Vartavarian LM, Secor DL, Vinters HV: Progression of clinical deterioration and pathological changes in patients with Alzheimer disease evaluated at biopsy and autopsy. Arch Neurol 1999;56:1254-1261.
45. Cummings JL: Cognitive and behavioral heterogeneity in Alzheimer's disease: seeking the neurobiological basis. Neurobiol Aging 2000;21:845-861.
46. Perl DP, Olanow CW, Calne D: Alzheimer's disease and Parkinson's disease: distinct entities or extremes of a spectrum of neurodegeneration? Ann Neurol 1998;44:S19-S31
47. Waldemar G: Functional brain imaging with SPECT in normal aging and dementia. Methodological, pathophysiological, and diagnostic aspects. Cerebrovasc Brain Metab Rev 1995;7:89-130.
48. Mann UM, Mohr E, Gearing M, Chase TN: Heterogeneity in Alzheimer's disease: progression rate segregated by distinct neuropsychological and cerebral metabolic profiles. J Neurol Neurosurg Psychiatry 1992;55:956-959.
49. Cagnin A, Myers R, Gunn RN, et al. Imaging activated microglia in the ageing human brain. J Cereb Blood Flow Metab 1999; 19: S820(Abstract)
50. Juottonen K, Laakso MP, Partanen K, Soininen H: Comparative MR analysis of the entorhinal cortex and hippocampus in diagnosing Alzheimer disease. Am J Neuroradiol 1999;20:139-144.
51. Syed GM, Eagger S, Toone BK, Levy R, Barrett JJ: Quantification of regional cerebral blood flow (rCBF) using ^{99} Tc^{m}-HMPAO and SPECT: choice of the reference region. Nucl Med Commun 1992;13:811-816.
52. Joachim CL, Morris JH, Selkoe DJ: Diffuse senile plaques occur commonly in the cerebellum in Alzheimer's disease. Am J Pathol 1989;135:309-319.
53. Rozemuller JM, Stam FC, Eikelenboom P: Acute phase proteins are present in amorphous plaques in the cerebral but not in the cerebellar cortex of patients with Alzheimer's disease. Neurosci Lett 1990;119:75-78.
54. Talbot PR, Lloyd JJ, Snowden JS, Neary D, Testa HJ: Choice of reference region in the quantification of single-photon emission tomography in primary degenerative dementia. Eur J Nucl Med 1994;21:503-508.
55. Pickut BA, Dierckx RA, Dobbeleir A, Audenaert K, Van Laere K, Vervaet A, De Deyn PP: Validation of the cerebellum as a reference region for SPECT quantification in patients suffering from dementia of the Alzheimer type. Psychiatry Res 1999;90:103-112.

56. Torres SR, Frode TS, Nardi GM, Vita N, Reeb R, Ferrara P, Ribeiro-Do-Valle RM, Farges RC: Anti-inflammatory effects of peripheral benzodiazepine receptor ligands in two mouse models of inflammation. Eur J Pharmacol 2000;408:199-211.
57. Klegeris A, McGeer EG, McGeer PL: Inhibitory action of 1-(2-chlorophenyl)-N-methyl-N-(1- methylpropyl)-3-isoquinolinecarboxamide (PK 11195) on some mononuclear phagocyte functions. Biochem Pharmacol 2000;59:1305-1314.
58. Waterfield JD, McGeer EG, McGeer PL: The peripheral benzodiazepine receptor ligand PK 11195 inhibits arthritis in the MRL-lpr mouse model. Rheumatology 1999;38:1068-1073.

CHAPTER SEVEN

ROLE AND DISTRIBUTION OF SEROTONIN TYPE 2A RECEPTORS IN ALZHEIMER'S DISEASE

ROLE OF SEROTONIN AND SEROTONIN TYPE 2A RECEPTORS IN ALZHEIMER'S DISEASE

INTRODUCTION

Serotonin or 5-hydroxytryptamine (5-HT) is widely distributed in the whole brain and each receptor subtype has a specific regional distribution. It plays a role in a great variety of behaviours such as activity rhythms, food intake, sexual behaviour and emotional states. Serotonin type 2A ($5\text{-}HT_{2A}$, formerly called $5\text{-}HT_2$) receptors, with a mainly cortical distribution, have been implicated in several largely 'neuroexcitating' brain functions, such as appetite control, thermoregulation and sleep and play an important role in the pathophysiology of mood and anxiety disorders, schizophrenia, ageing and also Alzheimer's disease (AD). The following part explains the potential role of serotonin and serotonin type 2A receptors in Alzheimer's disease.

ROLE OF SEROTONIN AND SEROTONIN TYPE 2A RECEPTORS IN COGNITIVE BEHAVIOUR

Alzheimer's disease is typically characterised by a progressive memory impairment, predominantly a loss of short-term memory [5]. The 5-HT receptor is involved in various cognitive functions, especially learning, (working) memory and attentional processes [1]. These functions are not independent from each other or from other behavioural levels. For example, there are some connections between anxiety and memory, or between memory and attentional processes so 5-HT may modulate learning and memory by both direct and indirect ways [4]. Concerning the receptor subtypes, evidence exists that $5\text{-}HT_{2A/2C}$ agonists prevent memory impairment and facilitate learning (consolidation) in situations involving a high cognitive demand [4,7]. The $5\text{-}HT_{2A}$ receptor is thought to mediate also attentional rather than memory processes and acts by stimulating phospholipase C [3]. Finally, several interactions exist between the serotonergic and other neurotransmitter systems involved in memory. One of these interactions, especially for spatial memory, is the interaction between and modulation of the cholinergic system where 5-HT regulates the central cholinergic activity by modulating hippocampal and neocortical acetylcholine release, this through substance P interneurons. Also, the serotonergic role in learning and memory is made possible by interacting with the glutamatergic, dopaminergic or GABAergic systems [6].

ROLE OF SEROTONIN AND SEROTONIN TYPE 2A RECEPTORS IN NON-COGNITIVE BEHAVIOUR

Probably the most important role of the serotonin receptor lies in the non-cognitive aspects of Alzheimer's disease. Indeed, serotonin plays an important role in a great variety of behaviours such as food intake, activity rhythms, sexual behaviour and emotional states. After all, in many cases these non-cognitive features of AD are the main reason for hospitalisation and cause the greatest distress to caregivers. For example, $5\text{-}HT_{2A}$ receptor polymorphisms have been associated with both visual and auditory hallucinations and prominent psychotic symptoms [8,11].

ROLE OF SEROTONIN AND SEROTONIN TYPE 2A RECEPTORS IN AMYLOID FORMATION

Alzheimer's disease amyloid consists of amyloid β-peptides (Aβ) derived from the larger precursor amyloid precursor protein (APP). Non-amyloidogenic APP processing involves regulated cleavage within the Aβ domain followed by secretion of the ectodomain (APPs). Both the synthesis of the

amyloid precursor protein (APP) and its processing (i.e. to amyloidogenic Aβ peptides, soluble non-amyloidogenic APPs, and other APP fragments) are regulated by neurotransmitters. As such APP secretion is influenced by norepinephrine, prostaglandins, and muscarinic acetylcholine receptors [9]. However, the 5-HT_{2A} receptor has been suggested to regulate in a dose-dependent way APPs secretion, which could eventually lead to the formation of amyloidogenic derivatives [12].

IMMUNOLOGICAL ROLE OF SEROTONIN AND SEROTONIN TYPE 2A RECEPTORS IN ALZHEIMER'S DISEASE

5-HT has also a role in natural immunity in general, and more specifically in the superoxide production, phagocytosis, and the optimal accessory cell function of macrophages for natural killer and T-cells, which could eventually influence the removal of amyloid plaques [10]. Finally, the cerebral availability of plasma tryptophan, the precursor of 5-HT, decreases with activation of the immune system, the latter believed to be upregulated in AD [2]

REFERENCES

[1] Barnes NM, Sharp T. A review of central 5-HT receptors and their function. Neuropharmacology 1999;38(8):1083-152.

[2] Bonaccorso S, Lin A, Song C, Verkerk R, Kenis G, Bosmans E, Scharpe S, Vandewoude M, Dossche A, Maes M. Serotonin-immune interactions in elderly volunteers and in patients with Alzheimer's disease (DAT): lower plasma tryptophan availability to the brain in the elderly and increased serum interleukin-6 in DAT. Aging (Milano) 1998;10(4):316-23.

[3] Buhot MC. Serotonin receptors in cognitive behaviors. Curr Opin Neurobiol 1997;7(2):243-54.

[4] Buhot MC, Martin S, Segu L. Role of serotonin in memory impairment. Ann Med 2000;32(3):210-21.

[5] Cummings JL, Cole G. Alzheimer disease. JAMA 2002;287(18):2335-8.

[6] Feuerstein TJ, Gleichauf O, Landwehrmeyer GB. Modulation of cortical acetylcholine release by serotonin: the role of substance P interneurons. Naunyn Schmiedebergs Arch Pharmacol 1996;354(5):618-26.

[7] Harvey JA. Serotonergic regulation of associative learning. Behav Brain Res 1996;73(1-2):47-50.

[8] Holmes C, Arranz MJ, Powell JF, Collier DA, Lovestone S. 5-HT2A and 5-HT2C receptor polymorphisms and psychopathology in late onset Alzheimer's disease. Hum Mol Genet 1998;7(9):1507-9.

[9] Lee RK, Wurtman RJ. Regulation of APP synthesis and secretion by neuroimmunophilin ligands and cyclooxygenase inhibitors. Ann N Y Acad Sci 2000;920261-8.

[10] Mossner R, Lesch KP. Role of serotonin in the immune system and in neuroimmune interactions. Brain Behav Immun 1998;12(4):249-71.

[11] Nacmias B, Tedde A, Forleo P, Piacentini S, Guarnieri BM, Bartoli A, Ortenzi L, Petruzzi C, Serio A, Marcon G, Sorbi S. Association between 5-HT(2A) receptor polymorphism and psychotic symptoms in Alzheimer's disease. Biol Psychiatry 2001;50(6):472-5.

[12] Nitsch RM, Deng M, Growdon JH, Wurtman RJ. Serotonin 5-HT2a and 5-HT2c receptors stimulate amyloid precursor protein ectodomain secretion. J Biol Chem 1996;271(8):4188-94.

IMAGING OF THE 5-HT$_{2A}$ SYSTEM: AGE-, GENDER-, AND ALZHEIMER'S DISEASE-RELATED FINDINGS

Jan J Versijpt[a,b*] MD, Koen J Van Laere[b] MD PhD DrSc, Filip Dumont[c] Pharm PhD, Danny Decoo[d] MD, Marleen Vandecapelle[c] Chem, Patrick Santens[e] MD, Ingeborg Goethals[b] MD, Kurt Audenaert[f] MD PhD, Guido Slegers[c] Chem Pharm PhD, Rudi A Dierckx[b] MD PhD, Jakob Korf[a] Chem PhD

[a]Department of Biological Psychiatry, Groningen University Hospital, the Netherlands
[b]Division of Nuclear Medicine, Ghent University Hospital, Belgium
[c]Department of Radiopharmacy, Ghent University, Belgium
[d]Department of Neurology, Elisabeth Hospital, Sijsele, Belgium
[e]Department of Neurology, Ghent University Hospital, Belgium
[f]Department of Psychiatry and Medical Psychology, Ghent University Hospital, Belgium

Neurobiol Aging 2003, in press

ABSTRACT

Serotonin (5-HT) and more specifically the 5-HT$_{2A}$ receptor is involved in cognitive and non-cognitive behavior and plays an important role in Alzheimer's disease (AD). The objective was to assess the 5-HT$_{2A}$ binding potential (BP) in healthy volunteers and AD with SPECT and ^{123}I-5-I-R91150, a selective radio-iodinated 5-HT$_{2A}$ receptor antagonist. Twenty-six controls and 9 AD patients were included. A semiquantitive analysis with normalization on cerebellar uptake provided estimates of BP for 26 cortical regions of interest. An age-related decline of neocortical BP was found (11.6 % per decade). Compared to age-matched controls, a generally decreased neocortical BP in AD was found with a significant regional reduction in the orbitofrontal, prefrontal, lateral frontal, cingulate, sensorimotor, parietal inferior, and occipital region. These results are in line with previous postmortem, in vitro, and PET findings. The age-related decline highlights the necessity for matched advanced age study samples. The fact that the 5-HT$_{2A}$ receptor is differentially affected in AD patients has implications for both the etiological basis and therapeutic management of AD.

INTRODUCTION

Approximately 90% of the total body amount of serotonin (5-HT) acts in the gastrointestinal system. Only 1-2% is present in the central nervous system where 5-HT receptors are generally involved in sleep, pain, behavior, learning, and memory [5,10]. More specifically, serotonin type 2A (5-HT_{2A}) receptors have been implicated in several brain functions, such as appetite control, sexuality, thermoregulation, and sustained attention and play an important role in the pathophysiology of mood, depressive, anxiety, and psychotic disorders, schizophrenia, ageing and also Alzheimer's disease [2,5,9,18,30,31,42].

Alzheimer's disease (AD), the most common form of dementia, is typically characterized by progressive impairment of recent memory. However, in the course of AD, other cognitive dysfunctions, behavioral and psychiatric symptoms emerge and become at least equally important [21]. The role of the $5\text{-HT}_{(2A)}$ receptor in AD is manifold. Firstly, the 5-HT_{2A} receptor has been suggested to play a role in the amyloid precursor protein secretion. Since this is linked to the ß-amyloid fibrillogenesis, this could eventually lead to the subsequent formation of amyloid plaques, typically seen in AD [24,25,35,36]. Secondly, several genetic associations between 5-HT_{2A} receptor polymorphisms and the AD symptomatology e.g. visual or auditory hallucinations have been reported [23,34]. Thirdly, 5-HT has a role in natural immunity in general, and more specifically in the superoxide production, phagocytosis, and the optimal accessory cell function of macrophages for natural killer and T-cells, which could eventually influence the removal of amyloid plaques [32]. Moreover, the cerebral availability of plasma tryptophan, the precursor of 5-HT, decreases with activation of the immune system, the latter believed to be upregulated in AD [1,8]. Finally, a decrease in serotonergic cells in the central nervous system could eventually lead to a disturbance of functional interactions between the serotonergic on one hand and the cholinergic or dopaminergic system on the other hand [16,19,40,44].

^{123}I radiolabeled R91150 is a radio-iodinated 5-HT_{2A} receptor antagonist with high affinity ($K_D = 0.11 \pm 0.01$ nM). The selectivity of this ligand for 5-HT_{2A} receptors as compared to other neurotransmitter receptor binding sites such as 5-HT_{1A}, 5-HT_{1B}, 5-HT_{1D}, 5-HT_{2C}, 5-HT_3, dopamine D_2 receptors, α_1 and α_2 adrenoreceptors and histamine H_1 receptors, is at least a factor of 50. ^{123}I-5-I-R91150 binding is saturable and displaceable with the known 5-HT_{2A} receptor antagonist ketanserin and proved suitable for the imaging of 5-HT_{2A} receptors with single photon emission computed tomography (SPECT) in the human brain [11].

The objectives of the present study were, firstly, to study the age and gender effect of the 5-HT_{2A} receptor binding potential in a large group of healthy subjects (n=26) with an age range of 22 to 85 years and, secondly, to determine whether there are abnormalities in the 5-HT_{2A} receptor binding potential in AD patients compared to age-matched healthy controls, and if so, whether these abnormalities are correlated with cognitive defects or depressive symptomatology.

METHODS

PATIENTS

The study was approved by the medical ethics committee of the Ghent University Hospital and all patients gave informed (proxy-)consent. Nine AD patients (two males, mean age 81 ± 6 yrs, range 73-88 yrs) according to the NINCDS-ADRDA criteria were included with the diagnosis made by a board-certified neurologist [27]. The diagnosis was supported by the fact that there was evidence of cerebral atrophy on computed tomography or magnetic resonance imaging in all AD patients and by the fact that structural imaging did not reveal any brain disease causing dementia other than Alzheimer's disease. The control group consisted of 26 healthy subjects (11 males; mean age 51 ± 24 yrs; range 22-85 yrs). For the comparison with the AD patient group, only the oldest age group was used consisting of 9 healthy subjects (3 males; mean age 77 ± 5 yrs, range 70-85 yrs). These two groups did neither differ significantly concerning age (*Mann-Whitney U test*, p = 0.16) or sex (Pearson Chi-Square test, p = 0.6).

METHODS

^{123}I-5-I-R91150 SPECT

Radionuclide synthesis and injection

$Na^{123}I$ was purchased from Bristol-Myers Squib Pharma Belgium N.V. formerly Dupont Pharmaceuticals Ltd. (Brussels, Belgium). R91150 (4-amino-N-[1-[3-(4-fluorophenoxy)propyl]4-methyl-4-piperidinyl] 5-iodo-2-methoxybenzamide) is an original product of Janssen Pharmaceutica (Beerse, Belgium). ^{123}I-5-I-R91150 was synthesized by electrophilic substitution on the 5-position of the methoxybenzamide group of R91150, followed by purification with high-performance liquid chromatography. The specific activity of the labeled compound was 370 GBq/μmol while the radiochemical purity of the final product yielded more than 99%. Thyroid was blocked with Lugol's solution for all subjects (5% iodine and 10% potassium iodide; one-day protocol of 20 drops one hr before radioligand injection). The administered dose was 185 MBq.

Image acquisition and reconstruction

All subjects were scanned on a triple-headed gamma camera (Toshiba GCA9300A, Dutoit Medical, Wijnegem, Belgium) equipped with low-energy super-high-resolution lead fan-beam collimators (measured resolution 8.1 mm) and ^{153}Gd transmission rod sources allowing transmission scanning prior to emission scanning, enabling image coregistration [46]. Since previously published work with sequential dynamic brain scans has shown that the cortico-cerebellar ratio reaches pseudo-equilibrium between 90 and 110 min postinjection and remains stable thereafter for up to 4 h, acquisition was started between 110 and 140 min after tracer injection [11]. Emission images were acquired in a 128×128 matrix with 90 projections during 40 min consisting of 4 sequential frames of 10 min in order to omit frames when the subject was unable to complete the whole imaging session (at least two frames required for high enough count statistics). After triple-energy window scatter correction and uniform attenuation correction (μ=0.09 cm^{-1}), images were processed by means of filtered backprojection and a post-reconstruction Butterworth filter of order 8 and a cut-off frequency of 0.08 cycles/cm [47].

Estimation of binding potential

After image registration into Talairach space, a volume of interest (VOI) analysis was performed making use of a predefined in-house modified VOI-map sampling the whole brain and consisting of 26 cortical, 6 subcortical, 2 cerebellar, and one pons 3D-volumes of interest (Brass, Nuclear Diagnostics, Hägersted, Sweden) [46]. Every registration with the subsequent VOI analysis was carefully checked for errors. In two subjects, a manual adjustment was necessary where the lower cerebellar slices were not completely imaged due to subject positioning on the camera (at least five cerebellar slices had to be visualized for final inclusion). The binding potential for a specific region was defined as the activity per volume element in that specific region divided through the activity per volume element in the cerebellum (void of 5-HT_{2A} receptors), expressed as a percentage. The neocortical binding potential was defined as the unweighted average of the binding potential of frontal, temporal, parietal, and occipital regions. For the comparison of AD patients to healthy controls, the binding potential values for symmetrical regions were summed to achieve improved statistics in the relatively small sample under study. An asymmetry index (AI) was calculated, defined as AI = (R-L)/(R+L)*200 (%).

Psychiatric and neuropsychological testing

All AD patients, except one, underwent a screening for depressive symptomatology by means of the geriatric depression scale (GDS), a reliable and validated self-rating 30 items depression screening scale for elderly populations with scores ranging from 0 to 30 with a cut-off of 9 for mild and 19 for severe depression [50,51]. Also, AD patients underwent a Mini-Mental State Examination (MMSE), a method for grading the cognitive state consisting of a series of short subtests designed to elicit information about orientation, registration, attention and calculation ability, recall, language, and praxis. It has a total score ranging from 0 to 30 with 30 representing pefect performance, with a generally accepted cut-off of 27 for the exclusion of mental impairment and 23 to 24 for the diagnosis of dementia [17,20]. Finally all AD patients underwent a screening battery for cognitive impairment (Amsterdam dementia screening test, ADS6) containing the following subtests: picture recognition (n=8), orientation (n=8), drawing alternating sequences (n=8), verbal fluency (n=8), copying geometric figures (n=7), and free recall (n=7) [14]. Not every (sub)test could be performed in all patients due to non-compliance.

Statistical analysis

Data were analyzed by means of SPSS v10.0 for Windows (Chicago, IL, USA). For normality testing, a Kolmogorov-Smirnov test statistic was applied. For differences between groups, a two-tailed *independent samples t test* or a *Mann-Whitney U test* was applied when appropriate. A p-value lower than 0.05 was considered as significant. Data are given as means ± one standard deviation.

RESULTS

Age, sex, GDS, MMSE-score, and cognitive deficits of the AD patients are presented in Table 1.

Age	Sex	GDS	MMSE	Most prominent cognitive defects
81	F	-	-	memory
88	F	2	9	memory, orientation, attention, visuoconstruction
76	F	9	15	(visual) memory, orientation
78	F	9	21	(visual) memory
73	F	7	25	verbal memory and attention, visuospatial aspect, orientation
86	M	9	9	orientation, visuoconstruction, memory, word fluency, learning
85	F	15	20	memory, understanding, orientation
85	M	3	25	orientation, memory
74	F	19	17	visuoconstruction, language, visual memory

Table 1 Demographic variables of the AD patient group

^{123}I-5-I-R91150 SPECT uptake values

THE DISTRIBUTION OF RADIOLIGAND UPTAKE IN HEALTHY CONTROLS

The distribution of radioligand uptake throughout the brain as measured in 26 healthy volunteers is shown in figure 1. Relative regional specific uptakes compared to the cerebellum varied between 174 for the occipital cortex and 160 for the sensorimotor area. As for asymmetries in radioligand uptake, two statistically significant asymmetries were found consisting of a 2% asymmetry in frontal uptake in favor of the right side ($p = 0.003$) with the greatest difference in the prefrontal cortex (3%; $p = 0.001$) and another 3% asymmetry in favor of the left side for the temporal cortex ($p = 0.002$), with the greatest difference in the temporal superior cortex (5%; $p < 0.001$).

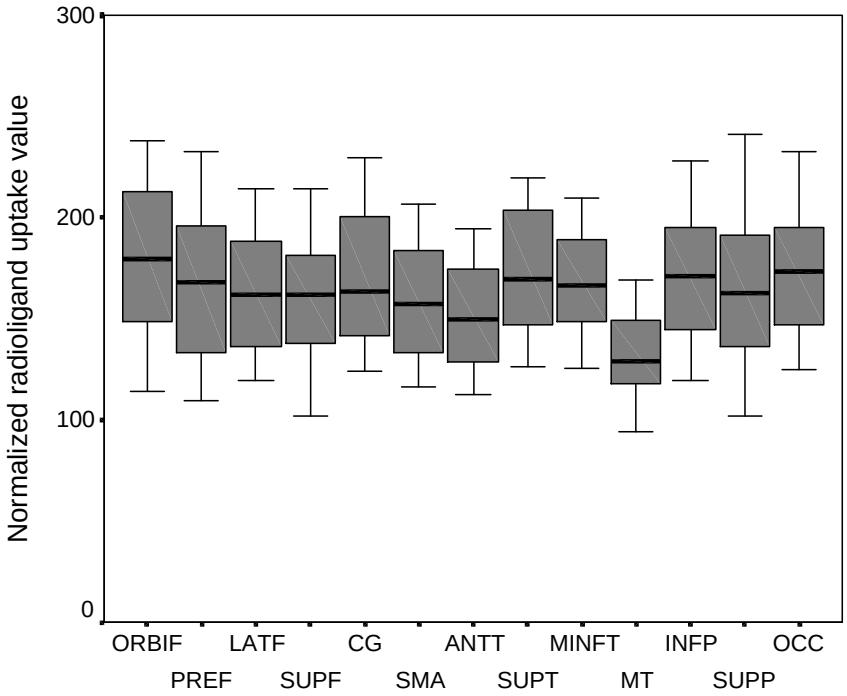

Figure 1. The distribution of radioligand uptake throughout the brain as measured in 26 healthy volunteers.
ORBIF = orbitofrontal; PREF = prefrontal; LATF = lateral frontal; SUPF = superior frontal; CG = cingulate gyri; SMA = sensorimotor area; ANTT = anterior temporal; SUPT = superior temporal; MINFT = medial inferior temporal; MT = mesotemporal; INFP = inferior parietal; SUPP = superior parietal; OCC = occipital

NEOCORTICAL BINDING POTENTIAL IN HEALTHY VOLUNTEERS AND RELATION WITH AGE AND GENDER

There was no statistically significant difference in radioligand uptake according to sex for any volume of interest. Concerning the age effect, the average neocortical binding potential varied between 217 at 23 years and 119 at 73 years. There was a significant age-related decline of neocortical binding potential (linear regression analysis: $R^2 = 0.87$, $p < 0.001$) resulting in an average decline of 11.6 ± 0.9 % per decade (figure 2). When only subjects over 60 years old were included, no significant age-related decline was present ($n = 13$; $R^2 = 0.1$, $p = 0.3$). Moreover, when only subjects over 70 years old were included ($n = 8$), the receptor binding potential as measured with ^{123}I-5-I-R91150 SPECT seemed to increase visually, however, this did not reach statistical significance ($p = 0.4$). The distribution of radioligand uptake throughout the brain compared between the 13 youngest (up to 52 years old) and the 13 oldest subjects (from 62 years on) is shown in figure 3. The highest age-related decline was reached in the posterior cingulate with a decrease of 14.2 % per decade ($R^2 = 0.78$, $p < 0.001$) while the lowest age-related decline was found in the left and the right mesotemporal region with a mean decrease of 7.6 % per decade ($R^2 = 0.8$, $p < 0.001$). There was no statistically significant asymmetry change according to age for any region.

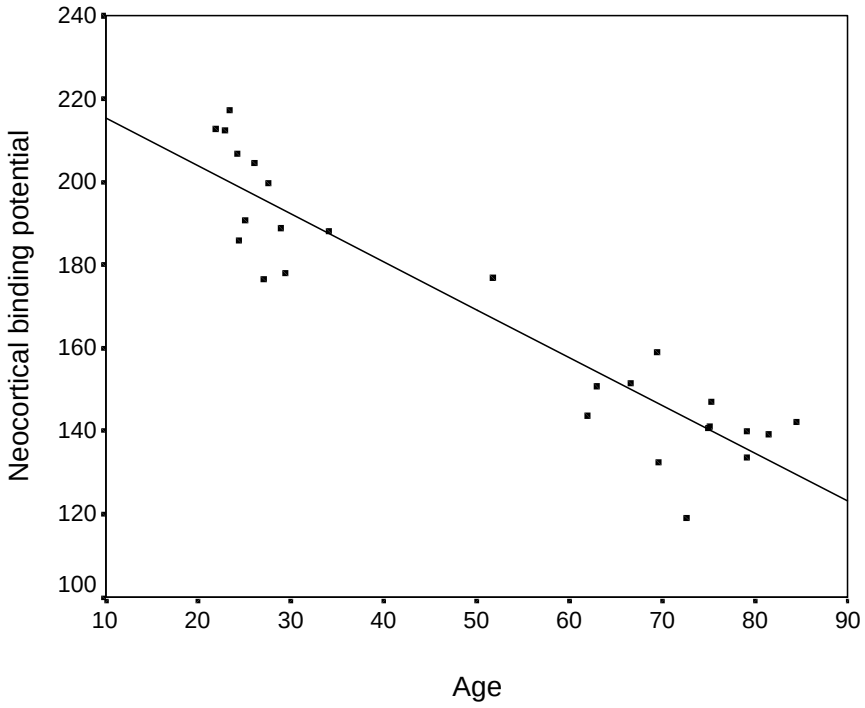

Figure 2. Age-related decline of the 5-HT_{2A} receptor neocortical binding potential as measured with ^{123}I-5-I-R91150 SPECT.

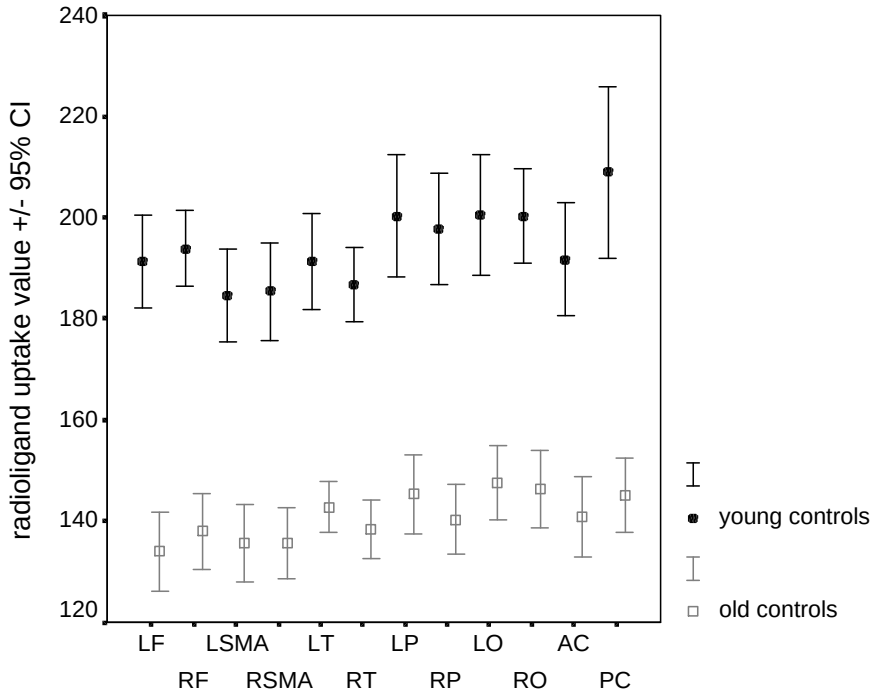

Figure 3. The distribution of radioligand uptake throughout the brain compared between the 13 youngest and the 13 oldest subjects (22-52 versus 62-85 yrs). LF = left frontal; RF = right frontal; LSMA = left sensorimotor; RSMA = right sensorimotor; LT = left temporal; RT = right temporal; LP = left parietal; RP = right parietal; LO = left occipital; RO = right occipital; AC = anterior cingulate; PC = posterior cingulate

ALZHEIMER'S DISEASE PATIENTS VERSUS AGE-MATCHED CONTROLS

Grouped mean uptake values for AD patients and age-matched controls are displayed in figure 4.

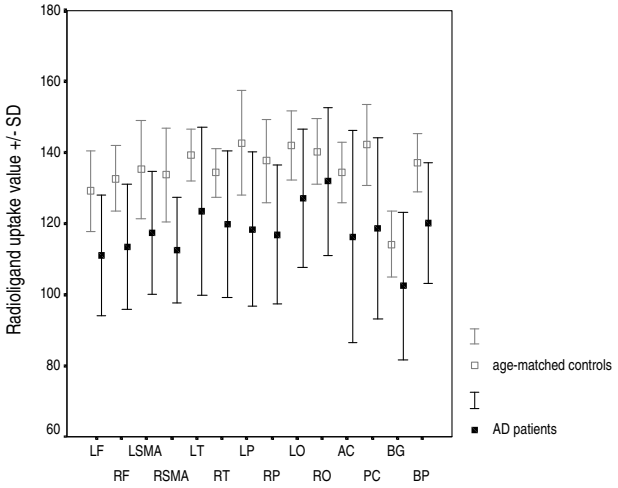

Figure 4. Grouped mean uptake values ± SD for AD patients and age-matched controls.

A generally decreased neocortical binding potential was found in the AD patient group (p = 0.02). Mean regional uptake values for AD patients and controls are shown in Table 2.

	AD patients		**age-matched controls**		**p-value, uncorrected**
	UV	SD	UV	SD	
Orbitofrontal	117.6	21.5	139	14.5	0.04*
Prefrontal	107.7	18.6	126.7	12.3	0.03*
Lateral frontal	116.8	15.1	135.2	8.6	0.008*
Superior frontal	110.4	25.3	128.2	16.1	0.1
Cingulate gyri	117.3	25.4	137.7	7.6	0.02*
Sensorimotor	114.9	14.9	134.5	12.2	0.004*
Temporal anterior	112.3	24.8	128.7	10.9	0.2
Temporal superior	125.5	26.4	142.4	10.9	0.06
Temporal medial inferior	129.4	22.9	144.3	7.4	0.09
Mesotemporal	100.6	17.9	113.3	11.8	0.16
Parietal inferior	121.6	17.3	141.8	9.5	0.01*
Parietal superior	108.0	33.3	136.3	21.4	0.06
Occipital	129.5	19.3	141.2	8.2	0.04*

*statistically significant p-values

Table 2. ^{123}I-5-I-R91150 regional uptake values (UV) and standard deviation (SD) for AD patients compared to age-matched controls

For the individual regions, a statistically significant decreased binding potential in AD patients compared to controls was found in the orbitofrontal, prefrontal, lateral frontal, cingulate, sensorimotor, parietal inferior, and occipital region ($p_{uncorrected} < 0.05$). After Bonferroni correction for multiple comparisons, only the difference in radioligand uptake for the sensorimotor region yielded significance ($p = 0.05$).

Concerning asymmetries, a statistically significant asymmetry was found for the mesotemporal region in favor of the left side ($p = 0.02$). However, individually neither the left or right mesotemporal area differed significantly from age-matched controls concerning radioligand uptake.

Figure 5 shows the radioligand uptake values for AD patients and age-matched controls for the right sensorimotor and left orbitofrontal region. Figure 6 shows a representative slice of an age-matched healthy volunteer and an AD patient with the specific radioligand uptake decreases in the lateral frontal, sensorimotor, and posterior cingulate region.

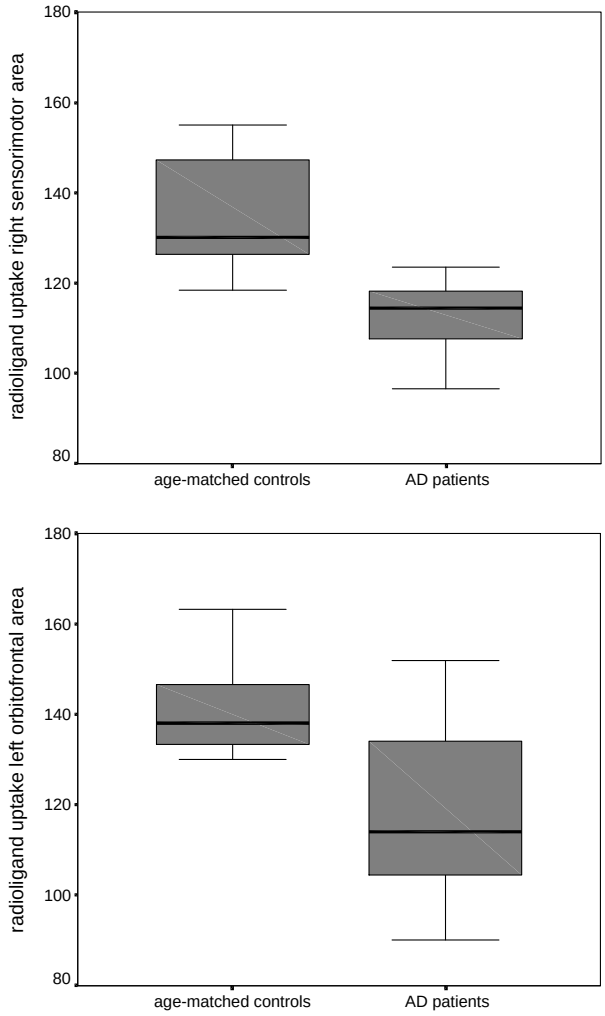

Figure 5. Boxplots of the ^{123}I-5-I-R91150 uptake values for AD patients and age-matched controls for the right sensorimotor (upper) and the left orbitofrontal (lower) region.

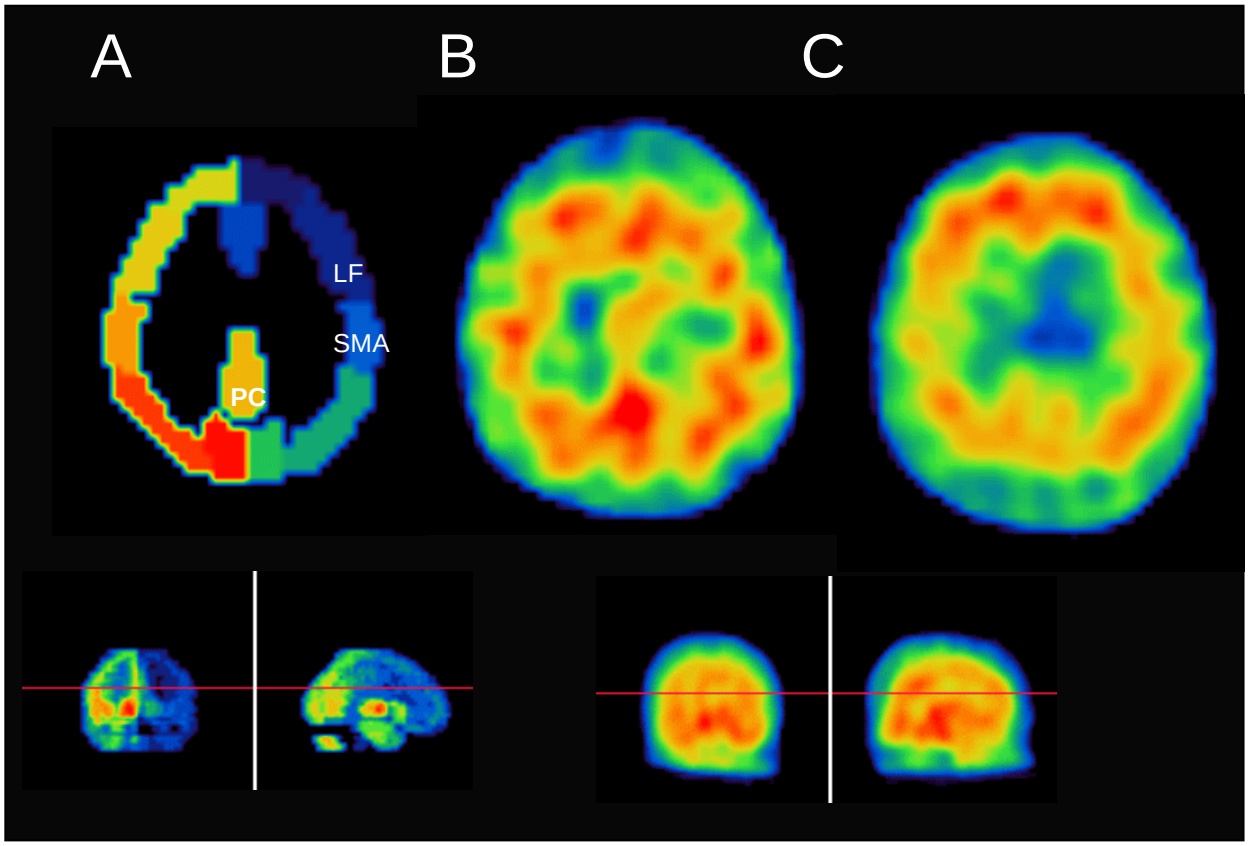

Figure 6. Figure of the VOI-map (A) together with a representative slice of an age-matched healthy volunteer (B) and an AD patient (C). Mark the cerebellum, representing free ligand and non-specific binding and also the specific uptake decreases in the lateral frontal (LF), sensorimotor (SMA) and the posterior cingulate region (PC) in the AD patient.

Neuropsychological testing and correlation with the 123I-5-I-R91150 uptake values

The mean Mini-Mental State Examination score (MMSE) yielded 18 ± 6 (range 9-25). The mean score on the geriatric depression scale (GDS) was 9.1 ± 6 (range 2-19), where, according to the cut-offs used, two mildly and no severely depressed patients were included. No effect of depression score on regional or neocortical binding potential was present within the AD patient group. A significant positive correlation was found between the ^{123}I-5-I-R91150 uptake value in the left orbitofrontal region and the global cognitive deficit as assessed with the MMSE-score (Spearman's σ correlation coefficient of 0.7; $p < 0.05$). No correlation was found between ^{123}I-5-I-R91150 uptake values for any region and global or subscores on the ADS6 cognitive screening battery.

DISCUSSION

The present findings concerning age dependency of 5-HT_{2A} receptor density are in agreement with previous ex vivo distribution studies demonstrating a general decrease in cortical 5-HT and more specifically 5-HT_{2A} receptor density [39]. This decline is also consistent with clinical observations of age-related changes in behaviors such as sleep or executive functioning, known to be linked to serotonergic function [15,33]. Moreover, peak minus baseline prolactin responses to fenfluramine (a serotonin-releasing agent) were shown to be negatively correlated with age [26]. Concerning the regional age-dependent decreases in 5-HT_{2A} receptor density, a very recent study with [^{18}F]altanserin found the highest age-related decline in the cingulate region while the lowest decline was found in the hippocampus, which is in concordance with the regional age-related decreases found in the present study [43].

This decrease in 5-HT_{2A} receptor density gradually declines, reaching a minimum between the 5th and the 6th decade [45]. As for in vivo imaging studies, several studies confirmed this linear decrease in cortical 5-HT_{2A} receptor binding in the living human brain with a more rapid decline in the first half of adult life, directly reflecting the loss of specific 5-HT_{2A} receptors with age [7,41,49]. Moreover, one study used the same radioligand as in the present study in a healthy control group up to 60 years old [4]. Also, it was previously shown that the effect of atrophy is relatively small compared to the large change in 5-HT_{2A} receptor binding in healthy aging [29]. The present study extends these previously published data since healthy subjects up to an age of 85 years were included where no significant age-related effect from the age of 60 on could be demonstrated. On the contrary, the receptor density seemed to slightly increase again from the age of 70, however, this did not reach statistical significance. This phenomenon of a parabolic relationship between aging and 5-HT_{2A} receptor density with an upswing from the age of 60 has also been reported previously for the prefrontal cortex and the hippocampal dentate using [^{3}H]ketanserin autoradiography [22]. Concerning gender, our data could not show any significant gender difference in radioligand uptake for any brain region. Up till now only one PET study with [^{18}F]altanserin, a 5-HT_{2A} receptor antagonist, has reported a gender difference in cortical 5-HT_{2A} receptor uptake in healthy subjects with a higher binding capacity in men in general with the greatest differences in the frontal and cingulate cortices [6].

Concerning the present findings about radioligand uptake in the AD patient group, our results are in line with previously published ex vivo data. Indeed, most postmortem studies showed, in addition to mostly frontal deficits, also deficits in cingulate and parietal 5-HT_{2A} binding sites [37]. However, an important issue concerning post-mortem studies is that some of these results, due to the nature of many of these studies, are potentially biased, firstly towards Alzheimer's disease of end-stage severity and secondly by post mortem delay. However, also two previously published PET studies with [^{18}F]setoporone and [^{18}F]altanserin showed this specific decrease in 5-HT_{2A} receptor density for AD patients, with the greatest deficits in frontal, cingulate, and temporal regions [7,28]. Interestingly, the reduction in radioligand uptake in the sensorimotor cortex, in fact the only statistically significant difference compared to age-matched

controls proof against formal Bonferroni correction, is somewhat unexpected but in line with recently published PET results using [^{18}F]altanserin [28]. Hypothetically, this could be related to a reduction in planned motor behavior and a reduction in sensory processing. Both aspects have been described in literature and are often observed in clinically demented patients [38,48].

Since binding potential may reflect changes in receptor density (B_{max}) as well as receptor affinity (K_D), abnormalities in either or both measures may contribute to the finding of a difference or, alternatively, a lack of difference in regional binding potential between different study groups. However, most postmortem binding assays and saturation binding experiments of 5-HT_{2A} receptor ligands in AD brains have shown abnormal B_{max} values and normal K_D values [12,13]. Therefore, it is likely that the low specific binding potential for several brain regions found in the present study is the result of a corresponding loss of 5-HT_{2A} receptors. This is similar to what has already been reported for most neuroreceptor changes in AD for e.g. the nicotinic, 5-HT_1, glutamate, NMDA, somatostatin or neuropeptide Y receptor sites [37].

Concerning the dynamic content of the measured receptor data, static scans were acquired and no full kinetic modelling of the receptor binding potential was measured. As mentioned already, pseudo-equilibrium conditions were assumed and the relative measure of neocortical to (nearly receptor-free) cerebellar activity was taken as a measure of the binding index, as has been shown in previous literature both by our group as well as others [3,4,11]. Under pseudo-equilibrium circumstances, the delivery phase of the tracer (initial flow) is not a determinant of the binding index anymore and therefore, regional estimates of perfusion need not to be correlated directly to the 5-HT_{2A} binding data.

No effect of depression score on global or regional binding potential was present within the AD patient group, although the low number of depressed subjects precluded a definitive examination of the 5-HT_{2A} receptor status in AD patients with concommittant depression. This is however in agreement with a previous PET study where no significant abnormalities in 5-HT_{2A} receptor binding potential as measured with [^{18}F]altanserin were observed in 11 patients with late-life depression according to DSM-IV and Hamilton depression scale criteria. Moreover, no effect of depression on neither global nor regional binding potential was present within the AD patient group (3 out of 11 with concurrent depression) [28]. These findings are consistent with the hypothesis that the 5-HT_{2A} receptor is differentially affected in late-life depression and AD, a finding that has implications for the etiological basis of mood and cognitive features of neuropsychiatric disorders of late life.

In conclusion, the results of the present study agree with and extend previous postmortem, in vitro and PET/SPECT in vivo findings. The age-related decline in 5-HT_{2A} receptor binding potential with a tendency towards a slight upswing towards later life highlights the necessity for age-matched controls in (clinical and) imaging studies and the need for larger study samples at advanced age. Moreover, it stresses the

etiological and potential therapeutic implications concerning mood changes and psychotropic drug dosing for older age groups. The fact that the 5-HT_{2A} receptor is differentially affected in AD patients compared to age-matched controls has implications for both the etiological basis and the therapeutic management of AD.

REFERENCES

[1] Akiyama H, Barger S, Barnum S, Bradt B, Bauer J, Cole GM, Cooper NR, Eikelenboom P, Emmerling M, Fiebich BL, Finch CE, Frautschy S, Griffin WS, Hampel H, Hull M, Landreth G, Lue L, Mrak R, MacKenzie IR, McGeer PL, O'Banion MK, Pachter J, Pasinetti G, Plata-Salaman C, Rogers J, Rydel R, Shen Y, Streit W, Strohmeyer R, Tooyoma I, Van Muiswinkel FL, Veerhuis R, Walker D, Webster S, Wegrzyniak B, Wenk G, Wyss-Coray T. Inflammation and Alzheimer's disease. Neurobiol Aging 2000;21(3):383-421.

[2] Arias B, Gutierrez B, Pintor L, Gasto C, Fananas L. Variability in the 5-HT(2A) receptor gene is associated with seasonal pattern in major depression. Mol Psychiatry 2001;6(2):239-42.

[3] Audenaert K, Van Laere K, Dumont F, Slegers G, Mertens J, van Heeringen C, Dierckx RA. Decreased frontal serotonin 5-HT 2a receptor binding index in deliberate self-harm patients. Eur J Nucl Med 2001;28(2):175-82.

[4] Baeken C, D'haenen H, Flamen P, Mertens J, Terriere D, Chavatte K, Boumon R, Bossuyt A. ^{123}I-5-I-R91150, a new single-photon emission tomography ligand for 5-HT_{2A} receptors: influence of age and gender in healthy subjects. Eur J Nucl Med 1998;25(12):1617-22.

[5] Barnes NM, Sharp T. A review of central 5-HT receptors and their function. Neuropharmacology 1999;38(8):1083-152.

[6] Biver F, Lotstra F, Monclus M, Wikler D, Damhaut P, Mendlewicz J, Goldman S. Sex difference in 5HT2 receptor in the living human brain. Neurosci Lett 1996;204(1-2):25-8.

[7] Blin J, Baron JC, Dubois B, Crouzel C, Fiorelli M, Attar-Levy D, Pillon B, Fournier D, Vidailhet M, Agid Y. Loss of brain 5-HT_2 receptors in Alzheimer's disease. In vivo assessment with positron emission tomography and [^{18}F]setoperone. Brain 1993;116(3):497-510.

[8] Bonaccorso S, Lin A, Song C, Verkerk R, Kenis G, Bosmans E, Scharpe S, Vandewoude M, Dossche A, Maes M. Serotonin-immune interactions in elderly volunteers and in patients with Alzheimer's disease (DAT): lower plasma tryptophan availability to the brain in the elderly and increased serum interleukin-6 in DAT. Aging (Milano) 1998;10(4):316-23.

[9] Buhot MC. Serotonin receptors in cognitive behaviors. Curr Opin Neurobiol 1997;7(2):243-54.

[10] Buhot MC, Martin S, Segu L. Role of serotonin in memory impairment. Ann Med 2000;32(3):210-21.

[11] Busatto GF, Pilowsky LS, Costa DC, Mertens J, Terriere D, Ell PJ, Mulligan R, Travis MJ, Leysen JE, Lui D, Gacinovic S, Waddington W, Lingford-Hughes A, Kerwin RW. Initial evaluation of ^{123}I-5-I-R91150, a selective 5-HT_{2A} ligand for single-photon emission tomography, in healthy human subjects. Eur J Nucl Med 1997;24(2):119-24.

[12] Cross AJ, Crow TJ, Ferrier IN, Johnson JA, Bloom SR, Corsellis JA. Serotonin receptor changes in dementia of the Alzheimer type. J Neurochem 1984;43(6):1574-81.

[13] Crow TJ, Cross AJ, Cooper SJ, Deakin JF, Ferrier IN, Johnson JA, Joseph MH, Owen F, Poulter M, Lofthouse R. Neurotransmitter receptors and monoamine metabolites in the brains of patients with Alzheimer-type dementia and depression, and suicides. Neuropharmacology 1984;23(12B):1561-9.

[14] de Jonghe JF, Krijgsveld S, Staverman K, Lindeboom J, Kat MG. Differentiation between dementia and functional psychiatric disorders in a geriatric ward of a general psychiatric hospital using the 'Amsterdam Dementia-Screening Test'. Ned Tijdschr Geneeskd 1994;138(33):1668-73.

[15] Degl'Innocenti A, Agren H, Zachrisson O, Backman L. The influence of prolactin response to d-fenfluramine on executive functioning in major depression. Biol Psychiatry 1999;46(4):512-7.

[16] Dewey SL, Smith GS, Logan J, Brodie JD. Modulation of central cholinergic activity by GABA and serotonin: PET studies with ^{11}C-benztropine in primates. Neuropsychopharmacology 1993;8(4):371-6.

[17] Eefsting JA, Boersma F, Van Tilburg W, Van Den BW. [Usefulness of the 'Mini-Mental State Test'for the diagnosis of dementia; study of criterion validity in a Dutch rural population]. Ned Tijdschr Geneeskd 1997;141(43):2066-70.

[18] Einat H, Clenet F, Shaldubina A, Belmaker RH, Bourin M. The antidepressant activity of inositol in the forced swim test involves 5-HT(2) receptors. Behav Brain Res 2001;118(1):77-83.

[19] Feuerstein TJ, Gleichauf O, Landwehrmeyer GB. Modulation of cortical acetylcholine release by serotonin: the role of substance P interneurons. Naunyn Schmiedebergs Arch Pharmacol 1996;354(5):618-26.

[20] Folstein MF, Folstein SE, McHugh PR. "Mini-mental state". A practica l method for grading the cognitive state of patients for the clinician. J Psychiatr Res 1975;12(3):189-98.

[21] Geldmacher DS, Whitehouse PJ. Evaluation of dementia. N Engl J Med 1996;335(5):330-6.

[22] Gross-Isseroff R, Salama D, Israeli M, Biegon A. Autoradiographic analysis of age-dependent changes in serotonin 5-HT2 receptors of the human brain postmortem. Brain Res 1990;519(1-2):223-7.

[23] Holmes C, Arranz MJ, Powell JF, Collier DA, Lovestone S. 5-HT2A and 5-HT2C receptor polymorphisms and psychopathology in late onset Alzheimer's disease. Hum Mol Genet 1998;7(9):1507-9.

[24] Lee RK, Knapp S, Wurtman RJ. Prostaglandin E2 stimulates amyloid precursor protein gene expression: inhibition by immunosuppressants. J Neurosci 1999;19(3):940-7.

[25] Lee RK, Wurtman RJ. Regulation of APP synthesis and secretion by neuroimmunophilin ligands and cyclooxygenase inhibitors. Ann N Y Acad Sci 2000;920261-8.

[26] Lerer B, Gillon D, Lichtenberg P, Gorfine M, Gelfin Y, Shapira B. Interrelationship of age, depression, and central serotonergic function: evidence from fenfluramine challenge studies. Int Psychogeriatr 1996;8(1):83-102.

[27] McKhann G, Drachman D, Folstein M, Katzman R, Price D, Stadlan EM. Clinical diagnosis of Alzheimer's disease: report of the NINCDS-ADRDA work group under the auspices of the Department of Health and Human Services Task Force on Alzheimer's Disease. Neurology 1984;34939-44.

[28] Meltzer CC, Price JC, Mathis CA, Greer PJ, Cantwell MN, Houck PR, Mulsant BH, Ben Eliezer D, Lopresti B, Dekosky ST, Reynolds CF, III. PET imaging of serotonin type 2A receptors in late-life neuropsychiatric disorders. Am J Psychiatry 1999;156(12):1871-8.

[29] Meltzer CC, Smith G, Price JC, Reynolds CF, III, Mathis CA, Greer P, Lopresti B, Mintun MA, Pollock BG, Ben Eliezer D, Cantwell MN, Kaye W, Dekosky ST. Reduced binding of [^{18}F]altanserin to serotonin type 2A receptors in aging: persistence of effect after partial volume correction. Brain Res 1998;813(1):167-71.

[30] Meneses A. 5-HT system and cognition. Neurosci Biobehav Rev 1999;23(8):1111-25.

[31] Meyer JH, Kapur S, Eisfeld B, Brown GM, Houle S, DaSilva J, Wilson AA, Rafi-Tari S, Mayberg HS, Kennedy SH. The effect of paroxetine on 5-HT(2A) receptors in depression: an [(18)F]setoperone PET imaging study. Am J Psychiatry 2001;158(1):78-85.

[32] Mossner R, Lesch KP. Role of serotonin in the immune system and in neuroimmune interactions. Brain Behav Immun 1998;12(4):249-71.

[33] Myers BL, Badia P. Changes in circadian rhythms and sleep quality with aging: mechanisms and interventions. Neurosci Biobehav Rev 1995;19(4):553-71.

[34] Nacmias B, Tedde A, Forleo P, Piacentini S, Guarnieri BM, Bartoli A, Ortenzi L, Petruzzi C, Serio A, Marcon G, Sorbi S. Association between 5-HT(2A) receptor polymorphism and psychotic symptoms in Alzheimer's disease. Biol Psychiatry 2001;50(6):472-5.

[35] Nitsch RM, Deng M, Growdon JH, Wurtman RJ. Serotonin 5-HT2a and 5-HT2c receptors stimulate amyloid precursor protein ectodomain secretion. J Biol Chem 1996;271(8):4188-94.

[36] Nitsch RM, Wurtman RJ, Growdon JH. Regulation of APP processing. Potential for the therapeutical reduction of brain amyloid burden. Ann N Y Acad Sci 1996;777175-82.

[37] Nordberg A. Neuroreceptor changes in Alzheimer disease. Cerebrovasc Brain Metab Rev 1992;4(4):303-28.

[38] Ortiz AT, Lopez-Ibor MI, Martinez CE, Fernandez LA, Maestu UF, Lopez-Ibor JJ. Deficit in sensory motor processing in depression and Alzheimer's disease: a study with EMG and event related potentials. Electromyogr Clin Neurophysiol 2000;40357-63.

[39] Pazos A, Probst A, Palacios JM. Serotonin receptors in the human brain--IV. Autoradiographic mapping of serotonin-2 receptors. Neuroscience 1987;21(1):123-39.

[40] Quirion R, Richard J, Dam TV. Evidence for the existence of serotonin type-2 receptors on cholinergic terminals in rat cortex. Brain Res 1985;333(2):345-9.

[41] Rosier A, Dupont P, Peuskens J, Bormans G, Vandenberghe R, Maes M, de Groot T, Schiepers C, Verbruggen A, Mortelmans L. Visualisation of loss of 5-HT2A receptors with age in healthy volunteers using [^{18}F]altanserin and positron emission tomographic imaging. Psychiatry Res 1996;68(1):11-22.

[42] Roth BL, Berry SA, Kroeze WK, Willins DL, Kristiansen K. Serotonin 5-HT2A receptors: molecular biology and mechanisms of regulation. Crit Rev Neurobiol 1998;12(4):319-38.

[43] Sheline YI, Mintun MA, Moerlein SM, Snyder AZ. Greater loss of 5-HT_{2A} receptors in midlife than in late life. Am J Psychiatry 2002;159(3):430-5.

[44] Siever LJ, Kahn RS, Lawlor BA, Trestman RL, Lawrence TL, Coccaro EF. Critical issues in defining the role of serotonin in psychiatric disorders. Pharmacol Rev 1991;43(4):509-25.

[45] Sparks DL. Aging and Alzheimer's disease. Altered cortical serotonergic binding. Arch Neurol 1989;46(2):138-40.

[46] Van Laere K, Koole M, D'Asseler Y, Versijpt J, Audenaert K, Dumont F, Dierckx R. Automated stereotactic standardization of brain SPECT receptor data using single-photon transmission images. J Nucl Med 2001;42(2):361-75.

[47] Van Laere K, Koole M, Kauppinen T, Monsieurs M, Bouwens L, Dierckx R. Nonuniform transmission in brain SPECT using ^{201}Tl, ^{153}Gd, and ^{99m}Tc static line sources: anthropomorphic dosimetry studies and influence on brain quantification. J Nucl Med 2000;41(12):2051-62.

[48] Wallin A, Blennow K. Neurologic motor signs in early and late onset Alzheimer's-disease. Dementia 1992;3314-9.

[49] Wong DF, Wagner HN, Jr., Dannals RF, Links JM, Frost JJ, Ravert HT, Wilson AA, Rosenbaum AE, Gjedde A, Douglass KH, . Effects of age on dopamine and serotonin receptors measured by positron tomography in the living human brain. Science 1984;226(4681):1393-6.

[50] Yesavage JA, Brink TL, Rose TL. The geriatric depression rating scale: comparison with other self-report and psychiatric rating scales. In: Crook T, Gerris S, Bartus R, editors. Assessment in geriatric psychopharmacology. New Canaan: Mark Powley Associates, 1983. p. 153-65.

[51] Yesavage JA, Brink TL, Rose TL, Lum O, Huang V, Adey M, Leirer VO. Development and validation of a geriatric depression screening scale: a preliminary report. J Psychiatr Res 1982;17(1):37-49.

SUMMARY, DISCUSSION AND PERSPECTIVES

The present thesis aims at being an aid in clarifying the pathophysiology of Alzheimer's disease by means of functional radionuclide imaging, this in order to reveal certain aspects of its disease process and finally aid its therapeutic management.

The option of functional radionuclide imaging being either positron emission tomography (PET) or single photon emission computed tomography (SPECT) was chosen because of its properties of allowing the non-invasive detection of specific cells and tissues involved in the pathophysiological process all depending of the radioligand of choice. This whereas the capability of structural imaging lies in visualising (mostly non-specific) structural changes and describing their detailed spatial relationship. As such, in general, the disease process must be already at an advanced stage before it can be depicted by structural imaging modalities, giving rise to its poor *pathophysiological sensitivity* at the early stages (when anatomical changes are not detectable yet). Also, for chronic processes like Alzheimer's disease, structural changes may be detectable that do not reflect the actual state of disease activity.

As for the newer structural or metabolic imaging tools however, for example *proton MR spectroscopy* seems more specific in assessing the pathophysiological process by means of for example measuring neurocellular viability or neuroaxonal integrity (N-acetyl aspartate) and glial (choline and especially myo-inositol) markers which, according to some authors, could be able to predict and monitor the response to therapy, giving rise to an individual optimised treatment. Likewise, *magnetisation transfer imaging* (MTI) seems valuable in measuring brain involvement and provides information about brain damage with increased pathological specificity detecting subtle microscopic abnormalities in brain tissue, which go undetected with conventional scanning. As such, a low MTI ratio indicates a reduced capacity of the macromolecules in brain tissue membranes to exchange magnetisation with the surrounding water molecules, reflecting damage to these membranes. Also, coefficients of water diffusion can be measured with *diffusion tensor MRI* where an increased water diffusivity reflects a disintegration of brain tissue compartments. As for *functional magnetic resonance imaging*, some studies suggest that fMRI can be used to diagnose Alzheimer's disease in its earliest stage, detecting subclinical deterioration of the memory function and may be useful to predict the future decline of memory in people with genetic or other risk factors.

This thesis is divided in two parts. One part (chapter two to six) deals with the *neuroinflammatory hypothesis* while the second part (chapter seven) deals with the *serotonergic hypothesis* in Alzheimer's disease.

In **chapter two**, in an *introductory section*, the epidemiology, clinical features, pathophysiology, and treatment of Alzheimer's disease is reviewed. A *second section* discusses three topics.
Firstly, the basic neuroinflammatory mechanisms and its biochemical characteristics, the potential

neurotoxic mediators during activation of microglia (i.e. the brain resident macrophages), and the current status of inflammation with respect to neurodegeneration is reviewed. Indeed, in the past decades, our understanding of the central nervous system has evolved from one of an immune-privileged site, to one where inflammation is pathognomonic for some of the most prevalent and tragic neurodegenerative diseases. Inflammation, whether in the brain or periphery, is almost always a secondary response to a primary pathogen. In head trauma, for example, the blow to the head is the primary event. What typically concerns the neurologist and neurosurgeon more, however, is the secondary inflammatory response that will ensue and likely cause more neuron loss than the initial injury. Current research indicates that diseases as diverse as multiple sclerosis, stroke and Alzheimer's disease exhibit inflammatory processes that contribute to cellular dysfunction or loss.
Secondly, the immune-related pathogenesis of Alzheimer's disease is thoroughly reviewed. It is clearly shown that inflammation contributes to neurodegeneration in Alzheimer's disease, not simply as a secondary phenomenon, but primarily as a significant source of pathology. As such, visualising this neuroinflammation would be of interest, firstly for clarifying the pathophysiology, secondly for selecting patient subgroups that are more eligible for anti-inflammatory treatment(s) and finally, for monitoring patients during trials with these anti-inflammatory agents.
Thirdly, the currently available neuroinflammatory imaging modalities, both structural and mainly functional, are critically reviewed and discussed. It is shown that, whereas structural imaging shows merely late anatomical consequences of an inflammatory response, functional imaging is a strong potential candidate to bridge the gap between *in vitro* and *in vivo* knowledge. In this perspective, a number of radioligands have been recently explored which allow the early *in vivo* visualisation of inflammatory responses, and, as such, open a promising window on both *understanding* as well as possible *clinical management* of inflammatory neurodegenerative disorders.

In the light of the aforementioned goals of neuroinflammatory imaging, a first attempt is made with ^{57}Co and SPECT. Indeed, previous studies showed that ^{57}Co SPECT is able to visualise inflammatory lesions, probably by means of the final common pathway of the Ca^{2+}-homeostasis disturbance in both neuronal degeneration and inflammation. **Chapter three** describes this attempt to visualise inflammation *in vivo* in Alzheimer's disease patients by detecting ^{57}Co SPECT changes and investigates whether ^{57}Co SPECT can generate additional information which cannot be obtained with conventional neuroimaging techniques or neuropsychological testing (NPT). As such, ^{57}Co SPECT data are compared with data obtained from Magnetic Resonance Imaging (MRI), perfusion SPECT, and neuropsychological testing, and finally findings in Alzheimer's disease patients are compared with patients suffering from vascular dementia and frontal lobe-type dementia. It is shown that ^{57}Co SPECT scans were not able to show any regional raised uptake and in this way ongoing tissue decay or inflammation, irrespective of the type of dementia, depth or extent of perfusion defects, presence of atrophy on MRI, or the results of NPT. In an attempt to explain these results it is concluded that the limitations of ^{57}Co SPECT are manifold. Due to the long physical half-life of 270 days, only a limited dose can be injected which is responsible for the low count rate and the resulting low statistics. Moreover, whether ^{57}Co visualises specific aspects of neuronal damage or blood-brain barrier integrity

is still uncertain. To what extent ^{57}Co really visualises calcium-mediated processes (*in vitro* and more importantly *in vivo*), and therefore resembles identical molecular uptake mechanisms, has yet to be determined, although the cerebral uptake of intravenously administered radioactive ^{45}Ca and ^{60}Co in neuronal damage is highly similar. Finally, its exact cellular site of accumulation of radioactivity is, as yet, not known.

After this, the development and validation of another radioligand for the visualisation of neuroinflammatory lesions is described. Indeed, the peripheral benzodiazepine receptor (PBR) was reported to reflect neuro-inflammatory damage by an upregulation on activated microglia. As such, radiolabelled PK11195, a high affinity ligand for the PBR, could be an ideal candidate. In **chapter four**, the biodistribution and dosimetry of [^{123}I]iodo-PK11195, a potential SPECT radioligand is described in humans. For this, sequential whole body scans were performed up to 72 hours post-injection of ^{123}I labelled iodo-PK11195. Multiple blood samples were taken, and urine was collected to measure the fraction voided by the renal system. Decay corrected regions of interest of the whole-body images were analysed, and geometric mean count rates were used to determine organ activity. Organ absorbed doses and effective dose were calculated using the MIRD method. It was seen that [^{123}I]iodo-PK11195 was rapidly cleared from the blood, mainly by the hepatobiliary system. Approximately 22% was voided in urine after 48 hours. Average organ residence times were 0.74, 0.44, and 0.29 hrs for the liver, upper large intestine, and lower large intestine respectively. The testes received the highest dose, 109.4 μGy/MBq. All other organs investigated received doses of less than 50 μGy/MBq. The effective dose was 40.3 μSv/MBq. It was concluded that ^{123}I labelled iodo-PK11195 is a suitable agent for the visualisation of the PBR and indirectly for the imaging of neuroinflammatory lesions. Taking into account the radiation burden of 7.46 mSv following an administration of 185 MBq, a ^{123}I labelled iodo-PK11195 investigation should as such be considered as an ICRP risk category IIb investigation.

Thereafter, in **chapter five**, the validation of radiolabelled PK11195 as a neuroinflammatory tracer is described, this by applying the radiolabelled ligand in multiple sclerosis, the prototype neuroinflammatory disorder with its pathophysiological involvement of microglia. In an *introductory section*, the history, epidemiology, pathophysiology, clinical features and disease course, and treatment of multiple sclerosis is reviewed. In a *second section*, the visualisation of activated microglia in multiple sclerosis patients using [^{11}C]PK11195 and PET is studied. For this, semiquantitative [^{11}C]PK11195 uptake values were assessed for multiple sclerosis patients compared to healthy controls with a normalisation on cortical gray matter. It was found that the radioligand uptake in Gadolinium-lesions was significantly increased compared to normal white matter. Uptake in T2-lesions was generally decreased, suggesting a PBR downregulation. However, uptake values for T2-lesions increased whenever a clinical or MR-relapse was present, all suggestive for a dynamic process with a transient PBR upregulation. During disease progression, an increase of normal-appearing white matter (NAWM) radioligand uptake was found, propagating NAWM as the possible real burden of disease. It was concluded that [^{11}C]PK11195 PET imaging has an additional value over MRI concerning the immuno-pathophysiological process and is able

to demonstrate inflammatory processes with microglial involvement in multiple sclerosis. In a *third section* of this chapter, brain atrophy and microglial activation was assessed in multiple sclerosis patients during different disease stages and the relationship between inflammation, atrophy, and clinical measures was investigated. It was found that atrophy was significantly greater in multiple sclerosis patients compared to age-matched controls. Moreover, a significant correlation was found between brain atrophy and both disease duration and disability, as measured with the expanded disability status scale (EDSS). For NAWM, microglial activation as measured with [^{11}C]PK11195 uptake increased with the amount of atrophy, while T_2-lesional [^{11}C]PK11195 uptake values decreased according to increasing brain atrophy. It was concluded that brain atrophy, correlating with disease duration and disability, is directly related to NAWM and T_2-lesional inflammation as measured by this *PET probe* for microglial activation.

Chapter six describes the assessment of microglial activation using radiolabelled PK11195 for SPECT in Alzheimer's disease ànd its relation with findings obtained from perfusion SPECT and neuropsychological testing. For this, [^{123}I]iodo-PK11195 SPECT images were realigned into stereotactic space where binding indices, normalized on cerebellar uptake, were calculated. It was found that the mean [^{123}I]iodo-PK11195 uptake was increased in Alzheimer's disease compared to controls in nearly all neocortical regions, however, statistical significance was only reached in the frontal and right mesotemporal regions. Significant correlations were found between regional increased [^{123}I]iodo-PK11195 uptake values and specific cognitive deficits as assessed with neuropsychological testing. It is concluded that [^{123}I]iodo-PK11195 is a cellular disease activity marker allowing the *in vivo* assessment of microglial inflammation in Alzheimer's disease. Future optional work could be both at a technical and clinical level. Technically, a direct comparison between the PET and SPECT radioligand should be accomplished whereas feasable methods for absolute quantification of radioligand uptake should be further validated and implemented. From the clinical level, the inclusion of more patients at different stages of the disease, the comparison with proton MR spectroscopy for the measurement of glial markers, or the assessment of radioligand uptake changes during (anti-inflammatory) therapy could be very useful. Also, new ligands could be developed for the neuroinflammatory visualisation depending on the eventual development of the current anti-inflammatory treatment of choice. Ideally, this new radioligand should be rapidly cleared from blood and other non-target tissues and moreover, the interaction of the ligand and its receptor should be characterized by a high binding affinity and specificity (shown by autoradiography, receptor blockade, or studies with control agents). For neuroimaging studies in pathologies without blood-brain barrier breakdown (like Alzheimer's disease), the ligand should be able to easily penetrate this blood-brain barrier.

In a second part of this thesis (**chapter seven**) dealing with the serotonergic hypothesis of Alzheimer's disease, the role and distribution of serotonin (5-HT) type 2A receptors in healthy controls and Alzheimer's disease patients is described. In an *introductory section* the role of serotonin in general and serotonin type 2A receptors specifically in cognitive and non-cognitive behaviour and its relation with Alzheimer's disease in general and the inflammatory hypothesis more specifically is briefly

reviewed. In a *second section*, the imaging of the 5-HT_{2A} system in healthy controls and Alzheimer's disease patients is performed. Using ^{123}I-5-I-R91150, a selective radio-iodinated 5-HT_{2A} receptor antagonist and SPECT, the 5-HT_{2A} binding potential (BP) in healthy volunteers and Alzheimer's disease patients is calculated. For this, a semiquantitive analysis with normalisation on cerebellar uptake provided estimates of BP for 26 cortical regions of interest. An age-related decline of neocortical BP was found in healthy controls (11.6 % per decade). Compared to age-matched controls, a generally decreased neocortical BP in Alzheimer's disease was seen with a significant regional reduction in the orbitofrontal, prefrontal, lateral frontal, cingulate, sensorimotor, parietal inferior, and occipital region. These results are in line with previous postmortem, *in vitro*, and PET findings. As such, the age-related decline highlights the necessity for matched advanced age study samples. The fact that the 5-HT_{2A} receptor is differentially affected in Alzheimer's disease patients compared to controls has implications for both its etiological basis and therapeutic management.

As presented in the aforementioned manuscripts, both *neuroinflammatory* and *serotonergic* imaging yield different specific regional changes in binding potential for Alzheimer's disease patients, which raises the question of their (inter)relationship in terms of the Alzheimer's disease pathophysiology. Unfortunately, for reasons of logistics, no study was performed where both radiolabelled PK11195 and ^{123}I-5-I-R91150 was used in the same patients, however, one can assume that both populations included in these two studies are, however small, representative for a, if existing, *true* Alzheimer's disease population making these differences in regional binding potential changes in fact *true differences* reflecting as such not differences in the characteristics of the patients included, but reflecting a different point of view or part regarding the Alzheimer's disease pathophysiology. In fact, there are three options. Firstly, there is the notion of disease heterogeneity where questions have been raised about the existence of Alzheimer's disease as a single nosological entity. Although many researchers have tried to unify the different hypotheses concerning the aetiology and pathophysiology of Alzheimer's disease, many scientific arguments exist pointing to the possibility that there may not be just one *Alzheimer's disease* we are looking at. Indeed, many authors have raised the option of Alzheimer's disease patients with for example different neuropsychological or clinical profiles or different perfusion disturbances, not to mention the overlap both concerning risk factors and concerning clinical presentation between Alzheimer's disease and vascular dementia. Secondly, there is the option of a chronology in the pathophysiology of Alzheimer's disease in which different *brain systems* are more or less affected during the disease time course. In the light of the present thesis, the *series of events* presented here would be firstly the inflammatory response following a primary event (amyloid burden, …) followed by functional neurotransmitter or more specifically serotonergic changes finally followed by structural changes like atrophy. Thirdly, there is the option of a co-existence of pathophysiological changes at the same time with a different regional sensitivity explaining these differences in regional binding potential changes. Indeed, one can speculate why the sensorimotor cortex is spared regarding perfusion but heavily affected concerning the 5-HT_{2A} system or why the mesotemporal area is largely affected by tissue loss and relatively spared concerning the serotonergic system.

To answer these and other questions it would be worthy to study in the same patients several pathophysiological points of view for example amyloidogenic, neuroinflammatory, perfusion, cholinergic, serotonergic and structural changes and this on different time points in order to label different pathophysiological mechanisms to different time courses of the disease. Ideally, this should also be done making use of different markers for measuring the same aspect of its pathophysiology, for example both neuroimaging (structural, functional, and metabolic), laboratory (serum, CSF, …) as post-mortem neuropathological markers. This certainly, in an era where more and more treatment is available in order to be of any help in deciding when to apply which kind of treatment.

SAMENVATTING, DISCUSSIE EN TOEKOMSTPERSPECTIEVEN

Het huidig proefschrift tracht een hulp te zijn bij de opheldering van de pathofysiologie van de ziekte van Alzheimer door middel van functionele beeldvorming met behulp van radionucliden, dit om uiteindelijk aspecten van het ziekteproces te doorgronden and finaal mogelijks het therapeutisch beleid te beïnvloeden.

De optie van functionele beeldvorming zij het òfwel *positron emissie tomografie* (PET) ofwel *enkelvoudige foton emissie tomografie* (*single photon emission computed tomography* of SPECT) was verkozen gezien deze techniek ons in staat stelt tot een niet invasieve detectie van specifieke cellen en weefsels betrokken bij het pathofysiologisch proces, dit afhankelijk van het gekozen radioligand. Dit staat haaks tegenover de mogelijkheid van structurele beeldvorming die zich meer situeert in het in beeld brengen van (meestal aspecifieke) structurele veranderingen en het beschrijven van de gedetailleerde ruimtelijke relatie hiervan. Zodoende dient in het algemeen het ziekteproces reeds in een geavanceerd stadium te zijn vooraleer het kan gedetecteerd door middel van structurele beeldvormingsmodaliteiten wat aanleiding geeft tot zijn minder goede *pathofysiologische gevoeligheid* in de eerste stadia van de ziekte, wanneer anatomische veranderingen nog niet detecteerbaar zijn. Bovendien kunnen voor chronische aandoeningen zoals de ziekte van Alzheimer structurele veranderingen detecteerbaar zijn die de huidige ziektetoestand niet correct weergeven.

Wat betreft de nieuwere structurele of metabole beeldvormingsmodaliteiten echter lijkt bijvoorbeeld *proton MR spectroscopie* meer specifiek in het in kaart brengen van het pathofysiologisch proces, dit door middel van het meten van neurocellulaire viabiliteits- of neuro-axonale integriteits- (N-acetyl-aspartaat) en gliale (choline en vooral myo-inositol) merkers die, volgens sommige auteurs, in staat zijn om het antwoord op de ingestelde therapie te voorspellen èn te volgen mogelijks leidend tot een geïndividualiseerde meer optimale behandeling. Evenzeer lijkt *magnetisation transfer imaging* (MTI) waardevol in het meten van de betrokkenheid van het brein in het ziekteproces en verschaft zodoende informatie over hersenschade met een verhoogde pathologische specificiteit door subtiele microscopische abnormaliteiten in het hersenweefsel te ontdekken welke nog niet gedetecteerd kunnen worden met conventionele beeldvormingsmodaliteiten. In die zin zou een verlaagde MTI ratio op een verminderde capaciteit wijzen van de macromoleculen in de membranen van het hersenweefsel om magnetisatie uit te wisselen met de omgevende watermoleculen wijzend op schade aan deze membranen. Verder kunnen coëfficiënten van waterdiffusie gemeten worden met behulp van *diffusion tensor MRI* waarbij een verhoogde waterdiffusie-coëfficiënt een desintegratie van hersenweefselcompartimenten reflecteert. Wat betreft functionele magnetische resonantiebeeldvorming (fMRI) suggereren sommige studies dat fMRI in staat zou zijn om de ziekte van Alzheimer in een vroegtijdig stadium te diagnosticeren door het detecteren van subklinische deteriorations van de geheugenfunctie waardoor het in die zin nuttig zou kunnen zijn om toekomstig geheugenverlies te voorspellen en dit vooral bij mensen met genetische of andere risicofactoren.

Het huidig proefschrift is opgedeeld in twee delen. Eén deel (hoofdstuk twee tot en met zes) behandelt de *neuro-inflammatoire hypothese*, terwijl het tweede deel (hoofdstuk zeven) de *serotonerge hypothese* bij de ziekte van Alzheimer behandelt.

In **hoofdstuk twee** wordt in een *inleidende sectie* de epidemiologie, klinische verschijnselen, pathofysiologie en de behandeling van de ziekte van Alzheimer toegelicht. Een *tweede sectie* bediscussieert drie topics.

In een eerste topic wordt de basis omtrent neuro-inflammatoire mechanismen en zijn biochemische karakteristieken, de mogelijk neurotoxische mediatoren tijdens de activatie van microglia (de hersenmacrofagen) en de huidige status met betrekking tot inflammatie en neurodegeneratie toegelicht. Inderdaad, in de laatste decades is ons begrip van het centraal zenuwstelsel geëvolueerd van dat van een immuun-geprivilegeerde plaats tot dat van een plaats waar inflammatie kenmerkend is voor enkele van de meeste voorkomende en tragische neurodegeneratieve aandoeningen. Inflammatie, zij het centraal of perifeer, is meestal een secundaire respons op een primair pathogeen. Bij een hoofdtrauma bijvoorbeeld is de slag op het hoofd het primaire event. Wat de neuroloog en de neurochirurg vooral zal interesseren echter is de secundaire inflammatoire respons die erop zal volgen en mogelijks meer neuronaal verlies zal berokkenen dan het initieel incident. Huidig onderzoek wijst erop dat ziektes zoals multipele sclerose, beroerte en de ziekte van Alzheimer inflammatoire processen vertonen welke een bijdrage leveren tot het verlies of de dysfunctie van neuronale cellen.

Ten tweede wordt de immuungerelateerde pathogenese van de ziekte van Alzheimer grondig toegelicht. Het wordt duidelijk dat inflammatie bijdraagt tot neurodegeneratie in de ziekte van Alzheimer, dit niet enkel als een secundair fenomeen maar ook primair als een significante bron van pathologie. In die zin zou het in beeld brengen van deze inflammatie interessant zijn, ten eerste voor een bijdrage te leveren wat betreft de kennis van de pathofysiologie, ten tweede voor het selecteren van patiëntengroepen die in aanmerking zouden komen voor behandeling met (een) anti-inflammatoire therapie(ën) en ten slotte voor het opvolgen van deze patiënten tijdens deze trials met anti-inflammatoire medicatie.

Ten derde wordt de huidige stand van zaken omtrent neuro-inflammatoire beeldvormingsmodaliteiten en dit zowel structureel als vooral functioneel kritisch toegelicht en bediscussieerd. Het wordt duidelijk dat, terwijl structurele beeldvorming meestal late anatomische veranderingen van een inflammatoire respons aantoont, functionele beeldvorming een sterke kandidaat is om de kloof tussen *in vitro* en *in vivo* kennis te dichten. In dit perspectief zijn recent een aantal radioliganden bestudeerd die ons toelaten tot het vroeg *in vivo* visualiseren van inflammatoire veranderingen en op die manier een perspectief bieden op zowel *het begrijpen* als het uiteindelijke *klinische beleid* van inflammatoire neurodegeneratieve aandoeningen.

In het licht van deze hierboven vermelde objectieven van neuro-inflammatoire beeldvorming werd een eerste poging gedaan met ^{57}Co en SPECT. Inderdaad, vroegere studies wezen erop dat ^{57}Co SPECT in staat is om inflammatoire letsels in beeld te brengen dit mogelijks door middel van de *final common*

pathway van de Ca^{2+}-homeostase-stoornis en dit zowel in neuronale degeneratie als in inflammatie. **Hoofdstuk drie** beschrijft deze poging tot het in beeld brengen van inflammatie *in vivo* in patiënten met de ziekte van Alzheimer door middel van het detecteren van ^{57}Co SPECT veranderingen en investigeert of ^{57}Co SPECT in staat is tot het genereren van additionele informatie die niet vergaard kan worden door middel van conventionele beeldvormingsmodaliteiten of neuropsychologische testen. In die zin werden ^{57}Co SPECT data vergeleken met data verkregen door middel van MRI, perfusie SPECT en neuropsychologische testen en werden deze resultaten bij patiënten lijdend aan de ziekte van Alzheimer vergeleken met deze van patiënten lijdend aan vasculaire en frontale dementie. Er wordt aangetoond dat ^{57}Co SPECT niet in staat is om regionaal verhoogde opnames en in die zin weefselverval of inflammatie in beeld te brengen en dit ongeacht van het type dementie, de ernst en de uitgebreidheid van de doorbloedingsdefecten, de aanwezigheid van atrofie op MRI noch van de resultaten van de neuropsychologische testen. In een poging om de hierboven vermelde resultaten te verklaren wordt geconcludeerd dat de beperkingen van ^{57}Co SPECT veelvuldig zijn. Door het lang fysisch halfleven van namelijk 270 dagen kan slechts een beperkte dosis geïnjecteerd worden hetgeen verantwoordelijk is voor de lage *count rate* en de resulterende lage beeldvormingsstatistieken. Bovendien is het nog steeds niet zeker of ^{57}Co specifieke aspecten van neuronale schade dan wel bloed-hersenbarrière-doorbraak in beeld brengt. In hoeverre ^{57}Co werkelijk Calcium-gemedieerde processen in beeld brengt (*in vitro* en nog belangrijker *in vivo*) en in die zin staat voor identieke moleculaire opnamemechanismen dient nog bepaald te worden, hoewel de cerebrale opname van intraveneus toegediend ^{45}Ca en ^{60}Co bij neuronale schade zeer veel gelijkaardige kenmerken vertoont. Tenslotte is de exacte cellulaire opnameplaats van de radioactiviteit nog niet gekend.

Hierna wordt de ontwikkeling en validatie van een nieuw radioligand voor de beeldvorming van neuro-inflammatoire letsels beschreven. Zo wordt gebruik gemaakt van de *perifere benzodiazepine receptor* (PBR) die in staat is om neuro-inflammatoire schade in beeld te brengen dit door middel van een upregulatie op geactiveerde microglia. Aldus zou radioactief gemerkt PK11195, een hoog-affiniteitsligand voor deze PBR, een ideale kandidaat zijn. In **hoofdstuk vier** wordt de biodistributie en dosimetrie van [^{123}I]iodo-PK11195, een potentieel SPECT radioligand beschreven bij mensen. Hiervoor worden sequentiële *whole body* opnames verricht tot 72 uur na de injectie van ^{123}I gemerkt iodo-PK11195. Meerdere bloedafnames werden verricht en de urine werd verzameld voor het meten van de fractie welke geklaard werd door het renaal systeem. Voor verval gecorrigeerde regio's van deze *whole body* opnames werden geanalyseerd en geometrisch gemiddelde activiteitsverdelingen werden gebruikt om orgaanactiviteiten te bepalen. De geabsorbeerde en de effectieve dosissen werden berekend gebruik makende van de MIRD methode. Er werd vastgesteld dat [^{123}I]iodo-PK11195 snel geklaard werd vanuit het bloed, dit hoofdzakelijk door het hepatobiliair systeem. Ongeveer 22% was terug te vinden in de urine na 48 uur. De gemiddelde orgaan-residentietijden waren 0.74, 0.44 en 0.29 uur voor de lever, bovenste dikke darm en onderste dikke darm respectievelijk. De testis ontvingen de hoogste dosis namelijk 109.4 µGray/MBq. Alle andere organen ontvingen dosissen van minder dan 50 µGray/MBq. De effectieve dosis was 40.3 µSv/MBq.

Zodoende konden we concluderen dat [^{123}I]iodo-PK11195 een geschikt radioligand is voor de beeldvorming van de PBR en indirect voor de beeldvorming van neuro-inflammatoire letsels. Rekening houdend met de stralingsbelasting van 7.46 mSv na een toediening van 185 MBq kan men een [^{123}I]iodo-PK11195 onderzoek beschouwen als een ICRP risicocategorie IIB investigatie.

Hierna wordt in **hoofdstuk vijf** de validatie van radioactief gemerkt PK11195 als neuro-inflammatoir radioligand beschreven, dit door het toepassen ervan in multipele sclerose, het prototype van de neuro-inflammatoire aandoening met zijn pathofysiologische betrokkenheid van microglia. In een *inleidende sectie* wordt de historiek, epidemiologie, pathofysiologie, klinische kenmerken en ziekteverloop en de behandeling van multipele sclerose toegelicht. In een *tweede sectie* wordt de beeldvorming van geactiveerde microglia in multipele sclerose patiënten door middel van [^{11}C]PK11195 en PET bestudeerd. Hiervoor worden semi-kwantitatieve [^{11}C]PK11195 opnamewaarden berekend voor multipele sclerose patiënten en vergeleken met gezonde vrijwilligers, dit met een normalisatie ten opzichte van corticale grijze stof. Er wordt geconcludeerd dat de opname van het radioligand in gadoliniumletsels significant gestegen is in vergelijking met de opname in de normale witte stof. De opname in T2-letsels is over het algemeen verminderd, suggestief voor een PBR downregulatie. Hiertegenover staat een toename van de opnamewaarden wanneer een klinische of MRI-opstoot aanwezig is, suggestief voor een dynamisch ziekteproces met een voorbijgaande PBR-upregulatie. Tijdens de ziekteprogressie wordt een toename van de opname van het radioligand bemerkt ter hoogte van de normaal-uitziende witte stof wat erop wijst dat deze normaal-uitziende witte stof aan de grondslag ligt van het ziekteproces. Als conclusie kunnen we stellen dat [^{11}C]PK11195 PET beeldvorming een additionele waarde heeft tegenover MRI wat betreft het immunopathofysiologisch proces, en in staat is om inflammatoire processen met een microgliale betrokkenheid aan te tonen in multipele sclerose. In een derde sectie van dit hoofdstuk werd hersenatrofie en microgliale activatie opgemeten in multipele sclerose patiënten tijdens de diverse ziektestadia en werd de relatie tussen inflammatie, atrofie en klinische evaluatieschalen geïnvestigeerd. Er werd vastgesteld dat atrofie significant toegenomen was bij multipele sclerose patiënten in vergelijking met leeftijdsgenoten. Bovendien was er een positieve correlatie tussen hersenatrofie en zowel ziekteduur als invaliditeit, dit laatste gemeten aan de hand van de *expanded disability status scale* (EDSS). Voor de normaal-uitziende witte stof was er een gestadige toename van microgliale activatie (gemeten met behulp van [^{11}C]PK11195 PET) en de hoeveelheid atrofie, dit terwijl de microgliale activatie ter hoogte van de T_2-letsels afnam naar gelang het toenemen van de hersenatrofie. Als besluit kunnen we stellen dat hersenatrofie correleert met ziekteduur en invaliditeit en gerelateerd is aan inflammatie ter hoogte van de normaal uitziende witte stof en de T_2-letsels dit gemeten door middel van deze *PET-probe* voor microgliale activatie.

Hoofdstuk zes beschrijft de meting van microgliale activatie door middel van radioactief gemerkt PK11195 voor SPECT bij de ziekte van Alzheimer en zijn relatie met de bevindingen verkregen door perfusie SPECT en neuropsychologische testen. Hiervoor werden [^{123}I]iodo-PK11195 SPECT beelden gerealigneerd in een stereotactische ruimte waarvoor bindingspotentialen (relatief ten

opzichte van het cerebellum) berekend werden. Er werd gemiddeld een verhoogde [^{123}I]iodo-PK11195 opname vastgesteld bij patiënten lijdend aan de ziekte van Alzheimer in vergelijking met controlepersonen en dit in bijna alle neocorticale regio's hoewel statistische significantie enkel bereikt werd in de frontale en rechter mesotemporale regio's. Directe correlaties werden gevonden tussen regionaal toegenomen [^{123}I]iodo-PK11195 opnamewaarden en cognitieve defecten. Zodoende kan men stellen dat [^{123}I]iodo-PK11195 een cellulaire merker is van de ziekteactiviteit die ons in staat stelt tot het *in vivo* evalueren van microgliale inflammatie bij de ziekte van Alzheimer. Toekomstig werk zou zowel technisch als klinisch kunnen zijn. Methodologisch zou er een directe vergelijking dienen te gebeuren tussen de PET en SPECT radioligand terwijl eveneens bruikbare methodes voor de absolute quantificatie verder gevalideerd en geïmplementeerd zouden moeten worden. Klinisch zou de inclusie van meer patiënten en dit tijdens verschillende ziektestadia, de vergelijking met proton MR spectroscopie voor de meting van gliale merkers of de evaluatie van wijzigingen in de opname van dit radioligand tijdens (anti-inflammatoire) behandelingsstrategieën zeer nuttig kunnen zijn. Evenzeer zouden nieuwe radioliganden ontwikkeld kunnen worden voor neuro-inflammatoire beeldvorming, afhankelijk van de eventuele ontwikkeling van nieuwere anti-inflammatoire behandelingsmodaliteiten. Idealiter moet dit nieuw radioligand in staat zijn om snel geklaard te worden uit het bloed en andere *non-target* weefsels en dient de interactie tussen het radioligand en de receptor gekenmerkt te zijn door een hoge bindingsaffiniteit en specificiteit, zoals aangetoond door middel van autoradiografie, receptorblokkadestudies of studies met controle-agentia. Voor neuro-beeldvormingsstudies bij pathologieën zonder bloed-hersenbarrière doorbraak (zoals bij de ziekte van Alzheimer) dient het radioligand tevens in staat te zijn deze snel en eenvoudig te kunnen penetreren.

In het tweede deel van dit proefschrift (**hoofdstuk zeven**) handelend over de serotonerge hypothese van de ziekte van Alzheimer wordt de rol en de verdeling van serotonine type 2A receptoren bij gezonde controlepersonen en patiënten lijdend aan de ziekte van Alzheimer beschreven. In een *inleidende sectie* wordt de rol van serotonine en vooral serotonine type 2A receptoren voor cognitief en niet-cognitief gedrag en zijn relatie met de ziekte van Alzheimer in het algemeen en de inflammatoire hypothese in het bijzonder kort geëxploreerd. In een *tweede sectie* wordt de beeldvorming van het 5-HT_{2A} systeem in gezonde vrijwilligers en patiënten lijdend aan de ziekte van Alzheimer beschreven. Gebruik makende van I^{123}-5-I-R91150, een selectief radioactief gemerkte 5-HT_{2A} receptor antagonist en SPECT wordt de 5-HT_{2A} bindingspotentiaal in gezonde vrijwilligers en patiënten lijdend aan de ziekte van Alzheimer berekend. Hiervoor wordt een semi-kwantitatieve analyse (relatief ten opzichte van het cerebellum) verricht, welke bindingspotentialen oplevert voor 26 corticale regio's. Er werd een leeftijdsafhankelijke afname van de neocorticale bindingspotentiaal gevonden voor gezonde vrijwilligers (11.6% per decade). In vergelijking met leeftijdsgenoten was er een algemeen gedaalde neocorticale bindingspotentiaal in patiënten lijdend aan de ziekte van Alzheimer met een significant regionale vermindering in de orbitofrontale, prefrontale, lateraal frontale, sensorimotore, inferopariëtale en occipitale regio en de gyri cinguli. Deze resultaten zijn in overeenstemming met vroeger *post mortem*, *in vitro* en PET bevindingen. Aldus stelt deze leeftijdsafhankelijke afname de noodzaak in het licht voor *gematchte* hoogbejaarde studiegroepen.

Het feit dat de 5-HT_{2A} receptor aangetast is bij patiënten lijdend aan de ziekte van Alzheimer in vergelijking met leeftijdsgenoten heeft implicaties voor zowel de etiologie als het therapeutisch beleid hiervan.

Zoals vermeld bij de hierboven voorgestelde resultaten leveren neuro-inflammatoire en serotonerge beeldvorming verschillende specifieke regionale veranderingen in bindingspotentiaal op voor patiënten lijdend aan de ziekte van Alzheimer, hetgeen de vraag doet rijzen naar hun respectievelijke relatie met betrekking tot de pathofysiologie van de ziekte van Alzheimer. Jammer genoeg werd er om logistieke redenen geen enkele studie verricht waarbij zowel radioactief gemerkt PK11195 en ^{123}I-5-I-R91150 gebruikt werd bij dezelfde patiënten hoewel men kan veronderstellen dat beide populaties welke geïncludeerd werden in deze twee studies, hoewel klein, toch representatief zijn voor een, indien ze al bestaat, *waarachtige* populatie van patiënten lijdend aan de ziekte van Alzheimer hetgeen de verschillen in regionale bindingspotentiaalwijzigingen tot *echte verschillen* maakt als dusdanig, niet wijzend op verschillen in de geïncludeerde patiëntenkarakteristieken maar wijzend op een verschillend aspect van de pathofysiologie van de ziekte van Alzheimer. Hiervoor zijn er minstens drie mogelijke verklaringsmodellen. Ten eerste is er de notie van de heterogeniteit van de ziekte van Alzheimer waar vragen rijzen omtrent het bestaan van de ziekte van Alzheimer als een enkelvoudige pathophysiologische entiteit. Hoewel meerdere onderzoekers getracht hebben de verschillende hypotheses betreffende de etiologie en pathofysiologie van de ziekte van Alzheimer te verenigen, zijn er toch diverse wetenschappelijke argumenten wijzend op de mogelijkheid dat er niet één *ziekte van Alzheimer* bestaat. Inderdaad, reeds vele auteurs hebben gewezen op patiënten lijdend aan de ziekte van Alzheimer met bijvoorbeeld enerzijds verschillende neuropsychologische of klinische presentaties of anderzijds verschillende doorbloedingsstoornissen om nog maar te zwijgen over de overlap betreffende zowel risicofactoren als klinische presentatie tussen patiënten lijdend aan de ziekte van Alzheimer en patiënten lijdend aan vasculaire dementie. Ten tweede is er de optie van een chronologie in het pathofysiologisch proces van de ziekte van Alzheimer waarin verschillende hersensystemen min of meer aangetast zijn gedurende het ziekteproces. In het licht van de huidige thesis zou de hier voorgestelde opeenvolging van gebeurtenissen vooreerst de inflammatoire respons zijn, volgend op een primair event (amyloïde accumulatie, ...), hierna gevolgd door functionele neurotransmitter of meer specifiek serotonerge wijzigingen finaal gevolgd door structurele veranderingen zoals atrofie. Ten derde is er de optie van co-existentie van pathofysiologische veranderingen met een verschillende regionale gevoeligheid welke een verklaring bieden voor de verschillen in regionale bindingspotentiaalwijzigingen. Inderdaad kan men zich afvragen waarom de sensorimotore cortex relatief onaangetast is wat betreft perfusie maar zwaar aangetast betreffende het serotonine 2A systeem of bijvoorbeeld de mesotemporale regio voornamelijk aangetast is door atrofie en relatief onaangetast betreffende het serotonerge systeem.

Om deze en andere vragen te kunnen beantwoorden zou het waardevol zijn om verschillende pathofysiologische aangrijpingspunten bij dezelfde patiënten te bestuderen, bijvoorbeeld amyloïdogene, neuro-inflammatoire, cholinerge, serotonerge, perfusionele en structurele veranderingen en dit op verschillende tijdstippen van het ziekte-evolutie om zodoende in staat te zijn

de diverse pathofysiologische mechanismen te kunnen toeschrijven aan verschillende tijdstippen van het ziekteproces. Idealiter zou dit moeten gedaan worden gebruik makende van verschillende meetinstrumenten voor het evalueren van hetzelfde pathofysiologisch proces bijvoorbeeld zowel beeldvorming (structureel, functioneel en metabool), laboratoriuminvestigaties (bloed, cerebrospinaal vocht, ...) als post mortem neuropathologisch onderzoek. Dit zeker in een tijdstip waar meer en meer behandeling beschikbaar wordt om zodoende van enig nut te kunnen zijn bij de beslissing welke therapie wanneer toe te passen.

DANKWOORD

Uiteraard zou niks van dit alles mogelijk geweest zijn zonder de steun en assistentie van een ganse groep mensen waar ik steeds op kon rekenen en die ik bij deze hartelijk wil danken. Op het gevaar af van mensen over het hoofd te zien wil ik vooreerst beginnen met die anonieme groep van 'vergetenen' uitgebreid te danken. Zij verdienen deze *dankuwel* eigenlijk ook het meest gezien deze mensen er in slagen zaken vooruit te helpen alsof het evident is en zonder dat dit overdreven in het daglicht gesteld wordt.

Toch zou ik graag enkele specifieke mensen en groepen een woord van dank toegooien.

Het is natuurlijk allemaal begonnen op de dienst Isotopen alias *P7* waar ik ooit - reeds deels de geneeskunde de rug toegekeerd - verzeild raakte. Ik trof er een dienst aan met een nooit geziene transparantie, amicaliteit en een nagenoeg legendarisch horizontale gezagstructuur. Het is in dit klimaat dat ik langzaam overtuigd werd van het feit dat ik alsnog een rol in de medische wereld kon vervullen. Ik wil dan ook specifiek Prof. Dierckx bedanken voor de broeikas te *managen* waarin dit geheel kon gedijen. In deze biosfeer heb ik op het traject van mijn onderzoeksperiode eveneens een aantal mensen leren kennen die ik ook expliciet wil bedanken voor de hechte vriendschap welke ik met hen mocht en hopelijk nog lang mag delen. Duizendmaal dank aan *gli ingegneri* van wie ik zo graag één van hen wou zijn… Frederic, jij was de ultieme belichaming van het positivisme dat onze dienst uitademde. Je hebt er geen idee van hoezeer wij jou missen, als collega maar vooral als vriend. Olivier en Ingeborg, dank om met mij zolang het toch wel gezellige bureautje te willen delen maar vooral om mijn neurotische *bureau-moet-leeg-met-hierop-alles-netjes-in-bakjes-gerangschikt-trekjes* te tolereren.

Het werkelijke startschot werd natuurlijk gegeven met het promotorschap van Prof. Korf die ik dan ook van harte wil bedanken voor zijn wetenschappelijke onbevangenheid gekoppeld aan een (ogenschijnlijk) schier grenzeloos vertrouwen, enthousiasme(ringsvermogen) en zijn rol als continue inspiratiebron.

Een bijzonder woord van dank zou ik toch willen richten aan Koen Van Laere zonder wie een groot deel van dit werk niet mogelijk zou geweest zijn. Zelden iemand ontmoet die een wetenschappelijk gefundeerde glasheldere zin voor precisie en gedrevenheid zo perfect wist te combineren.

Dank ook voor de meer dan prettige samenwerking met de diensten Radiofarmacie (onder het vakkundig leiderschap van Prof. Slegers, Filip Dumont, Filip De Vos, Marleen Vandecapelle, …), Neurologie (Jan Debruyne, Patrick Santens, Danny Decoo), Psychiatrie (Kurt Audenaert) en Radiologie (Eric Achten).

Dank aan familie en vrienden voor de gegeven levenskansen en de continue steunbetuigingen in deze soms toch wel op zijn minst lang lijkende lijdensweg. Ik wil me dan ook oprecht excuseren voor het soms *afwezig* zijn omwille van alweer eens een wetenschappelijk obstakel. Gelukkig is alles uiteindelijk op zijn pootjes gevallen…

Hartelijke dank,
Jan

LIST OF PUBLICATIONS IN PEER-REVIEWED INDEXED JOURNALS

- Absolute 24 h quantification of $^{99}Tc^{m}$-DMSA uptake in patients with severely reduced kidney function: a comparison with ^{51}Cr-EDTA clearance
  Van de Wiele C, van den Eeckhaut A, Verweire W, van Haelst JP, Versijpt J, Dierckx RA
  Nucl Med Commun 1999;20(9):829-32

- In vivo evaluation in mice and metabolism in blood of human volunteers of [^{123}I]iodo-PK11195: a possible single-photon emission tomography tracer for visualization of inflammation
  Dumont F, De Vos F, Versijpt J, Jansen HM, Korf J, Dierckx RA, Slegers G
  Eur J Nucl Med 1999;26(3):194-200

- Laparoscopic adjustable silicone gastric banding leakage assessed by ^{99m}Tc-pertechnetate scintigraphy
  Van den Eeckhaut AC, Villeirs GM, Van de Wiele C, Versijpt JJ, Pattyn P, Dierckx RA
  J Nucl Med 1999;40(5):783-5

- The contribution of bone scintigraphy in occupational health or medical insurance claims: a retrospective study
  Versijpt J, Dierckx RA, De Bondt P, Dierckx I, Lambrecht L, De Sadeleer C
  Eur J Nucl Med 1999;26(8):804-11

- Accurate differentiation of parkinsonism and essential tremor using visual assessment of [^{123}I]-FP-CIT SPECT imaging: the [^{123}I]-FP-CIT study group
  Benamer TS, Patterson J, Grosset DG, Booij J, de Bruin K, van Royen E, Speelman JD, Horstink MH, Sips HJ, Dierckx RA, Versijpt J, Decoo D, Van Der Linden C, Hadley DM, Doder M, Lees AJ, Costa DC, Gacinovic S, Oertel WH, Pogarell O, Hoeffken H, Joseph K, Tatsch K, Schwarz J, Ries V
  Mov Disord 2000;15(3):503-10

- Antisaccadic effects of a dopamine agonist as add-on therapy in advanced Parkinson's patients
  Crevits L, Versijpt J, Hanse M, De Ridder K
  Neuropsychobiology 2000;42(4):202-6

- Biodistribution and dosimetry of [^{123}I]iodo-PK 11195: a potential agent for SPET imaging of the peripheral benzodiazepine receptor
  Versijpt J, Dumont F, Thierens H, Jansen H, De Vos F, Slegers G, Santens P, Dierckx RA, Korf J
  Eur J Nucl Med 2000;27(9):1326-33

- Verbal fluency as a prefrontal activation probe: a validation study using ^{99m}Tc-ECD brain SPET
  Audenaert K, Brans B, Van Laere K, Lahorte P, Versijpt J, van Heeringen K, Dierckx R
  Eur J Nucl Med 2000;27(12):1800-8

- ^{57}Co SPECT, ^{99m}Tc-ECD SPECT, MRI and neuropsychological testing in senile dementia of the Alzheimer type
  Versijpt J, Decoo D, Van Laere KJ, Achten E, Audenaert K, D'Asseler Y, Slegers G, Dierckx RA, Korf J
  Nucl Med Commun 2001;22(6):713-9

- ^{99m}Tc-ECD brain perfusion SPET: variability, asymmetry and effects of age and gender in healthy adults
  Van Laere K, Versijpt J, Audenaert K, Koole M, Goethals I, Achten E, Dierckx R
  Eur J Nucl Med 2001;28(7):873-87

- ^{99}Tc^{m} labelled HL91 versus computed tomography and biopsy for the visualization of tumour recurrence of squamous head and neck carcinoma
  Van de Wiele C, Versijpt J, Dierckx RA, Moerman M, Lemmerling M, D'Asseler Y, Vermeersch H
  Nucl Med Commun 2001;22(3):269-75

- Automated stereotactic standardization of brain SPECT receptor data using single-photon transmission images
  Van Laere K, Koole M, D'Asseler Y, Versijpt J, Audenaert K, Dumont F, Dierckx R
  J Nucl Med 2001;42(2):361-75

- Non-uniform versus uniform attenuation correction in brain perfusion SPET of healthy volunteers
  Van Laere K, Koole M, Versijpt J, Dierckx R
  Eur J Nucl Med 2001;28(1):90-8

- Regional brain perfusion in 10 normal dogs measured using Technetium-99m ethyl cysteinate dimer SPECT
  Peremans K, De Bondt P, Audenaert K, Van Laere K, Gielen I, Koole M, Versijpt J, Van Bree H, Verschooten F, Dierckx R
  Vet Radiol Ultrasound 2001;42(6):562-8

- Transfer of normal ^{99m}Tc-ECD brain SPET databases between different gamma cameras
  Van Laere K, Koole M, Versijpt J, Vandenberghe S, Brans B, D'Asseler Y, De Winter O, Kalmar A, Dierckx R
  Eur J Nucl Med 2001;28(4):435-49

- Analysis of clinical brain SPECT data based on anatomic standardization and reference to normal data: an ROC-based comparison of visual, semiquantitative, and voxel-based methods
  Van Laere KJ, Warwick J, Versijpt J, Goethals I, Audenaert K, Van Heerden B, Dierckx R
  J Nucl Med 2002;43(4):458-69

- Considering depression as a consequence of activation of the inflammatory response system
  Korf J, Klein HC, Versijpt J, den Boer J, ter Horst GJ
  Acta Neuropsychiatrica 2002;141-10

- Experimental Performance Assessment of SPM for SPECT Neuroactivation Studies Using a Subresolution Sandwich Phantom Design
  Van Laere KJ, Versijpt J, Koole M, Vandenberghe S, Lahorte P, Lemahieu I, Dierckx RA
  Neuroimage 2002;16(1):200-16

- Perfusion SPECT changes after acute and chronic vagus nerve stimulation in relation to prestimulus condition and long-term clinical efficacy
  Van Laere K, Vonck K, Boon P, Versijpt J, Dierckx R
  J Nucl Med 2002;43(6):733-44

- Semiquantification of the peripheral-type benzodiazepine ligand [^{11}C]PK11195 in normal human brain and application in multiple sclerosis patients
  Debruyne JC, Van Laere KJ, Versijpt J, De Vos F, Keppens J, Strijckmans K, Santens P, Achten E, Slegers G, Korf J, Dierckx RA, De Reuck JL
  Acta Neurol Belg 2002;102(3):127-35

- SPECT neuropsychological activation procedure with the Verbal Fluency Test in attempted suicide patients
  Audenaert K, Goethals I, Van Laere K, Lahorte P, Brans B, Versijpt J, Vervaet M, Beelaert L, van Heeringen K, Dierckx R
  Nucl Med Commun 2002;23(9):907-16

- Scintigraphic visualisation of inflammation in neurodegenerative disorders
  Versijpt J, Van Laere KJ, Dierckx RA, Dumont F, De Deyn PP, Slegers G, Korf J
  Nucl Med Commun 2003;24:209-221

- Imaging of the 5-HT$_{2A}$ system: age-, gender-, and Alzheimer's disease-related findings
  Versijpt J, Van Laere KJ, Dumont F, Decoo D, Vandecapelle M, Santens P, Goethals I, Audenaert K, Slegers G, Dierckx RA, Korf J
  Neurobiol Aging 2003;in press

- PET visualisation of microglia in multiple sclerosis patients using [^{11}C]PK11195
  Versijpt J, Debruyne JC, Van Laere KJ, De Vos F, Keppens J, Strijckmans K, Achten E, Slegers G, Dierckx RA, Korf J, De Reuck JL
  Eur J Neurol 2003;in press

- Assessment of neuroinflammation and microglial activation in Alzheimer's disease with radiolabelled PK11195 and single photon emission computed tomography: a pilot study
  Versijpt J, Dumont F, Van Laere KJ, Decoo D, Santens P, Audenaert K, Achten E, Slegers G, Dierckx RA, Korf J
  Eur Neurol 2003;in press

- Imaging of microglial activation with PET and atrophy with MRI in multiple sclerosis: interrelationship and clinical correlates
  Versijpt J, Debruyne JC, Van Laere KJ, De Vos F, Keppens J, Strijckmans K, Achten E, Slegers G, Dierckx RA, Korf J, De Reuck JL
  J Neurol Sci 2003;submitted

- ^{99m}Tc-HMPAO labelled white blood cell scanning for the detection of infection in End-Stage-Renal-Disease
  Casier K, Versijpt J, Van de Wiele C, Vanholder R, van Haelst JP, Dierckx RA
  Eur J Nucl Med 2003;submitted

CURRICULUM VITAE

Jan Jozef Albert Versijpt is geboren op 10 november 1972 te Sint-Amandsberg. Vanuit een basisinteresse voor wetenschappen met een humane *touch* koos hij in 1990 voor de artsenstudie aan de Universiteit van Gent, welke hij in 1997 beëindigde. Steeds geboeid door de fysiopathologie van het menselijk brein leek het dan ook een ideale mogelijkheid om aansluitend te kunnen starten met wetenschappelijk onderzoek en dit handelend over de ziekte van Alzheimer en nucleaire functionele beeldvorming, onder het promotorschap van Prof. J. Korf (vakgroep Biologische Psychiatrie, Rijksuniversiteit Groningen) en het co-promotorschap van Prof. Dr. R.A. Dierckx (dienst Nucleaire Geneeskunde, Universitair Ziekenhuis Gent). Als dusdanig is Jan (co-)auteur van 27 manuscripten in geïndexeerde tijdschriften en van meer dan 50 communicaties op (inter)nationale congressen. Eveneens werd hij de laureaat van twee reisbeurzen uitgereikt door de *International Society of Cerebral Blood Flow and Metabolism* en won hij een prijs uitgereikt door het wetenschappelijk comité van het *Belgisch Genootschap voor Nucleaire Geneeskunde*. Blijvend geïntrigeerd door het *in vivo-tracer*-principe van nucleaire geneeskunde als specialiteit en gecharmeerd door de nauwe samenwerking van deze discipline met zowel basis – als toegepaste wetenschappen besloot hij in deze richting verder te gaan. Voor het verder afwerken van deze opleiding tot geneesheer specialist in de Nucleaire Geneeskunde was hij vanaf oktober 2001 tewerkgesteld op de dienst Inwendige Ziekten, AZ St. Jan te Brugge en is hij momenteel werkzaam in de Kliniek H. Familie te Gent, dienst Isotopen. Wat betreft vrije tijd houdt Jan zich vooral bezig met improvisatietheater, salsa en sport.

'*Wie herinnert zich niet in zijn kindsheid theoloog, in zijn jeugd metafysicus en op zijn mannelijke leeftijd fysicus geweest te zijn?'*
Auguste Comte in *Cours de philosophie positive* (1842)

Financial support for publication of this thesis has kindly been provided by:

Nuclear Diagnostics
Veenstra Instruments
Amersham Health
Bristol-Myers Squibb
Tyco Healthcare